MICROWAVE POWER TRANSMISSION SYSTEM STUDIES

VOLUME III SECTION 8-MECHANICAL SYSTEMS AND FLIGHT OPERATIONS

RAYTHEON COMPANY
EQUIPMENT DIVISION
ADVANCED DEVELOPMENT LABORATORY
SUDBURY, MASS. 01776

prepared for

NATIONAL AERONAUTICS AND SPACE ADMINISTRATION

1. Report No. NASA CR-134886	2. Government Accession No.	3. Recipient's Catalog No.
4. Title and Subtitle MICROWAVE POWER TRANSMISSION SYSTEM STUDIES Volume III - Mechanical Systems and Flight Operations (Section 8)		5. Report Date December 1975
		6. Performing Organization Code
7. Author(s) O. E. Maynard, W. C. Brown, A. Edwards, J. T. Haley, G. Meltz, J. M. Howell - Raytheon Co.; A. Nathan - Grumman Aerospace Corp.		8. Performing Organization Report No. ER75-4368
		10. Work Unit No.
9. Performing Organization Name and Address Raytheon Company Equipment Division 528 Boston Post Road Sudbury, Massachusetts 01776		11. Contract or Grant No. NAS 3-17835
		13. Type of Report and Period Covered Contractor Report
12. Sponsoring Agency Name and Address National Aeronautics and Space Administration Washington, D.C. 20546		14. Sponsoring Agency Code

16. Abstract

A study of microwave power generation, transmission, reception and control was conducted as a part of the NASA Office of Applications' joint Lewis Research Center/Jet Propulsion Laboratory five-year program to demonstrate the feasibility of power transmission from geosynchronous orbit. This volume (3 of 4) summarizes the efforts and presents recommendations associated with preliminary design and concept definition for mechanical systems and flight operations. Technical discussion in the areas of mission analysis, antenna structural concept, configuration analysis, assembly and packaging with associated costs are presented. Technology issues for the control system, structural system, thermal system and assembly including cost and man's role in assembly and maintenance are identified. Background and desired outputs for future efforts are discussed.

ORIGINAL PAGE IS
OF POOR QUALITY

17. Key Words (Suggested by Author(s)) Microwave power transmission; power from space; satellite power transmission; phased array power transmission; rectifying antenna (rectenna).	18. Distribution Statement Unclassified - Unlimited		
19. Security Classif. (of this report) Unclassified	20. Security Classif. (of this page) Unclassified	21. No. of Pages 233	22. Price* $3.00

* For sale by the National Technical Information Service, Springfield, Virginia 22161

NASA-C-168 (Rev. 10-75)

PREFACE

This section was prepared by Grumman Aerospace Corporation
for Raytheon as the final report on the Mechanical System and Flight
Operations tasks of Preliminary Analysis and Concept Definition. The
baseline MPTS assumed for these tasks was derived from the prior
feasibility study (Reference 4). The principal difference between
this baseline and the system description that evolved during the Con-
ceptual Design Phase was the increase in weight of the MPTS waveguide
to reflect an increase in wall thickness to 0.5 mm. This increase
does not materially effect the study results since the structure de-
sign driver is the thermal environment, and the orbital transportation-
assembly costs are normalized to cost per unit weight.

A similar evolution to higher weight took place in the estimate
for the solar photovoltaic power source used as an example for the
complete SPS. The preliminary and final estimates are as follows for
an aluminum-amplitron configuration and 5 GW ground output power:

	Preliminary Weight - kg x 10^6	Final Weight - kg x 10^6
Solar Array	9.8	11.8
Transmitting Antenna	1.7	6.1 (*)
	11.5	17.9

(*) Final Transmitting Antenna Weight – kg x 10^6

Power Distribution	0.51
Converters	2.22
Antenna	3.33
	6.06

TABLE OF CONTENTS

VOLUME I - EXECUTIVE SUMMARY

VOLUME II - Sections 1 through 7 with Appendices A through G

TABLE OF CONTENTS -- Continued

TABLE OF CONTENTS -- Continued

TABLE OF CONTENTS -- Continued

TABLE OF CONTENTS -- Continued

TABLE OF CONTENTS -- Continued

TABLE OF CONTENTS -- Continued

TABLE OF CONTENTS -- Continued

TABLE OF CONTENTS -- Continued

TABLE OF CONTENTS -- Continued

ILLUSTRATIONS

ILLUSTRATIONS (continued)

ILLUSTRATIONS (continued)

ILLUSTRATIONS (continued)

ILLUSTRATIONS (continued)

LIST OF NON-STANDARD TERMS

AFCRL	Air Force Cambridge Research Laboratory
ATC	Air Traffic Control
ATS	Applications Technology Satellite
CFA	Crossed Field Amplifier
CPU	Central Processor Unit
GaAs	Gallium Arsenide
HLLV	Heavy Lift Launch Vehicle
Met	Meteorological
MPTS	Microwave Power Transmission System
MW	Microwave
N. F.	noise factor
PPM	periodic permanent magnet
ROM	Rough Order of Magnitude
SCR	Silicon Controlled Rectifier
SEPS	Solar Electric Propulsion Stage
Sm-Co(SMCO)	Samarium Cobalt
SPS	Satellite Power System
SSPS	Satellite Solar Power Station
TDRS	Tracking and Data Relay Satellite
TEC	Total Electron Content

Section 1

INTRODUCTION

The objective of the Grumman study effort is to provide refined inputs for mechanical systems, structure and thermal control for Raytheon's overall investigation of the Microwave Power Transmission System (MPTS). This system will be used to transmit, receive and control large amounts of power from space. Grumman's efforts identified structural design options, the driver parameters for both weight and cost, and established requirements for the structural and flight operations systems.

An orbiting electric power station has several major elements: the power source or converter, the electrical power distribution system and the microwave generator/ transmitting antenna. An antenna can be hypothesized that would be independent of the power source except for the mechanical control system interface. The purpose of Task 1, Preliminary Design, was to evaluate this mechanical interface. To achieve the depth needed to gain an understanding of accuracy and stability, a power source and spacecraft had to be selected. Because more data on physical characteristics were available on the Satellite Solar Power Station (SSPS), this power source/spacecraft was used in the preliminary assessment.

Selection of the antenna structure required evaluation of 1) basic antenna geometry, 2) the impact of MW conversion thermal waste on structural material selection and feasible structural flatness, and 3) the mode of transportation and assembly. A broad matrix of antenna geometries, structural materials and transportation modes have been evaluated. Figure 1-1 summarizes this matrix of design options considered during the Task 1 Preliminary Design Phase.

The three materials, aluminum, graphite/epoxy and Kevlar polyimide, were selected on the basis that they represent a broad range of strength, weight, cost and thermal characteristics. Aluminum represents a low cost, high weight option that would thermally limit the power level selected for the system. Graphite/epoxy represents a material with excellent thermal expansion characteristics, high strength and low weight. Kevlar polyimide would be low weight at modest cost with a resin that could withstand a high temperature environment.
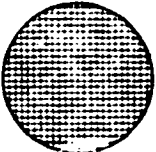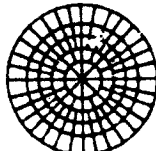
The four transportation modes selected for Task 1 represent the near term Space Transportation System capabilities. A Transtage was selected, both in an expendable and reusable version, as being most representative of the performance of the Interim Upper Stage (IUS). A Full Capability Cryo Tug was used to represent the STS performance capability in the 1984 time frame. The fourth option, Shuttle/Low Altitude Assembly, was introduced into the matrix to determine the impact of assembly altitude on overall system selection.

Antenna geometry options include a rectangular grid and a radial spoke structural layout. Both these structural arrangements are acceptable in terms of available layouts for the power distribution system. Antenna diameters between 0.7 to 1.4 km were included in the design matrix after Raytheon's preliminary results indicated that optimum system performance would fall within these bounds.

The Task 1 study logic for control analysis and thermal structural analysis and cost parametrics are outlined in Fig. 1-2. The output of the three principal tasks are recommendations for a limited number of control system, structural and flight operations options for detailed concept definition in Task 2.

The limited number of design options recommended in Task 1 were evaluated in greater detail in Task 2, Concept Definition, using the study logic shown in Fig. 1-3. Information generated during Concept Definition will permit Raytheon to carry out technical and economic evaluation leading to selection of a single configuration to be the basis for ground demonstration test.

Flight plans were generated for assembly of the SSPS at a low altitude which is within the performance range of the Shuttle with integral OMS, and at an altitude above the Van Allen belts. Traffic rates and fleet size requirements were established for a one and two year assembly period. Packaging densities of SSPS components were considered in establishing the method of assembly using manipulative devices, maneuvering units, and EVA. Assumptions concerning degree of human skills are outlined as well as the potential capability of support ancillary equipment. Sensitivity analysis of various levels of ground prefabrication compared to corresponding levels of orbital assembly was performed to determine the most cost effective approach to structural assembly.

TRANSPORTATION MODE		MATERIALS		
		ALUMINUM	GRAPHITE/ EPOXY	KEV.. POLYIMIDE
I	SHUTTLE/ EXPENDABLE TRANSTAGE	√	√	√
II	SHUTTLE/ REUSABLE TRANSTAGE	√	√	√
III	SHUTTLE/ CRYO TUG	√	√	√
IV	SHUTTLE/ LOW ORBIT ASSEMBLY	√	√	√
V	SHUTTLE/ CRYO TUG/ SPACE STATION	√	√	√

STRUCTURAL ARRANGEMENT	DIAMETER (Km)		
	0.7	1.0	1.4
RECTANGULAR GRID	√	√	√
RADIAL SPOKE		√	

√ STUDY CONCEPTS EVALUATED

Fig. 1-1 Preliminary Design Option Matrix
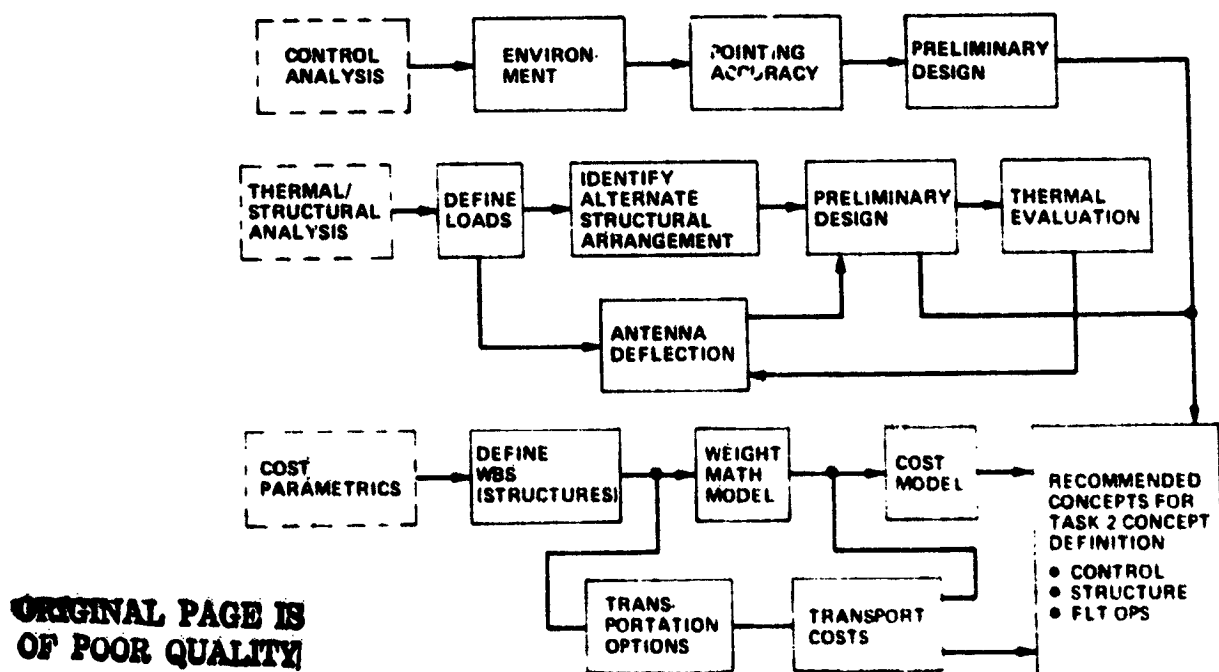
Fig. 1-2 Task 1 Preliminary Design Study Logic, Mechanical Systems and Flight Operations

TASK 3.2.1	3.2.1-1	3.2.1-2	3.2.1-3	3.2.1-4	
FLIGHT OPERATIONS	ASSEMBLY ALTITUDE SELECTION	TRANSPORTATION SYSTEM PERFORMANCE	TIME LINES	ASSEMBLY SCHEDULE	FLT PLAN

TASK 3.2.2	3.2.2-1	3.2.2-2	3.2.2-3	3.2.2-4
DESIGN DEFINITION	GENERAL ARRANGEMENT	WEIGHT STATEMENT	SUBASSEMBLY DEFINITION	PACKAGING ASSESSMENT

TECHNOLOGY ISSUES

TASK 3.2.3	3.2.3-1	3.2.3-2	3.2.3-4	3.2.3-5
PRELIMINARY STRUCTURAL ANALYSIS	CROSS SECT. SELECTION	THERMAL NODAL ANALYSIS	STRUCTURAL DEFLECTION ASSESSMENT	MATERIALS ASSESSMENT

FINAL REPORT

TASK 3.2.4	3.2.4-1	3.2.4-2	3.2.4-3
COST ANALYSIS	ASSEMBLY COST ESTIMATE APPROACH	ORBIT ASSEMBLY COMPLEXITY FACTORS	CONCEPT COMPARISON

Fig. 1-3 Task 2 — Concept Definition Study Logic

Antenna general arrangements, interface drawings and weight statements are in-
.... d in this document for use during the remainder of the MPTS studies. Detail thermal
and structural evaluations have been performed to determine the limitations the structure
impose on electronic layout and phase front control concepts. Mechanical options to a
fully electronic control system have been identified and are shown to desensitize the
tolerance on structural assembly accuracy and impact of thermal deflections over a wide
range of sun-to-spacecraft geometries.

Section 2

SUMMARY

2.1 TASK 1 - PRELIMINARY DESIGN

2.1.1 Control Analysis

Qualitative estimates of requirements and desi;n options for antenna mechanical steering indicates that pointing accuracy of better than 1 arc-min can be achieved. The mechanical system, if integrated with the electronics microwave beam phase front control, could improve overall system efficiency with minimal impact on system weight and cost.

Figure 2-1 summarizes the design environment for mechanical steering. The antenna gravity gradient torques are a major externally induced disturbance. Other factors, such as torque caused by solar pressure, or electromagnetic forces, are small. The most significant torque is the friction torque at the rotary joint. This torque varies as a function of system power level and power transfer technique. Base motions of the SSPS are caused by normal limit cycle operations and by solar array bending dynamics.

Figure 2-2 is a composite of system accuracy and torque requirements as a function of mechanical control system frequency. An azimuth accuracy of 40 arc-sec can be achieved with a control system frequency of 1 rad/sec. This control frequency would require 1,020,000 N·m (750,000 ft-lb) peak control torque (measured on load side of the gear train). This control system frequency is well above the first structural frequency of the SSPS and antenna. Peak horsepower requirements at 1 rad/sec is 0.18 and 1.75 hp in azimuth (East-West rotation) and elevation (North-South rotation), respectively.

A review of top level methods for implementing mechanical steering favors a motor-gearing mechanical system as opposed to a reaction jet system. Because control system frequencies are well above the first structural bending frequencies, no instabilities are foreseen. A mechanical system could be configured against wear by providing sufficient redundancy. The reaction jet approach, in which jets are mounted to the antenna, would be advantageous because the antenna structure could be more readily isolated from spacecraft dynamics than a mechanical system using gear trains. The shortcomings of the jet system, however, include:

- ● ANTENNA TORQUES

	AZIMUTH	ELEVATION
– GRAVITY GRADIENT ~ N·m (FT·LB)	1800 (1330)	2280 (1682)
– FRICTION DUE TO ROLLERS ~ N·m (FT·LB)	4300 (3168)	1150 (792)
– FRICTION DUE TO SLIP RINGS ~ N·m (FT·LB)	1,020,000 (750,000)	N/A

- ● BASE MOTION

	AZIMUTH	ELEVATION
– SSPS LIMIT CYCLE		
□ POSITION ~ DEG	±1	±1
□ RATE ~ DEG/SEC	±3.94	±2
□ ACCELERATION ~ DEG/SEC^2	9×10^{-7}	2×10^{-8}
– ANTISYMMETRIC BENDING MODE		
□ POSITION ~ RAD	.0027	.0027
□ RATE ~ RAD/SEC	4.86×10^{-5}	4.86×10^{-5}
□ ACCELERATION ~ RAD/SEC^2	8.66×10^{-8}	8.66×10^{-8}

Fig. 2-1 Control System Requirements

Fig. 2-2 Control System Requirements
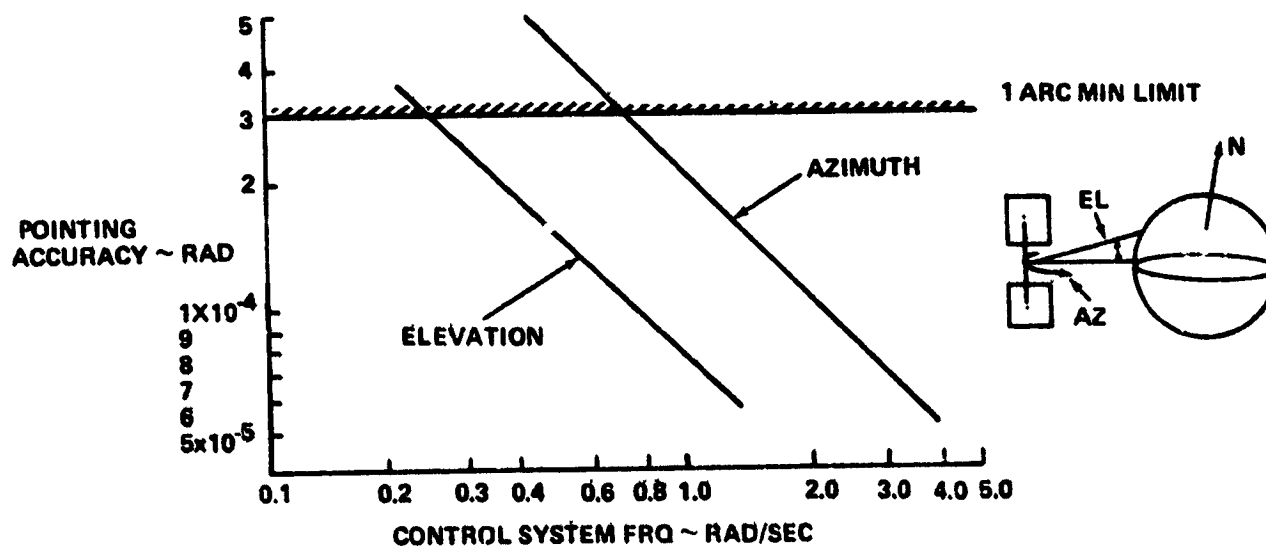
- ● CONTROL PEAK TORQUE
  - – AZ ≈ CONSTANT WITH CONT'L FREQ = 1,020,000 N·m
  - – EL ≈ CONSTANT WITH CONT'L FREQ = 2780 N·m

- ● PEAK OPERATING HP
  - – AZ ≈ CONSTANT WITH CONT'L FREQ = .18 HP
  - – EL ≈ CONSTANT WITH CONT'L FREQ = 1.75 HP

- Requirement for propellant resupply

- Contamination of waveguide functions.

Figure 2-3 lists mechanical system options considered in Task 1 and identifies configurations recommended for Task 2 Concept Definition. Also included in Fig. 2-3 are recommended technology studies which could provide a more optimum design. Power clutches or rotary transformers are power transfer advanced space techniques that could lead to a reduction in interface friction, and increased life. Spur gears are recommended for the gear train, but a direct drive motor system would eliminate gears and may be easier to implement, provided sufficient accuracy could be achieved. Individual rollers are recommended as baseline because of ease of implementation. Ball bearings offer an advantage in terms of lower friction torques and should be considered as an alternate. DC brush torque motors are recommended; however, linear induction motors may show advantages in terms of life and inherent capability to isolate the spacecraft dynamics from the antenna dynamics.

2.1.2 Thermal/Structural Analysis

A thermal/structural analysis has been carried out to determine deformations to be used in establishment of requirements for phase front control, and to determine cost and weight factors for overall system selection.

2.1.2.1 Preliminary Design Options

Figure 2-4 is a weight comparison of principal structural design layouts. The rectangular grid approach was found to be lighter than the radial spoke arrangement. Two compression member designs were considered; a singular tube, 100 m long, and a triangular girder with thin walled circular tubes at the apex with cross tubes and diagonal wire bracing. The triangular girder approach was found to be significantly lighter than the singular tube.

Assessment of structural deflections included analysis of load, thermal and assembly tolerance induced deformations. The assembly tolerances were found to be the largest source of deformation with a worst case tip deflection of 0.17 degree. Deflections due to thermal bending can be kept below 1 arc-min if thermal gradients between the upper and lower primary structural caps can be controlled to less than $4°K$. Deflections due to loads were found to be insignificant.

BASELINE

	AZ	EL	TECHNOLOGY STUDIES RECOMMENDED

● **POWER TRANSFER**

  – SLIP RING AND BRUSH ——————→√
  – FLEX HARNESS ———————————————→√
  – POWER CLUTCH —————————————————————————→√
  – ROTARY TRANSFORMER ————————————————————→√
  – ROLLING CONTACT

● **GEARS**

  – SPUR GEARS ————————————√———————→√
  – WORM GEARS
  – HARMONIC DRIVE GEARS
  – HELICAL GEARS ————————————————————————————→√
  – CHAIN DRIVE ————————————————————————————

● **BEARINGS**

  – BALL BEARINGS ————————————————————————————→√
  – ROLLER BEARINGS
  – INDIVIDUAL ROLLERS ——————→√

● **MOTORS**

  – DC BRUSH TYPE TORQUE ————√
  – DC BRUSHLESS TORQUE ————————→√———————→√
  – INDUCTION ————————————————————————————→√
  – AC SYNCHRONOUS
  – AC TORQUE

Fig. 2-3 Mechanical System Options Recommended for Task 2 Study

2.1.2.2 Thermal Evaluation

Preliminary thermal analysis of the MPTS centered about studies that would indicate the sensitivity of temperature level and thermal gradient on antenna size, power level, microwave converter selection, and distribution.

2.1.2.2.1 Temperature Level - Structural temperature levels, material and antenna size combine to place limitations on the power that can be transmitted by the antenna. Figure 2-5 shows the limit power level for antenna diameters between 0.7 and 1.4 km. Aluminum, epoxy and polyimide are shown as representative materials. Aluminum and graphite/epoxy lose their strength characteristics at approximately 450°K. This limits system power levels for 1 km diameter antenna to 17 gw with a 90% efficient microwave converter and to 4 gw with a 70% efficient converter. Limit power levels can be significantly increased with the use of polyimide composite materials.

2.1.2.2.2 Thermal Gradient - Figure 2-6 presents the thermal gradients between primary structural caps for distances of 40 and 90 meters. The trend indicates that to limit tip deflections to less than 1 arc-min, the average distance between caps should be somewhat less than 40 meters. This would keep temperature gradients below 4°C. The worst case thermal gradients occur when the antenna microwave surface shades the structure from the sun.

2.1.3 Design Options and Groundrules for Task 2 Concept Definition

Task 1 resulted in recommendations that a frequency of 2.45 GHz be selected and four configurations of slotted waveguide transmitting arrays be studied in Task 2. These configurations involve combinations of amplitrons with aluminum structure and array, amplitrons with graphite composite structure and array, and a klystron with the same two materials.

Task 1 also showed that a 5 gw ground output power level would be a reasonable choice for all Task 2 study vehicles. An antenna diameter of 1 km was selected based on the relative insensitivity of this parameter to overall system cost and performance. Figure 2-7 summarizes the guidelines for Task 2 study.
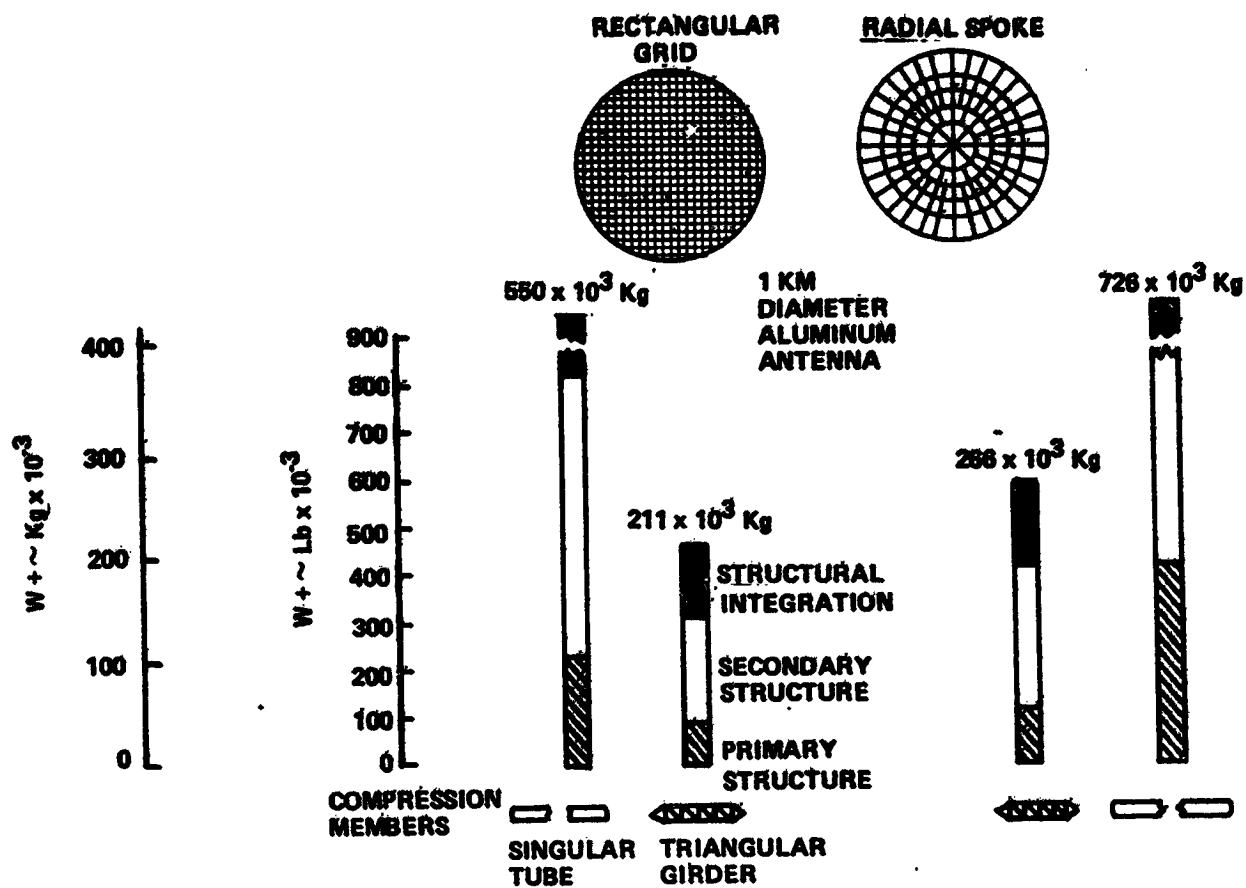
Fig. 2-4 Antenna Geometry Tradeoff
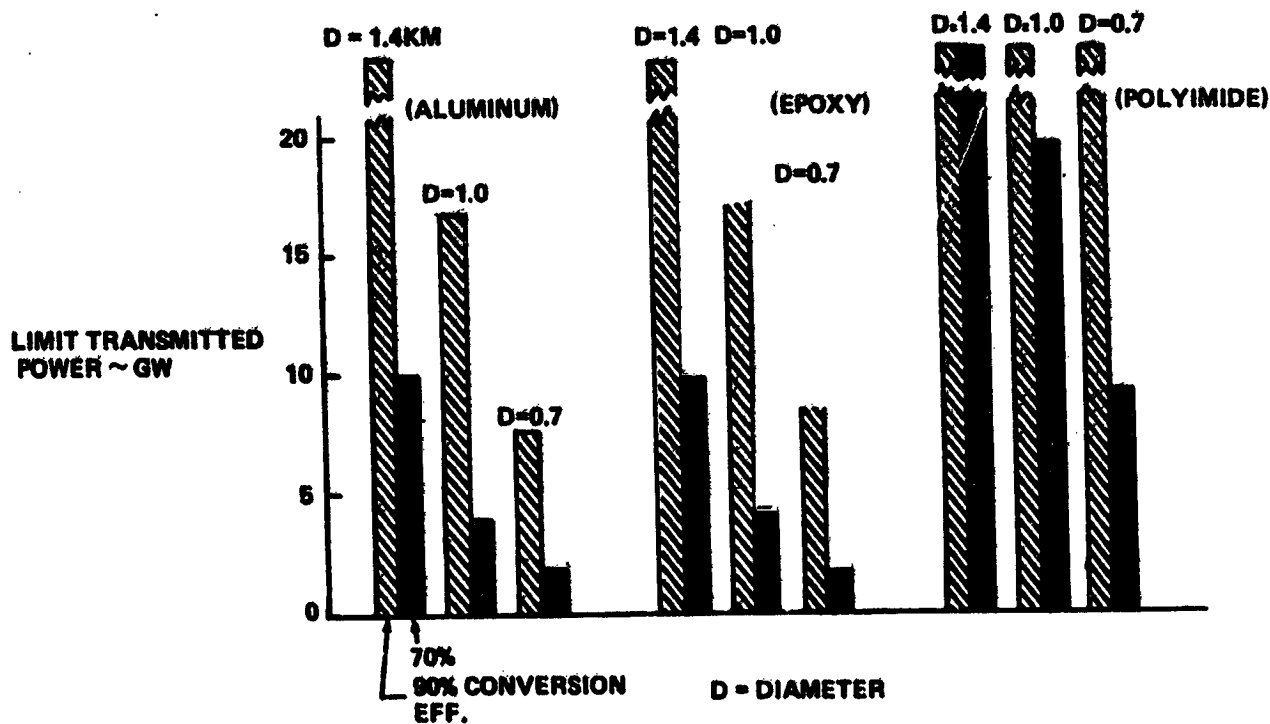
Fig. 2-5 Power Level Limitations Due to Material Thermal Properties

$\Delta T \sim °K$

DISTANCE FROM CENTER LINE OF ANTENNA, METERS

TEMPERATURE OF MEMBER
LOCATED 50 METERS
ABOVE ANTENNA MINUS
TEMPERATURE OF MEMBER
AT 10 METERS

TEMPERATURE OF MEMBER
LOCATED 100 METERS
ABOVE ANTENNA MINUS
TEMPERATURE OF MEMBER
AT 10 METERS
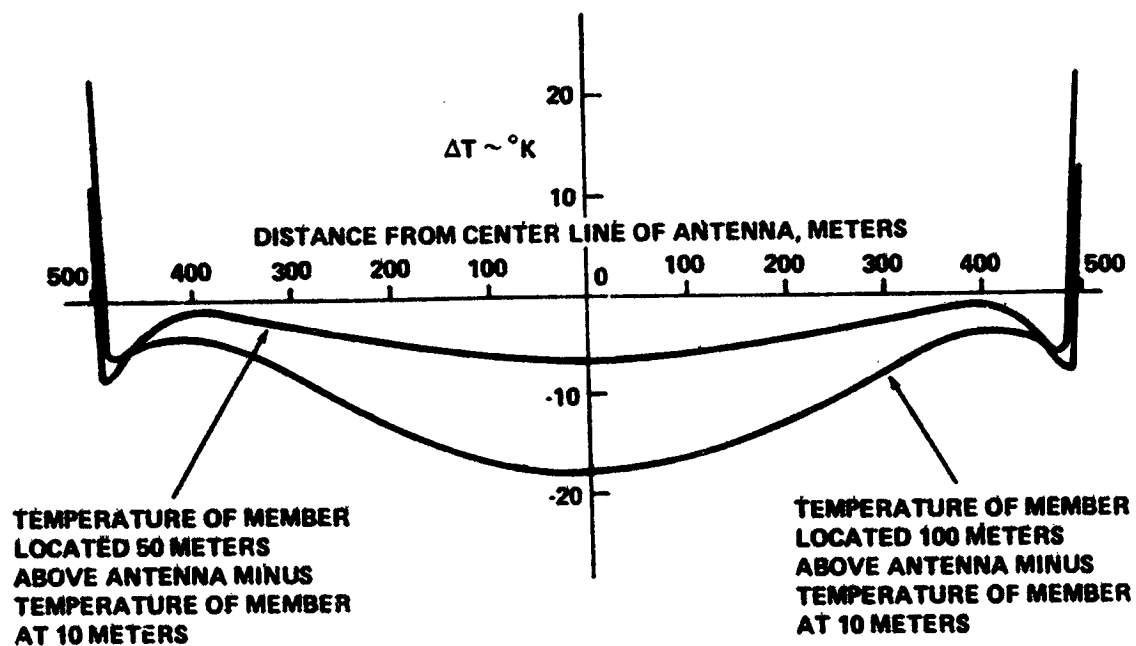
- POWER TRANSMITTED = 10 GW
- CONVERTER EFFICIENCY = 90%

Fig. 2-6 Temperature Difference Between Structural Member Located Different Distances above the Antenna Surface

FUNDAMENTAL PARAMETERS		
DESIGN POWER SOURCE		SOLAR PHOTOVOLTAIC
FREQUENCY		2.45 GHz
GROUND OUTPUT POWER (t_0+5 YR)		5 GW
USEFUL LIFE		30 YR
TRANSMITTING ARRAY:		
TYPE		SLOTTED ARRAY
STRUCTURE		RECTANGULAR GRID – GIRDER
MATERIAL	(1)	ALUMINUM
	(2)	GRAPHITE EPOXY
PHASE FRONT CONTROL	(1)	COMMAND
	(2)	COMMAND PLUS ADAPTIVE
DC-RF CONVERTER	(1)	AMPLITRON
	(2)	KLYSTRON
HEAT TRANSFER		CONDUCTION-RADIATION (NO HEAT PIPE)
RECEIVING ANTENNA		RECTENNA
TRANSPORTATION-ASSEMBLY	(1)	SHUTTLE ORBITER/CRYO TUG/SEPS – HIGH ALTITUDE ASSEMBLY
	(2)	SHUTTLE ORBITER/SEPS-LOW ALTITUDE ASSEMBLY

PROVISIONAL PARAMETERS	
TRANSMITTING ARRAY:	
DIAMETER	1 KM
ILLUMINATION	EXP $[-2.30 \, (^r/_a)^2]$
RADIATED POWER	6.45 GW
SUBARRAY SIZE	18M X 18M
AMPLITRON OUTPUT POWER	6KW
AMPLITRON EFFICIENCY	85%
KLYSTRON OUTPUT POWER	6KW
KLYSTRON EFFICIENCY	75%
PEAK GROUND POWER DENSITY	23 mw/cm^2
RECTENNA SIZE	10 km X 13 km

Fig. 2-7 Task 2 Baseline Design Guidelines

2.2 TASK 2 - CONCEPT DEFINITION

2.2.1 Mission Analysis

The mission analysis effort objective was to define flight scenarios for subsequent assessment of transportation system performance requirements. Figure 2-8 is a top level functional flow of the SSPS assembly sequence. Two flight plans for assembly and transport to geosynchronous orbit were developed:

- Low altitude assembly and transport to geosynchronous using solar electric propulsion (SEP)

- Assembly just above Van Allen belts and transport to geosynchronous using SEP.

A baseline SSPS, Fig. 2-9 was assumed for mission analysis and subsequent estimates of traffic models and fleet sizes. Performance capabilities of the transportation system are summarized in Fig. 2-10. Shuttle performance of 65,000 lb (29,400 Kg) can be expected up to an altitude of 190 n mi. The Cryo Tug, used in the flight plan with assembly at 7000 n mi, has a payload capability of 36,800 lb (16,700 Kg) in a Tug recoverable mode.

SEP size and performance data for the two flight modes are presented in Fig. 2-10. A SEP system efficiency of 0.7 and a specific weight of 15 lb/kw (6.8 Kg/kw) was assumed in the stage sizing. The 0.7 efficiency is equaled or exceeded by today's technology. Overall system specific weight is consistent with projected solar cell weights for the SSPS itself. Specific weight of the power conditioning and subsystems is based on a projected four fold improvement in technology (using today's technology would result in an overall system specific weight of 65 lb/kw = 29.5 Kg/kw).

A 190 n mi assembly site would require continuous orbit keeping propulsion to compensate for air drag. Figure 2-11 indicates that uncorrected air drag effects would result in assembly entry after one to 16 months depending upon configuration M/C_dA. The spread in M/C_dA (0.175 to 1.75) is indicative of the SSPS configuration with solar blankets deployed and retracted. A 16-lb thrust (70 newton) SEP stage would be required for the orbit keeping function. A propellant expenditure of 44 Klb (20,000 Kg) is projected.

2.2.2 Antenna Structural Definition

The MPTS antenna is 1 km in diameter by 40 meters deep, Fig. 2-12. The antenna is assembled in two rectangular grid structural layers. The primary structure is built-up in 108 x 108 x 35 meter bays using triangular girder compression members 18 meters long
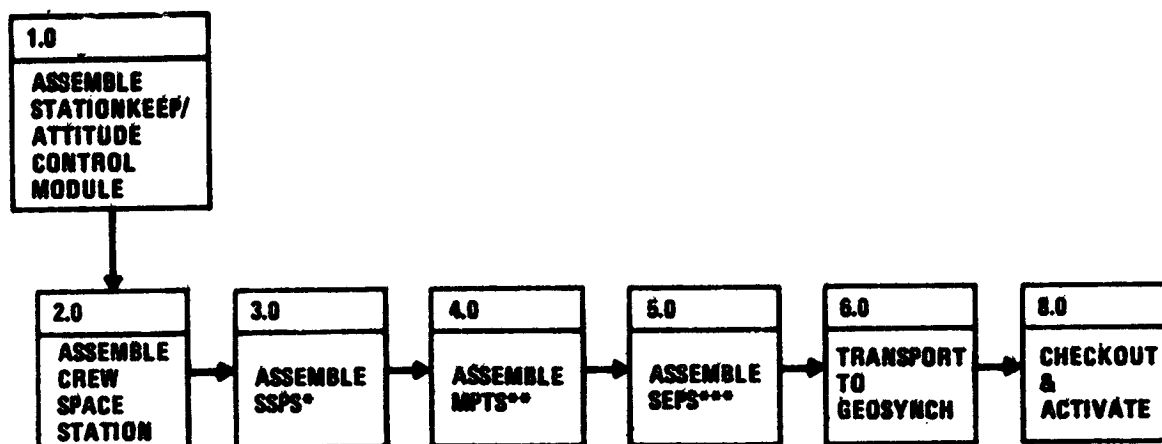
* SSPS: — SATELLITE SOLAR POWER STATION
** MPTS: — MICROWAVE POWER TRANSMISSION SYSTEM
*** SEPS: — SOLAR ELECTRONIC PROPULSION SYSTEM

Fig. 2-8 Level 1 Assembly Functional Flow

	WEIGHT	
	$Kg \times 10^6$	$LB \times 10^6$
SOLAR ARRAY	9.8	21.61
MW ANTENNA	1.66	3.65
CONTROL CONSUMABLES (1 YR)	0.02	0.04
TOTAL	11.48	25.30
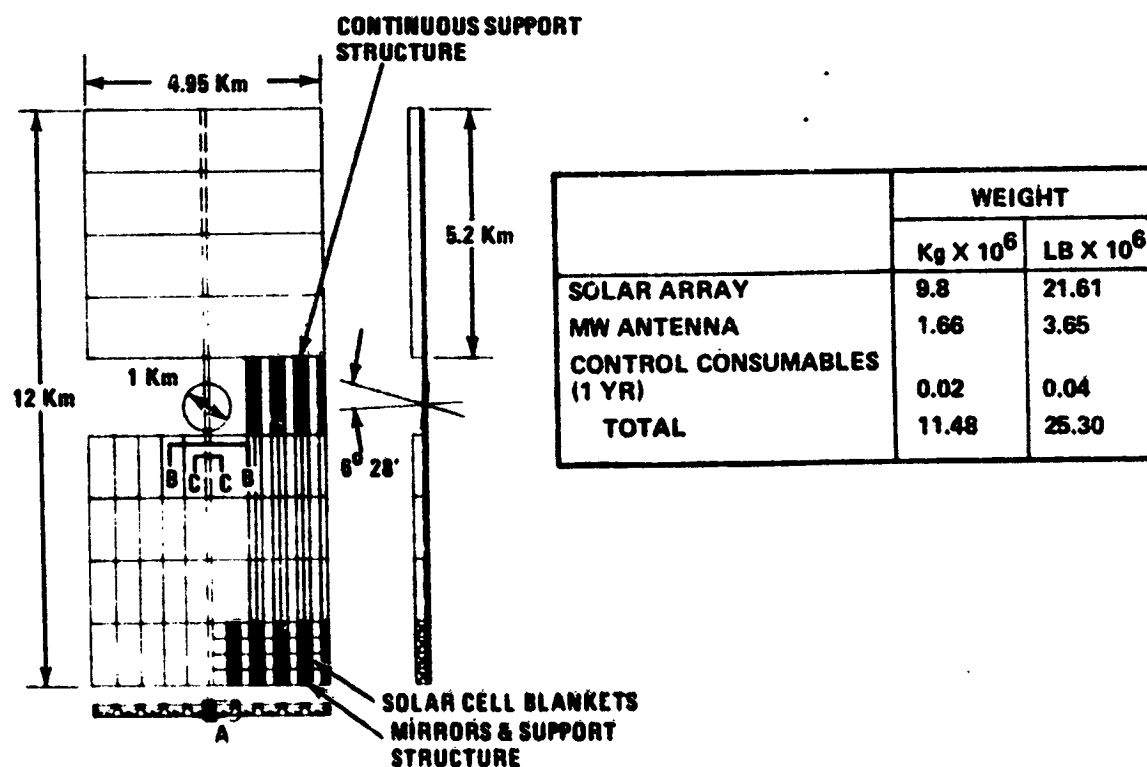
Fig. 2-9 Baseline SSPS

MISSION PLANS

1 — LOW EARTH ORBIT ASSY
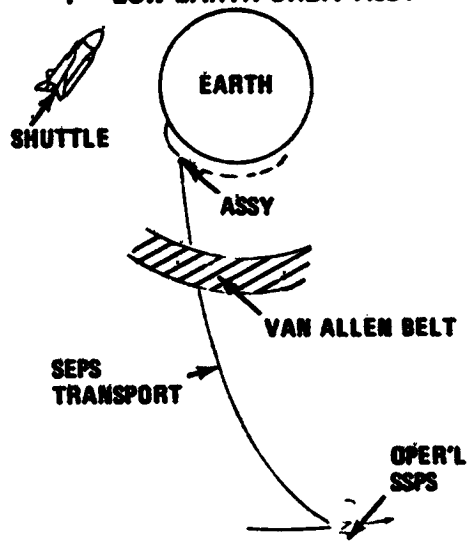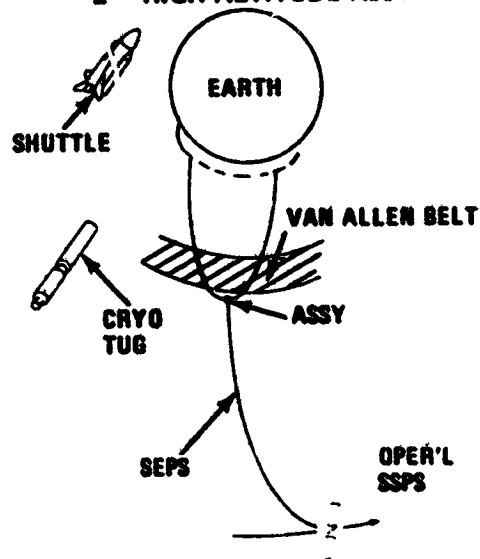
TRANSPORTATION SYSTEM PERFORMANCE

- SHUTTLE

  - MAX PAYLOAD = 65 KLB (29.4 x 10^3 Kg)
  - MAX ALT = 190 N M
  - INCLINATION = 28.5°

- CRYO TUG

  I_{SP} = 456.6 SEC
  λ' = 0.898
  P/L (190 TO 7000 N M) = 36,800 LB (16,670 Kg)

- SEPS

  (190 N M TO GEOSYNCH)

  P/L = 25.3 MLB (11.46 x 10^6 Kg)
  I_{SP} = 8000 SEC
  W_{FULL} = 3.55 MLB (1.61 x 10^6 Kg)
  W_{PROD} = 1.78 MLB (.81 x 10^6 Kg)
  THRUST = 454 LB (2019N)

  (7000 N M TO GEOSYNCH)

  P/L = 25.3 MLB (11.46 x 10^6 Kg)
  I_{SP} = 4625 SEC
  W_{FULL} = 2.63 MLB (1.2 x 10^6 Kg)
  W_{PROP} = 1.57 MLB (.71 x 10^6 Kg)
  THRUST = 400 LB (1779N)

2 — HIGH ALTITUDE ASSY

Fig. 2-10 Mission Options
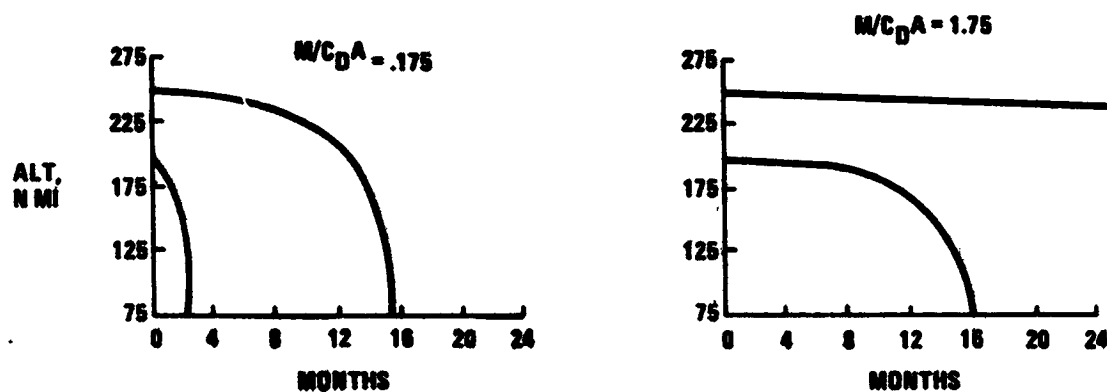
- 16 LB OF CONTINUOUS FORCE NEEDED TO MAINTAIN 190 N MI ORBIT
- 95 PERCENTILE ATMOSPHERE REDUCE ORBIT LIFE BY ~ 1/2
- HEAVIER BOOST CAPABILITY TO 255 N MI DESIRABLE

Fig. 2-11 SSPS Orbital Decay Due to Aerodynamic Drag

SECTION A-A
—SUB ARRAY

	ALUMINUM (2024-t6)		COMPOSITES (POLYIMIDE)	
• TEMP, °K	450		560	
• MODULUS OF ELASTICITY, Psi	9×10^6		6×10^6	
• DENSITY, LB/IN^3	0.101		0.055	
• THICKNESS RANGE, IN.	0.015 TO 040		0.020 TO 0.055	
• WEIGHT	**LB** (10^3)	**KG**	**LB** (10^3)	**KG**
SUBARRAY PRI STRUCT	300	137	207	94
SUBARRAY SEC STRUCT	103	47	66	30
ANT. SUPPORT STRUCT	233	106	157	71
YOKE & MECHANISMS	146	66	122	56
COATINGS	46	21	49	22
AMPLITRON SUPPORT				
CONTOUR CONTROL ACTUATORS	268	122	268	122
AMPLITRON ATTACH STRUCT	51	23	36	16
TOTAL	1147	522	904	411

Fig. 2-12 Antenna Structural Arrangement

and 3 meters deep. The secondary structure is used as support points for the waveguide subarrays and is built up as 18 x 18 x 5 meter bays. The total antenna structure/mechanical system weight is 522 x 10^3 Kg using aluminum and 411 x 103 Kg using graphite/epoxy (or polyimide).

The antenna-to-spacecraft interface uses a 360° rotary joint for antenna motion perpendicular to the orbit plane (azimuth joint) and a limited motion rotary joint, ± 10 deg, for North-South pointing (elevation joint), Fig. 2-13. Two slip ring assemblies (one for plus power and one for power return) are used for power transfer across the azimuth rotary joint and flex cable is used across the elevation joint. Both the azimuth and elevation joint drive assemblies utilize a geared rail about the diameter of the support structure and four DC brushless motor driven roller assemblies.

The structure to waveguide interface uses three gimballed screw jack assemblies (Fig. 2-14) to provide a mechanical tuning system for alignment of the waveguides after construction. Up to 40.5 cm of linear motion can be used to correct thermally induced antenna tip deflections and can also be used to correct a maximum expected 4 arc-min subarray misalignment.

Figure 2-15 is a typical conceptual design of a mechanical locking mechanism for structural joints. The girder interconnect f'tting is similar to a docking drogue which utilizes a spring-loaded ball lock for fastening with the tri-beam end fitting.

2.2.3 Configuration Analysis

2.2.3.1 Thermal Analysis

A refined thermal analysis of the antenna conceptual design concentrated efforts on the following:

- Selection of the tri-beam element longeron cross section to minimize maximum temperature and thermal gradients

- Identifying the limit waste heat at the center of the antenna as a function of structural vertical member material

- Defining range of thermal gradients between primary and secondary structural caps as a function of sun position relative to the antenna.

Figure 2-16 presents the maximum temperatures and thermal gradient across three candidate structural cross sections: tubular, rectangular hat, and triangular hat. The tube is the worst from a thermal standpoint. The use of aluminum tubing near the center

AZIMUTH JOINT

- ANTENNA SPEED = 0.728 X 10^{-4} RAD/SEC
- GEAR REDUCTION = 2.47 X 10^5
- MOTOR SPEED = 18.4 RAD/SEC
- MOTOR TORQUE = 2.8 FT·LB (12.3 N · m)
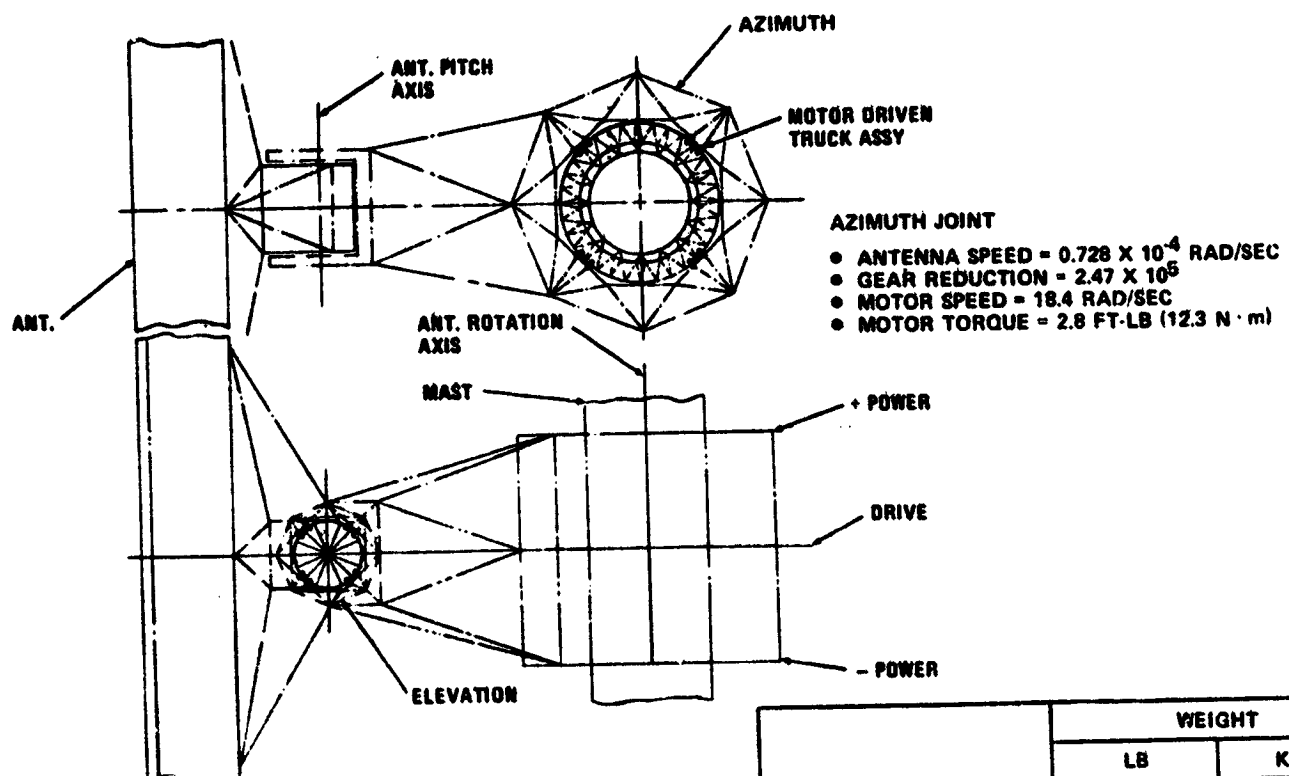
	WEIGHT	
	LB	KG
AZIMUTH		
GEAR BOX & MOTORS	24,065	10,938
DRIVE	2,389	1,086
SLIP RING/BRUSH	1,100	500
SUPPORT	21,196	9,634
TOTAL EACH	48,750	22,158
(TWO REQD)	(97,500)	(44,316)
ELEV TOTAL	24,300	11,045

Fig. 2-13 Rotary Joint

MECHANISM TRAVEL
- EXTENSION   16 IN. (40.5 CM)
- ROTATION   ± 4 ARC MINUTES

WAVEGUIDE ALIGNMENT SCREWJACK
AMPLITRON
WAVEGUIDE PANEL

ANTENNA SECONDARY STRUCTURE
GIMBAL
MOTOR-GEAR-BOX-SCREW JACK ASSY (3)
WAVEGUIDE ASSY
THERMAL ISOLATION FITTING

WAVEGUIDE/STRUCTURE INTERFACE
3 POINT SUPPORT

	WT / MECHANISM	
	LB	KG
SHAFT	20	9.1
WORM	3.8	1.7
MOTOR	5.0	2.3
THERMAL INSULATION	1.6	0.7
GEAR BOX & GIMBAL	6.6	3.0
	44	20

Fig. 2-14 Structure/Waveguide Interface

GIRDER INTERCONNECT FITTING

"TRIBEAM" GIRDER ASSEMBLY

GIRDER INTERCONNECT FITTING – DROGUE

GIRDER INTERCONNECT – BALL DETENTE

BALL LOCK

GIRDER END FITTING – PROBE

Fig. 2-15 Structural Joints
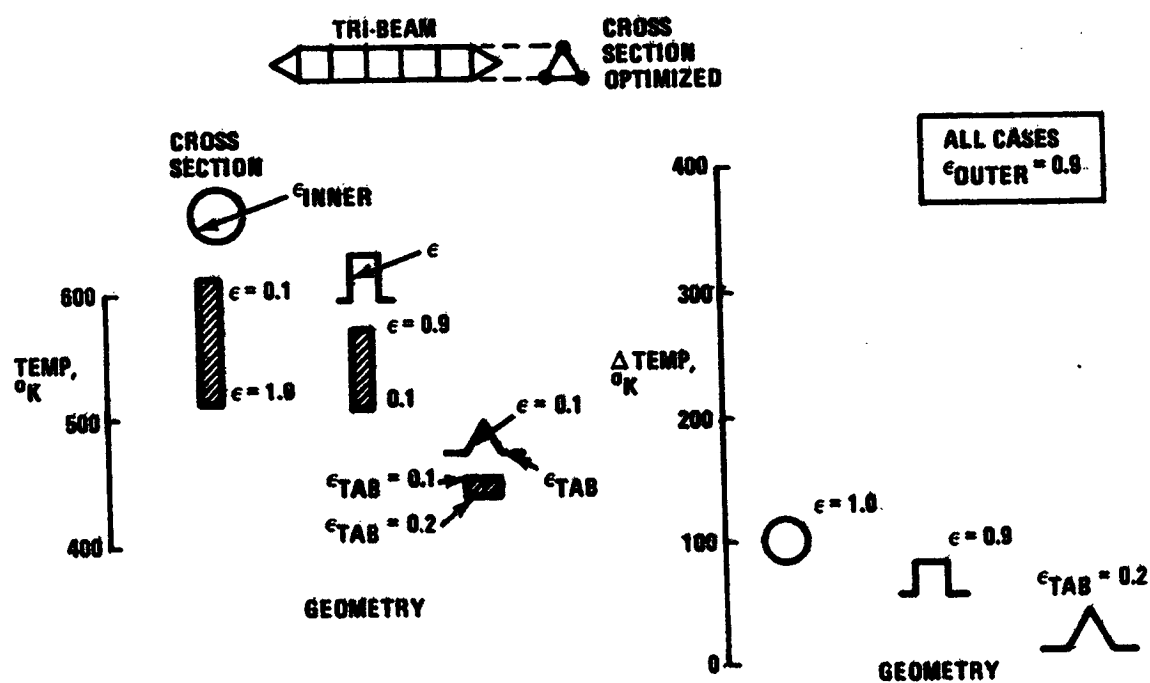
Fig. 2-16 Comparison of Maximum Temperature and Thermal Gradients

of the antenna will not be possible with this geometry. The rectangular high hat design is not an attractive structural geometry but does offer an improved temperature picture. The triangular hat design has the lowest maximum temperature level and minimum gradient of the concepts considered. Aluminum construction of the tri-beam horizontal members can be considered with this cross section.

The temperature profiles along the horizontal structural tri-beam caps were evaluated for various orbital positions during the equinoxes and solstices. Figure 2-17 presents the expected variation in thermal gradients between primary and secondary structural caps. The average primary structure thermal gradient is approximately 5°K at the center of the antenna. The expected variation in this gradient is $\pm 1°K$. The thermal gradients between secondary structural caps are small, $1/2° \pm 1/4°K$, and do not present a significant thermally induced deflection environment.

The vertical columns of the structure have the same view of the antenna surface and space, and consequently cannot be readily configured with coatings, insulation or geometry selection to minimize peak temperatures of the material. Figure 2-18 presents the maximum waste heat flux that will be experienced by the vertical columns for microwave converter efficiency of 85% and 70%. Eighty-seven percent of the waste heat generated by the converters is assumed radiated toward the structure. The parameter p is a scaling factor for the shape of the Gaussian distribution of microwave converters on the antenna surface. Limitations as to the taper of this distribution must be imposed depending upon the structural material selected. A near uniform distribution (1.5 to 1) must be used if the structure is aluminum or graphite/epoxy (70% converter efficiency). Selection of graphite/polyimide would be compatible with a desirable 10:1 taper for the converter Gaussian distribution.

2.2.3.2 Structural Analysis

The Task 2 structural analysis objective was to refine the design of the structural members and to perform a detailed assessment of thermally induced deflections. The following summarizes these assessments:

* The principal applied load for structure design is that induced by inertial response of the control system during breakaway from the 1.0×10^6 N·m slip-ring torque. This torque equates to a 100 lb (440N) end load on the upper and lower members.

- MICROWAVE CONVERTER EFFICIENCY = 75%
- SCALE FACTOR ρ = 488 METERS
- POWER RATIO = 10:1

RADIAL DISTANCE FROM CENTER OF ANTENNA, METERS

Δ TEMP, °K

PRIMARY STRUCTURE

SECONDARY STRUCTURE

$(T_{6 \text{ METER}} - T_{1 \text{ METER}})$

ORBITAL VARIATION (ANY SEASON)

TEMP OF MEMBER LOCATED 41 METERS ABOVE ANT. MINUS TEMP OF MEMBER AT 1 METER $(T_{41} - T_1)$
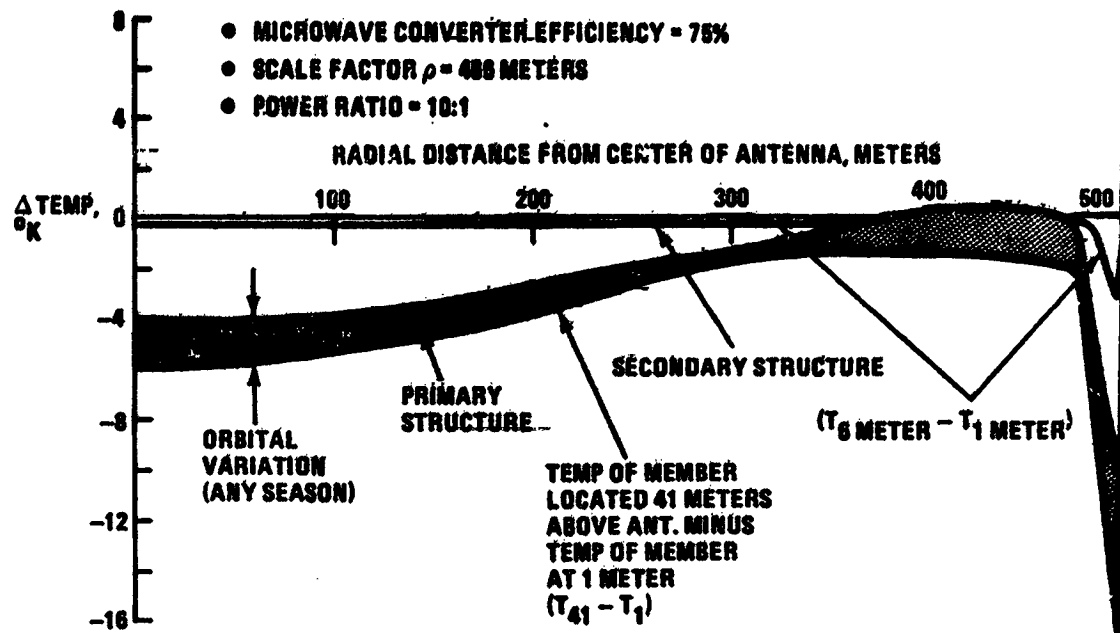
Fig. 2-17 Temperature Difference Between Beam Cap Members Located Different Distances Above Antenna Surface

- MICROWAVE CONVERTER SPACING = L_{MIN} *EXP$((R/\rho)^2)$
- ANTENNA DIAMETER = 1 Km
- WASTE HEAT TOWARD STRUCTURE = 87.5%

WASTE HEAT FLUX, KW/M²

MAX FOR POLYIMIDE

MAX FOR ALUMINUM GR/EP

MICROWAVE CONVERTER EFFICIENCY

70%

85%

SCALE FACTOR ρ, METERS
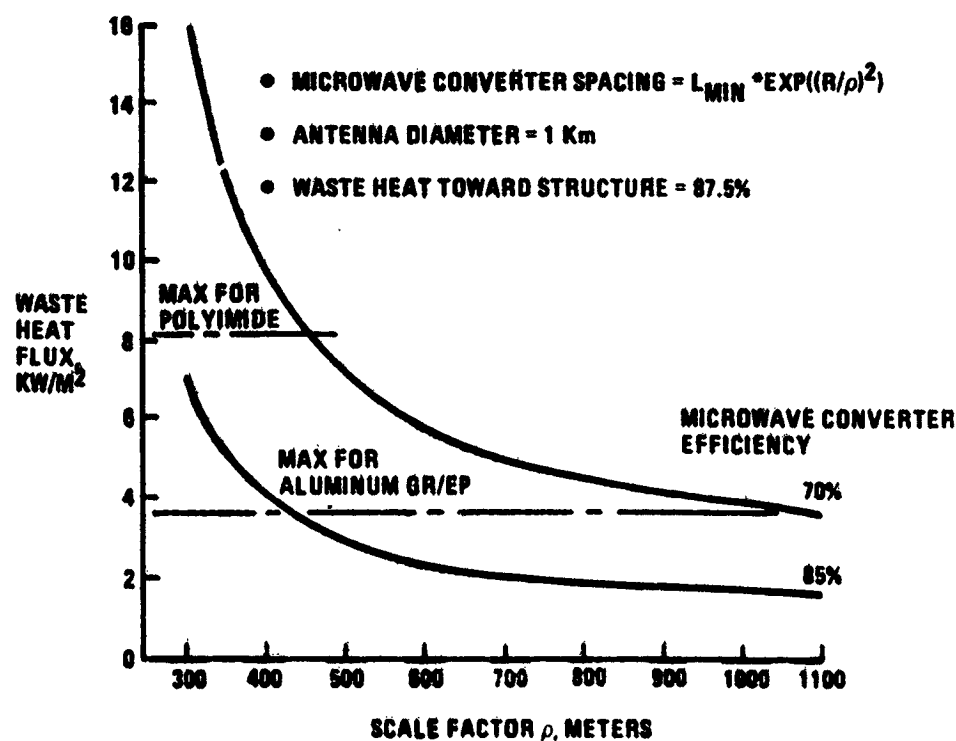
Fig. 2-18 Waste Heat Flux at Center of Antenna as Function of Scale Factor

2-20

- The optimized graphite/epoxy triangular hat longeron design is shown in Fig. 2-19 for a 450°K environment. The 20 mil thick material is composed of ten layers of 2-mil graphite fibers.

- The range of thermally induced deflections and local slope are presented in Fig. 2-20. Variations in slope with variations in orbital position exceeds 1 arc-min for an aluminum structure. The slope variations from a mean or average deformity is well within limits for graphite/epoxy. Assessment of secondary structure deformation shows that the worst deflections occur at the tips of the antenna, with maximum deflections not to exceed 10.5 mm over any one 18 x 18m subarray.

2.2.4 Assembly

2.2.4.1 Detail Parts Assembly

Sensitivity analysis of various levels of ground prefabrication compared to corresponding levels of orbital assembly was performed to determine the most cost effective approach to antenna structural assembly. Figure 2-21 outlines the three approaches which span the possible options for detail part fabrication. Case I assumes manufacture of articulated lattice tri-beams on the ground. These designs can be compressed to 1/30 of its deployed length for convenient packaging in the Orbiter. Case II assumes that the ground fabricates the longerons and intercostal elements of the tri-beam and that assembly of the beam is performed in a space station. Case III assumes ground personnel prepares flat stock with appropriate coatings for installation into an automatic manufacturing module in space.

Figure 2-22 summarizes the pertinent characteristics of these approaches. Although the articulated lattice beam is an efficient packaging arrangement, the packaging density in the Orbiter is extremely poor. As much as 440 Shuttle flights would be required for delivery of the 470 Klb (213 x 10^3 Kg) antenna structure. Transport of beam elements provides an improved packaging density, depending upon the cross-section selected. The number of crew members, however, required to fabricate the finished beam in space in a reasonable time would require deployment of as many as 24 12-man space stations. In-orbit automatic manufacture of the structural members appear to provide the clearest road to a low cost detail parts assembly method.

DESIGN CONDITIONS

- T = 450°K
- END LOAD = 440 NEWTON
- SUPPORT EVERY 3M
- MINIMUM 5 PLY
  COMPOSITE

3/16 R

.02

60°

1/8 R

1.75 IN.

.438
TYP.

3M (118")
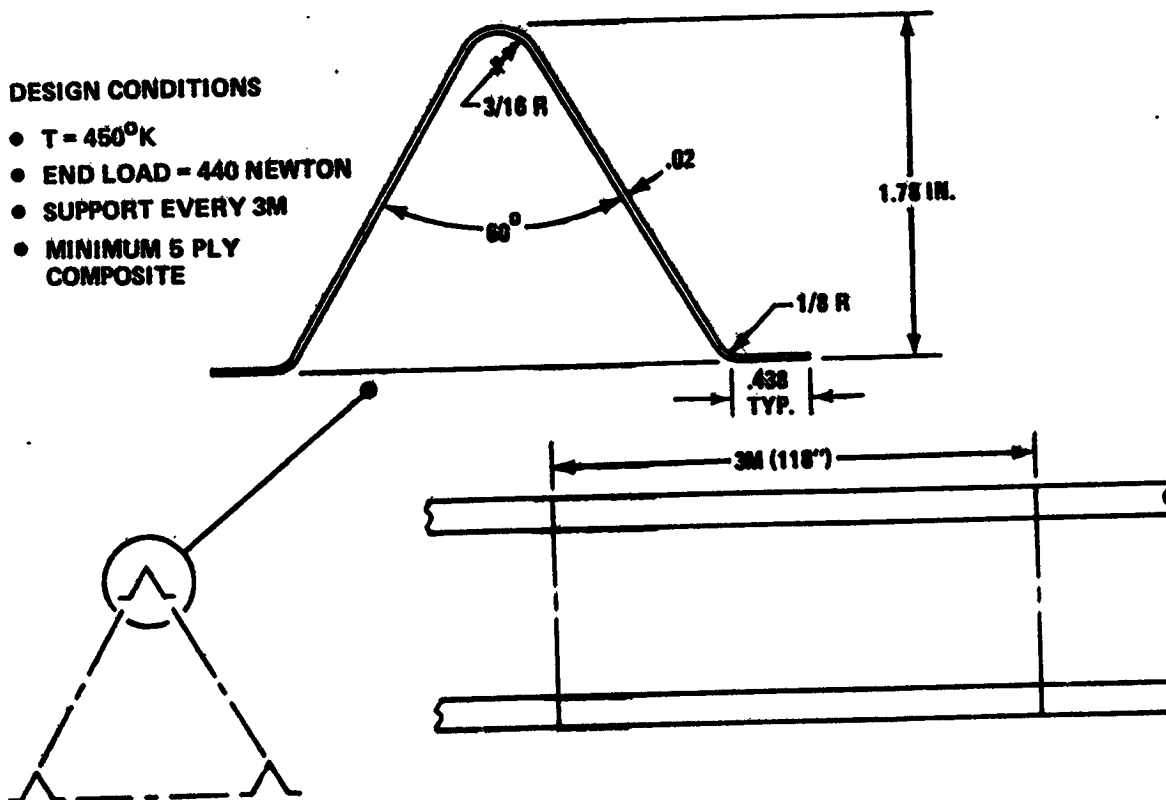
Fig. 2-19 Cross-Section Design
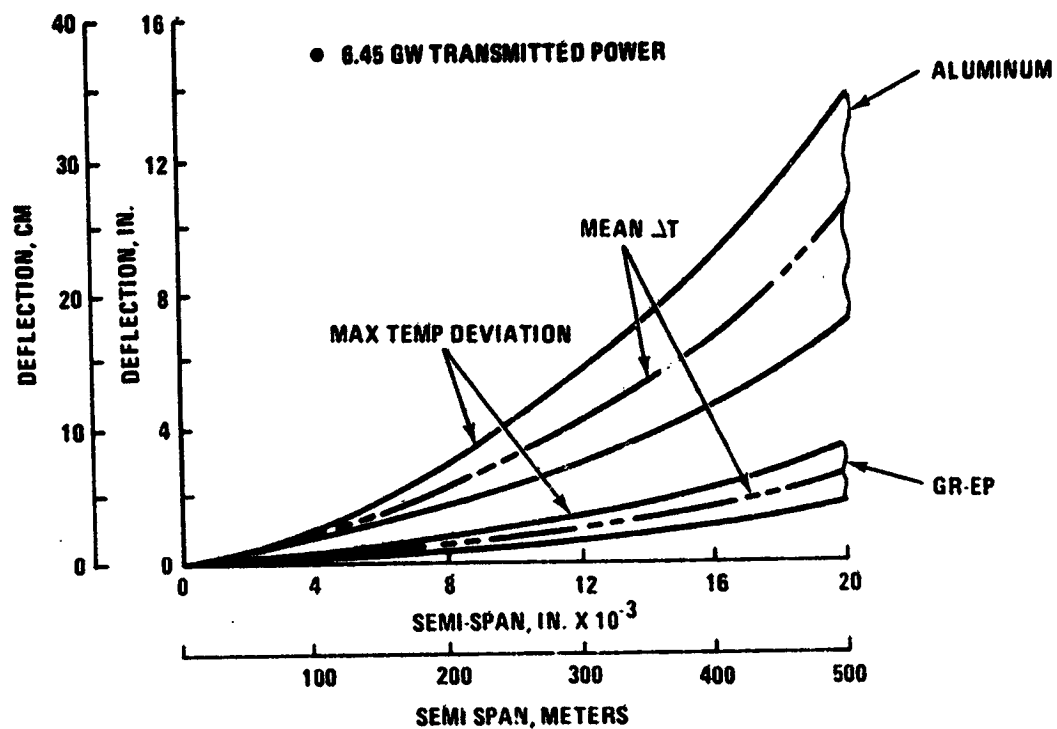
(a) Typical Antenna Deflection Due to Thermal Gradients (40 Meter Beam Depth)
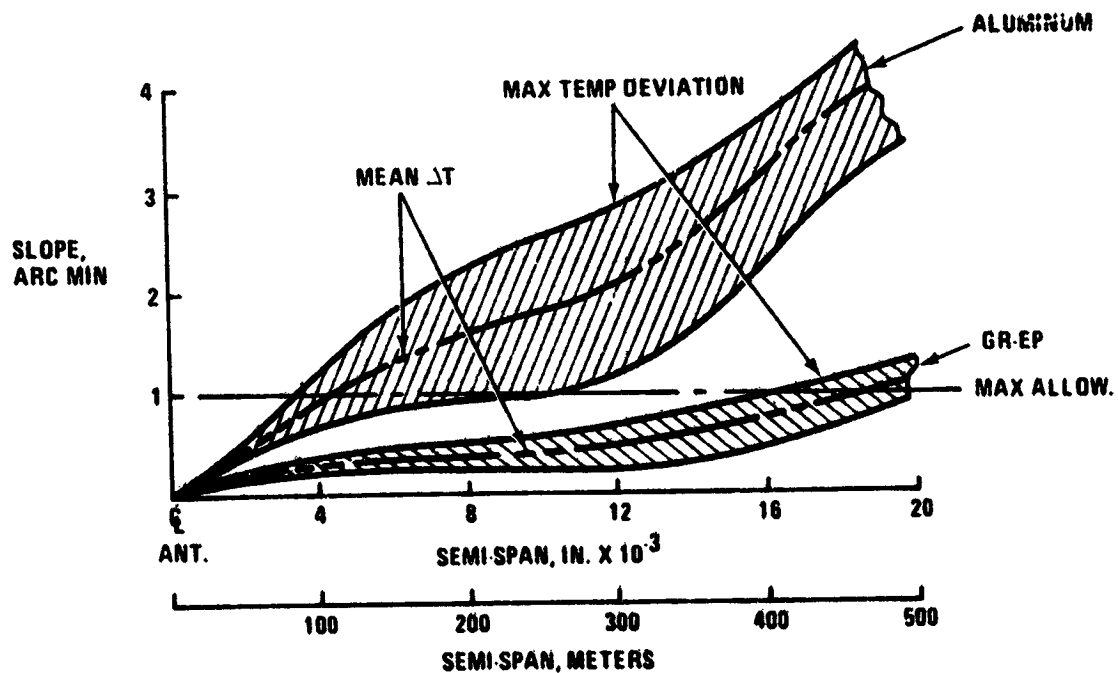
(b) Typical Slopes of Structure Due to Thermal Gradients

Fig. 2-20 Range of Thermally Induced Deflections and Local Slope

TRANSPORT

| | EARTH | | ON ORBIT |

CASE I — ASSEMBLE ARTICULATED LATTICE BEAMS ON GROUND → PACKAGE IN ORBITER → DEPLOY BEAMS IN ORBIT

CASE II — FABRICATE BEAM ELEMENTS ON GROUND → PACKAGE IN ORBITER → ASSEMBLE INTO TRI BEAMS AT SPACE STATION

CASE III — PRE FAB FLAT STOCK ON GROUND → PACKAGE IN ORBITER → AUTO MANUFACTURE ON ORBIT
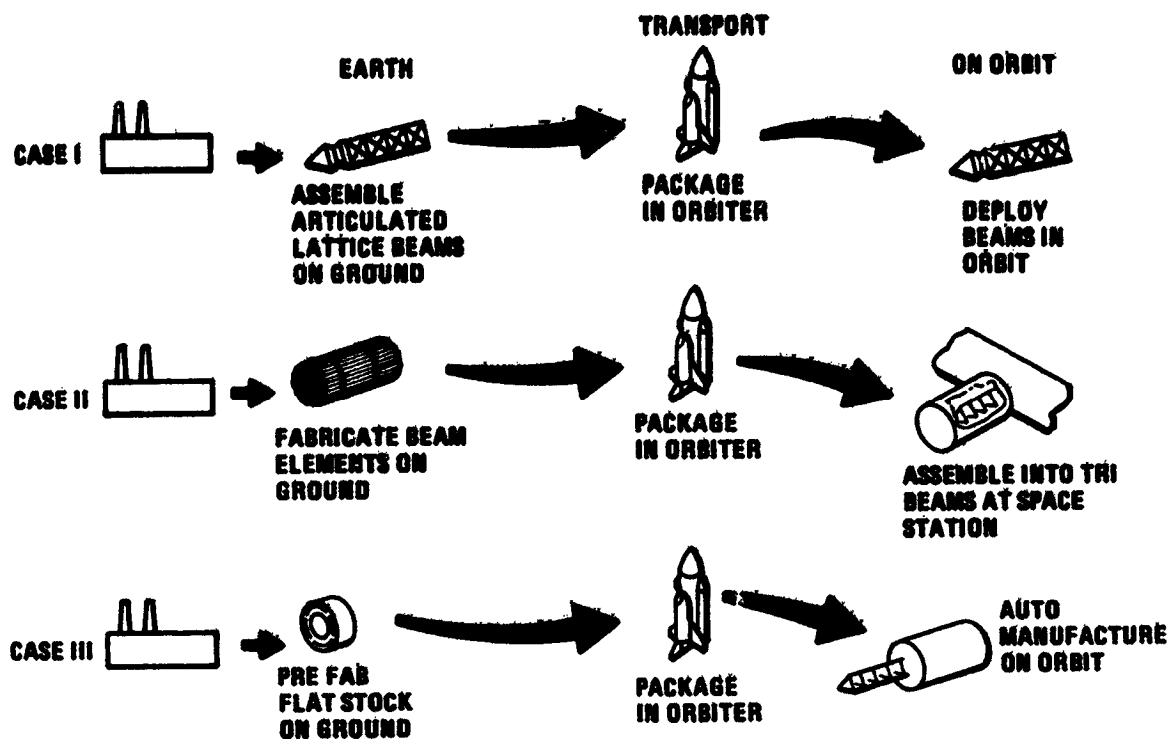
Fig. 2-21 Structural Detail Parts Assembly Options

CONDITION	CASE 1	CASE 2	CASE 3
– GROUND	ASSEMBLE ARTICULATED BEAMS	FORM LONGERONS & CROSS MEMBERS	PRE-PROCESS FLAT STOCK
– IN-ORBIT	DEPLOY	ASSEMBLE	MANUFACTURE
PACKAGING DENSITY (–SHUTTLE CAPACITY)	0.1 LB/FT^3 (6.1 LB/FT^3)	0.9 TO 75 LB/FT^3 (6.1 LB/FT^3)	100 LB/FT^3 (6.1 LB/FT^3)
NUMBER SHUTTLE FLTS TO DELIVER ANTENNA STRUCTURE	440	8 TO 49	8
SUPPORT EQUIPMENT	DEPLOYMENT CANNISTER	24 SPACE STATIONS	8 MFG MODULES
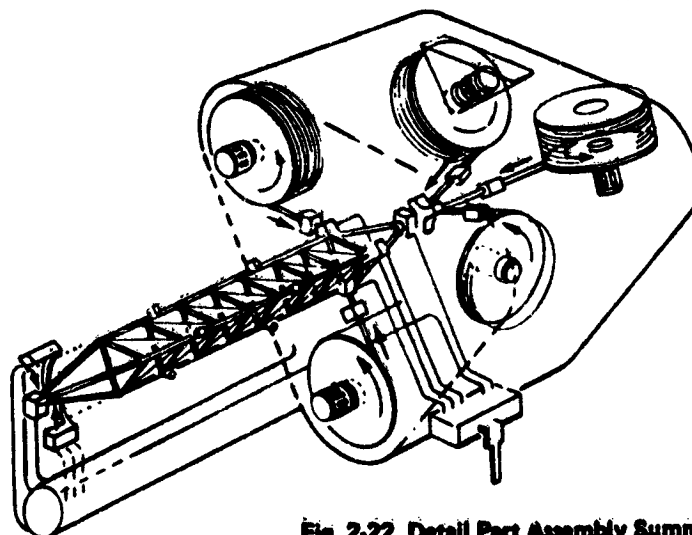
RECOMMENDED FOR STRUCTURE

Fig. 2-22 Detail Part Assembly Summary

2.2.4.2 Structural Assembly

Analysis concentrated on the most frequently used operation in the antenna structure assembly, namely, the time and motion assessment of joining beams. Assembly costs are generally a strong function of the quantity and complexity of the assembly operation. In the estimate, for example, of aircraft structural assembly, the major cost driver is the number of parts and the type fastener used. In the antenna structure and waveguide interface design, simple mechanical locking mechanisms similar in concept to a docking probe/ drogue was utilized when possible. Since most of the assembly will involve this type of operation, detail evaluations were performed on this beam assembly procedure.

Figure 2-23 outlines the antenna structure assembly flow. Assembly starts with installation of the rotary joint using the solar array central mast as the point of departure. The rotary joint to antenna interface follows, using the elevation rotary joint structure as an assembly base. Assembly of the primary and secondary structure is performed working radially from the center of the antenna. Installation of waveguides and electronics follow.

The alternate approaches evaluated include use of:

- Manned manipulator modules
- Remote controlled manipulator modules
- EVA with assist from remote controlled logistics modules.

The operations analysis approach is summarized in Fig. 2-24. The functional steps in the operation for the three options were identified and a time line analysis performed to determine the range of potential assembly rates. Estimates of consumables consumption of the free-flying modules were also made. Past Grumman simulation data, which relates complexity of manipulator operations in a static environment to operations in a dynamic environment, was used in estimating both manned and remote controlled manipulator performance. Skylab 3 data on the human performance in assembling the twin pole sunshade was used to estimate EVA assembly rates.

Figure 2-25 summarizes results of the operations studies. The following conclusions were drawn from this data:

- Remote controlled manipulator assembly offers the most cost effective approach
- EVA assembly with remote controlled logistics vehicles could be cost competitive if assembly times in excess of two years is acceptable and Space Station costs for a 50-man crew can be shown to be reasonable
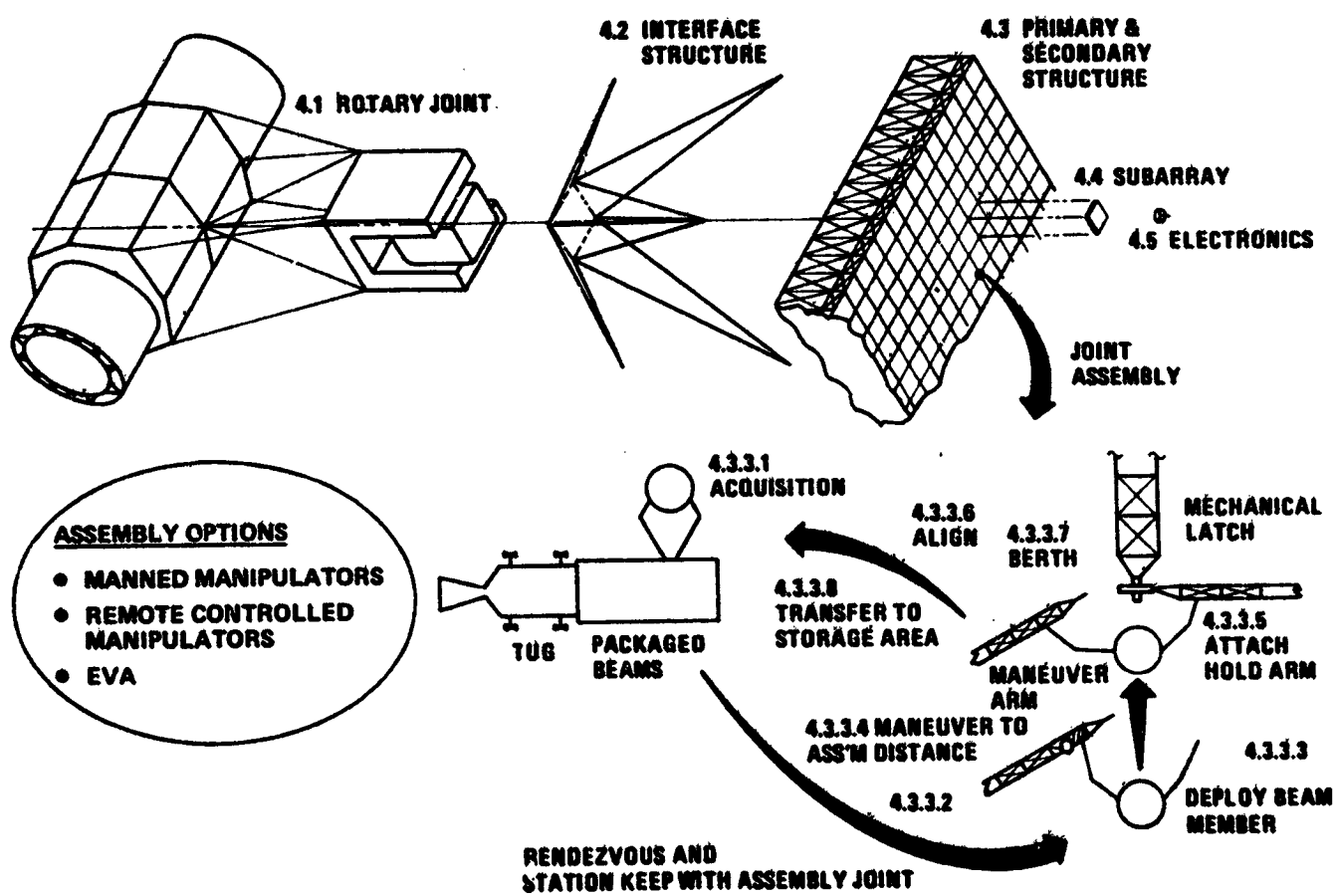
Fig. 2-23 MPTS Antenna Structural Assembly

EVENT	TIME, MINUTES				CONSUMABLES, LB			
	MINIMUM		MAXIMUM		PROPELLANT		ECS	
	ΔT	T	ΔT	T	MIN	MAX	MIN	MAX
4.3.3.1 ACQUIRE LOWER CAP FROM STORAGE	3.0	3.0	10.5	10.5	0.36	1.20		
4.3.3.2 TRANSPORT TO ASSY JOINT	6.0	9.0	6.0	16.5	4.72	4.72		
4.3.3.3 DEPLOY ASTROMAST	2.0	11.0	2.0	18.5	0.24	0.24	1.17	2.3
4.3.3.4 MANEUVER TO ASSY DISTANCE	0.5	11.5	0.5	19.0	3.0	3.0		
4.3.3.5 ATTACH HOLD ARM	3.0	14.5	10.5	29.5	0.36	1.20		
4.3.3.6 ALIGN MEMBER WITH ATTACH JOINT	3.0	17.5	10.5	40.0				
4.3.3.7 BERTH BEAM MEMBER WITH JOINT	1.0	18.5						
4.3.3.8 TRANSFER TO STORAGE AREA								

- EVALUATE STRUCTURAL ASSY OF JOINTS AS MOST FREQUENT OPERATION
- IDENTIFY FUNCTIONAL STEPS
- PERFORM TIME LINE ANALYSIS USING
  - PAST GRUMMAN MANIPULATOR SIM DATA
  - SKYLAB 3 TWIN POLE ASSY PERFORMANCE

Fig. 2-24 Assembly Operations Analysis Approach

	STRUCTURAL ASSEMBLY METHOD		
	MANNED MANIPU-LATOR MODULE	REMOTE MANIPU-LATOR MODULE	EVA WITH RE-MOTE CON-TROLLED LOGISTICS VEHICLE
● FREE FLYER CHARACTERISTICS			
– WGT	1360 Kg	136 Kg	136 Kg
– I_{SP}, SEC	300	300	300
– CONSUMABLES RATE (Kg/Kg STRUCTURES)	1.7	0.15	0.03
– # OF SHUTTLE RESUPPLY FLTS FOR ANTENNA STRUCT.	12	1	1
● ASSY RATE			
– MAX (Kg-STRUCT/HR)	13	13	25
– MIN (Kg-STRUCT/HR)	7	7	18
● NO. IN-ORBIT PERSONNEL AT MAX RATE			
– 1 YR ASSY	182	6	95
– 2 YR ASSY	91	6	48
● KEY ISSUE	SAFETY	TV COMMUNI-CATIONS	SAFETY

Fig. 2-25 Summary of Assembly Options

- Manned manipulator modules are not cost effective because of the high propellant consumption.

2.2.4.3 Support Equipment Requirements

Preliminary definition of support system requirements have been established for the low altitude and high altitude assembly sites using data generated during NASA studies of space stations, research applications modules and remote teleoperator vehicles. Figure 2-26 summarizes the transportation and assembly approach used as a strawman in establishing support equipment requirements. The following lists the major equipments over and above the basic transportation systems required in support of assembly at the two candidate assembly sites:

Low Altitude (190 N Mi)

- Remote controlled manipulators
- Shuttle crew accommodations
    - Crew support module
    - Communications module
- Manufacturing modules
- TDRS

High Altitude (7000 N Mi)

- Remote controlled manipulators
- Manufacturing modules
- Space station
- Crew transport module
- TDRS.

ASSY ORBIT	TRANSPORT SYSTEM (MATERIALS)	TRANSPORT CREW	DETAILED PARTS	ASSY METHOD	CREW ACCOM	TRANSPORT TO GEOSYNCH	COMM
LOW ORBIT – 190 N M – 28.5°	• SHUTTLE	• SHUTTLE	• AUTOMATIC IN-ORBIT (MFR MODULE)	• REMOTE MANIPU- LATOR	• SHUTTLE – 6 MEN – 30 DAYS	• SEPS	• TDRS
HIGH ORBIT – 7000 N M – 28.5°	• SHUTTLE • FULL CAP. TUG	• SHUTTLE • FULL CAP. TUG • CREW TRANSPORT MODULE	• AUTOMATIC IN-ORBIT (MFR. MODULE)	• REMOTE MANIPU- LATOR)	• SPACE STATION – 6 MEN – 180 DAYS	• SEPS	• TDRS

Fig. 2-26 Transportation and Assembly Elements

Figure 2-27 summarizes the weight and cost factors assumed in the overall cost assessment of the SSPS assembly operation. To achieve consistency of data, the $/Kg non-recurring and recurring cost estimate for the Space Station has been applied to the cost of all support equipment.

ELEMENT	PERFORMANCE	WEIGHT	COST/FLT	NON-RECURRING	RECURRING UNIT	SOURCE
SHUTTLE	65K TO 190 N M 100 FLT LIFE	N/A	$10.5M	N/A	$180M	GAC SHUTTLE STUDY
CRYO TUG	36.8 K LB TO 7000 N M 100 FLT LIFE	BURN OUT- 2680 Kg FULL - 24,900 Kg	$ 1.0M	N/A	$12M	MDAC TUG STUDY
FREE-FLYING TELE OPERATOR	5 YR LIFE	183 Kg	TBD	$5.95M	$1.24M	MSFC-PAYLOAD DESCRIPTION VOL II
RAM SUPPORT MODULE	30 DAY MISSION 5 YR LIFE	5000 Kg	$ 1.0M	$218M	$40M	WT DATA — NAS 8-27539 COST DATA — NAS 9-9953
RAM-COM MODULE	30 DAY MISSION 5 YR LIFE	8760 Kg	$ 1.0M	$283M	$59M	WT DATA — NAS 8-27539 COST DATA — NAS 9-9953
MANUFACTURE MODULE	5 YR LIFE	9100 Kg	TBD	$288M	$62.5M	SWAG
SEPS	1 YR TRIP TIME	FROM 190 N M = 1.18×10^6 Kg FROM 700 N M = $.556 \times 10^6$ Kg	$15.7M $ 9.0M	TBD TBD	$400M $400M	GAC RPT NO. ASP 583-R-8
SPACE STATION 6 MAN	5 YR LIFE	76,700 Kg	TBD	$2097.6M	$487.8M	NAS 9-9953
12 MAN	5 YR LIFE	102,000 Kg	TBD	$2309.9M	$759.1M	NAS 9-25051
CREW TRANSFER MODULE (4)	100 FLT LIFE	10,300 Kg	TBD	$326M	$71.2M	
TDRS	N/A	2038 Kg	N/A	$210M	$30-50M	HUGHS REPORT 30096-3514

Fig. 2-27 Transportation and Assembly System Fleet and Support Equipment Characteristics and Cost Summary (1974 $'s)

2.2.5 Cost

The Task 2 Conceptual Design objective was to refine the cost estimates established during preliminary design. Cost estimates of transportation and assembly were increased in scope to include the entire SSPS and associated support equipments. A more refined assessment of the antenna structural cost was performed on the rectangular grid 1 km structural arrangement using aluminum, graphite/epoxy and graphite/polyimide.

The following summarize the findings of these assessments:

- Low altitude assembly is significantly lower in cost than assembly above the Van Allen belts (575 $/Kg vs 1550 $/Kg)

- The major cost driver is Shuttle per flight costs

- Recurring unit costs for Shuttles, Tugs, Space Stations, and other support equipments represents 1/6th of the total assembly costs

- Aluminum is 4 to 5% lower in cost than composites.

Figure 2-28 summarizes the traffic and fleet size requirements for three flight plans. The total numbers of Shuttle flights required to assemble the entire SSPS includes flights for deployment of support equipments, transportation of personnel for monitoring the assembly operation and delivery of the consumables for the remote controlled manipulator modules. Flight Plan 1 and 3 assume one and two year assembly periods at the low altitude site, while Flight Plan 2 assumes a one year assembly time at the high altitude site. A significant difference exists in terms of total Shuttle flights needed for assembly at the high altitude site, primarily due to the added requirement to transport Tugs to and from orbit. The difference in total Shuttle flights required by Flight Plan 3 is not significantly different from Plan 1, but the average number of flights per day is within reason (1.37 vs 0.7 per day) particularly when considering the non-optimum launch opportunities available with a 190 n mi assembly altitude. Because of the orbital geometries, launches of as much as two to four Shuttles in one 15 minute launch window may be required with Flight Plan 1. The two year low altitude assembly plan is recommended based on the low number of Shuttle flights and reasonable launch rate.

Figure 2-29 presents a cost comparison of the three flight plans. The low altitude, two year assembly period is the lowest cost option (1301 $/kw). This cost could be reduced with increase in STS performance by a factor of two if a heavy lift, deploy only launcher with a payload capability of 120,000 lb (54,400 Kg) were developed from existing Shuttle

CONDITION	FLT PLAN 1	FLT PLAN 2	FLT PLAN 3
— ASSEMBLY ALT	190 N.M.	7000 N.M.	190 N.M.
— ASSEMBLY TIME	1 YR	1 YR	2 YR
— DETAIL PARTS	AUTO IN-ORBIT	AUTO IN-ORBIT	AUTO IN-ORBIT
— ASSEMBLY	REMOTE	REMOTE	REMOTE
● FLTS			
— SHUTTLE	491	1348	501
— TUG	—	855	—
— AVG SHUTTLE FLTS/DAY	1.37	3.68	0.7
— AVG TUG FLTS/DAY	—	2.34	—
● FLEET SIZE			
— SHUTTLE	24	59	16
— MANUFACTURE MODULES	8	8	4
— MANIPULATOR MODULES	182	176	91
— CREW SUPPORT MODULES	2	—	2
— TUGS	—	37	—
— SPACE STATION	—	1	—
— CREW TRANSPORT MODULE	—	2	—

RECOMMENDED

Fig. 2-28 Traffic and Fleet Size Summary

RECURRING
OPS
TOTAL

FLT PLAN 2
(1554 $/Kg)
(3537 $/KW)

FLT PLAN 1
(554 $/Kg)
(1352 $/KW)

FLT PLAN 3
(571 $/Kg)
(1301 $/KW)

FLT PLAN

1 – LOW ALT, 1 YR ASSY
2 – HIGH ALT, 1 YR ASSY
3 – LOW ALT, 2 YR ASSY

FLIGHT PLAN
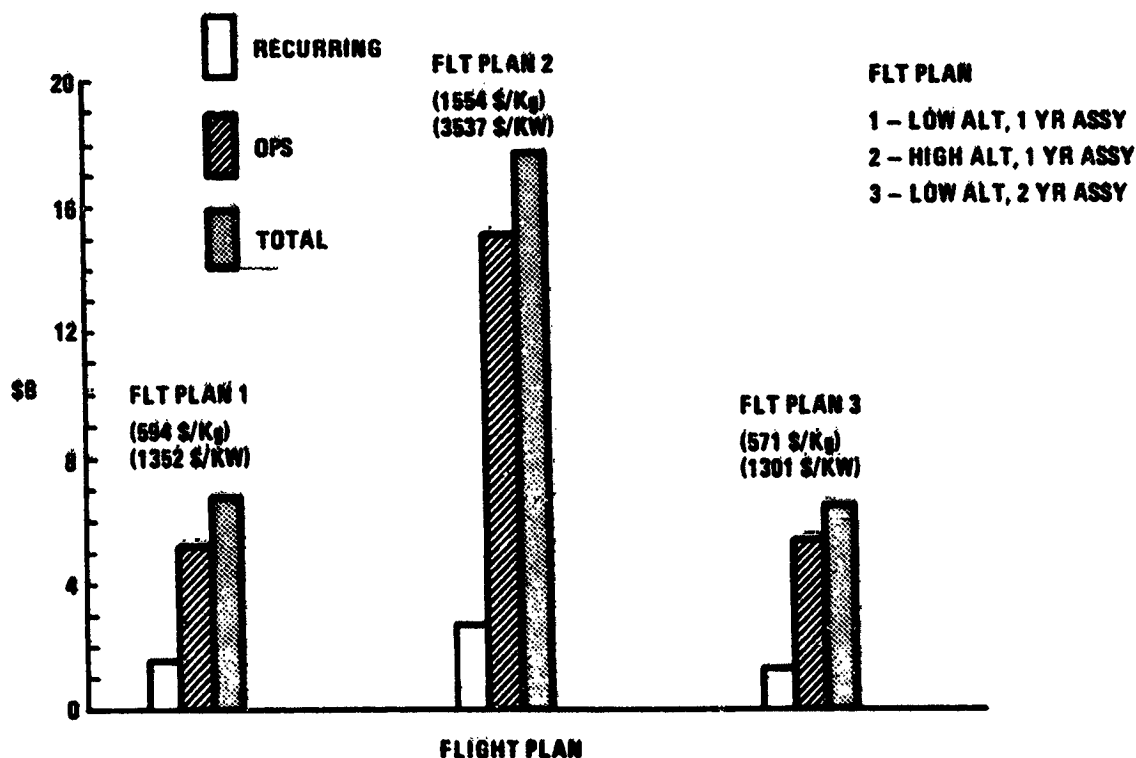
Fig. 2-29 Assembly Cost Comparison

components. An additional reduction could be achieved with development of the Fly-Back Booster. It is conceivable that a cost as low as 300 $/kw could be achieved.

An aluminum antenna structure is 4 to 5% lower in cost than a graphite/epoxy or graphite/polyimide structure (Fig. 2-30). This assumes that the basic structural elements can be made of the standard 5 mil fibers. Although the cost of composites are slightly higher than aluminum, technical factors such as thermal properties, could be the influencing factors in final selection.

2..3 RECOMMENDATIONS

The concepts and design options recommended for Task 3 study are listed in Fig. 2-31. Also included are concepts that show sufficient promise for further technology study.

Because of the greater cost associated with high altitude assembly, the transportation mode selection can be narrowed down to use of the Shuttle at a low altitude assembly site. Advanced transportation system with increased payload (heavy lift vehicle) and development of the Fly-Back Booster could further reduce transportation and assembly costs, and should be given greater study emphasis.

The rectangular grid structural arrangement should be retained. No technology issues arose during Concept Definition that would suggest a different approach. The light weight and standardized construction of the rectangular grid structure makes this approach the best of the options studied.

Materials selection cannot be clearly made at this time. Aluminum offers the lowest cost option with the least technology risk. The graphite composites are attractive in terms of thermal expansion properties and the potential to retain stiffness characteristics at high temperature (polyimides). Basic materials technology testing of composites is recommended to determine the outgassing and ultraviolet tolerance of these materials at the expected system operating temperatures.

The assembly of structure using remote controlled manipulators was found to be potentially the lowest cost approach. This assembly technique would minimize the man-in-space role and would therefore minimize the need for expensive life support equipments. The use of EVA in the assembly function showed the potential for increased production rates relative to remote controlled assembly. However, the cost of large support Space Stations may preclude selection of this approach. Study of man's role in assembly of large structure is recommended for investigation outside of the MPTS study.
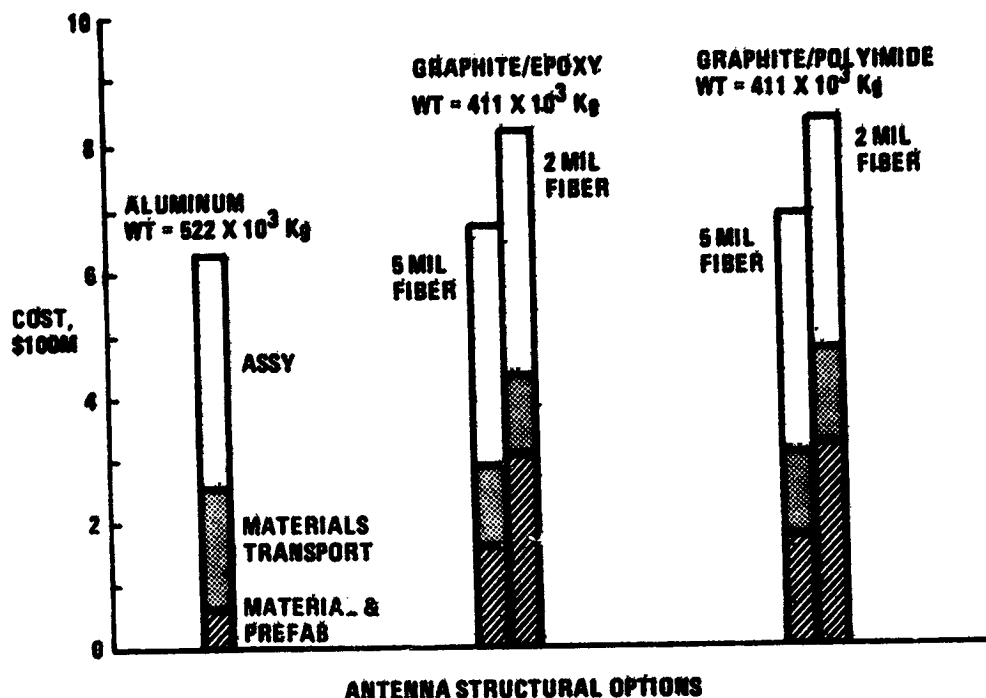
Fig. 2-30 Antenna Structural Cost Comparison

	TASK 3 STUDY	TECHNOLOGY STUDY
TRANSPORTATION MODE		
• SHUTTLE/EXPENDABLE TRANSTAGE		
• SHUTTLE/REUSABLE TRANSTAGE		
• SHUTTLE/CRYO TUG		
• SHUTTLE/LOW ORBIT ASSY	√	√
• ADVANCED TRANSPORT SYSTEMS		√
STRUCTURAL ARRANGEMENT		
• RECTANGULAR GRID	√	
• RADIAL SPOKE		
MATERIAL		
• ALUMINUM	√	
• GRAPHITE/EPOXY	√	√
• GRAPHITE/POLYIMIDE	√	√
• KEVLAR/POLYIMIDE		√
ASSEMBLY		
• MANNED MANIPULATOR		
• REMOTE CONTROLLED MANIPULATOR	√	√
• EVA		
DETAILED PARTS ASSEMBLY		
• GRD FAB OF DEPLOYABLE STRUCTURE		√
• MANNED IN-ORBIT FAB		
• AUTO SPACE FABRICATION	√	

Fig. 2-31 Recommendations for Task 3 Study

2-34

The method of fabricating detail parts of the assembly is strongly driven by the volume limitations of the transportation system. With the Shuttle volume characteristics, space fabrication of the low density components, such as structure, is recommended. If volume capabilities of the launch system were increased, ground prefabrication of deployable elements may become a more attractive option.

Section 3

TECHNICAL DISCUSSION

3.1 MISSION ANALYSIS

3.1.1 SSPS Configuration and Flight Mode Descriptions

The Satellite Solar Power Station (SSPS), as presently conceived, is a geosynchronous equatorial placed satellite whose function it is to collect solar energy and radiate it to the earth (see Fig. 3.1-1 and 3.1-2). Energy radiation to the earth would be accomplished by the Microwave Power Transmission System (MPTS), an integral part of the SSPS system. The overall size of the SSPS system (~5 km x 12 km) precludes launch into orbit by a single launch, but requires many launches to get the components of the system into low earth orbit. Once in low earth orbit (LEO) the system can be assembled and transported through the Van Allen belts to geosynchronous equatorial orbit. An alternate plan calls for SSPS assembly above the Van Allen belts (~7000 n mi) to avoid solar cell degradation which occurs while traversing the Van Allen radiation belts. The latter system would use a Tug to transport the SSPS components from LEO to 7000 n mi. Both assembly altitudes would use a Solar Electric Propulsion System (SEPS) to transport the assembled SSPS system from the assembly point to geosynchronous equatorial mission orbit. Similarly, both techniques would use Shuttles to transport materials from ground to LEO. In summary, the complete SSPS system consists of the following segments:

- SSPS structure

- MPTS antenna

- SEPS

- Stationkeep/control module (LEO assembly only).

Figure 3.1-3 depicts the two flight modes, i.e., the low earth orbit assembly mode (Plan 1), and the high earth orbit (HEO, 7000 n mi) assembly mode (Plan 2).

3.1.2 Transportation System Performance

3.1.2.1 Shuttle

Both of the flight modes described in the previous subsection utilize the Shuttle as the vehicle for transporting elements of the SSPS from ground to LEO. Due east Shuttle
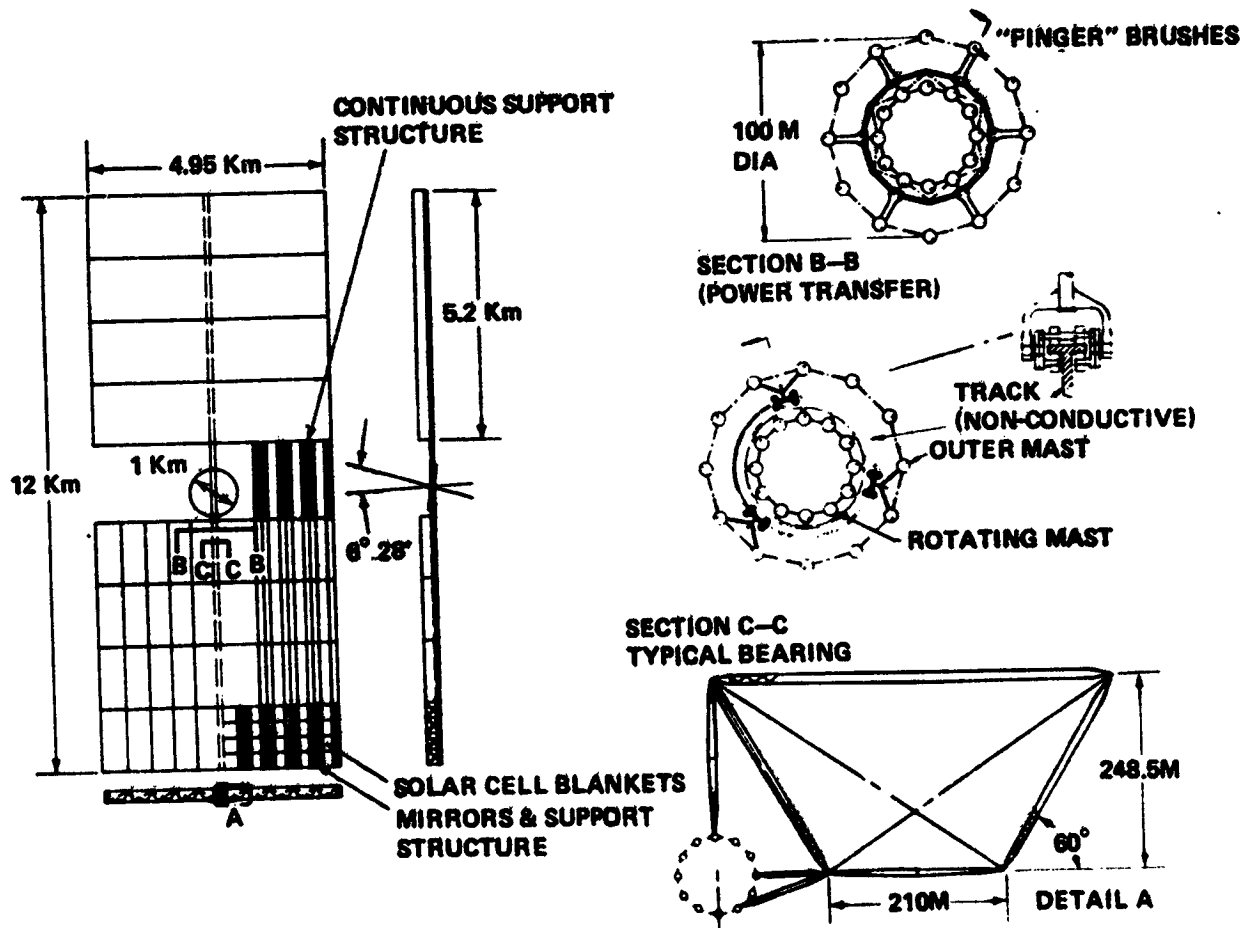
Fig. 3.1-1 SSPS Baseline Configuration

	Mass	
	kg x 10^6	lb m x 10^6
Solar Array	9.80	21.61
Blankets	6.11	13.47
Concentrators	0.93	2.05
Non-Conductive Structure	1.73	3.81
Busses, Switches	0.23	0.51
Mast & Rotary Joint	0.57	1.26
MW Antenna	1.66	3.65
Ref Phase Waveguide	0.02	0.04
Slotted Waveguides	0.68	1.50
Subarray Electronics and Detectors	0.03	0.07
Element Status and Cont. Data Bus	0.02	0.04
Switching and Power	0.06	0.13
MW Generators & Cooling	0.63	1.39
DC Busses	0.20	0.44
Structure incl. Rotary Joints	0.23	0.51
Installational Facilities	0.02	0.04
Control System incl. 1 year supply of Propellant	0.02	0.04
Total System	11.48	25.30

Centers of Gravity

X arm = 0.1 km
Y,Z arms = ± 0.026 km (85 ft)   (Variation is due to the rotation of the MW Antenna)

Moments of Inertia.

I_{xx} = 14.24 x 10^6 kgkm^2 (10.48 x 10^{12} slug ft^2)

I_{yy} = 123   x 10^6 kgkm^2 (90.528 x 10^{12} slug ft^2)

I_{zz} = 137   x 10^6 kgkm^2 (100.83 x 10^{12} slug ft^2)

Fig. 3.1-2 SSPS Mass Properties
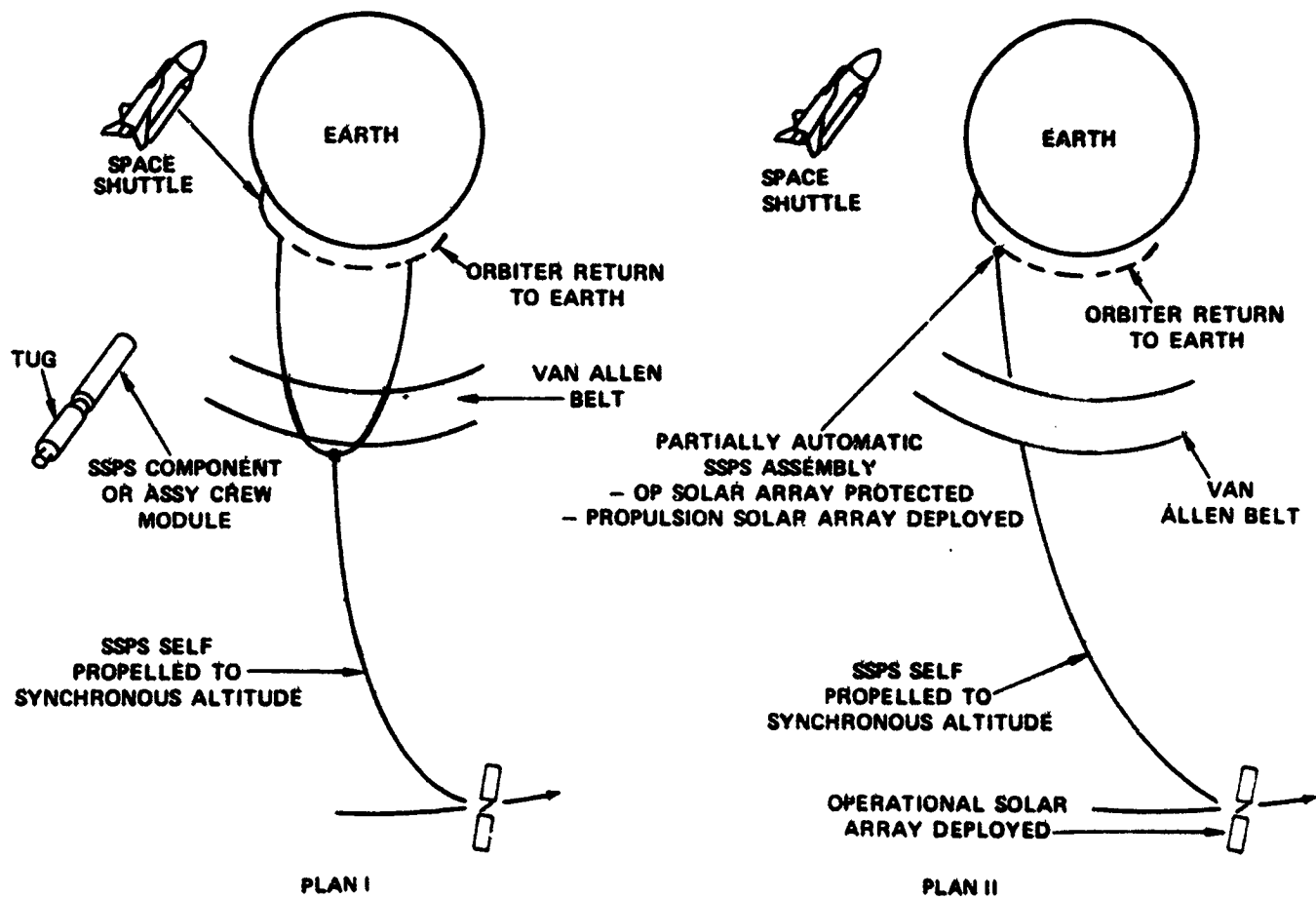
Fig. 3.1-3 Mission Options

launches from Kennedy Space Center (KSC) result in placement of the maximum payload of 65000 lb into low earth orbit at 28.5 deg inclination. Figure 3.1-4 presents the Shuttle payload capability as a function of circular orbit altitude for situations requiring a rendezvous by the Shuttle. As illustrated, 190 n mi is the maximum altitude that the Shuttle can deploy the maximum payload of 65000 lb. Shuttle performance degrades near linearly and rapidly above 190 n mi to 290 n mi, where no payload can be placed into orbit. Shuttle performance in this region can be increased with the addition of Orbit Maneuvering System (OMS) propellant in the Shuttle's payload bay; the obvious disadvantage of doing this is the loss of payload bay volume. Figure 3.1-5 presents similar performance information or cases not involving an ultimate rendezvous Shuttle. Maximum payload can be deployed to 290 n mi since no OMS propellant has been budgeted for rendezvous.

Since deployment of segments of the SSPS will require their being placed in close proximity to previously orbited segments, the rendezvous performance curve was used to determine Shuttle capabilities.

3.1.2.2 Tug

The Space Tug is an integral part of Flight Plan 2 operations since it will be used to transport, to 7000 n mi, the material delivered to LEO by the Shuttle. The Tug used throughout this analysis (see Ref 1) uses cryogenic propellant, is reusable and has the following characteristics:

- Propellant weight: 50177 lb (22730 Kg)

- Burnout weight: 5755 lb   (2607 Kg)

- Specific impulse (I_{sp}):   456.5 sec.

A typical Tug scenario starts with pick-up of a payload from a 190 n mi circular orbit, then delivering the payload to a 7000 n mi circular orbit, and returning to the shuttle in the original 190 n mi orbit. Figure 3.1-6 presents the Tug deploy capability while performing such a scenario. The performance is listed as a function of the delta V the Tug must expend to get the payload to its point of destination. This outbound delta-V can be related to the deployment altitude. The delta-V required to return the Tug to Shuttle has been assumed to be equal to that of the outbound leg of the journey.

Figure 3.1-7 shows the Tug configuration and summarizes its payload capability for three operation modes. The first, is for the aforementioned payload deploy scenario; it shows (as does Fig. 3.1-6) that the Tug can deploy 36800 lb (16770 Kg) to 7000 n mi. The
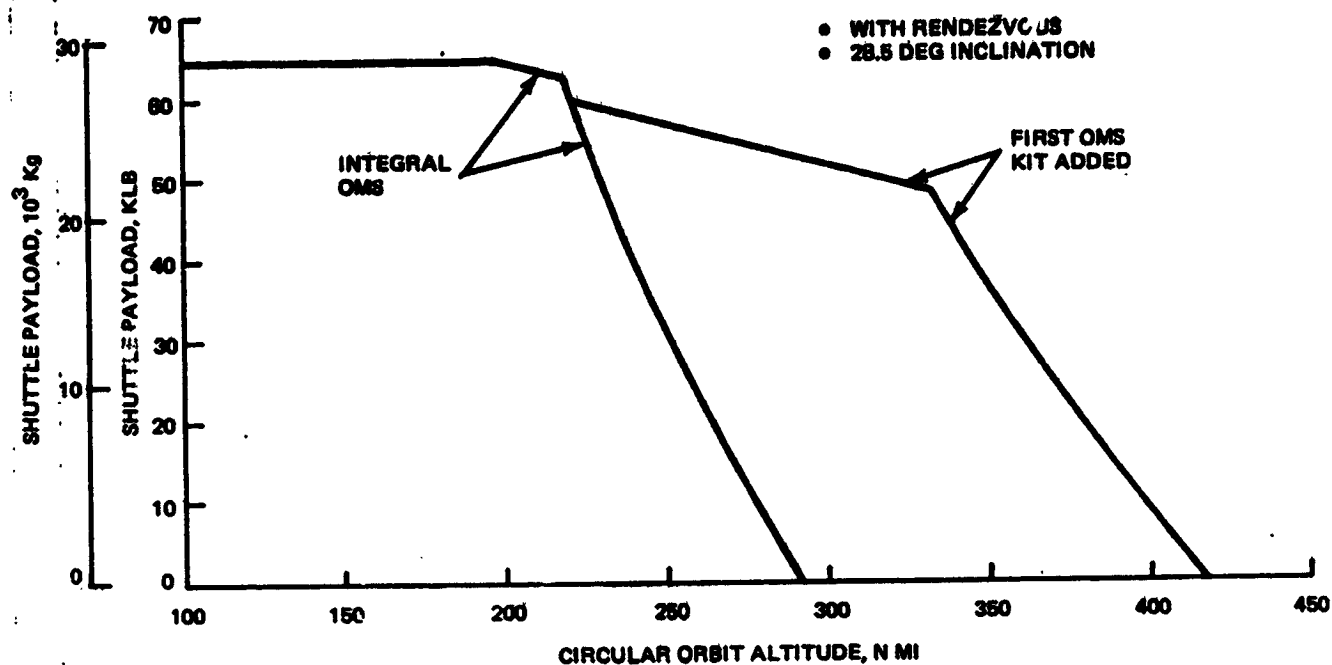
Fig. 3.1-4 Shuttle Payload Capability — Due East Launch from KSC
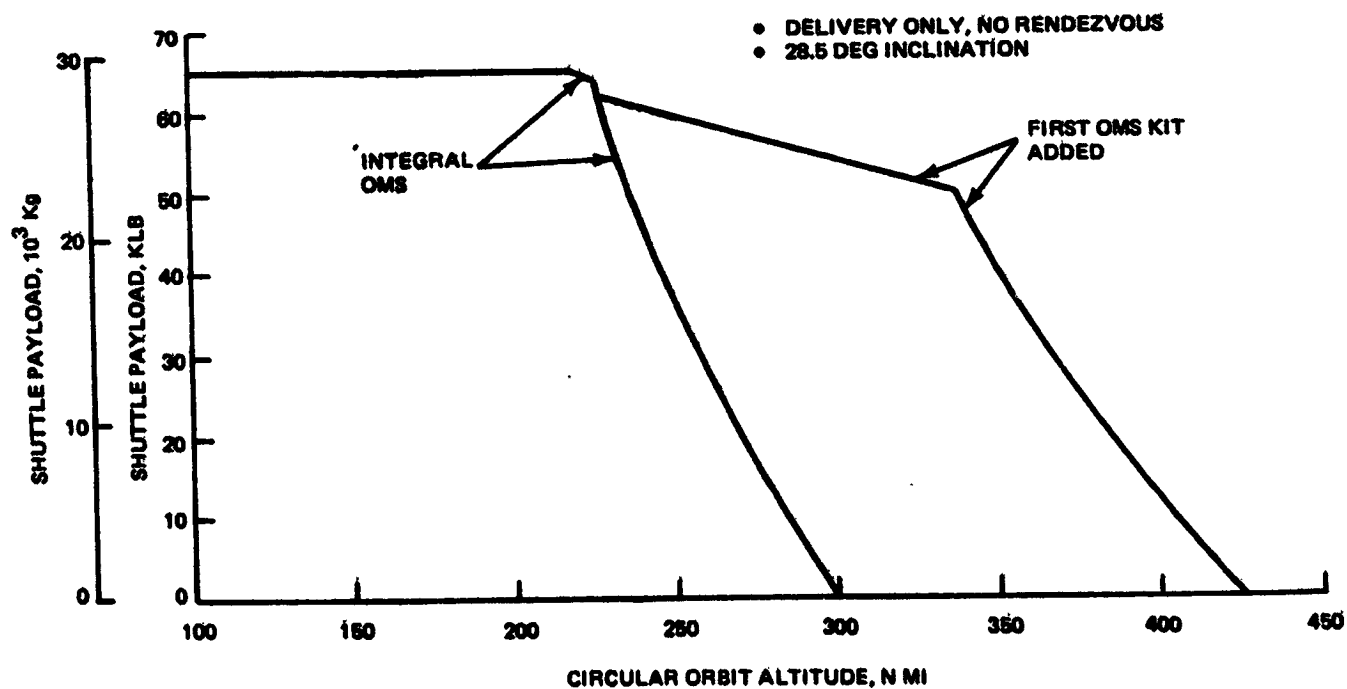
Fig. 3.1-5 Shuttle Payload Capability — Due East Launch from KSC

3.1-6
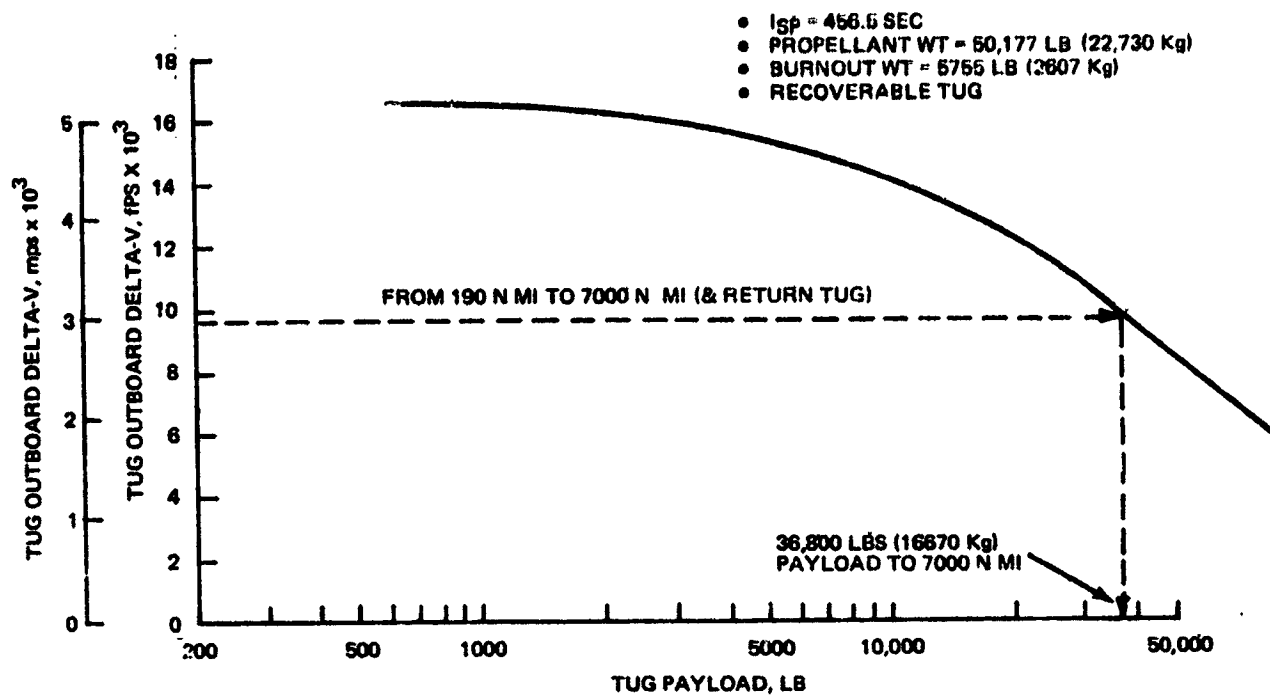
Fig. 3.1-6 Cryogenic Tug Deploy Performance
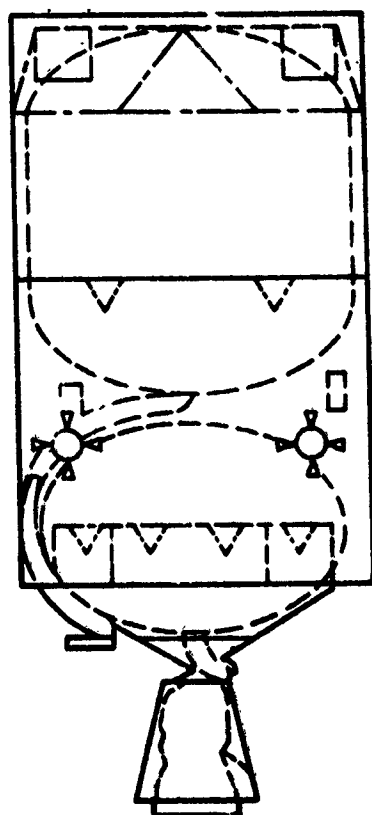
TOTAL WEIGHT, LB (Kg)	55,9⊥⊥ (25337)
PROPELLANT WEIGHT, LB (Kg)	50,177 (⌐)
DRY WEIGHT, LB (Kg)	575⊥ (2b⊥⊥)
SPECIFIC IMPULSE, SEC	456.5
PAYLOAD PERFORMANCE TO 7000 N MI	
● DEPLOY, LB (Kg)	36,800 (16670)
● RETRIEVE, LE (Kg)	19,000 (860)
● ROUN' TR·P, ⌐B (Kg)	12,500 (5662)

Fig. 3.1-7 Cryogenic Tug Configuration

3.1-7

second mode, payload retrieval, has a payload capability of 19000 lb (8607 Kg). The final mode involves deploying and retrieving a payload of equal weight to an orbit (roundtrip), and Fig. 3.1-7 lists 12500 lb (5662 Kg) as the capability.

3.1.2.3 Solar Electric Propulsion System (SEPS)

Ion propulsion system performance for both Plan 1, which calls for SSPS delivery from LEO to geosynchronous equatorial orbit, and Plan 2 which requires a similar delivery from 7000 n mi is dependent on SEPS thrust and SSPS weight. Figure 3.1-8 presents SEPS in-plane performance for a transfer from a 190 n mi circular orbit to geo-synchronous orbit (at 28.5°) for various thrust-to-weight ratios. The figure shows that approximately one year is required to reach mission orbit with the lowest thrust-to-weight ratio being considered: this traversal spends 120 days in the Van Allen radiation region, a period during which exposed solar cell effectiveness will be degraded by approximately 40%. This degradation will be accounted for when sizing the solar array which provides power for the ion propulsion system.

3.1.3 Altitude Selection

The issue of altitude selection is tied to both the Shuttle payload/altitude capability and air drag effects. The trades involved with selecting a LEO assembly altitude (Plan 1), or a high earth orbit assembly altitude (Plan 2) are centered around the consequences of supplying a Tug fleet for Plan 2 or an Orbit Keep/Altitude Control Module (OK/ACM) for assembly in LEO. Ultimately, the selection becomes one of cost and mission complexity. This subsection reports the effects of air drag on the SSPS in LEO, and will discuss the sizing of an OK/ACM system required to maintain the SSPS at the selected altitude.

Investigation of air drag effects on a satellite is dependent on the value of the satellites ballistic coefficient $(M/C_d A)$. Throughout this analysis, two values of $M/C_d A$ have been investigated, 0.175 and 1.75. These values were selected by assuming a total weight of 25 Mlbs, a C_d value of 2, and an order of magnitude difference in the area into the wind (A). The ballistic coefficient value of 0.175 assumes that the SSPS solar cells are covering the structure (as they would be in actual use) and that the SSPS has its edge into the wind. The ballistic coefficient value of 1.75 assumes that the solar cells are stored in a rolled window shade fashion, and the effective area is 10% of the nominal area. A one degree peak-to-peak oscillation about the center of the SSPS is also assumed. Since orientation of the SSPS edge perpendicular to the orbital velocity vector (edge into wind) follows a sinusoidal pattern, a mean area into the wind was computed. The computation considered the centroid of the
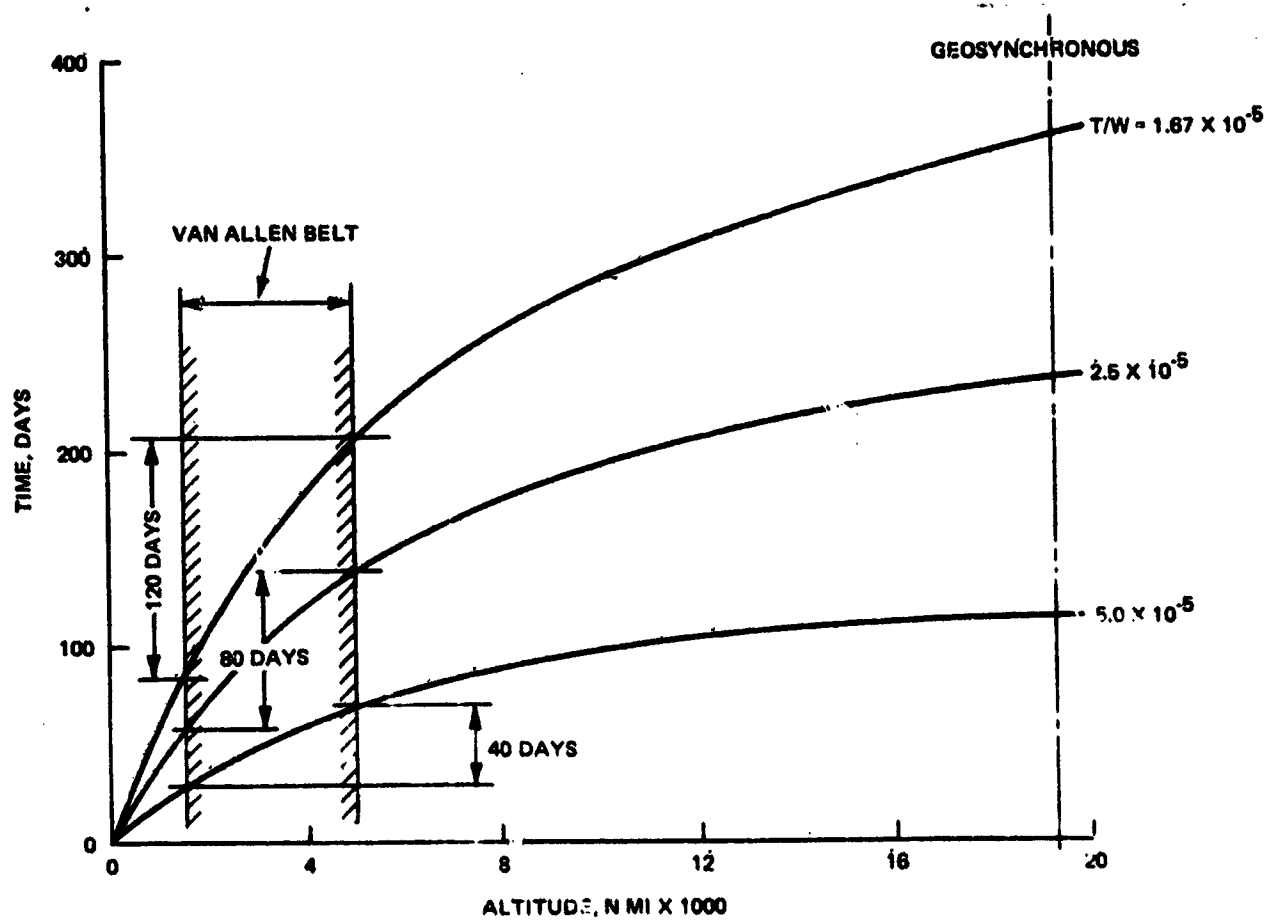
Fig. 3.1-8 Ion Propulsion Altitude vs Time from (100 N Mi Circular' – No Plane Change

limit-cycle sinusoid, and resulted in reducing the effective area by 60% over that of holding a fixed offset into the wind.

Figure 3.1-9 illustrates the effect of air drag on SSPS altitude over a 24 month period. The ballistic coefficient of 0.175 represents the SSPS with solar cell fully deployed. A nominal dynamic (Jacchia) mid-1979 atmosphere and a 95 percentile atmosphere were separately assumed. Considering the 95 percentile atmosphere and an initial altitude that Shuttle can reach with 65000 lb (29445 Kg) payload, the SSPS re-enters (assumed to be 75 n mi) after only one month in orbit. The nominal atmosphere assumption merely adds another month to the SSPS orbit life and indicates that an orbit keep module must be added to the SSPS if assembly is to be performed at 190 n mi. The figure shows that SSPS's with initial orbits of 250, 300, and 400 n mi will not re-enter within a year under nominal atmospheric conditions.

Figures 3.1-10 and 3.1-11 illustrate the wide variation in orbit lifetime which exists for vehicles with the two different ballistic coefficient values mentioned earlier. Figure 3.1-10 presents orbit decay characteristics for the SSPS at an initial 190 n mi altitude. Orbit lifetimes which differ by almost an order of magnitude result when the SSPS solar cells are fully deployed ($M/C_dA=0.175$) as compared to the case where they are stored in rolls. Storage of the cells then shows two advantages; first, air drag is reduced and secondly, solar cell degradation is reduced during Van Allen belt transit. Figure 3.1-11 shows similar information for an initial altitude of 250 n mi, and illustrates the distinct advantages of assembly at higher altitudes. The question of atmospheric density at 250 n mi becomes academic if a ballistic coefficient of approximately 1.75 can be assured. For these cases SSPS assembly could extend several years without even having to consider the addition of an orbit-keeping module to the SSPS. Unfortunately, Shuttle payload capability (on integral OMS) to 250 n mi is less than half of what it is to 190 n mi (see Fig. 3.1-4). If the present Shuttle is baselined as the SSPS launch vehicle, then fleet size and Shuttle traffic considerations dictate that 190 n mi be selected as the assembly altitude. The selection presupposes that an orbit-keeping module, which uses a reasonable amount of propellant over the assembly period (1 or 2 years), can be sized to maintain the 190 n mi altitude.

The orbit-keeping module has to supply a force equal in magnitude (and opposite in direction) to the air drag force. Figure 3.1-12 presents the forces required to compensate for air drag in low earth orbits. A constant force of 11 lb would maintain the SSPS at 190 n mi during the assembly period. The fact that the structure buildup will be progressive over the assembly period has been ignored. Rather, the conservative assumption which has
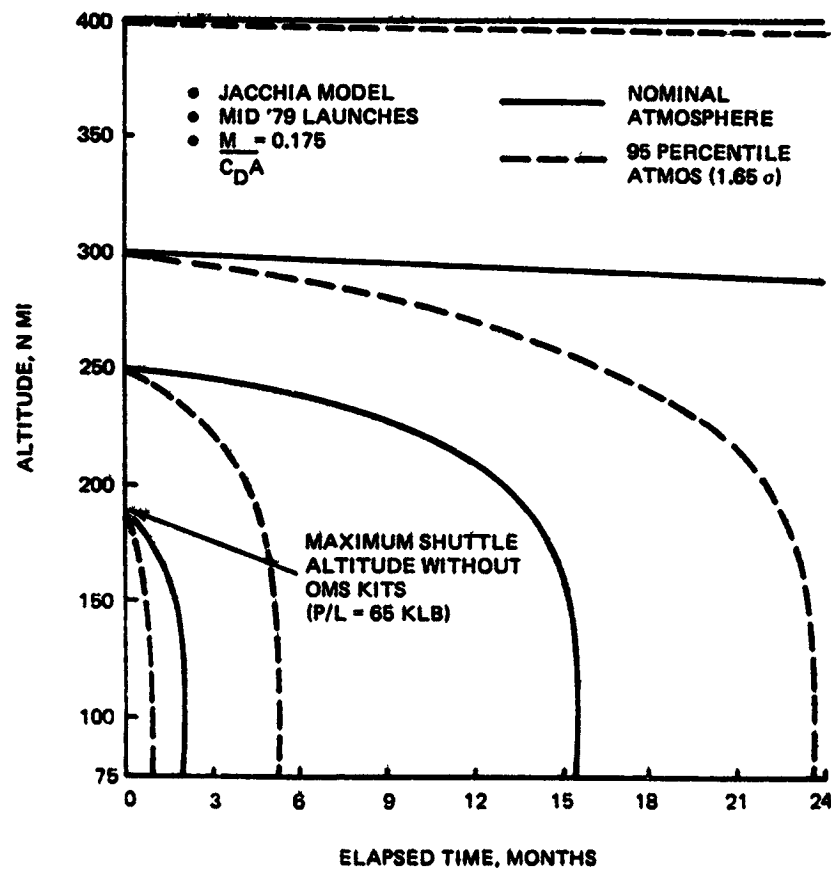
Fig. 3.1-9 SSPS Orbit Decay
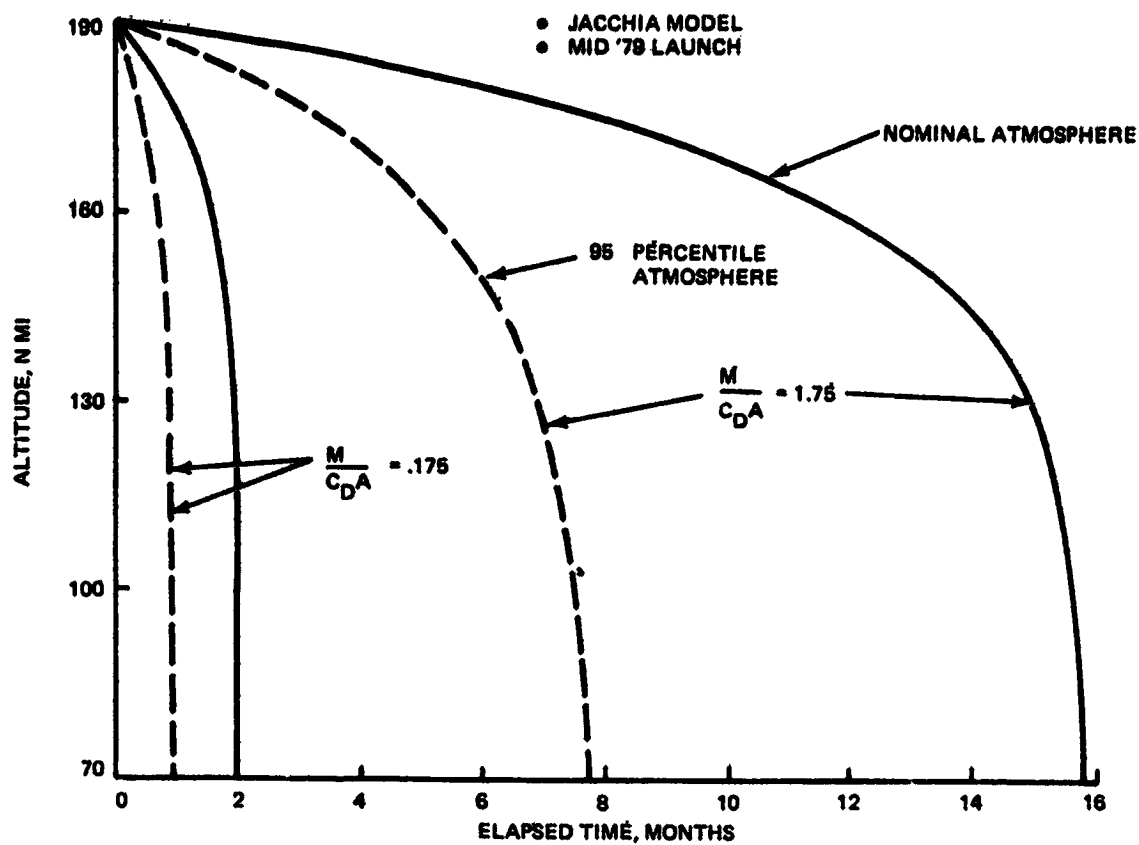
Fig. 3.1-10 SSPS Orbit Decay Characteristics
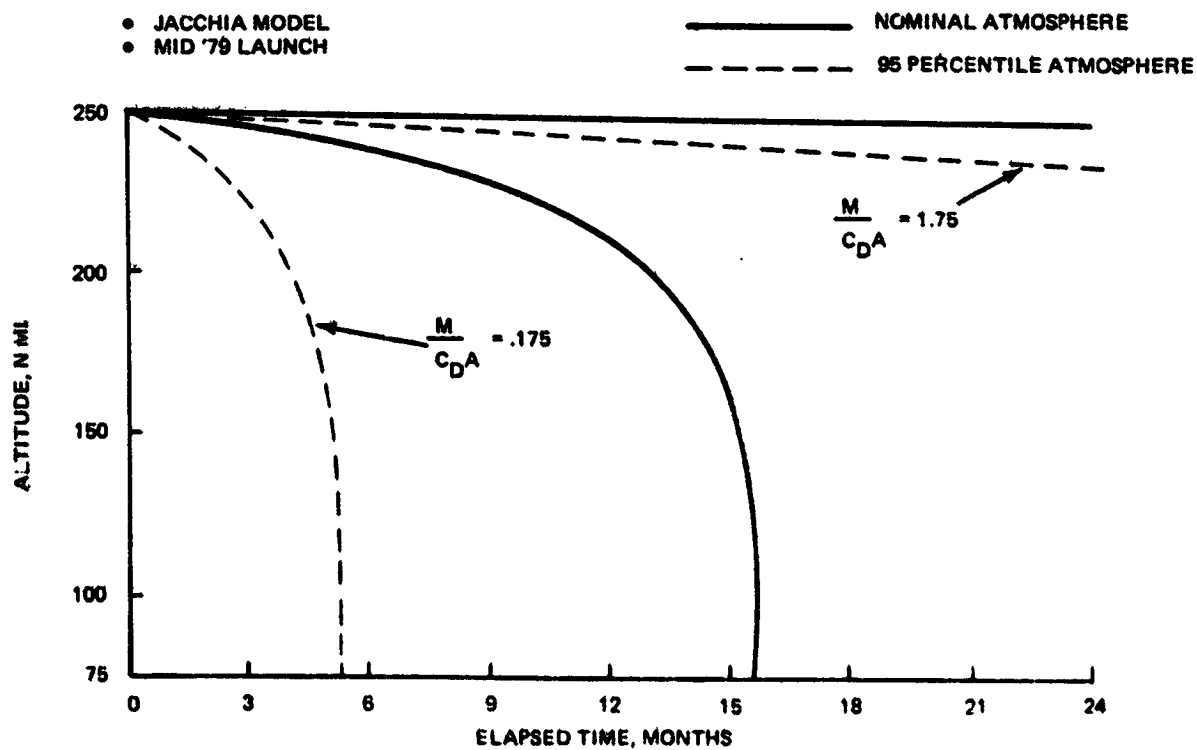
Fig. 3.1-11 SSPS Orbit Decay Characteristics
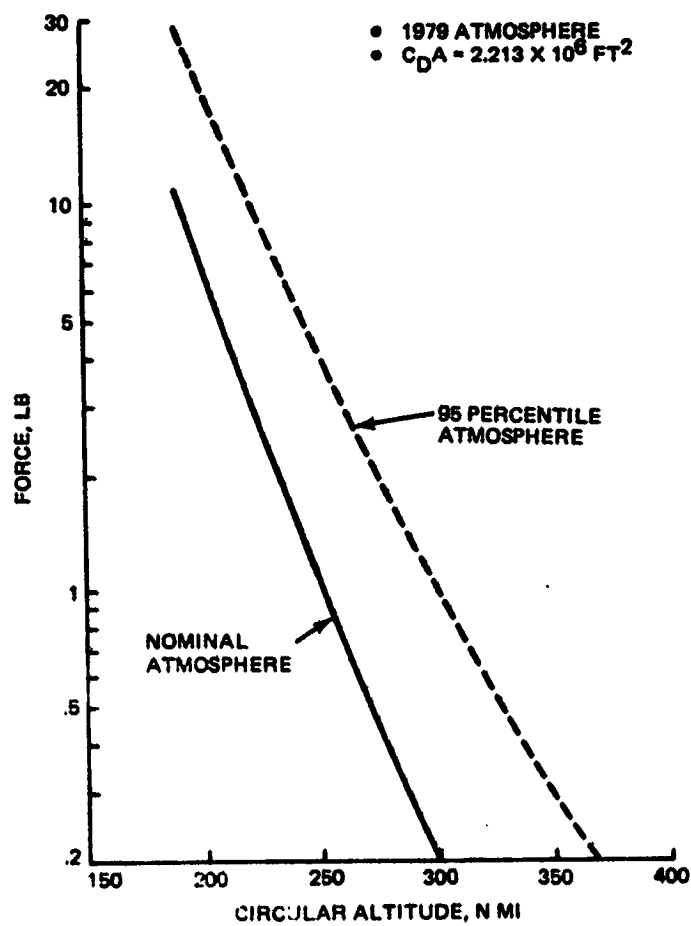
3.1-12

Fig. 3.1-12 Force Required to Compensate for Air Drag

been made is that the entire structure exists at the beginning of the orbit decay analysis time frame. An orbit-keeping module has been sized to maintain the SSPS at 190 n mi altitude. It represents a small version of the ion propulsion system proposed to transport the SSPS to geosynchronous orbit, and as such, has been sized using the procedure discussed in Subsection 3.1.4.

Power from the stationkeeping module ion engine is derived from solar photons impinging on solar cells. As the SSPS circles the earth in the 190 n mi assembly orbit, it will be in the earth's shadow approximately 40% of the time. Since the power source for the stationkeeping module will be inoperative during the shadow traverse, the force from the engine will drop off and the SSPS orbit will decay slightly. To compensate for this effect, the thrust required from the stationkeeping module has been increased from 11 to 16 lb. Characteristics of the stationkeeping module, which was sized to keep the SSPS at 190 n mi altitude under nominal air drag conditions, are as follows:

- Thrust   16 lb   (71.2N)
- Propellant   44 Klb/yr (19.9 x 10^3 Kg/yr)
- Total Module Weight   89 Klb   (40.3 x 10^3 Kg)

3.1.4 SEPS (Ion Engine) Sizing

3.1.4.1 Sizing Procedure

The factors affecting ion system size and a sizing procedure flow logic are depicted in Fig. 3.1.13. Maximizing payload ratio (λ_R) is the fundamental goal in sizing the ion propulsion. Unlike chemical propulsion, this is not achieved with maximum specific impulse (I_{sp}). The reduced propellant weight requirement with associated high I_{sp} must be traded against the increase in weight of the power supply required to achieve it. The factors affecting that trade are:

- System overall efficiency, $= \eta_U \cdot \eta_P$
    - η_U = propellant utilization efficiency = particles ionized per total particles
    - η_P = power efficiency = power in the thrust-producing ion jet per unit of power at the source
- Specific mass of the propulsion system, a = weight of all propulsion system hardware per unit of source electric power (lbm/kw)
- Propulsion time, t
- Mission ΔV.
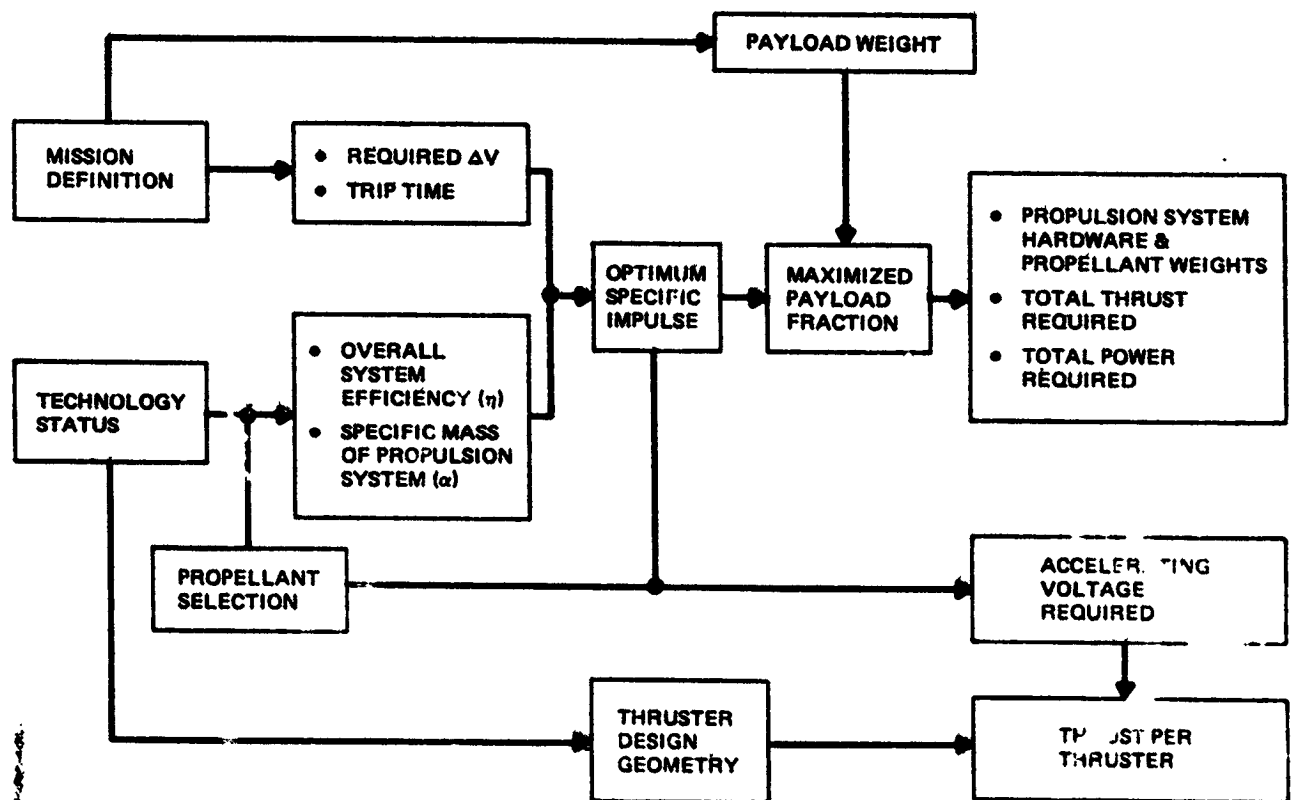
Fig. 3.1-13 Ion Propulsion System Sizing Factors

For a given value of sizing parameter $\eta t/a$ and mission ΔV, there exists an optimum I_{sp} which maximizes the non-propulsive payload ratio. Figures 3.1-14 and 3.1-15 show, respectively, the optimum specific impulse and corresponding maximized payload fraction as a function of $\eta t/a$*. Once the optimum I_{sp} and maximized payload fraction are established, many of the important propulsion system characteristics can be determined. The propulsion system weights, total thrust requirement, and total source power requirement can be calculated, as shown below, on the basis of a given non-propulsive payload weight (M_R):

- Payload + propulsion system weight, $M_o = M_R/\lambda R$ (3.1-1)

- Propulsion system weight, including propellant, $M_{ps} = M_o - M_R$ (3.1-2)

- Propellant weight, $M_p = M_o - M_{burnout} = M_o(1-e^{-\Delta V/I_{sp}g})$ (3.1-3)

- Total thrust required, $F = (M_p/t \text{ sec per yr}) I_{sp}$ (3.1-4)

- Source power requirement, $P = F I_{sp} g/2\eta$ x conversion
  factor to KW $(\frac{1}{740})$ (3.1-5)

3.1.4.2 SEPS Sized For Geosynchronous Delivery From 190 N Mi

Following the sizing procedures outlined in Subsection 3.1.4.1, the characteristics of a representative ion propulsion system for the SSPS delivery mission can be determined. The mission parameters assumed are:

- Delta-V = 16,000 fps (5000 mps)

- Trip time, t = 365 days

- Non-propulsive payload weight, $M_R = 26$ x 10^6 lbm (11.8 x 10^6 Kg).

The assumed mission delta-V corresponds to an ascension to geosynchronous orbit by continuous thrusting from an initial orbit altitude of approximately 190 n mi. A representative trip time of one year was selected to improve the $\eta t/a$ sizing parameter while keeping within the bounds of thruster system capability for continuous propulsion. Durations of approximately 8000 and 3500 hr have been demonstrated in ground and space tests, respectively. A three-year continuous-propulsion capability can readily be projected, at this time, for the SSPS time frame.

- - - - - - -

*Governing equations for Fig. 3.1-14 and 3.1-15 are derived in Ref (20).
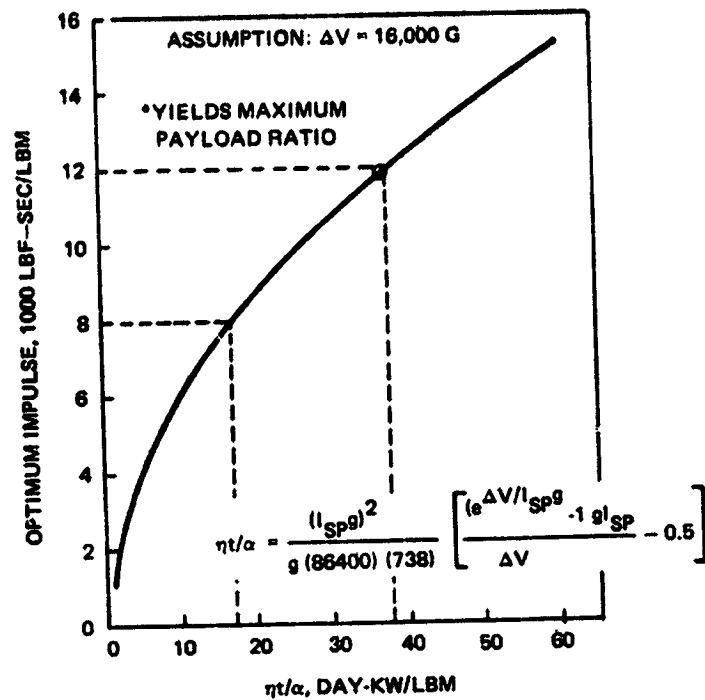
Fig. 3.1-14 Optimum Specific Impulse*

$$\eta t/\alpha = \frac{(I_{SP}g)^2}{g\,(86400)\,(738)} \left[\frac{(e^{\Delta V/I_{SP}g}-1)\,gI_{SP}}{\Delta V} - 0.5 \right]$$

$$\lambda_R = M_R/M_O = e^{-\Delta V/I_{SP}g} - \frac{\alpha\,(I_{SP}g)^2}{2\eta t} \left[1 - e^{-\Delta V/I_{SP}g} \right] \frac{1}{q} \qquad \frac{1}{(738)} \cdot \frac{1}{(86400)}$$
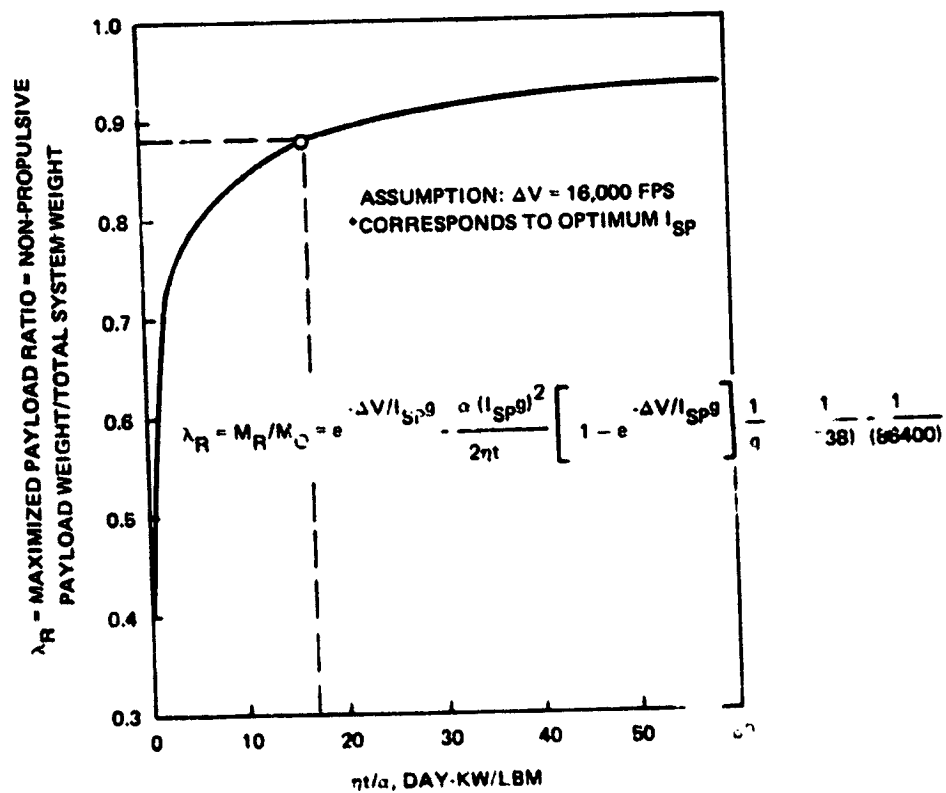
Fig. 3.1-15 Maximized Payload Ratio*

3.1-17

A mercury propellant, electron-bombardment ion propulsion system with a solar cell power source is assumed to have the following characteristics:

- System efficiency, $\eta = 0.7$
  - $\eta_U = 0.90$
  - $\eta_p = 0.78$
- Specific weight, $\alpha = 15$ lbm/kw.

Overall system efficiencies of 0.7 are equaled or exceeded with today's technology. The overall system specific weight assumption is based on an assumed power supply and conditioning specific weight of 5 lbm/kw, in line with projected solar cell weights for the SSPS itself, and propellant tankage, feed, thruster, structure, etc., specific weight of 10 lbm/kw. Current values for overall system specific weight fall in the range of 65-150 lbm/kw; however, the assumed value of 15 has precedence in literature (Ref 21).

The SSPS ion propulsion system, therefore, has a value of $\eta t/a = 17$ day-KW/lbm. It can now be determined from Fig. 3.1-14 and 3.1-15 that:

- Optimum $I_{sp} = 8000$ sec
- Maximized payload ratio, $\lambda_R = 0.88$

From Fig. (3.1-1) through (3.1-5):

- Total system weight, $M_o = 29 \times 10^6$ lbm (13.1×10^6 Kg)
- Propulsion system weight, $M_{ps} = 3.5 \times 10^6$ lbm (1.6×10^6 Kg)
- Propellant weight, $M_p = 1.8 \times 10^6$ lbm (0.82×10^6 Kg)
- Total thrust required, $F = 454$ lbf (2018N)
- Power required, $P = 113,000$ kw

3.1.4.3 SEPS Sized For Geosynchronous Delivery From 7000 N Mi

An ion propulsion system can be sized for a SSPS delivery to geosynchronous orbit from the candidate 7000 n mi assembly altitude. The method followed is identical to that outlined in Subsection 3.1.4.1. The mission parameters assumed are:

- Delta-V = 5,000 fps (1562 mps)
- Trip time, $t = 120$ days

- Non-Propulsive payload weight, $M_R = 26 \times 10^6$ lbm (11.78×10^6 Kg)

- System efficiency, $\eta = 0.7$

- Specific weight, $\alpha = 15$ lbm/KW (6.78 Kg/KW)

The resulting SEPS had the following characteristics:

- Optimum $I_{sp} = 4625$ sec

- Maximized payload ratio, $\lambda_R = 0.96$

- Total system weight, $M_O = 27 \times 10^6$ lbm (12.2×10^6 Kg)

- Propulsion system weight, $M_{ps} = 1.2$ M lbm (0.54×10^6 Kg)

- Propellant weight, $M_p = 0.9$ M lbm (0.4×10^6 Kg)

- Total thrust required, $F = 400$ lbf (1178N)

- Power required, $P = 43,000$ KW

3.2 ANTENNA STRUCTURAL CONCEPT

3.2.1 General Arrangement

The MPTS antenna is 1 km (3280 ft) in diameter by 40 meters (131.2 ft) deep. The antenna is assembled in two rectangular grid structural layers, Fig. 3.2-1. The primary structure is built up in 108 x 108 x 35 meter bays using triangular girder compression members 18 meters long and 3 meters wide. The secondary structure 18 x 18 x 5 meter bays (Section B-B, Fig. 3.2-1) are used as support points for the waveguide subarrays. Dimensions of the secondary structure will vary with selection of the optimum subarray size. (The 18 x 18 meter size is typical). A mechanical screw jack system (Detail C, Fig. 3.2-1) is used as the interface with the subarrays and provides the flexibility of mechanically aligning the waveguides in orientation and position. This feature desensitizes the configuration requirements on assembly tolerances and thermal deflection accuracies.

The antenna-to-spacecraft interface (Detail D, Fig. 3.2-2), uses a 360° rotary joint (azimuth) about the spacecraft (SSPS) central mast and a limited motion (±8°) rotary joint for North-South steering (elevation). The azimuth rotary joint uses two slip-rings and brush assemblies for power transfer (Section F-F, Fig. 3.2-2). One routes plus current, the other negative. The azimuth drive assembly utilizes a geared rail support structure (Section E-E, Fig. 3.2-2) and motor driven 4-wheel truck roller assembly. The elevation drive utilizes flexible cable for power transfer and a geared rail drive system similar to the mechanism used for azimuth control.

3.2.2 Rotary Joint

A recommended approach for concept definition consisting of rollers and tracks ha tentatively been made. Power is transferred across the azimuth interface by silver alloy brushes and slip rings, and across the elevation drive by flexible cable. The orientation drive is by DC torque motor with spur gear drive.

Design of the antenna mechanical interface requires selection of the gearing, bearings, motor, power transfer device and lubrication. Reference 8, containir design details and analysis for a space station solar array rotating joint, has been used as a source of pertinent design data. Applicable data from both Ref 7 and 8 has be acreated in this report for convenience.

3.2.2.1 Gears

The choice of gears to meet the 1 arc-min pointing accura requirement and 30-year life is a major issue in control system design. Depending upon the entitlement of the gear ratio,

backlash and jamming in an environment of high torque and low rotational rate, may preclude meeting requirements. The basic types of gears include spur gears, helical gears, worm gears, harmonic drive gears and bevel gears. The features of each of these options are presented in Fig. 3.2-3. The "no backlash" feature of the harmonic drive, in addition to the potential to achieve high gearing ratios with minimal packaging difficulty, would lead to selection of this approach. The major problem with the harmonic drive, however, is the poor life inhibited in limited tests of these gears. The worm gear approach, particularly for the elevation drive, is not recommended because of alignment difficulties, high friction and the inability to drive the gears backwards. A spur gear drive would provide a simple positive traction for transfer of torque; however, the design of gear teeth would have to provide a significant positive safety margin to preclude tooth breakage. Wear is not considered a problem due to the low speed environment.

3.2.2.2 Bearings

Bearings for the MPTS interface control system should be rolling-element types to provide the lowest friction possible. Options for selection include ball bearings, roller bearings or individual rollers. The individual roller approach was used in the SSPS design shown in Fig. 3.2-2. This approach results in high friction and has questionable fatigue life. A ball-bearing approach would minimize friction and provide better fatigue life. The large diameter (65 meters) of the azimuth interface would cause problems in design and assembly of conventional, machined-race, low-friction bearings. Because of the ball bearing design problem, it is recommended that the individual roller and track bearing arrangement be retained.

Further study and definition should include assessment of the following:

- Static load capacity
- Dynamic load capacity
- Fatigue life
- Stiffness
- Friction

- Tolerance to thermal gradients
- Lubrication
- Materials
- Maintainability

1 KM DIA

40 M

— 140 M —

— SEE DETAIL D
SHT 2

5M
40 M

18 M
(TYP)

18 M (TYP)

TYPICAL CABLE
SHEAR TIE

108 M
(TYP)

108 M
(TYP)

108 M
(TYP)

108 M
(TYP)

40 M REF

DET C

SEC A-A

18 M
(TYP)

35 M

5 M

SEC B-B

PLANE A

TYPICAL CONSTRUCTION

SHEAR TIE

18 M (REF) (TYP)
105 M (REF) (TYP)
140 M (REF)
5 M (REF)

35 M (REF)

5 M (REF)

PLANE A

AMPLITRON (TYP)

WAVEGUIDE PANEL

SCREW/JACK & DRIVE
3 REQ'D PER WAVEGUIDE PANEL

DETAIL C ROTATED 45" CW
SCALE 1" = 1 M

18 M (REF)

40 M REF
DET C
35 M
5 M
SEC B-D
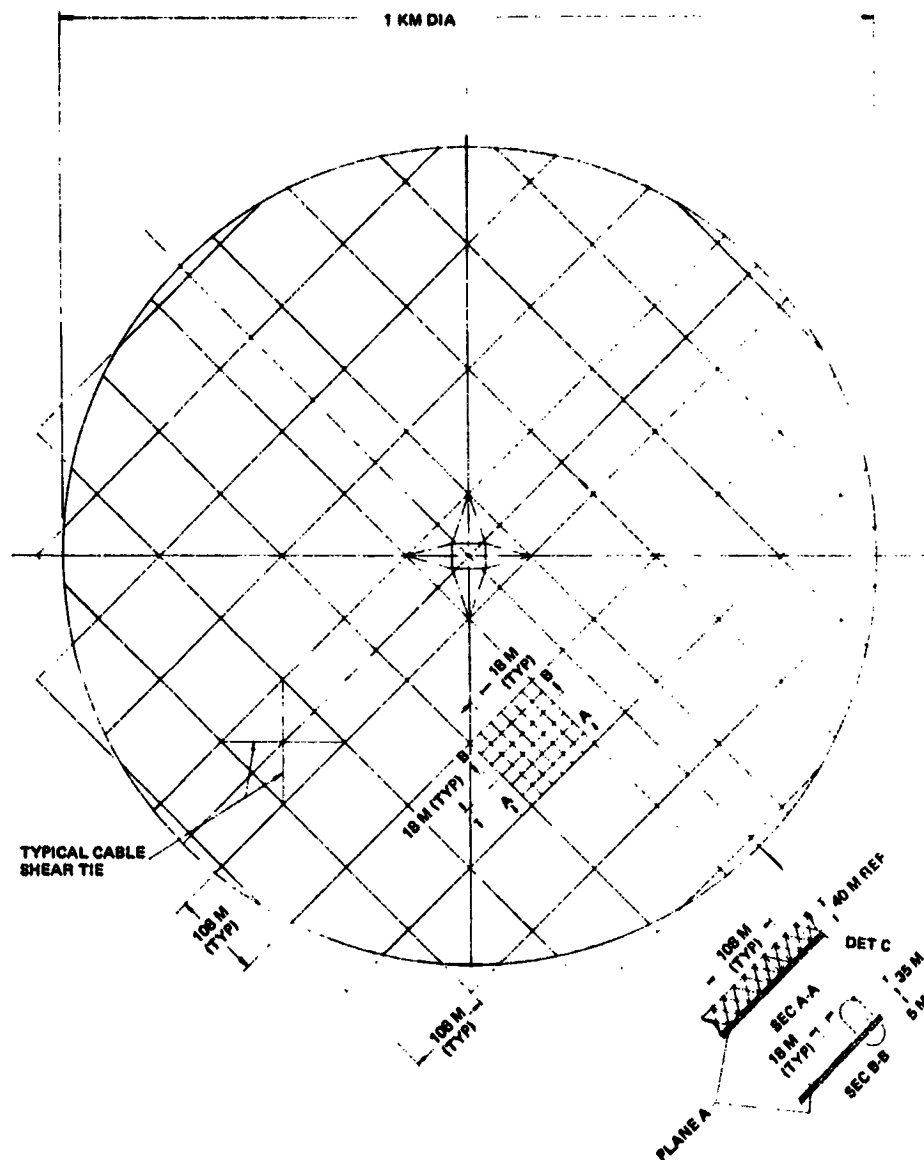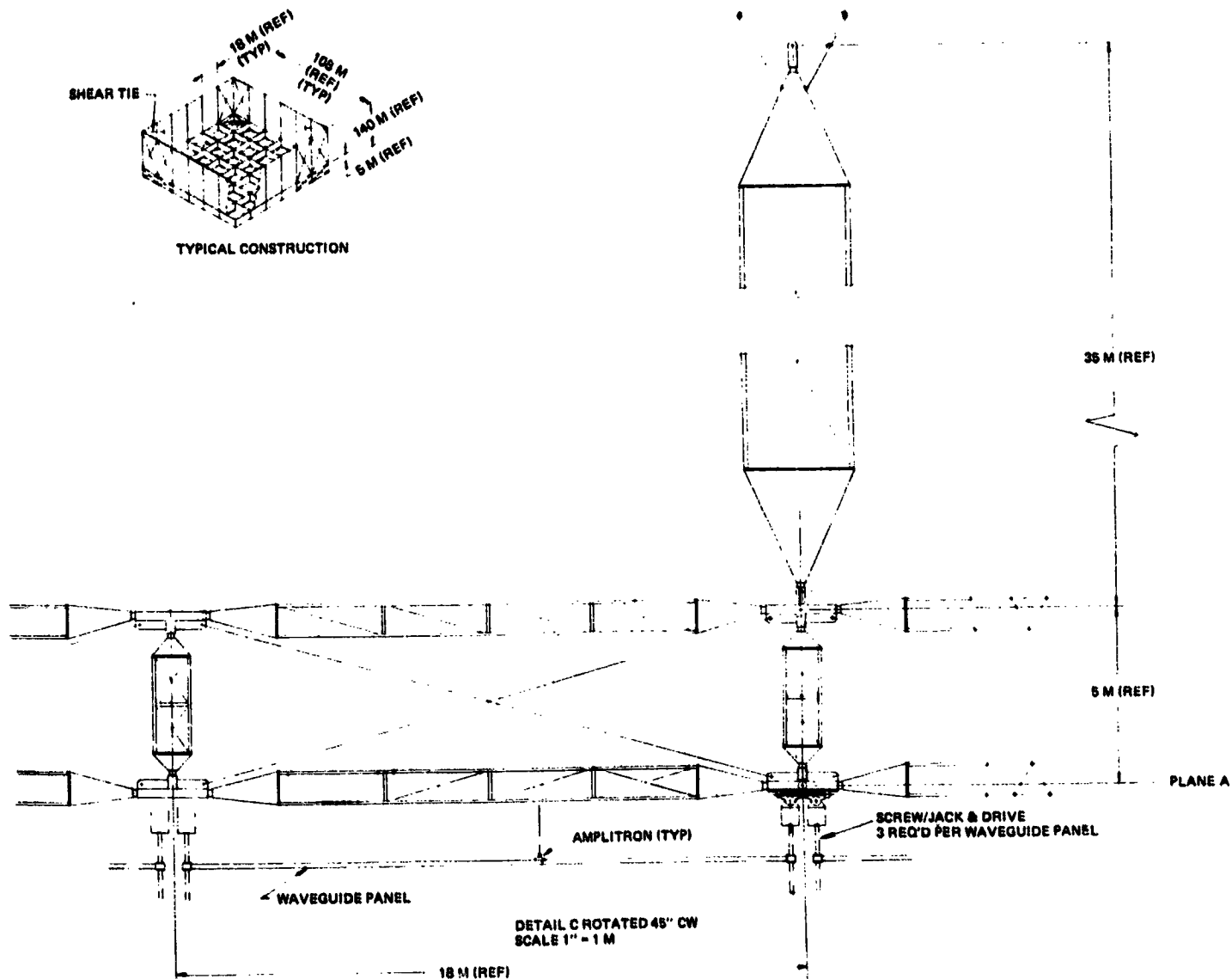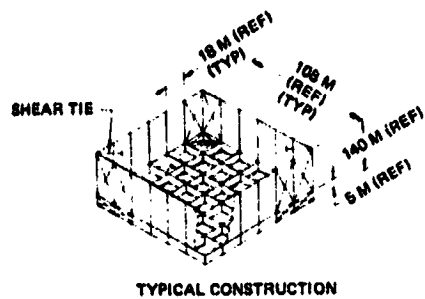
Fig. 3.2-1 Structural Arrangement MPTS Antenna

3.2-3

MOTOR DI
"TRUCK"

SECTION E-E

DETAIL D
SCALE 1" = 10 M

MOTOR DRIVEN
"TRUCK" ASSEMBLY

SLIP RING

SPRING LOADED
BRUSHES

BASIC MAST
STRUCTURE

F

E

F

SECTION F-F
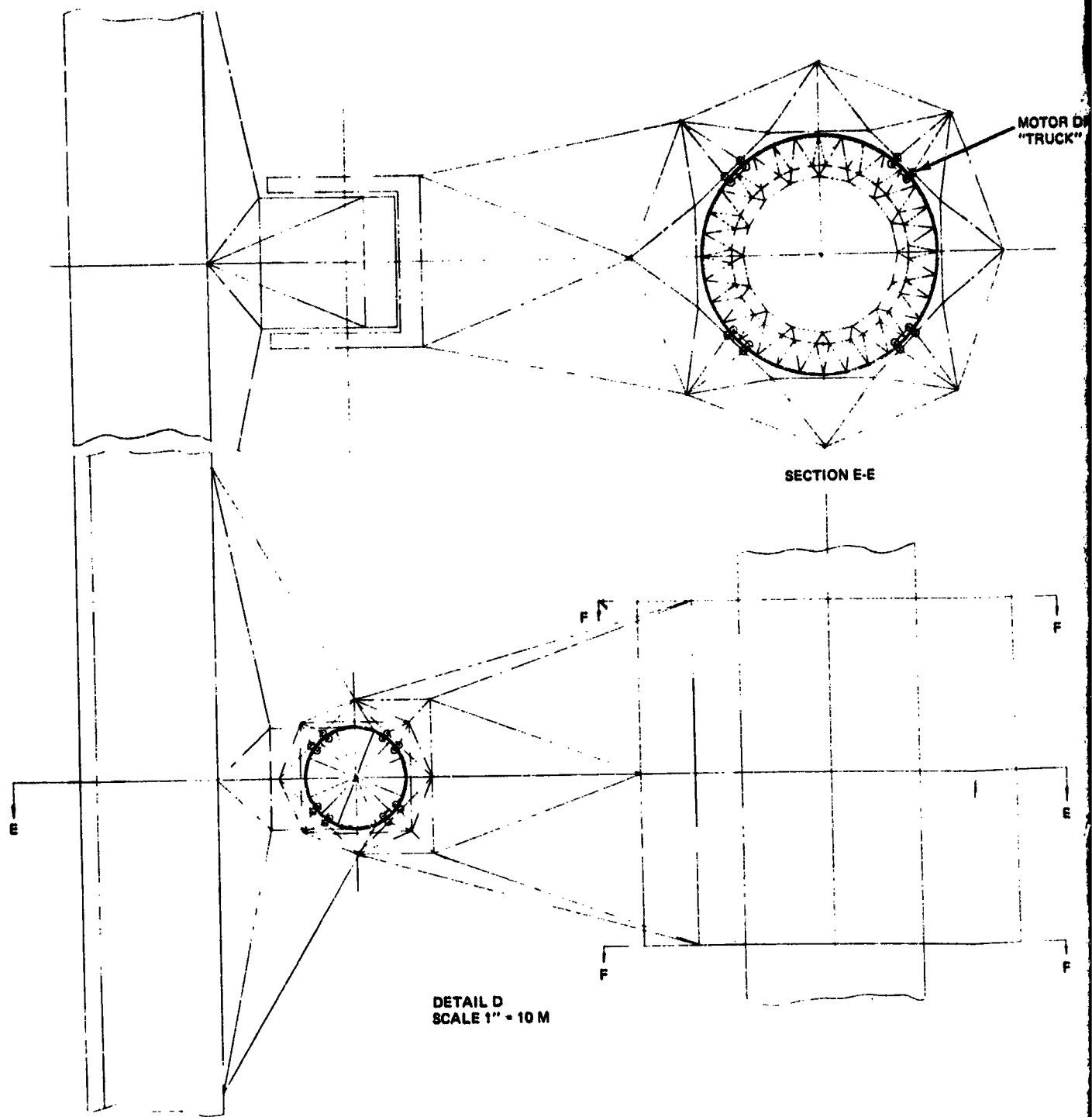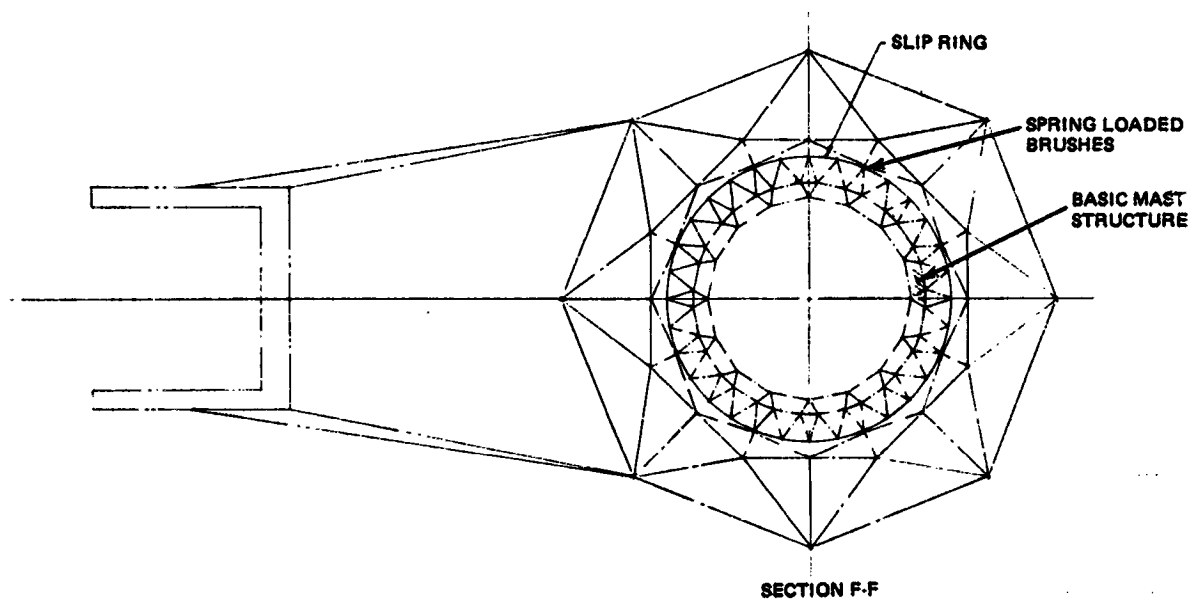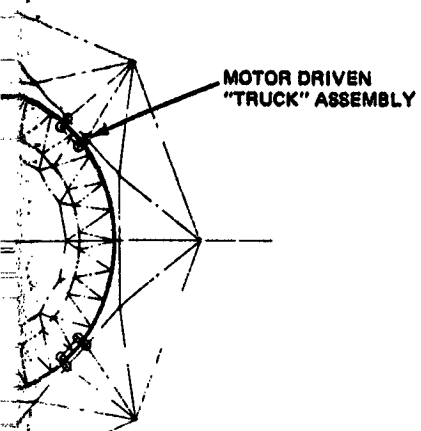
Fig. 3.2-2 Structural Arrangement MPTS Antenna

3.2-4

FOLDOUT FRAME 4

CONSIDERATIONS GEAR TYPE	TECHNOLOGY STATUS	EFFICIENCY PERCENT	FRICTION AND WEAR	BEARING LOADS	REMARKS
SPUR	• AVAILABLE IN MANY SIZES • AVAILABLE IN MANY MAT'LS • MTP'S SIZES TBD • MANUFÁCTURING TECHNIQUES	95 TO 98	MINIMUM (ROLLING CONTACT)	MINIMUM	• LARGE ANNULAR GEAR CAN BE PART OF LARGE BEARING • LOWER COST
HELICAL	• OFF THE SHELF SIZES UP TO 6" DIA.	95 TO 98	MINIMUM (ROLLING CONTACT)	SAME AS SPUR, EXCEPT AXIAL LOAD APPLIED TO SHAFT	LARGE LOAD/TOOTH CAPABILITY
WORM	• AVAILABLE UP TO 10" DIA. • AVAILABLE IN SEALED HOUSING	60 TO 80	HIGH (RUBBING CONTACT)	HIGH	• HIGH RATIO (100:1) AVAILABLE • CANNOT BE DRIVEN BACKWARDS • ALIGNMENT IS DIFFICULT
HARMONIC	• WELL DEVELOPED AND AVAILABLE IN SMALL SIZES	60 TO 90	LOW (ROLLING CONTACT)	NO DRIVE SHAFT-WAVE GENERATOR HAS SMALL LOADS	• NO BACKLASH • RATIX SFR 100:1 TO 200:1 AVAIL LE • NO LIFE TEST DATA AVAILABLE
BEVEL	• WELL DEVELOPED • AVAILABLE IN RELATIVELY SMALL SIZES	95 TO 98	MINIMUM (ROLLING CONTACT)	SAME AS SPUR, EXCEPT AXIAL LOAD APPLIED TO SHAFT	ANGLE OF SHAFTS USUALLY 90°

SEE REFERENCE 8

Fig. 3.2-3 Gear System

3.2.2.3 Motors

The following summarizes the motor requirements for the MPTS mechanical system interface:

Motor Characteristics	Azimuth Drive	Elevation Drive
• Torque (peak)	1.02×10^6 N·m	2.83×10^3 N·m
• Horsepower	0.18	1.8
• Time Constant	Less than 0.1 sec	

Figure 3.2-4 is a list of typical motor types that are considerations for the servo system design.

Control dynamics computations indicate that less than 134 watts power drain is required to drive the antenna in azimuth; however, startup inertia and response to control the effect of base dynamics will require a high starting torque motor. A DC motor is well suited to this application. The long life requirements (30 years) favors the brushless DC torque motor, though these devices are slightly heavier and less efficient than brush motors. Figure 3.2-5 presents a conceptual design for the rotary drive mechanism. The total weight for motors, gears, idler wheels and drive wheels is 12,024 Kg.

An attractive option to the motor-gear system would be the use of linear step motors mounted around the periphery of the drive assembly support. These devices have an excellent thrust-to-weight ratio (10:1) and would eliminate the wear problems associated with gears. Figure 3.2-6 is a conceptual layout and weight estimate of a three-phase variable reluctance linear motor system. A significant weight reduction relative to the motor gear approach is indicated. The attractiveness of this approach in terms of reliability, simplicity and low weight strongly suggest that technology efforts be initiated to determine the feasibility of application to the MPTS rotary joint drive mechanism.

3.2.2.4 Power Transfer Devices

Figure 3.2-7 summarizes power transfer options and the major considerations in selection. Consideration of all factors leads to a tentative selection of slip rings for the azimuth drive and flex cables for the elevation drive.

3.2.2.5 Slip Rings and Brushes

A possible configuration would employ two coin silver slip rings around the mast mounted near the roller tracks for gap tolerance stability. Self-lubricating brushes would

MOTOR TYPE	WEIGHT (LB)	SIZE	TORQUE EFFICIENCY LB-FT/WATT	GEARING ADAPTABILITY	CONTROL SYSTEM COMPATIBILITY	LIFE (DOES NOT INCLUDE BEARINGS)	REMARKS
DC BRUSH TYPE TORQUE	7.0	6" DIA X 1-3/4"	0.027	PANCAKE MOUNTING, NO PROBLEM WITH GEARING	EXCELLENT	BRUSHES ARE ONLY WEAR ELEMENTS.	• CAN HANDLE LARGE INERTIA LOADS. • IMPRESSIVE HISTORY OF SUCCESSFUL SPACE APPLICATIONS
DC BRUSH LESS TYPE TORQUE	4	4-3/4" DIA X 2-1/4"	0.022	PANCAKE MOUNTING, NO PROBLEM WITH GEARING	ELECTRONIC COMPLEXITY OTHERWISE EXCELLENT	LONG LIFE FEASIBLE	• CAN HANDLE LARGE INERTIA LOADS. • VERY COMPLEX ELECTRONICS
SERVO MOTOR	2 LB MOTOR 5 LB GEARHEAD	NO UNIT MFGR WITH TORQUE RQMTS EXCEPT WITH EXTRA GEARHEAD	0.00026 AT MOTOR	GEAR SIZE MATCHING PROBLEM	MORE COMPLEX ELECTRONICS TO CONTROL AC	LOW : LIFE FEASIBLE	• POOR TORQUE PER WATT RATIO. • INVERTER LOSSES MUST BE CHARGED AGAINST DRIVE
DC STEPPER	4	4-3/4" DIA . 2-1/4"	0.022	PANCAKE MOUNTING - GEARING MUST ABSORB REPEATED MECH. SHOCK	COMPLICATED ELECTRONICS	QUESTIONABLE DUE TO REPEATED MECH SHOCK	• HIGH SURGE CURRENTS, DOES NOT DRIVE INERTIA LOADS WELL. • DETENT TORQUE COULD BE USEFUL.
AC STEPPER	1 LB MOTOR 7 LB GEARHEAD	NO UNIT MFGR TO TORQUE RQMTS EXCEPT WITH GEARHEAD	0.00002	GEAR SIZE MOUNTING PROBLEM	COMPLICATED ELECTRONICS	QUESTIONABLE DUE TO REPEATED MECH SHOCK	• POOR TORQUE EFFICIENCY, HIGH SURGE CURRENTS DOES NOT DRIVE INERTIA LOADS WELL
INDUCTION	2C	3" DIA 11" LONG	0.0007	NO PROBLEM	MORE COMPLEX ELECTRONICS TO CONTROL AC	LONG LIFE FEASIBLE	• LOW STARTING TORQUE, HIGH STARTING SURGE CURRENT. INVERTER INEFFICIENCY MUST BE CHARGED TO DRIVE
AC SYNCHRONOUS	7	10" C 14"	POOR. DEPENDS ON STARTING METHOD	NO PROBLEM	MORE COMPLEX ELECTRONICS TO CONTROL AC	LONG LIFE FEASIBLE	• POOR STARTING TORQUE WITHOUT AUX. MEANS. INVERTER LOSSES MUST BE CHARGED TO DRIVE.
AC TORQUE	40	15" DIA X 4"	0.002	NO PROBLEM	MORE COMPLEX ELECTRONICS TO CONTROL AC	LONG LIFE FEASIBLE	• POOR TORQUE PER WATT RATIO. • POOR TORQUE PER POUND RATIO. INVERTER LOSSES CHARGED TO DRIVE.

SEE REFERENCE 8

Fig. 3.2-4 Typical Motor Options

MOTOR DRIVEN GEAR

CABLE

IDLER WHEEL

"FIXED" STRUCTURE

CABLE/SEGMENTED GEAR RACK

AZIMUTH DRIVE CHARACTERISTICS

ANTENNA SPEED	$= 0.728 \times 10^{-4}$ RAD/SEC
GEAR REDUCTION	$= 2.47 \times 10^{5}$
MOTOR SPEED	$= 18.4$ RAD/SEC
MOTOR TORQUE	$= 2.8$ FT/LB (3.8 N m)

WT, GEAR BOX & MOTORS = 24,065 LB (10938 Kg)

WT, DRIVE TRUCK & CABLE = 2389 LB (1086 Kg)
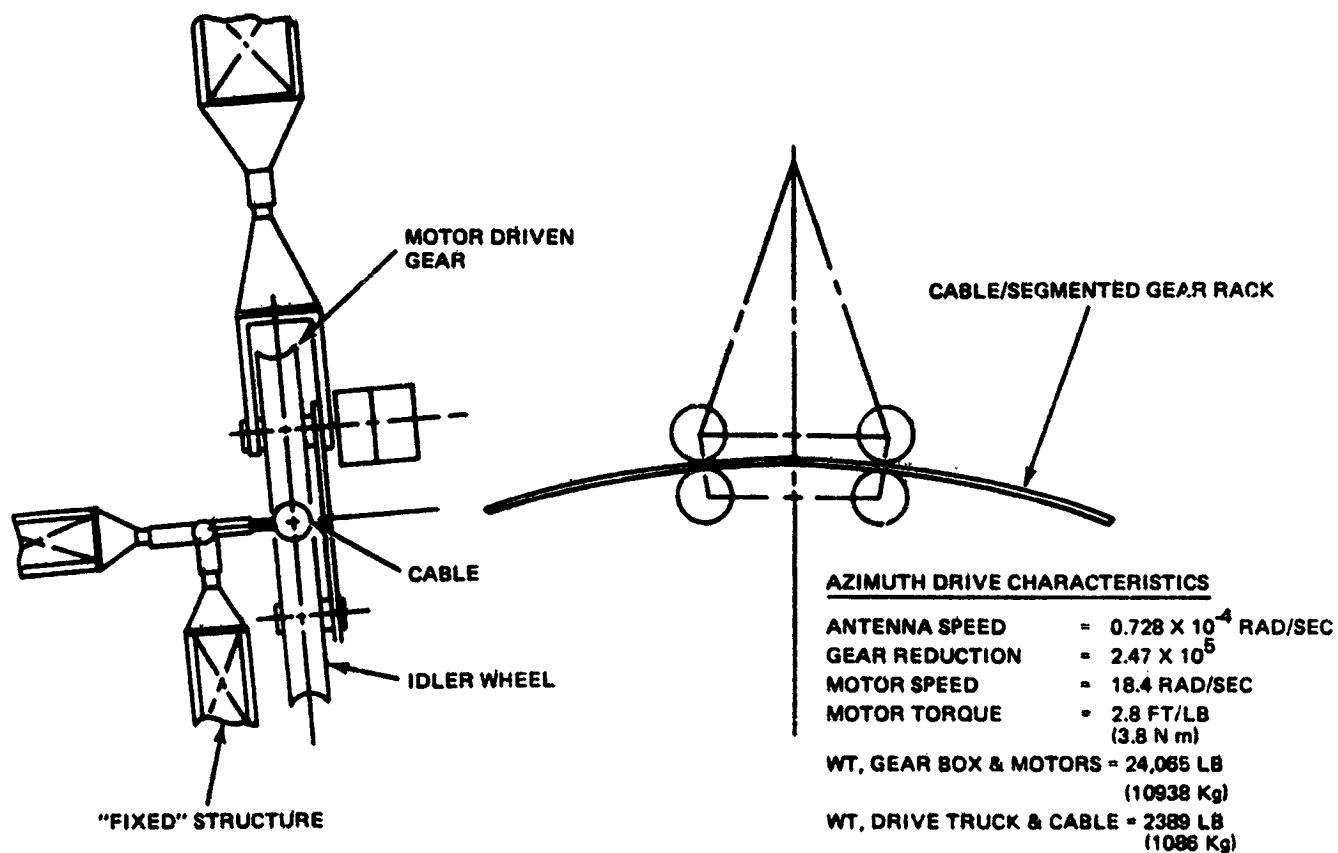
Fig. 3.2-5 Rotary Drive Concept
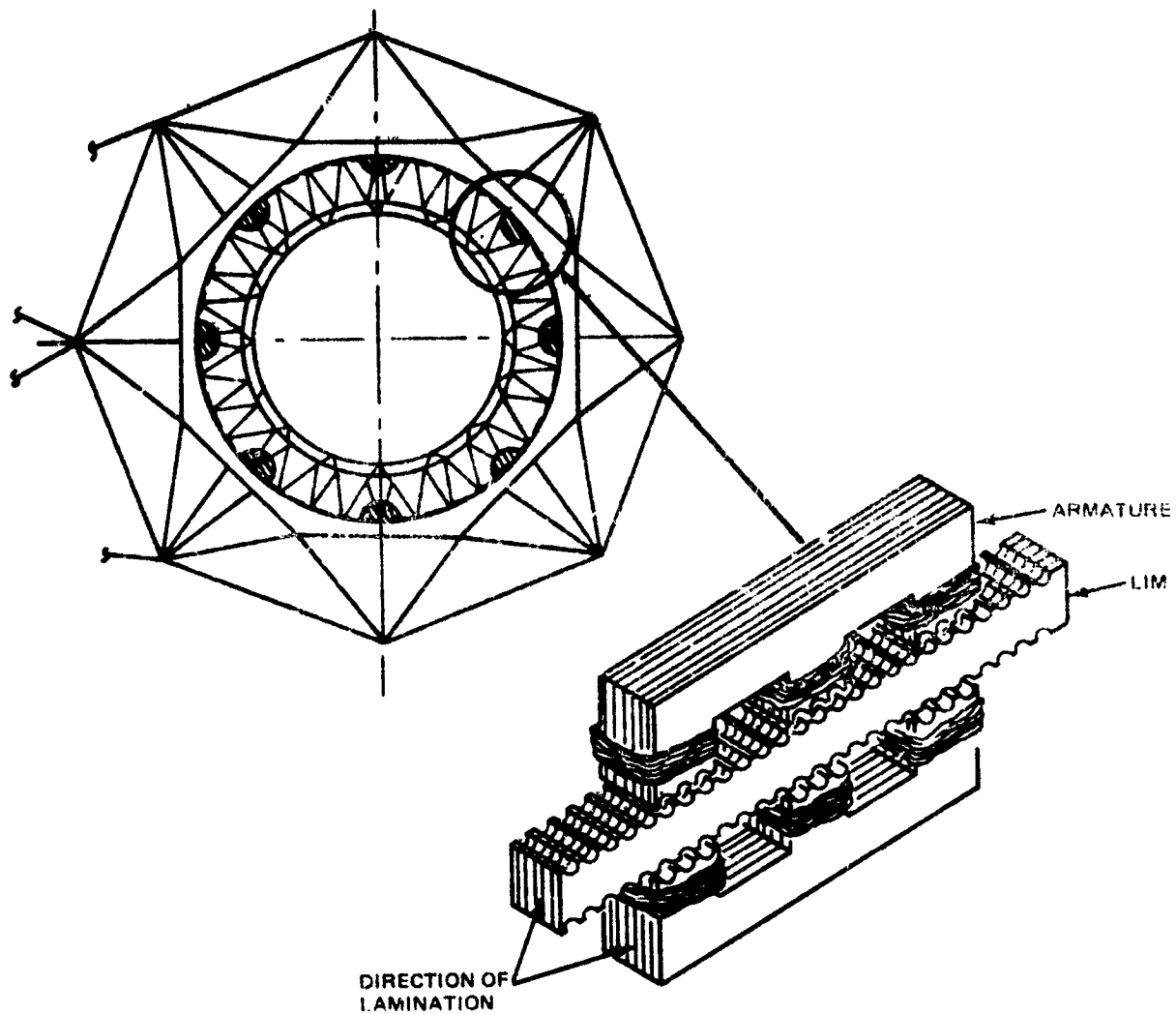
	WEIGHT	
	LB	Kg
LIM	2214	0⁻⁾
ARMATURE	432	1⁹
	2ₒ⁴⁾	1116

Fig. 3.2-6 Antenna Rotary Joint (Frictionless Linear Motor Concept)

be spring loaded and made of silver/niobium diselenide carrying from 7.75×10^4 to 15.5×10^4 amp/m^2 (50 to 100 a p/in.^{2}). Brush pressure would be from 27,550 to 68,940 N/m^2 (4 to 10 psi). Brush speed is low, so no arcing problems are anticipated. Brush height would be designed for the life of the SSPS at very small penalty, or life/reliability goals could be met by an unloaded set of standby brushes to be actuated by command when wearout of the initial set was imminent. Life predictions for such designs have been estimated to be possible for over 100 years. The main problem is providing for oil vapor lubrication to supplement the NbSe$_2$ solid lubricant. Oil vapor lube extends the life of brushes, but requires some form of reservoir and labyrinth seal to minimize vapor loss. Mass estimate has yet to be made, but the specific weight will probably be small relative to structure, bearings, and buses.

Figure 3.2-8 is a schematic of the slip ring and brush design concept for the azimuth rotary joint. The total weight of brushes and slip rings is estimated at 1100 lb (504 Kg).

Slip rings and brushes possess a well-developed technology and have unlimited rotational freedom in one axis. Their performance is not degraded by stopping, starting or reversing. Slip rings have high reliability over long operating periods. Slip rings, however, are relatively heavy and because of their large size would present problems in assembly. The major consideration to overall system design is the high thermal inputs to the structural interface due to I^2R losses at the brush slip ring interface. Figure 3.2-9 and 3.2-10 summarize the operating temperatures and voltage drop for some candidate brushes and slip ring combinations. Considering a system power level of 5 GW and a voltage level of 20 KV, there will be approximately 20,000 amperes per bus bar. To achieve a medium current density of 7.75 amperes per square meter requires 3.23 square meters of brush/slip ring contact area. According to Fig. 3.2-10, the voltage drop across the brush/slip ring interface will be approximately 0.2 volt which will generate 40 KW of waste heat at each interface. To ensure reasonable operating temperatures for the brushes, methods for efficiently "dumping" this waste heat should be considered.

3.2.2.6 Liquid Metal Slip Rings

No information on successful application of this concept has been uncovered to date. The state-of-the-art is such as to leave most questions unanswered, so development risk is considered high. Reference 8 gave no technical information relative to liquid slip rings but did not list them with SKF as origin. SKF had tried to use a mercury liquid metal slip ring for instrumentation noise suppression on a 24,000 rpm bearing research program but had dropped development in favor of a silver/silver graphite solid brush system.

DEVICE	SIZE & WEIGHT	LONG LIFE & MAINT	POWER CONSUMPTION	COST & SCHEDULE	TECHNOLOGY STATUS	LUBRICATION
SLIP RING	INTERMEDIATE	POSSIBLE	INTERMEDIATE I^2R. OVERCOME BRUSH FRICTION	SECOND	STATE-OF-THE-ART	DRY LUBE INCORPORATED IN BRUSHES
POWER CLUTCH	INTERMEDIATE	POSSIBLE. COMPONENTS REPLACEABLE.	INTERMEDIATE I^2R. HAVE TO RESET	THIRD	CONCEPT STAGE	NO LUBE ON CONTACTS MOTOR PARTS NEED MISCELLANEOUS LUBRICATION
FLEX CABLE	LOWEST	POSSIBLE.	LOWEST I^2R.	FIRST (LOWEST)	STATE-OF-THE-ART	INDIVIDUAL STRANDS LUBRICATED WITHIN SHEATH
ROTARY TRANSFORMER	HIGHEST	POSSIBLE.	HIGHEST LOSSES (DUE TO INVERTER)	DEPENDENT ON SIZE AND EFFICIENCY.	INDUSTRIAL UNITS OFF THE SHELF. SPACE UNITS NEED DEV	NONE
ROLLING CONTACT	INTERMEDIATE	FATIGUE PROBLEMS.	INTERMEDIATE I^2R. OVERCOME BEARING FRICTION.	FOURTH	WORKING MODELS BUT NEED DEVELOPMENT.	CONDUCTIVE DRY LUBE

SEE REFERENCE 8

Fig. 3.2-7 Power Transfer Device Selection Considerations
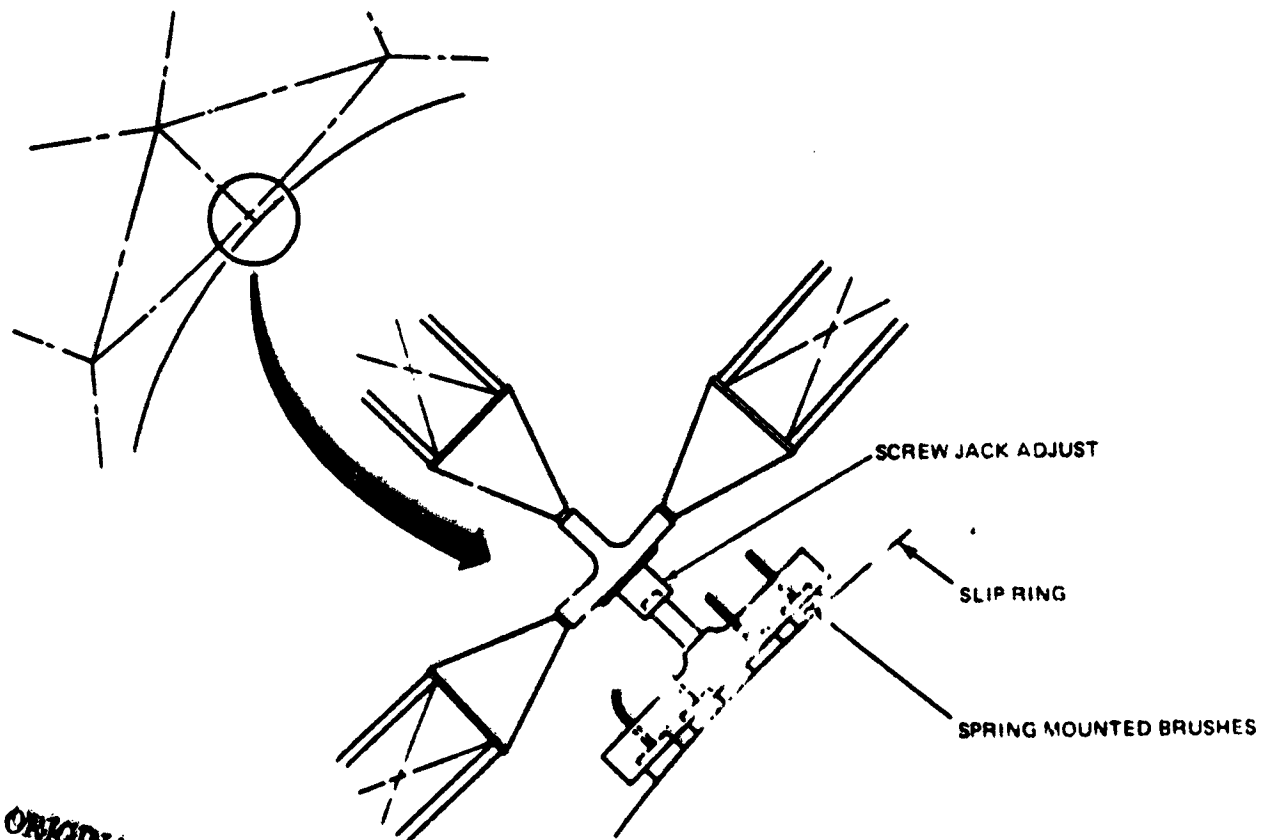
Fig. 3.2-8 Brush/Slip Ring Concept

SCREW JACK ADJUST

SLIP RING

SPRING MOUNTED BRUSHES

	VAC KOTE LUBED SILVER/GRAPHITE		MoS$_2$ LUBED SILVER/COPPER	NbSe$_2$ LUBED SILVER
	50 A/IN^2	100 A/IN^2	50 A/IN^2	60 A/IN^2
COPPER SLIP RINGS				
SLIDING				
4 PSI	88; 73-74	—		
8 PSI	63; 60-63	—		
10-12 PSI	80-81	—		
13-16 PSI	50-60			
STATIC				
4 PSI	76	—		
8 PSI	54	—		
10-12 PSI	75-78	—		
13-16 PSI	50-61	—		
SILVER SLIP RINGS				
SLIDING				
4 PSI	72-76	100-102	49-56	61-63
8 PSI	35-58	38-51	—	—
STATIC				
4 PSI	58-62	82-88	44-49	50-51
8 PSI	32-46	39-47	—	—

Fig. 3.2-9 Operating Temperatures (^{O}C) of Candidate Brushes

BRUSHES	VAC KOTE LUBED SILVER/GRAPHITE				MoS$_2$ LUBED SILVER/ COPPER	NbSe$_2$ LUBED SILVER
	50 A/IN^2		100 A/IN^2		50 A/IN^2	50 A/IN^2
COPPER SLIP RINGS						
SLIDING FOR:	~ 200 HR	~ 650 HR				
4 PSI	0.25	0.18				
8 PSI	0.18	0 17				
10-16 PSI	0.22	—				
STATIC FOR:	~ 375 HR					
4 PSI	0.14					
8 PSI	0.14					
10-16 PSI	0.17					
SILVER SLIP RINGS						
SLIDING FOR:	~ 200 HR		~ 200 HR		200 HR	200 HR
4 PSI	0.25		0.34		0 09	0 08
8 PSI	0.20		0.23		—	—
STATIC FOR:	~ 375 HR		~ 375 HR	~ 1200 HR	~ 375 HR	~ 375 HR
4 PSI	0.20		0.27	0.25	0 073	0.066
8 PSI	0.19		0.21	0.20		

Fig. 3.2-10 Voltage Drop for Candidate Brushes (for Single Contacts)

Liquid sodium has potential as a slip ring liquid because of good conductivity, wetting and viscosity characteristics. Theoretically, such a device would carry current with low power loss and low torque drag. The main problem is foreseen as development of a long life, low friction seal to keep the liquid contained. Such a seal would be sensitive to temperature change, contamination, and corrosion. It might prove difficult to lubricate and on-line maintenance or seal replacement could prove complicated.

Because of high development risk, lack of design information, constraints on structural configuration, and lower life/reliability rating than conventional slip rings, liquid metal slip rings are not recommended for baseline development but should be considered as a potential technology study.

3.2.2.7 Power Clutch and Flexible Cable

A power clutch holds two contacts fixed together while they move through part of a revolution, and then the contacts break apart and reset to an initial position, and the cycle repeats. The relative motion is allowed for by a flexible cable. For SSPS application, two sets of contacts would be required so one could carry the load while the other reset. The advantage is a lower contact resistance and lower wear rate than with brushes and slip rings, but the greater mechanical complexity and redundant mechanism required would probably trend toward higher weight and lower reliability.

3.2.2.8 Rotary Transformer

A rotary transformer could be designed to operate at high efficiency with no wear (no contact), but the high efficiency would require heavy core material and a close tolerance gap. Since SSPS is a DC system, an additional penalty would have to be added for DC-DC power conversion. Rotary transformers do provide low friction and should be considered as a potential technology study.

3.2.2.9 Rolling Contact

A rolling contact device transferring power through either gears or bearings is inefficient as an electrical conduction path because contact areas are essentially lines or points unless there is deformation - in which case metal fatigue becomes a problem. It is not recommended.

3.2.2.10 Lubrication

Lubricant options include oil, grease and solids. Figs 3.2-11 and 3.2-12 (based on data from Ref 8) summarize test data on various candidate oils and grease. The 30-year life

TEST CONDITIONS:

LOAD	10 KG (INITIAL HERTZ STRESS = 210,000 PSI)
SPEED	600 RPM (45 FT/MIN SLIDING)
DURATION	90 MINUTES
BALLS	52100 STEEL

CANDIDATE OIL	MIN. COEF. OF FRICTION			WEAR SCAR DIA., MM		
	38°C	70°C	100°C	38°C	70°C	100°C
VAC KOTE PETROLEUM	0.089 0.094	0.096	0.096	0.401 0.432	0.479	0.483
VAC KOTE ESTER	0.065	0.088	0.093	0.280	0.276	0.273
VAC KOTE ETHER	0.122	0.118	0.114 0.113	0.241	0.220	0.224 0.207
KRYTOX 143 AB	0.113*	0.105*	0.098*	0.381	0.308	0.363
XRM 217D	0.080	0.073	0.073	0.211	0.195	0.198
VERSILUBE F-50	0.096*	ERRATIC*	0.080*	0.491	0.445	0.488
FS-1265	0.065	0.083	0.072	0.194	0.207	0.381
* NOISY SLIDING						
SEE REFERENCE 8						

Fig. 3.2-11 Friction and Wear Properties of Oils (Four-Ball Test)

TEST CONDITIONS:

LOAD	10 KG (INITIAL HERTZ STRESS = 210,000 PSI)
SPEED	600 RPM (45 FT/MIN SLIDING)
DURATION	90 MINUTES
BALLS	52100 STEEL

CANDIDATE GREASE	MIN. COEF. OF FRICTION			WEAR SCAR DIA., MM.		
	38°C	70°C	100°C	38°C	70°C	100°C
VAC KOTE ESTER BASE	0.071	0.083	0.098	0.379	0.389	0.384
VAC KOTE PETRO. BASE	0.080	0.073	0.071	0.416	0.494	0.525
DUPONT PL-631	0.120**	0.106	0.100	0.413	0.298	0.256
KRYTOX 240 AC	0.106**	0.110**	0.120	0.517	0.424	0.368
SUPERMIL M125	0.089**	0.083**	0.077‡* (60 MIN)	0.384	0.445	0.328* (60 MIN)
VERSILUBE G-300	0.174‡* (13 MIN)	0.093‡* (15 MIN)	0.22‡* (ZERO MIN)	0.504* (13 MIN)	0.456 (15 MIN)	0.560* (ZERO MIN)

* FAILED AT TIME INDICATED DUE TO HIGH FRICTION (≥ 0.22)
** NOISY SLIDING

Fig. 3.2-12 Friction and Wear Properties of Greases (Four-Ball Test)

requirement is the most significant consideration, with little or no data to support a selection. Vac Kote lubricants have proven highly reliable in OSO and other spacecraft slip ring, gear and motor applications. Greases have the same basic characteristics as the oils with appropriate thickening agents added. Greases should be used only where leakage is too high to retain an oil. Solids would have application for slip ring and motor brushes.

3.2.3 Primary/Secondary Antenna Structure

The basic structure consists of 20 major beams perpendicular to each other to form a grid of squares 108 meters on each side. The secondary structure located within these grids form a denser grid of squares 18 meters on each side. The major beam "upper" caps are girder/columns consisting of three longitudinal members equidistant apart. At appropriate intervals, cross bracing and tension wires are added to balance the shear loads. The "lower" cap of the primary structure is identical to the secondary structure which is a beam consisting of girder/columns five meters apart. These are of similar construction to the primary members but scaled down. All beams are given shear capability by virtue of wire/cables connected in the manner of a drag truss. Horizontal shear capability is obtained in a like manner by attaching cables at the upper beam caps across the 108 meter bays. See Fig. 3.2-13 for a typical 108 meter bay structural arrangement.

3.2.4 Structure/Waveguide Interface

Two methods of attaching the waveguide assembly to the secondary structure have been identified:

- The Single Point Pickup (Fig. 3.2-14) consists of a two-axis motor driven gimbal located at each 18 meter intersection. Lugs on this unit attach to composite structural members which support the waveguide assembly and effectively prevent any conductive heat transfer. The gimbal provides means of varying the mounting attitude of the waveguide assembly to account for structural/thermal deformations in the structure.

- The Three Point Support (Fig. 3.2-15) requires three motor driven screw jacks at each 18 meter intersection. Each one is mounted on a two axis gimbal which, when coupled to the screw jack action, provides rotational and translational adjustment. Conductive heat transfer is minimized by the use of composite fittings to interface with the screw jacks.
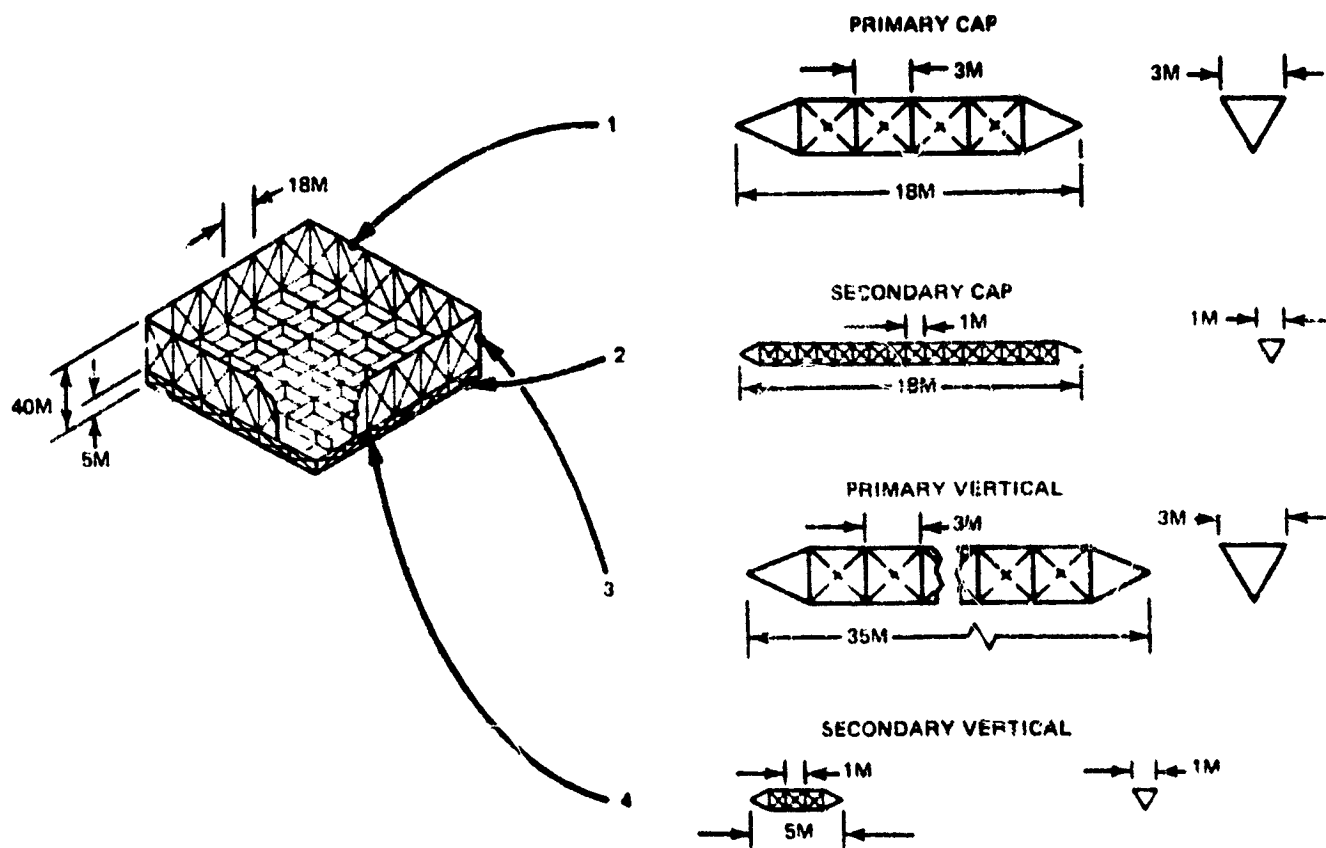
Fig. 3.2-13 Structural Members

ANTENNA SECONDARY STRUCTURE

GIMBAL

COMPOSITE STRUTS
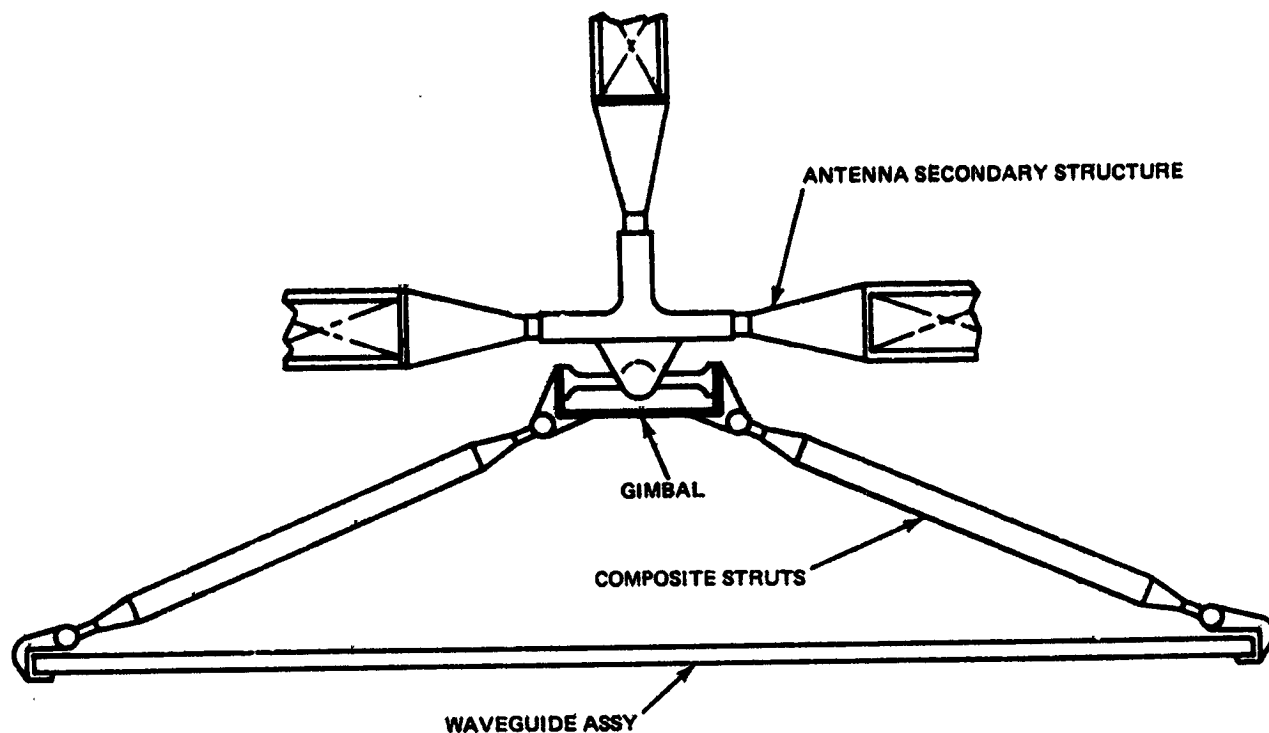
WAVEGUIDE ASSY

Fig. 3.2-14 Waveguide/Structure Interface, Single Point Support

REQUIREMENTS

- EXTENSION 16 IN. (40.6 CM)
- ROTATION ±4 ARC MINUTES

WT EST/ACTUATOR (ALUM)		
	LB	Kg
SHAFT	20.0	9.06
WORM	3.8	1.72
MOTOR	5.0	3.89
THERMAL ISOL	1.6	0.72
GEAR BOX & GIMBAL	6.6	2.98
	44.0	19.93

ANTENNA SECONDARY STRUCTURE

GIMBAL

MOTOR GEAR BOX-SCREW JACK ASSY (3)

WAVEGUIDE ASSY

THERMAL ISOLATION FITTING
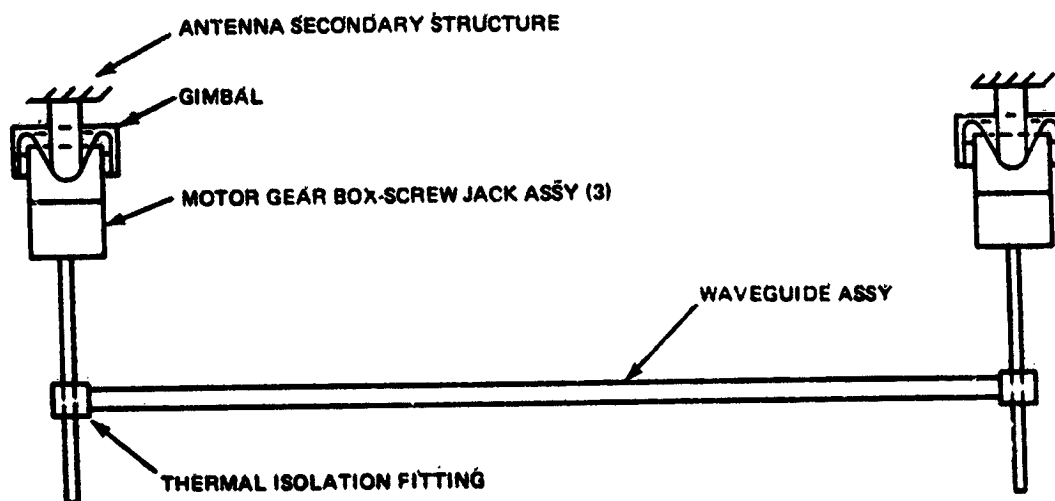
Fig. 3.2-15 Waveguide/Structure Interface, Three Point Support

C.2

3.2.5 Antenna Weight and Mass Properties

Weight of the structural installation for the SSPS microwave antenna evolved from considerations and analysis of the effect of weight on antenna size, materials and coatings, type of construction, manufacturing tolerances, deployment and space assembly, carrier system integration, SSPS life requirements in space environment, and thermal design requirements. The assumptions, weight drivers, weight trades and the resulting detail weight estimate for the antenna structure is included in the following discussion of study results.

3.2.5.1 Antenna Structure Weight

Weight of the antenna structure itemized in Fig. 3.2-16 is 410920 kg (904032 lb). The assumptions made to estimate weight are:

- Antenna diameter: 1 Km

- Material: Graphite/epoxy with thermal coatings (weight of graphite/polyimide is same as for graphite/epoxy)

- Primary Structure: Rectangular grid beams at 108 meter intervals. The structure is built up from structural beams 18 meters long, each of which is constructed from three longitudinal members 18 meters long braced at 3 meter intervals. The height of the primary structure is 35 meters

- The secondary structure is built up from 18 meter beams braced at three meter intervals. The secondary structure height is 5 meters and forms the grid for antenna electronic equipment support and spans across the primary structure spacing of 108 meters.

- Weight penalties for the power distribution bus are not included.

3.2.5.2 Alternate Materials and Structural Shape Study

Weight study results considering two types of structural shapes (tubular and triangular hat sections) and two materials (2024 T-6 Aluminum and graphite/epoxy) show that graphite/epoxy is 41% lighter than aluminum for a tubular section and 21% lighter for the triangular hat section. The triangular hat section is 40% heavier than the tubular section (in graphite/epoxy) (Fig. 3.2-17 and 3.2-18).

3.2.5.3 Weight Parametrics and Drivers

- <u>Loads</u> - The primary antenna loads are introduced into the antenna by the control actuators which must overcome the slip ring force. Gravity gradient, atmospheric, and magnetic forces are small when compared to the actuator force.
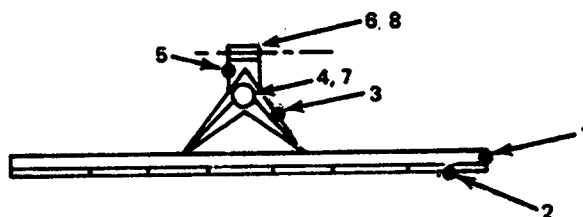
	ITEM	WEIGHT	
		LB	KG
1	SUBARRAY PRIMARY STRUCTURE	206,873	94,034
2	SUBARRAY SECONDARY STRUCTURE	65,452	29,749
3	ELEVATION JOINT SUPPORT	10,082	4,582
4	ELEVATION YOKE	42,241	19,200
5	AZIMUTH JOINT SUPPORT	8,951	4,069
6	AZIMUTH YOKE	95,633	43,470
7	ELEVATION MECHANISMS	97,500	44,318
8	AZIMUTH MECHANISMS & ATTACH.	24,300	11,045
9	AMPI 'TRON SUPPORT & ACTUATORS	304,000	138,131
10	COA INGS	49,000	22,272
	TOTAL ANTENNA STRUCTURE	904,032	410,920

Fig. 3.2-16 Antenna Structure Weight Summary (Graphite/Epoxy Triangular Hat)

	ALUMINUM (2024-t6)		COMPOSITE (GR/EP)	
• TEMPERATURE, °F	350		400	
• MODULUS OF ELASTICITY, PSI	9×10^6		9×10^6	
• DENSITY, LB/IN.^{3}	0.101		0.055	
• THICKNESS RANGE, IN.	0.006 TO 0.011		0.006 (3 PLIES)	
• WEIGHT	LB 10^3	KG	LB (10^3)	KG
— SUBARRAY PRIMARY STRUCTURE	214	97	104	47
— SUBARRAY SECONDARY STRUCTURE	101	46	53	24
— ANTENNA SUPPORT STRUCTURE	105	48	52	24
— YOKE AND MECHANISMS	111	51	90	41
— COATINGS	60	27	44	20
— AMPLITRON SUPPORT				
• CONTOUR CONTROL ACTUATORS	268	122	268	122
• AMPLITRON ATTACH STR	51	23	36	16
TOTAL	910	414	647	294

Fig. 3.2-17 Antenna Weight Comparison (Aluminum vs Composites Tubular Section)

	ALUMINUM (2024-t6)		COMPOSITES (GR/EP)	
• TEMPERATURE, °F	350		400	
• MODULUS OF ELASTICITY, PSI	9×10^6		6×10^6	
• DENSITY, LB/IN^3	0.101		0.055	
• THICKNESS RANGE, IN.	0.015 TO 0.040		0.020 TO 0.055	
• WEIGHT	LB (10^3)	KG	KB (10^3)	KG
— SUBARRAY PRIMARY STRUCTURE	300	137	207	94
— SUBARRAY SECONDARY STRUCTURE	103	47	65	30
— ANTENNA SUPPORT STRUCTURE	233	106	157	71
— YOKE AND MECHANISMS	146	66	122	56
— COATINGS	46	21	49	22
— AMPLITRON SUPPORT				
• CONTOUR CONTROL ACTUATORS	268	122	268	122
• AMPLITRON ATTACH STR	51	23	36	16
TOTAL	1147	522	904	411

Fig. 3.2-18 Antenna Weight Comparison (Aluminum vs Composites Triangular Hat Section)

- **Materials** – Materials considered for further analysis during the study were anodized aluminim and graphite composites. The latter appears to be a promising choice for the antenna structure due to its lower thermal expansion and high stiffness/density ratio.

- **Element Member Shape** – Two structural shapes were considered in the weight analysis, namely thin walled tube and a triangular hat section. The triangular hat section, although heavier than the tube, has considerably smaller thermal gradients across the section and is therefore a more desirable section.

- **Type of Construction** – Two methods of structural arrangement have been compared on a weight basis; rectangular grid and a radial grid. The results showed that the rectangular grid has a 25% weight advantage over the radial design.

- **Manufacturing Tolerances** – The wall thickness tolerances on standard commercially available tubes are ±10%. A + 10% tolerance on tube weight would increase the antenna structured weight by 13,600 Kg (30000 lb).

- **Antenna and Antenna Bay Size** – During Task 1 of this study, antenna sizing relation-ships were established to aid in selecting major antenna dimensions. Figure 3.2-19 shows the result of these studies using early configurations. The trends are valid for the final reported configuration weight.

- **Antenna Mass Properties** – Figure 3.2-20 gives the weight, center of gravity, and moments of inertia of the SSPS antenna. The moments about the antenna center of gravity and about the azimuth yoke pivot are given for a total SSPS antenna weight of 1.67×10^6 kg.

3.2.5.4 Antenna Structural Weight Derivation

The antenna structural weights were derived using the results of preliminary load, thermal, and stress analyses together with "Structural Arrangement for the MPTS Antenna" (DWG No. MPTS-001). Individual members were sized using a weight optimization technique which equates the Euler column buckling stress to the local buckling stress and the applied stress. The sections resulting from this analysis will be optimum for given material proporties, section shape loading requirements and end fixity requirements. Figure 3.2-21 summarizes the weight, dimensions and quantities of the elements and beams which make up the structure of the SSPS antenna. Included are weight estimates of the antenna azimuth and

ASSUMPTIONS:

L = 25M

DIA

H
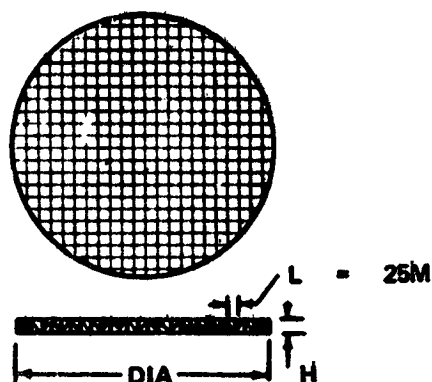
CAPS

- 100 LB LOAD END
  OF 25 METER CAP

- SIZE SO THAT LOCAL
  WALL BUCKLING AND
  COLUMN STRESS ARE
  EQUAL

  - RADIUS = 2.2 CM

  - THICK* = .0128 CM

*T$_{MIN}$ = .0128 CM

25M
5 M

H = 55M
40
25
10

WEIGHT RATIO

DIAMETER—METERS

500   1000   1500

PRIMARY BAY
SIZE

WEIGHT RATIO

1.5
1.0
0.5

50   100   150

BAY SIZE-METERS
(PRIMARY STR.)

SECONDARY BAY
SIZE

WEIGHT RATIO

1.2
1.0
0.8

0   5   10

BAY SIZE-METERS
(SECONDARY STR.)
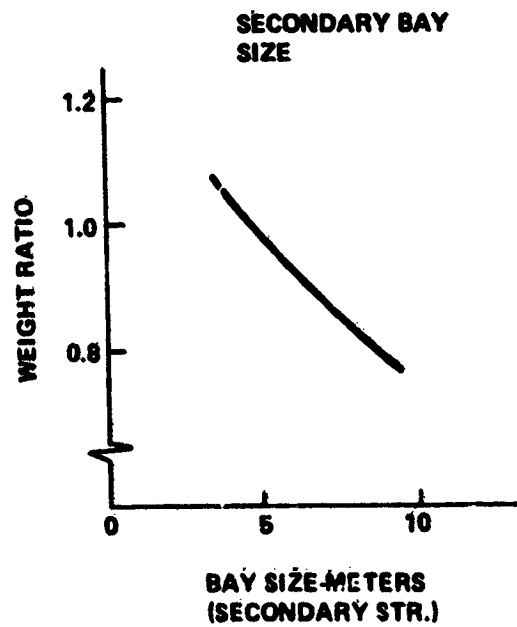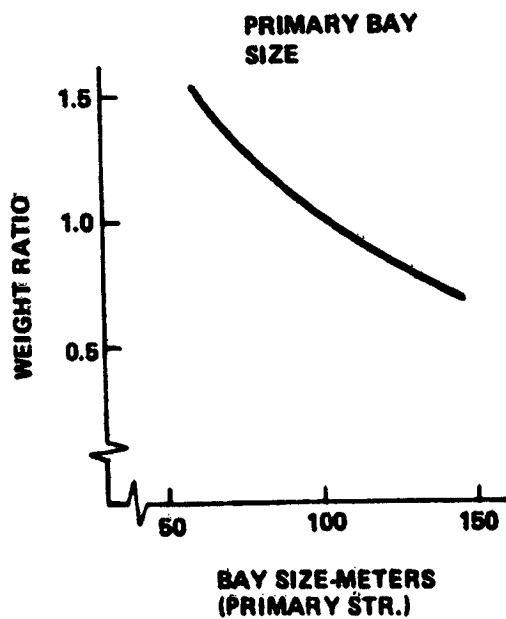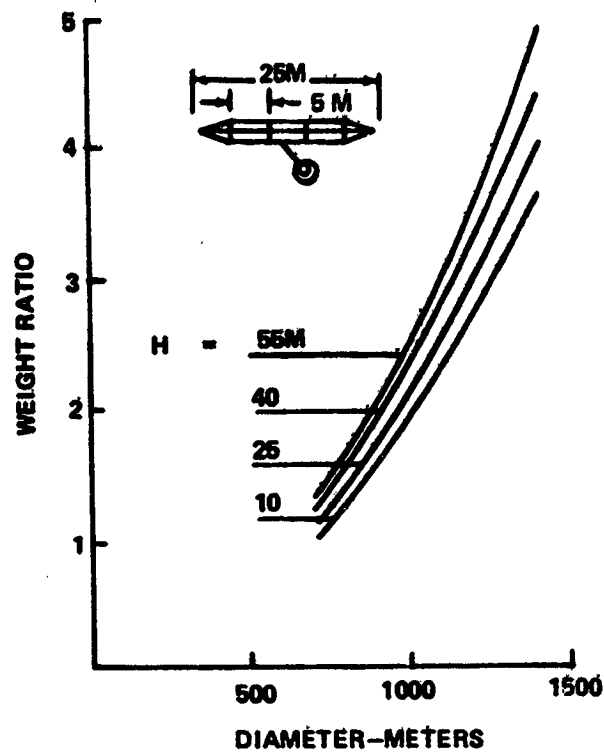
Fig. 3.2-19 Structure Weight vs Antenna Dimension

3.2-22
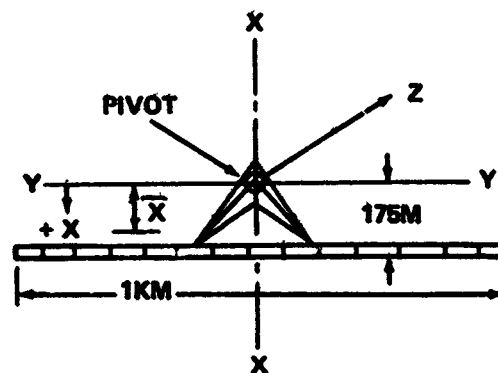
1. MASS PROPERTIES ABOUT ANTENNA C.G.

WEIGHT		3.68×10^6 LB	$(1.67 \times 10^6$ Kg)	
$\bar{X}$	=	466 FT	(142 METERS)	
$\bar{Y}$	=	0	(0)	
$\bar{Z}$	=	0	(0)	
I_{XX}(CG)		125756×10^6 SLUG-FT^2	$(170487 \times 10^6$	Kg-M^2)
I_{YY}(CG)		66332×10^6 " "	$(89926 \times 10^6$	Kg-M^2)
I_{ZZ}(CG)		66332×10^6 SLUG "	$(89926 \times 10^6$	Kg-M^2)

2. MASS PROPERTIES ABOUT PIVOT

WEIGHT		3.68×10^6 LB	$(1.67 \times 10^6$ Kg)	
$\bar{X}$	=	466 FT	(142 METERS)	
$\bar{Y}$	=	0	(0)	
$\bar{Z}$	=	0	(0)	
I_{XX}(PIVOT)	=	125756×10^9 SLUG-FT^2	$(170487 \times 10^6$	Kg)
I_{YY} (PIVOT)	=	91169×10^6 " "	$(123597 \times 10^6$	Kg-M^2)
I_{ZZ}(PIVOT)	=	91169×10^6 " "	$(123597 \times 10^6$	Kg-M^2)

Fig. 3.2-20 SSPS Microwave Antenna Mass Properties

Fig. 3.2-21 Antenna Structure Weight

ITEM	BEAM LENGTH, M	ELEMENT SIZE		L, M(1)	BEAM UNIT WT		BEAM QTY	TOTAL WEIGHT	
		HEIGHT, CM	THICK, MM		LB	KG		LB	KG
SUBARRAY PRIMARY STRUCTURE								(206873)	(94034)
CAPS – UPPER CIRCUM	18	3.89	0.51	3.0	33.1	15.1	174	5769	2618
CAPS – UPPER TRANSV	18	3.89	0.51	3.0	33.1	15.1	792	26216	11916
POSTS – CIRCUM	35	6.21	0.76	6.0	128.3	57.5	174	21976	9969
POSTS – TRANSV	35	6.21	0.76	6.0	128.3	57.5	684	86388	39288
SHEAR TIES–UPPER	152	–	0.40	–	8.5	3.9	62	530	241
SHEAR TIES – VERT.	39.4	–	0.31	–	1.35	0.6	966	1310	595
SHEAR TIES – LOWER	25	–	0.31	–	0.85	0.4	2240	1900	864
CAPS – LOWER CIRCUM	18	2.36	0.203	3.0	7.40	3.4	174	1288	585
CAPS – LOWER TRANSV	18	2.36	0.263	3.0	7.40	3.4	4717	34906	15966
BEAM CONNECT FITTINGS		10.16	2.5	6.5			3941	21800	9910
SHAFT-ELEVATION JOINT		6.27	0.13	3.0				4800	2182
SUBARRAY SECONDARY STRUCTURE								(85452)	(38749)
CAPS–LOWER CIRCUM	18	2.36	0.20	3.0	7.40	3.4	174	1288	585
CAPS–LOWER TRANSV	18	2.36	0.20	3.0	7.40	3.4	4717	34906	15966
POSTS–CIRCUM	5	2.36	0.20	3.0	2.09	0.94	174	364	165
POSTS–TRANSV	5	2.36	0.20	3.0	2.09	0.94	2777	5804	2638
SHEAR TIES–TRANSV	25	–	0.31	–	0.68	0.39	2240	1930	877
SHEAR TIES–VERTICAL	18.7	–	0.31	–	0.65	0.30	4981	3160	1436
BEAM CONNECT FITTINGS		10.16	2.54	6.5			3081	18000	8182
ANTENNA SUPPORT STRUCTURE					LB/FT	Kg/M	LENGTH,M	(1569071)	(713221)
ELEVATION JOINT SUPPORT	–	6.27	1.27	3.0	2.30	3.44	1283	10082	4582
ELEVATION YOKE	–	6.27	1.27	3.0	2.65	3.95	4876	42241	19200
AZIMUTH JOINT SUPPORT	–	6.55	1.30	3.0	2.65	3.95	1030	8951	4069
AZIMUTH YOKE	–	6.55	1.39	3.0	2.68	3.95	9832	95633	43470
MECHANISMS								(121800)	(55363)
AZIMUTH-JOINT								97500	44318
ELEVATION JOINT								24300	11045
AMPLITRON SUPPORT & ACTUATORS	– –							(304000)	(138181)
COATINGS	– –							(49000)	(22272)
TOTAL ANTENNA STRUCTURE								904032	410920

elevation joint mechanisms. Figure 3.2-22 through 3.2-32 give the detail sizes and assumptions made for each item in Fig. 3.2-21.

An investigation was made to consider the use of a Linear Induction Motor (LIM) for the rotary joint actuation in lieu of a motorized gear drive. Figure 3.2-33 compares the weight of the motorized gear drive with a large (4000 lb) LIM used on the TACRV (Grumman contract to the Department of Transportation) and a multiple step motor concept. The antenna requirements of low speed and high torque make the multiple step motor a contender as the drive for the antenna.
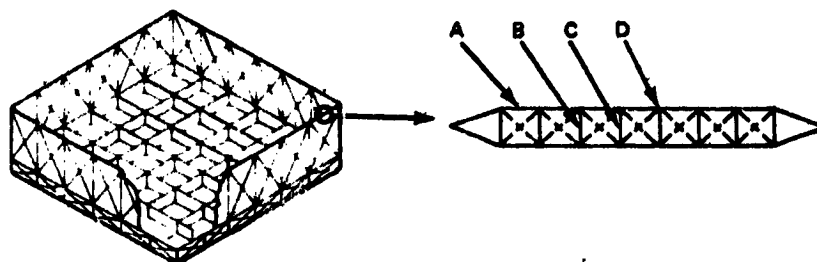
	LENGTH, M	HEIGHT, CM	t, MM	NUMBER/ BEAM	TOTAL WEIGHT	
					LB	KG
A. LONGITUDINALS	18	3.89	0.508	3	13.0	5.9
B. LATERALS	3	3.89	0.508	15	10.8	4.9
C. WIRES	4.2	0.31	—	24	1.7	0.8
D. FITTINGS & ATTACHMENTS					7.6	3.5
TOTAL UNIT BEAM WEIGHT					33.1	15.1

TOTAL NUMBER REQD/ANTENNA

CIRCUMFERENCE   174
TRANSVERSE   792

ASSUMPTIONS: PCAP 360 LB, MODULUS OF ELASTICITY 6×10^6 PSI
L = 118 INCHES/ELEMENT, GRAPHITE-EPOXY

Fig. 3.2-22 Primary Structure (Upper Caps)
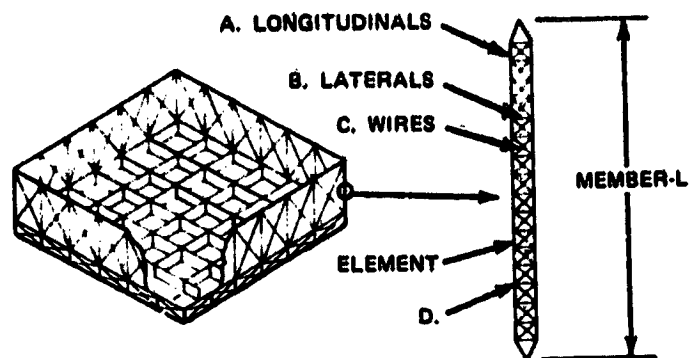
	LENGTH, M	HEIGHT, CM	t, MM	NUMBER/ POST	TOTAL WEIGHT	
					LB	KG
A. LONGITUDINALS	35	6.71	0.762	3	65.3	29.7
B. LATERALS	3	6.71	0.762	15	27.9	12.7
C. WIRES	8.5	0.31	—	24	3.9	1.8
D. FITTINGS & ATTACHMENTS					29.2	13.3
TOTAL BEAM WEIGHT					126.3	57.5

NUMBER RFQD/ANTENNA

CIRCUMFERENCE = 174
TRANSVERSE = 684

ASSUMPTIONS: P_{POST} = 750 LB, MODULUS OF ELASTICITY 6 X 10^6 PSI
L = 230 INCHES/ELEMENT, GRAPHITE/EPOXY

Fig. 3.2-23 Primary Structure (Posts)

	LENGTH, M	DIA, CM	t, MM	NUMBER/ BEAM	TOTAL WEIGHT LB	TOTAL WEIGHT Kg
A. LONGITUDINALS	18	2.36	0.203	3	3.22	1.5
B. LATERALS	0.9	2.36	0.203	15	0.83	0.4
C. WIRES	3.1	0.31	—	24	1.8	0.8
D. FITTINGS & ATTACHMENTS					1.55	0.7
TOTAL WEIGHT					7.40	3.4

NUMBER REQD/ANTENNA

    CIRCUMFERENCE   174
    TRANSVERSE   4717

ASSUMPTIONS: P_{CAP} = 30 LB, MODULUS OF ELASTICITY 6 X 10^6 PSI

                  L = 118 INCHES, GRAPHITE/EPOXY

* SAME AS SECONDARY UPPER STRUCTURE AND SECONDARY LOWER STRUCTURE.

Fig. 3.2-24 Primary Structure (Lower Caps*)
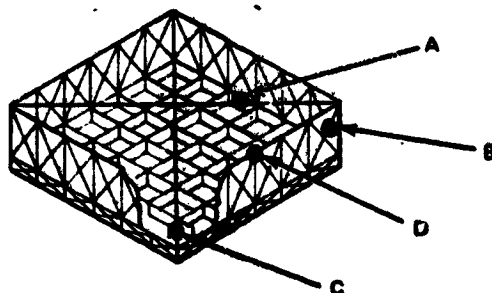
ITEM	LENGTH, M	DIA, CM	NUMBER/ ANTENNA	TOTAL WEIGHT LB	TOTAL WEIGHT Kg
A. UPPER SHEAR TIES	152.0	0.4	62	530	241
B. VERTICAL SHEAR TIES	39.4	0.31	968	1310	595
C. LOWER SHEAR TIES	25.0	0.31	2240	1900	864
D. FITTINGS-PRIMARY			3941	21,800	9910

Fig. 3.2-25 Primary Structure Integration Items

• UPPER AND LOWER CAPS

SAME AS PRIMARY STRUCTURE LOWER CAPS

• POSTS
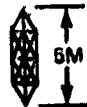
	LENGTH, M	DIA, CM	t, MM	NUMBER/ BEAM	TOTAL WEIGHT LB	TOTAL WEIGHT KG
1. LONGITUDINAL	6.0	2.36	0.203	3	0.81	2.37
2. TRANSVERSE	0.9	2.36	0.203	9	0.50	0.22
3. WIRES	1.4	0.31	—	12	0.30	0.14
4. FITTINGS & ATTACHMENTS					0.48	0.21
TOTAL BEAM WEIGHT						0.94

CAPS

NUMBER REQD/ANTENNA
    CIRCUMFERENCE   174
    TRANSVERSE   4717

POSTS

/ANTENNA
    CIRCUMFERENCE   174
    TRANSVERSE   2777

Fig. 3.2-26 Secondary Structure
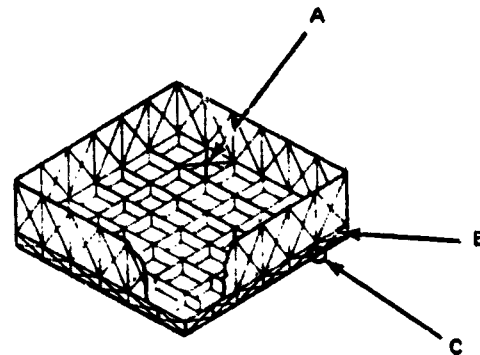
ITEM	LENGTH, M	DIA, CM	NUMBER· ANTENNA	TOTAL WEIGHT LB	TOTAL WEIGHT KG
A. LOWER SHEAR TIES	25	0 31	2240	1930	877
B. VERTICAL SHEAR TIES	18.7	0 31	4881	3160	1436
C. FITTINGS-SECONDARY			3019	18,000	8182

Fig. 3.2-27 Secondary Structure Integration Items

3.2-29
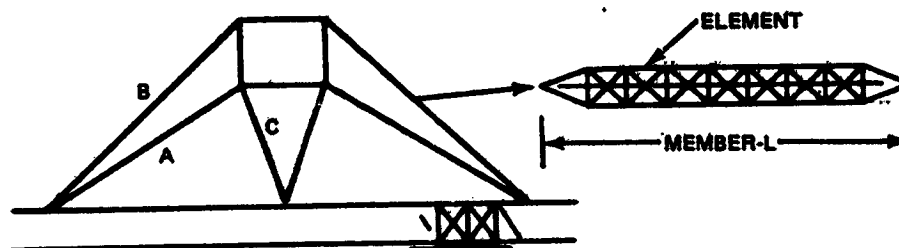
MEMBER	ELEMENT HEIGHT, CM	T, MM	MEMBER LENGTH, L, M	NUMBER/ ANTENNA	MEMBER WEIGHT, LB	TOTAL WEIGHT	
						LB	KG
A	6.27	1.27	66.7	8	604	4032	1838
B	6.27	1.27	79.3	8	599	4792	2178
C	6.27	1.27	28.7	4	217	868	394
FITTINGS				38		380	172
TOTAL PER ANTENNA						10,082	4582

ASSUMPTIONS.
Pmember = 4000 LB, MODULUS OF ELASTICITY 6 X 10^6 PSI, PINNED END,
118"/ELEMENT — GRAPHITE EPOXY

Fig. 3.2-28 Elevation Joint Support
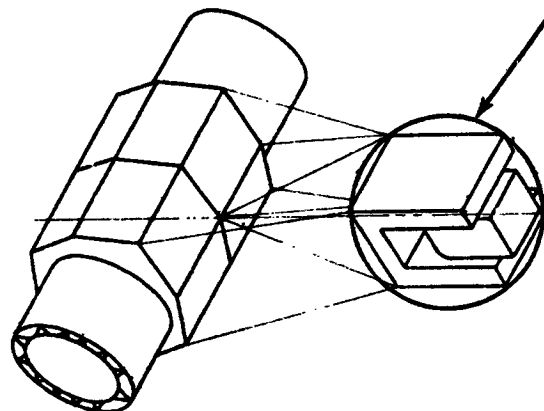
	6.27 CM
● ELEMENT HEIGHT	6.27 CM
● ELEMENT THICKNESS	1.27 MM
● ELEMENT SPACING	3 M
● BEAM WIDTH	3 M
● BEAM UNIT WEIGHT	3.44 Kg/METER
● TOTAL MEMBER LENGTH	4876 METERS

● WEIGHT	LB	Kg
— MEMBERS	36901	16773
— BEAM FITTINGS	1500	682
— MISC ATTACH.	3840	1745
TOTAL YOKE	42241	19200

ASSUMPTIONS:

P member = 5000 LB, MODULUS OF ELASTICITY 6 X 10^6 PSI PINNED END COLUMN
L = 118^0 INCHES/ELEMENT, GRAPHITE-EPOXY

Fig. 3.2-29 Elevation Yoke
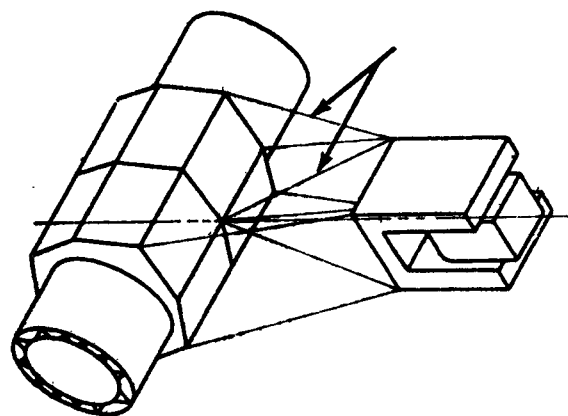
• ELEMENT DIAMETER	6.55 CM
• ELEMENT THICKNESS	1.39 CM
• ELEMENT SPACING	3M
• BEAM WIDTH	3M
• BEAM UNIT WEIGHT	3.95 Kg/METER
• TOTAL MEMBER LENGTH	1030 METERS
• TOTAL WEIGHT	8951 LB (4069 Kg)

ASSUMPTIONS:

P_{member} = 5000 LB, MODULUS OF ELASTICITY 6 X 10^6 PSI
L = 118 INCHES/ELEMENT, GRAPHITE-EPOXY

Fig. 3.2-30 Azimuth Yoke Support

		LB	Kg
• ELEMENT DIAMETER	6.5.`		
• ELEMENT THICKNESS	1.39 MM		
• ELEMENT SPACING	3M		
• BEAM WIDTH	3M		
• BEAM UNIT WEIGHT	3.95 Kg/METER		
• TOTAL MEMBER LENGTH	9832 METERS		
• WEIGHT		LB	Kg
— MEMBERS		85439	38836
— BEAM FITTINGS		1500	682
— ATTACHMENTS		8694	3952
TOTAL YOKE		95633	43470

ASSUMPTIONS: Pmember = 5000 LB, MODULUS OF ELASTICITY 6×10^6 PSI, PINNED END COLUMN L = 118 INCHES/ELEMENT, GRAPHITE/EPOXY

Fig. 3.2-31 Azimuth Yoke

AZIMUTH ROTARY JOINT

- ANTENNA SPEED 0.728×10^{-4} RAD/SEC
- GEAR REDUCTION 2.47×10^{5}
- MOTOR SPEED   18.4 RAD/SEC
- MOTOR TORQUE   2.8 FT-LB (THEORETICAL-NEGLECTING FRICTION)

- WEIGHT

	LB	Kg
— GEAR BOX & MOTORS	24065	10938
— DRIVE	2389	1086
— BRUSHES	1100	500
— SUPPORT	21196	9634
TOTAL EACH (TWO REQD)	48750	22158
	(97500)	(44316)

ELEVATION JOINT

- SCALED FROM ASMUTH ROTARY JOINT
- TOTAL WEIGHT = 12,150 X 2 REG = 24,300 LB (11,045 Kg)

Fig. 3.2-32 Mechanisms and Support

MECHANICAL (MOTOR/GEARS)		LINEAR INDUCTION MOTOR		
		LINEAR STEP		TACRV
	LB		LB	LB
GEARBOX	24065	LIM	2214	4000
DRIVE	2389	ARMATURE	432	1000
BRUSHES	1100	BRUSHES	1100	1100
SUPPORT	8987	SUPPORT	8000	6000
EACH	36541	EACH	11746	12100
2 REQD		(2)	23492	(2)24200
		POWER CONDITIONING	4000	12208
TOTAL LB	73802	TOTAL LB	27492	36408
Kg	(33216)	Kg	(12500)	(16100)

Fig. 3.2-33 Rotary Joint Drive (Mechanical vs Linear Induction Motor)

3.3 CONFIGURATION ANALYSIS

3.3.1 Control Analysis

The characteristics of a phased array Microwave Power Transmission System eliminates the need for mechanical fine pointing of the antenna. Signal phasing compensates for misalignment and distortions in antenna surface up to 1/16 of a wavelength with minimal loss in transmission efficiency. An overall antenna misalignment error of ± 1 arc-min can be tolerated by the subarrays. The purpose of this subtask is to define the environment and load requirements for the design of the antenna pointing system servomechanisms, define the best accuracy that can be achieved with this system and identify the likely design approach.

3.3.1.1 Spacecraft Torque Environment

Figure 3.3-1 summarizes the torque environment for the baseline SSPS system (Ref. 2). Torque calculations are based on the configuration data presented in Fig. 3.1-2 and the following additional groundrules:

- Baseline orbit - equatorial geosynchronous

- Baseline attitude - long axis (X-axis) perpendicular to orbit plane, the solar array normal (Z-axis) parallel to the projection of the sun vector onto the orbit plane.

The external disturbance torques are induced by aerodynamic, solar pressure, magnetic and gravity gradients. Gravity gradient torque predominates the induced torque environment by several orders of magnitude and will be the only source of external torque used to define mechanical system requirements.

Control system torque levels are limited by SSPS structural bending. A force level of 2980N (667 lb) used for orbit keeping and applied at the corners of the solar array, was found in Ref. 3 to be the maximum force at which structural deflections can be limited to ± 1 deg. This force, however, induces symmetric bending and does not affect antenna motion. A 44.5N (10 lb) coupled jet firing is used for attitude control and induces antisymmetric bending modes which do impact control system design.

3.3.1.1.1 <u>Antenna Motion Relative To Spacecraft</u> - Figure 3.3-2 shows a typical system that provides rotation in azimuth and elevation. The azimuth rotary joint is located at the mast interface between the antenna assembly and the solar arrays. Azimuth motion is provided by variable speed motor drives located at this interface. An actuator for elevation control could utilize proportional linear control (worm gears and linkage) and would be located at an offset distance from the main antenna-to-mast rotary joint.

SOURCE	TORQUE (T_i)	COMMENT
AERODYNAMIC	N/A	At an altitude of 19,333 n mi, the atmospheric density is equivalent to the plasma proton density: $= 3.4 \times 10^{-24}$ kgm m^3 $(3.0 \times 10^{-22}$ slug/ft^3) The resulting force on the SSPS is: $F = 22.4 \times 10^{-6}$ Newtons $(5 \times 10^{-6}$ lb) The relatively low magnitude and resulting torque can be ignored as a factor in design of mechanical interface (Ref. 1).
SOLAR	$T_x = 136$ newton-meter (100 ft-lb) $T_y = 5550$ newton-meter (4100 ft-lb) $T_z = 0.0$	Total Solar Collection area $= 49 \times 10^6$ m^2 Solar Pressure Constant $= 45 \times 10^{-6}$ newton/m^2 Separation of Cp from cg $= 25m$ (Ref. 1)
MAGNETIC	N/A	Adjacent Early unit magnetic field in the system has opposite polarity with a net magnetic torque of approximately zero. (Ref. 1)
GRAVITY	$T_y = 3100$ newton m/deg deviation (23,000 ft-lb/deg) $T_z = 27100$ newton m/deg deviation (10,000 ft-lb/deg) $T_{x_{max}} = 12.1 \times 10^4$ newton·m $(8.97 \times 10$ ft-lb)	The system X axis is perpendicular to the orbit plane resulting in zero nominal torque about y and z axis. Small limit cycle motions (± 10) cause destabilizing spring torques. The y and z axis rotate through 360° per orbit and produce torques with the max value shown when y and x axes are at 45° to the vertic.l. The period of this disturbance is twice a day. (Ref. 1)
CONTROL	$T_x = 6.754 \times 10^5$ newton-meter $(4.979 \times 10^5$ ft-lb) $T_y = 7.8 \times 10^6$ newton-meter $(5.78 \times 10^6$ ft-lb) $T_z = 7.9 \times 10^6$ newton-meter $(5.78 \times 10^6$ ft-lb)	Impulsive jet forces limited to 667 lb to limit SSPS structural deflections to less than $\pm 1°$. (Ref. 1) Max torques assume coupled firings.

Fig. 3.3-1 System Torque Environment
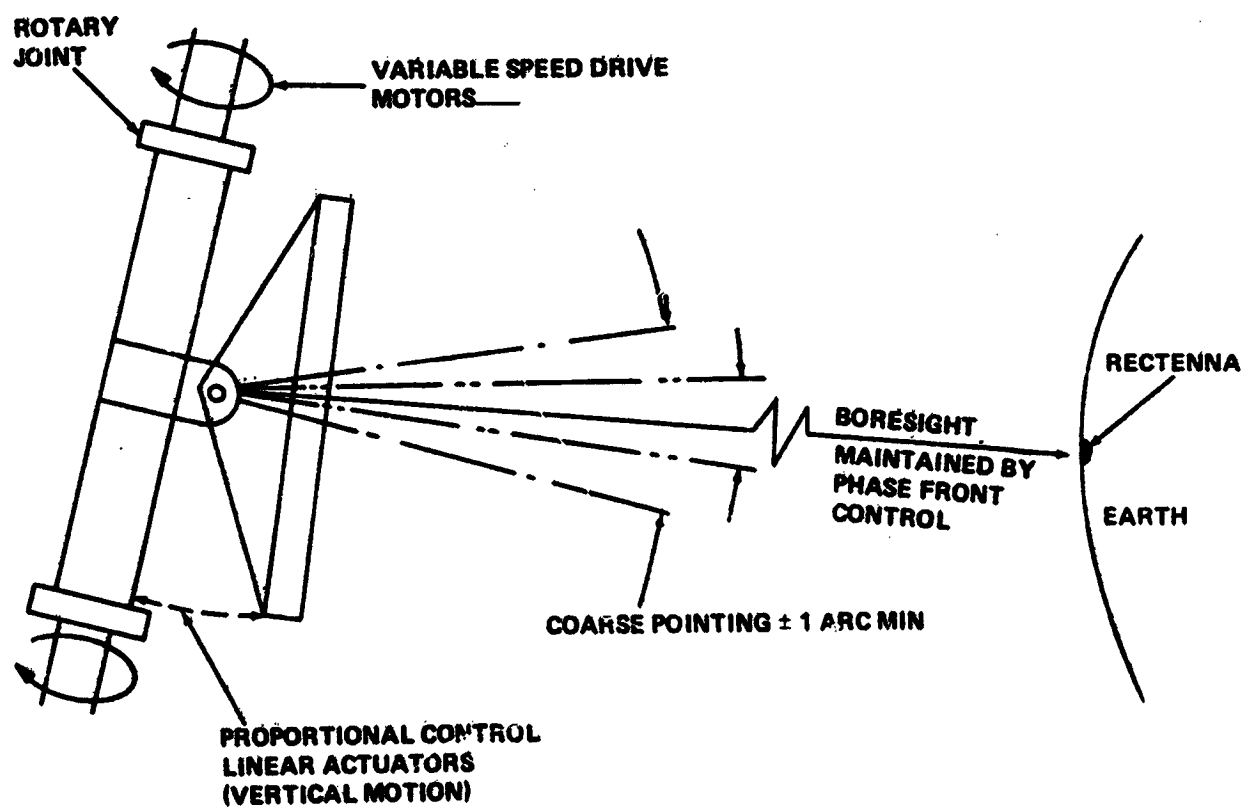
Fig. 3.3-2 Microwave Antenna Mechanical Pointing System

The elements defining required motion of the antenna relative to the spacecraft include the nominal motion between the sun-oriented SSPS and the earth pointing antenna, the normal SSPS control system limit cycle, and the bending motion of the SSPS mast at the antenna interface. The once-a-day 360° rotation of the antenna relative to the long axis of the solar pointing spacecraft is required to maintain boresight pointing to the rectenna. Additional antenna motion in azimuth and elevation is required to compensate for normal ±1° space-craft limit cycling. The modal characteristics of the SSPS affecting the antenna elevation drive is shown in Fig. 3.3-3. The normalized modal displacements, ϕ, and the normalized modal slopes, σ, corresponding to each mode, are identified at the ends of the axis where the control actuators and sensors for the SSPS are located (data presented in Ref 4). Also included is the anti-symmetric mode shape used to determine movement at the antenna interface driven by a coupled firing of the 44.5N SSPS attitude controllers. Maximum antenna motion due to bending will be approximately 0.15° at a frequency of 0.018 rad/sec.

Figure 3.3-4 summarizes the system angular motion requirements for design of mechanical interfaces between the spacecraft and antenna. Control error signals will be sinusoidal with a frequency equal to that of the SSPS control system limit cycle. Anti-symmetric bending motion is superimposed on the basic control motion. The minimum azimuth antenna rate is equal to orbital rate, while minimum rate in elevation is zero. Maximum azimuth rates occur just prior to SSPS jet firing and are induced by gravity gradient torques. Maximum accelerations occur at jet firings in azimuth and at peak energy points in the anti-symmetric bending oscillation in elevation.

3.3.1.1.2 Antenna Disturbance Torques - The rotary joint configuration shown in Fig. 3.2-2 consists of four equally spaced rollers attached to the solar array mast (Ref 5). The rollers slide on a track incorporated on the rotating mast. There are two sets of rollers at each rotary joint. Each set of bearings transmits bending moments through the mast segments by normal loads in each set of rollers. The critical mast bending moments result from loads induced by spacecraft gravity gradient correction torques. These torques produce a 3600N·m bending moment which results in rolling friction torque of 1077N·m in each set of rollers. (The Teflon coated rollers have a coefficient of friction against rolling of 0.05.)

The slip ring brushes also induce frictional torques. Contact pressures between the brushes and rotary joint ring will vary between 27,550N/m^2 and 68,940N/m^2 (4 and 10 psi) for optimum power transfer. At an assumed system voltage of 20 KV and a brush current rate of 7.75×10^4 A/m^2 (50 A/in^2), 6.45m^2 (10^4 in^2) of brush area is required to transfer 10 GW of power. The total normal force is 4.45×10^5N (10^5lb) at a coefficient of friction

ANTENNA LOCATION
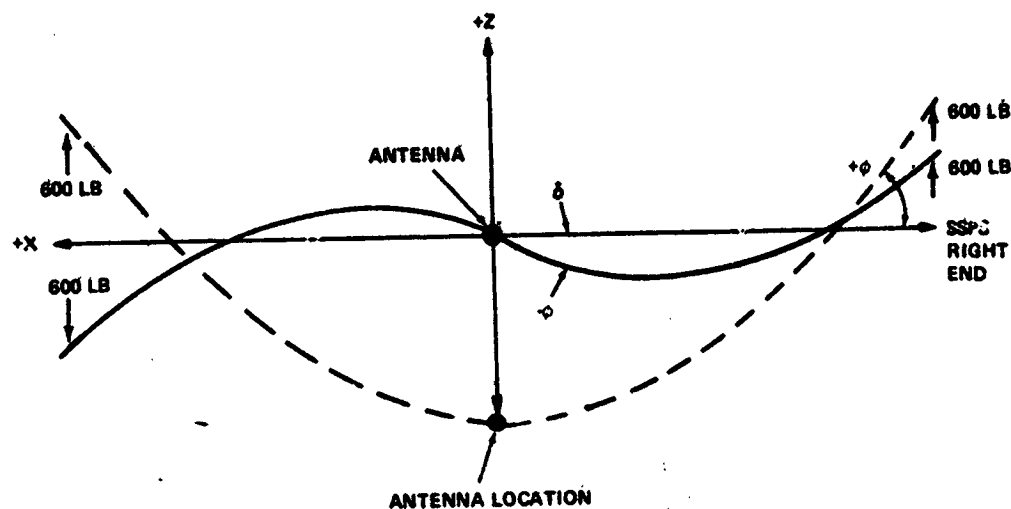
NORMALIZED DATA AT SSPS TIPS				
MODE	1ST SYMM	1ST ANTI-SYMM	2ND SYMM	2ND ANTI-SYMM
FREQUENCY RAD/SEC.	0.0076	0.0178	0.021	0.025
GENERALIZED MASS-SLUGS	189576.	159688.	143304.	140016.
STRUCTURAL DAMPING	0.0	0.0	0.0	0.0
RIGHT END NORMALIZED DISPLACEMENT	+1.0	+1.0	-0.793	+0.760
RIGHT END NORMALIZED SLOPE (RAD/FT)	$+0.864 \times 10^{-3}$	$+0.18 \times 10^{-3}$	-0.191×10^{-3}	$+0.353 \times 10^{-3}$

ANTISYMMETRIC DEFLECTIONS
AT ANTENNA GIMBAL MOUNT

FREQUENCY = .0178 RAD/SEC

$$\delta = \pm.0027 \text{ RAD}$$

SLOPE $$\dot{\delta} = \pm 4.87 \times 10^{-5} \text{ RAD/SEC}$$

$$\ddot{\delta} = \pm 8.66 \times 10^{-8} \text{ RAD/SEC}^2$$

Fig. 3.3-3 SSPS Bending Mode Data

PARAMETER	AZIMUTH SERVO	ELEVATION SERVO	COMMENT
CONTROL VARIABLE	$A(t) = W_e t + K \sin 2\omega_e t$	$E(t) = K_1 \sin 2\omega_e t + K_2 \sin \omega_m t$	ω_e = ORBITAL RATE ω_m = ANTI-SYMMETRIC MODE FREQ = .018 RAD/SEC K_1 = ATTITUDE DEAD BAND = $\pm 1^\circ$ K_2 = ANTI-SYMMETRIC BENDING MODE SLOPE = $\pm.00158$ RAD $K \sin 2\omega_e t$ SIMULATES CONTROL MOTION WITH A PERIOD EQUAL TO THAT OF GRAVITY GRADIENT TORQUE.
MIN RATE	$.728 \times 10^{-4}$ RAD/SEC	0.0	ORBITAL RATE
MAX RATE	$.69 \times 10^{-1}$ RAD/SEC	3.5×10^{-2} RAD/SEC	MAX. RATE BUILD-UP DUE TO GRAVITY GRADIENT
SLEW-RATE	$.728 \times 10^{-4}$ RAD/SEC	0.0	ORBITAL RATE
MAX ACCEL.	1.5×10^{-7} RAD/SEC^2	8.66×10^{-8} RAD/SEC^2	CONTROL TORQUE IN AZIMUTH; BENDING MODE RESPONSE IN ELEVATION
POSITION ACCURACY -	1 MIN	1 MIN	

Fig. 3.3-4 Servomechanism Environment

of 0.1 and a mast diameter of 50 meters, $1.02 \times 10^6 \mathrm{N \cdot m}$ (75×10^4 ft-lb) of torque is included by the slip rings. Figure 3.3-5 shows this torque variation with power level.

Antenna gravity gradient torques on the rotary joints are calculated using the equations shown in Fig. 3.3-6. The disturbance torque is approximately $354 \mathrm{N \cdot m/deg}$ (260 ft-lb/deg) offset between the antenna boresight and the local vertical. The nominal antenna azimuth angle is offset $2.6°$ as a result of locating the spacecraft at the stable node point, $123°$ West longitude, and the rectenna at $104°$ West longitude. An additional $3.5°$ offset results from eccentricity drift caused by solar pressure on the solar arrays. The elevation angle offset is $6.5°$ caused by locating the spacecraft on the equator and the rectenna at $40°$ North latitude.

The next highest disturbance on the antenna servo system results from electromagnetic radiation forces. An estimate of the force created by the electromagnetic energy radiation from the antenna has been computed (Ref 6) assuming a total power input of 10^{10} watts and a frequency of 3 GHz. The force is calculated by replacing the electromagnetic fields at the aperture of the slot array by equivalent current sources and computing the forces on the image currents which replace the aperture ground plane. The results predict an electromagnetic force pressure of $2.3 \times 10^{-5} \mathrm{N/m^2}$ normal to the antenna and a corresponding total force of 18N.

Although the electromagnetic forces do not place a significant design requirement on the antenna control system, the constant force in the radial direction does require the SSPS to continually perform orbital corrections. An acceleration along the radial direction does not significantly modify the energy of the orbit. The orbit will develop an eccentricity but the orbit period will remain almost constant. The force of 18 Newtons will cause a radial perturbation of

$$\pm \Delta R = 1.852 \text{ km} (1.00 \text{ n mi})$$

by the 80th day. (This same acceleration along the velocity vector would change the semi-major axis by (120 n mi) in the same time.) The propellant requirement to make an altitude correction of 1.0 n mi for an SSPS of 10^6 slugs and an ISP = 8000 seconds is,

$$W_p \approx 6.7 \text{ kg} (15 \text{ lb})$$

This would be equivalent to a yearly propellant requirement of,

$$W_p \approx 30.8 \text{ Kg} (68 \text{ lb})$$

3.3.1.2 Pointing and Control

Qualitative and limited quantitative data has been generated for defining mechanical steering of the transmitting antenna. This data will be used in an overall assessment of

CONTACT PRESSURE = 5 PSI
CURRENT RATE = 50 A/in.^{2}
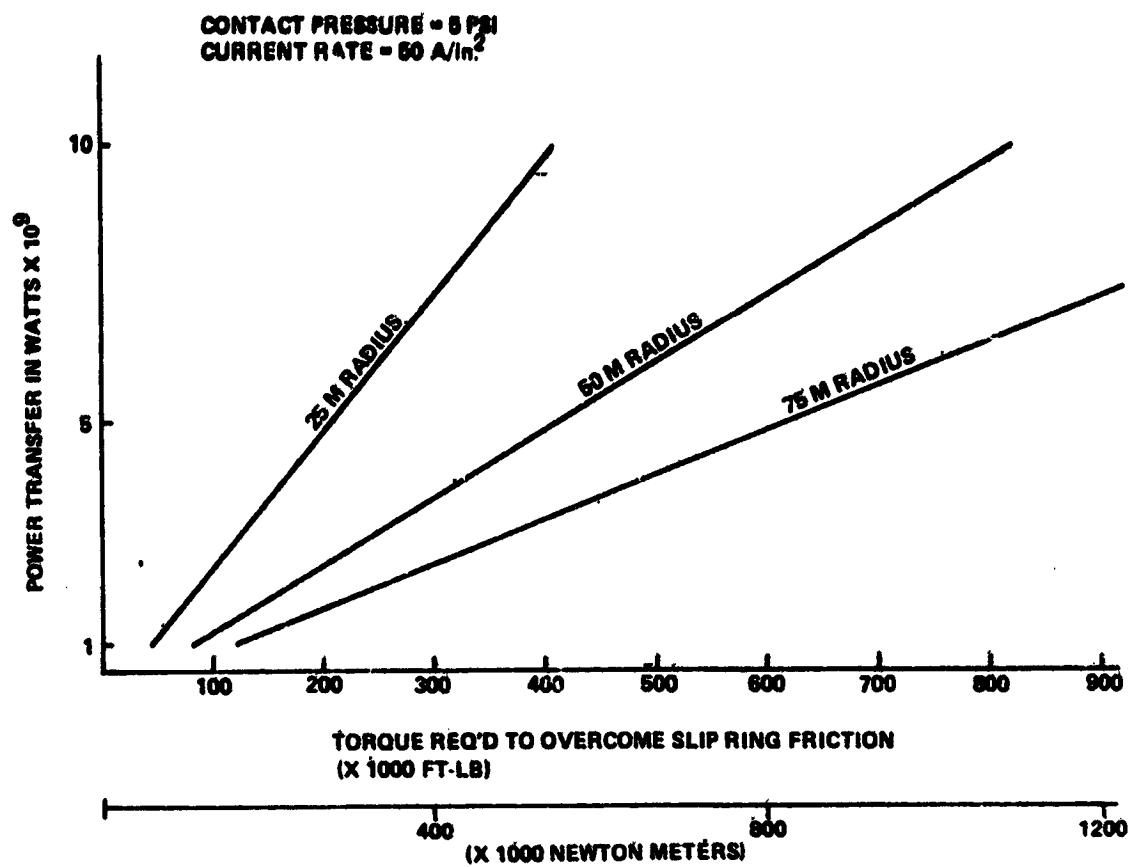
Fig. 3.3-5 Slip Ring Friction Torque
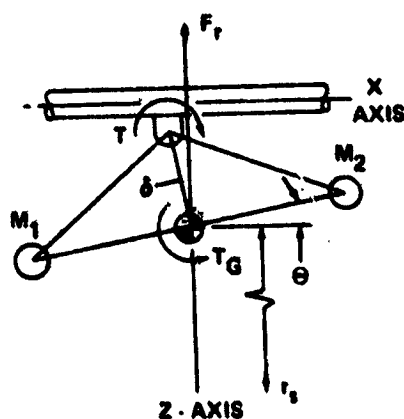
$$T = T_G + F_r d \sin \theta$$

$$T_G = \frac{3\mu}{2r_s^3} (I_Z - I_X) \sin 2\theta \qquad (\mu = 1.4 \times 10^{16})$$

$$F_r = 2 \frac{\mu}{r_s^3} + W_e^2$$

WHERE

T_G = GRAVITY GRADIENT TORQUE

F_r = RADIAL FORCE DUE TO DIFFERENCE IN S/C AND ANTENNA ORBIT MOTION

Fig. 3.3-6 Control System Requirements

3.3-8

microwave beam phase front control. The results of this effort indicate that mechanical steering of the antenna to accuracies better than 1 arc-min are readily achieved without substantial increase in control system torque or horsepower requirements.

Figure 3.3-7 summarizes control system design used in preliminary assessment. The initial response of the motor drive will be to relieve torque loads on the antenna induced by spacecraft (SSPS) disturbances. These spacecraft disturbances include gravity gradients, bending modes, and normal satellite limit cycling with a time constant of 12 hours.

Spacecraft bending modes couple through the rotary joint and are of the form:

$$\dot{\Theta} = A_s \cos \omega_s t.$$

This motion is coupled into the antenna through rotary joint friction in both elevation and azimuth. Antenna motion of the form

$$\Theta = A \sin \omega_s t$$

due to spacecraft bending dynamics which is coupled into the antenna only in elevation. This occurs because the antenna system uses only a 2-axis gimbal system. This coupled inertial load into the antenna is relatively small.

The gravity gradient disturbance has been neglected in this study because it is orders of magnitude less than the coupling disturbance and friction torque. The 1° satellite limit cycle is also neglected with the rationale that the 12-hour period is sufficiently long to assume that steady state conditions exist.

The preliminary system design is modeled as a motor directly driving the antenna through a shaft. Gearing dynamics and selection can be made with detail analysis at a later date. A study of control torque requirements and power requirements indicate that they are insensitive to variations of control frequency within the range studied. The system size requirements to achieve 1 arc-min are:

Az: 1.02×10^6 N·m torque;
0.18 hp

El: 2830 N·m torque;
1.8 hp

3.3.2 Thermal Evaluation

During Task 1, the analyses were centered about studies of the sensitivity of temperature level and temperature gradient within the antenna supporting structure (Fig. 3.3-3) to parameters such as antenna size, power transmitted, efficiency of microwave converter, thermal radiation properties of structure, and spacing of structural elements.

I	=	ANTENNA INERTIA (SLUG 6 FT^2)
K_{FF}	=	FRICTION COMPENSATION GAIN (SEC)
T_{FF}	=	FRICTION TORQUE MAGNITUDE (FT-LB)
W_c	=	CONTROL SYSTEM BANDPASS FREQUENCY (RAD/SEC)
T_M	=	MOTOR TIME CONSTANT (SEC)
Θ_{SA}	=	STRUCTURAL DISPLACEMENT AFFECTING ANTENNA POSITION (RADIANS)
$\dot{\Theta}_{SA}$	=	STRUCTURAL RATE AFFECTING FRICTION FORCES (RAD/SEC)
Θ_A	=	ANTENNA POSITION (RAD)
$\dot{\Theta}_A$	=	ANTENNA VELOCITY (RAD/SEC)
$\ddot{\Theta}_A$	=	ANTENNA ACCELERATION (RAD/SEC^2)
T	=	TOTAL ANTENNA TORQUE (FT-LB)
T_F	=	FRICTION TORQUE (FT-LB)
T_M	=	MOTOR TORQUE (FT-LB)

Fig. 3.3-7 Preliminary Design Control System

PRIMARY STRUCTURE

UPPER CAP

LOWER CAP

PLANE OF
ANTENNA
SUBARRAYS

GAUSSIAN
HEAT REJECTION
DISTRIBUTION

MW CONVERTER
RADIATORS

WAVEGUIDE
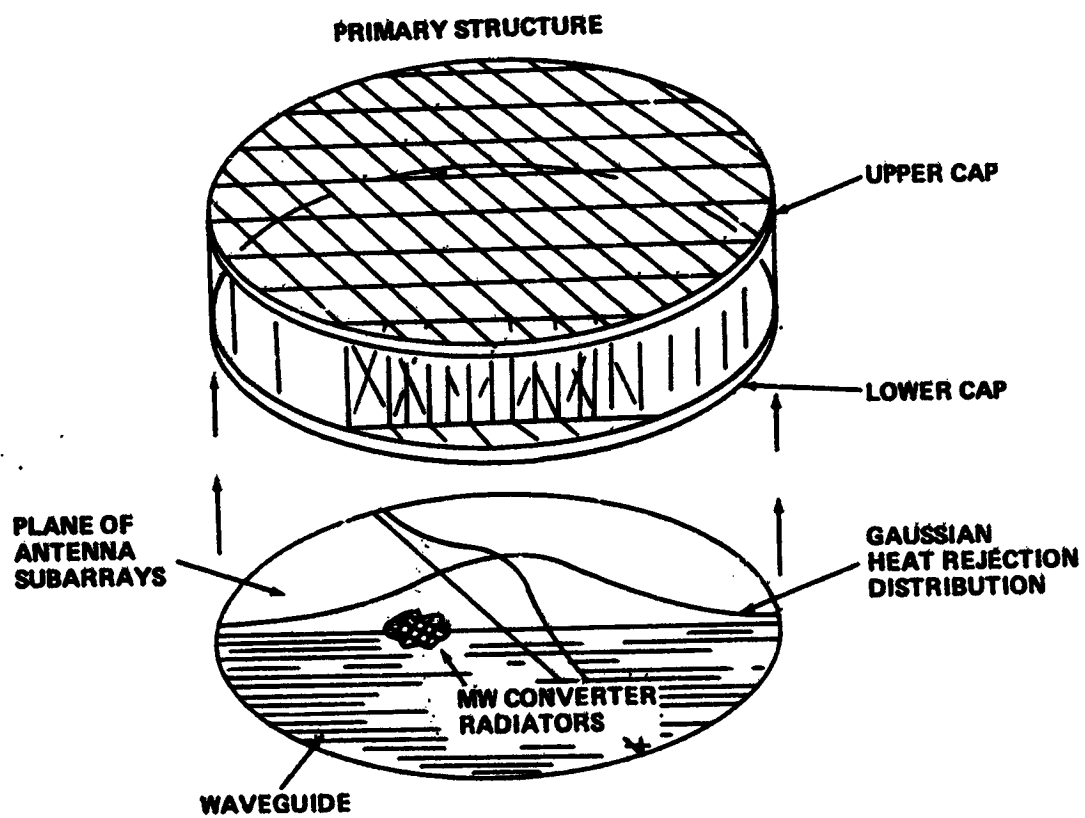
Fig. 3.3-8 Antenna Support Structure

For purpose of selecting candidate materials for the support structure, the maximum expected temperature must be determined. Should the support structure be used as an electrical distribution system from the solar arrays to the microwave converters, temperature level will also be required to establish the electrical resistance of the conductors.

Reference 11 states that the antenna power transmission distribution will be Gaussian in cross-section. With the present method of rejecting heat from the microwave converters, the radiant heat flux to the antenna support structure will also have a Gaussian distribution. Figure 3.3-9 gives such a distribution for a 1 km diameter antenna transmitting 10 GW with a microwave converter efficiency of 90%.

The maximum structural temperature will occur in the member that is closest to the center of the antenna where the radiant flux is maximum. Temperature magnitude will depend on the α_s/ϵ ratio of the element, the geometric shape of the element, to a minor extent the distance of the element from the antenna surface (for distances up to 50 meters the variation is less than 5^oK) and, to a major extent, the magnitude of the radiant flux at the center of the antenna. This last factor depends on microwave converter efficiency, spacing and power transmitted.

Figure 3.3-10 shows maximum structural temperatures as a function of transmitted power for three antenna diameters and two microwave converter efficiencies. The three basic trends are: (1) increasing the transmitted power increases the maximum structural temperature, (2) increasing the efficiency of the microwave power converter decreases the maximum structural temperature, and (3) increasing the diameter of the antenna decreases the maximum structural temperature.

After completion of Task 1, Raytheon selected the following values for the antenna parameters (Ref 13):

- Antenna diameter   1km
- Radiated power   6.45 GW
- Amplitron output power   6kw
- Amplitron efficiency   85%
- Klystron output power   6kw
- Klystron efficiency   75%
- Illumination $\exp(-2.30(r/a)^2)$

- **TOTAL ANTENNA POWER — 10GW**
- **MICROWAVE CONVERTER**
  - **EFFICIENCY = 90%**
  - **SPACING = .203 x $e^{(r/500)^2}$** meters
  - **POWER = 1350 W/AMPLITRON**
- **75% OF RADIATION ENERGY TOWARDS STRUCTURE**

WATTS/METER^2

DISTANCE FROM CENTER OF ANTENNA ~ METERS
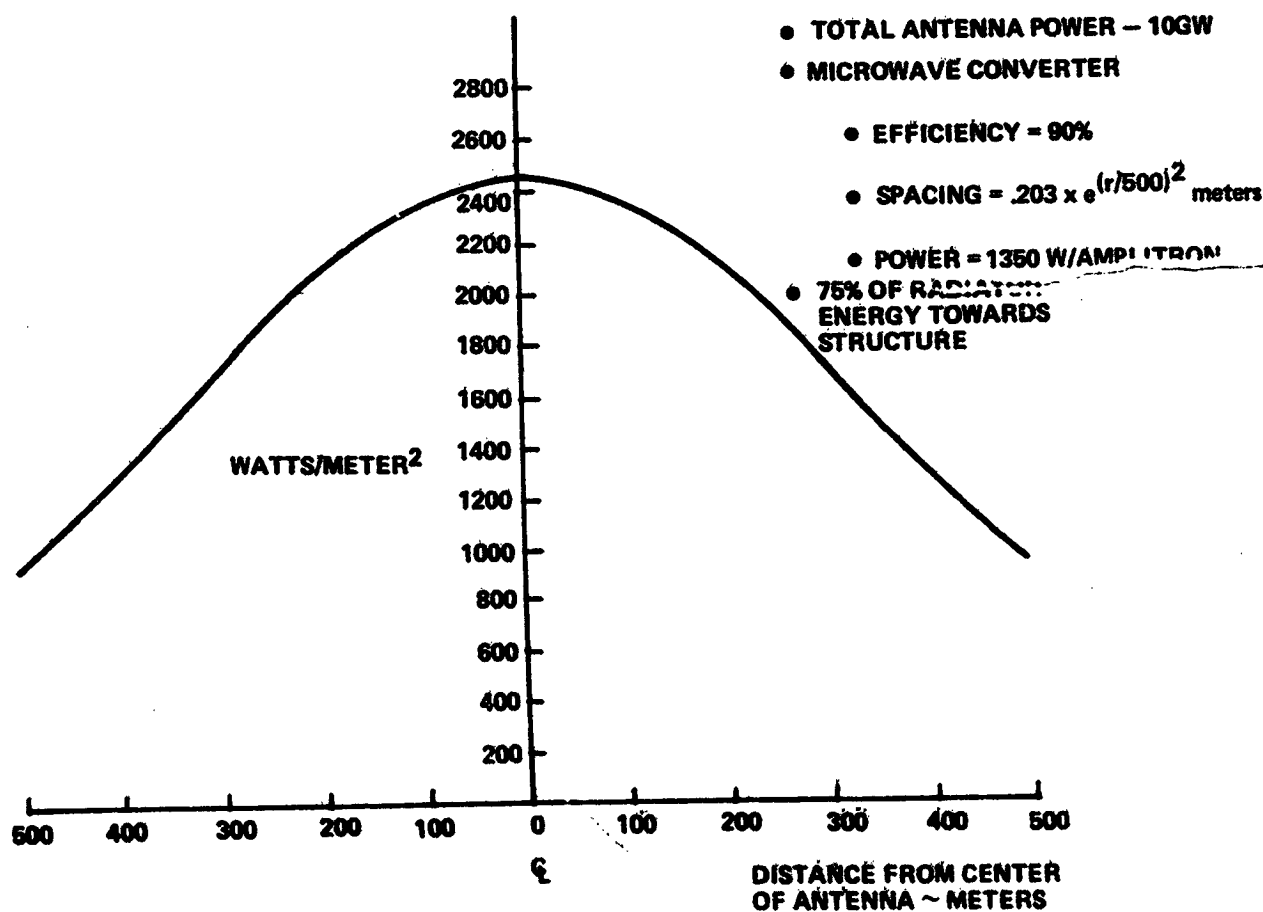
Fig. 3.3-9 Gaussian Radiative Heat Flux from Antenna Surface
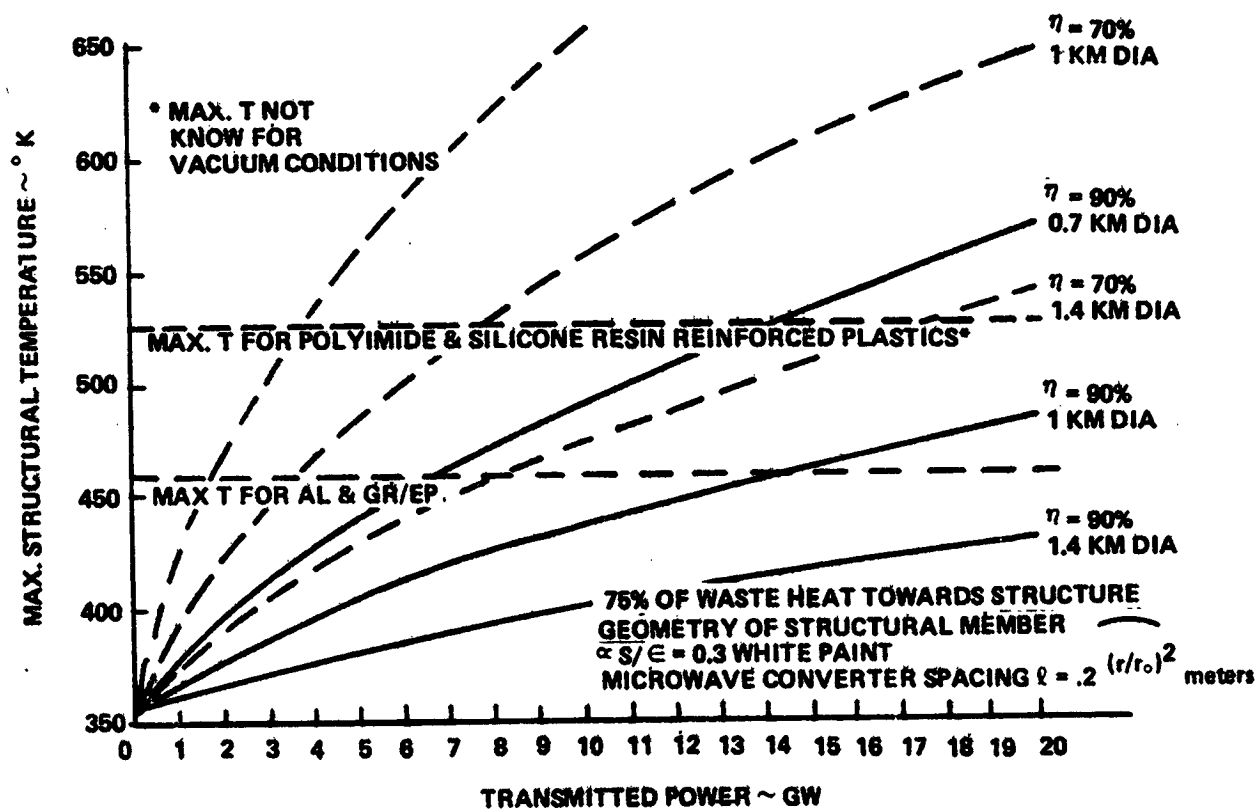
Fig. 3.3-10 Maximum Structural Temperature vs Transmitted Power

This illumination distribution results from a microwave converter spacing given by:

$$L = L_{min} \exp ((r/466)^2)$$

An analysis by Raytheon revealed that 87.5% of the waste heat generated in the microwave converter tubes would be radiated towards the antenna support structure, with the remaining 12.5% being radiated out of the opposite side of the antenna surface toward earth.

Thermal analyses of the following key problems were performed using the above values for the MPTS parameters: Geometry of beam cap elements, temperature difference between beam caps, column temperatures, and effect of microwave converter spacing on the waste heat profile with its attendant effect on beam and column temperatures.

3.3.2.1 Geometry of Beam Cap Elements

This study involved determining the maximum temperature and the temperature difference within structural members having tubular, high-hat and triangular cross-sections (Fig. 3.3-11 and 3.3-12). Maximum temperature is important from the materials selection and strength standpoint, while temperature gradient is important because of the induced thermal stresses. The structural members considered in this study are those that make up the beam cap and are in a plane parallel to the antenna surface (Fig. 3.3-11). (Members in a perpendicular plane were considered separately.) They are heated by radiation from the hot antenna surface below it. For this study the antenna surface at the center was taken to have an effective temperature of 600°K which is approximately the situation when the antenna is 1.0 km in diameter and transmitting 6.45 GW with a microwave converter efficiency of 75%.

The temperature analyses were performed by subdividing the particular geometry into nodes (between 8 and 11, depending on the shape) and determining the radiation couplings between the nodes themselves and between the nodes and the antenna surface as well as deep space (Fig. 3.3-13). The computer programs CONFAC (CONfiguration FACtor) and AF1 (script F) were used to determine the 50 or so significant radiation couplings. Conduction effects were neglected, which is a conservative approach, pending material and thickness selections. Once the mathematical mc lel of a geometry was established the computer program SSTA1 (Steady-State Thermal Analysis 1) was run to evaluate temperatures. The results of the investigation are discusse ext.

3.3.2.2 Tubular Cross-Section

Figure 3.3- esents the maximum emperature that a structural member with a tubular cross-section will experience as a function of the effective antenna surface
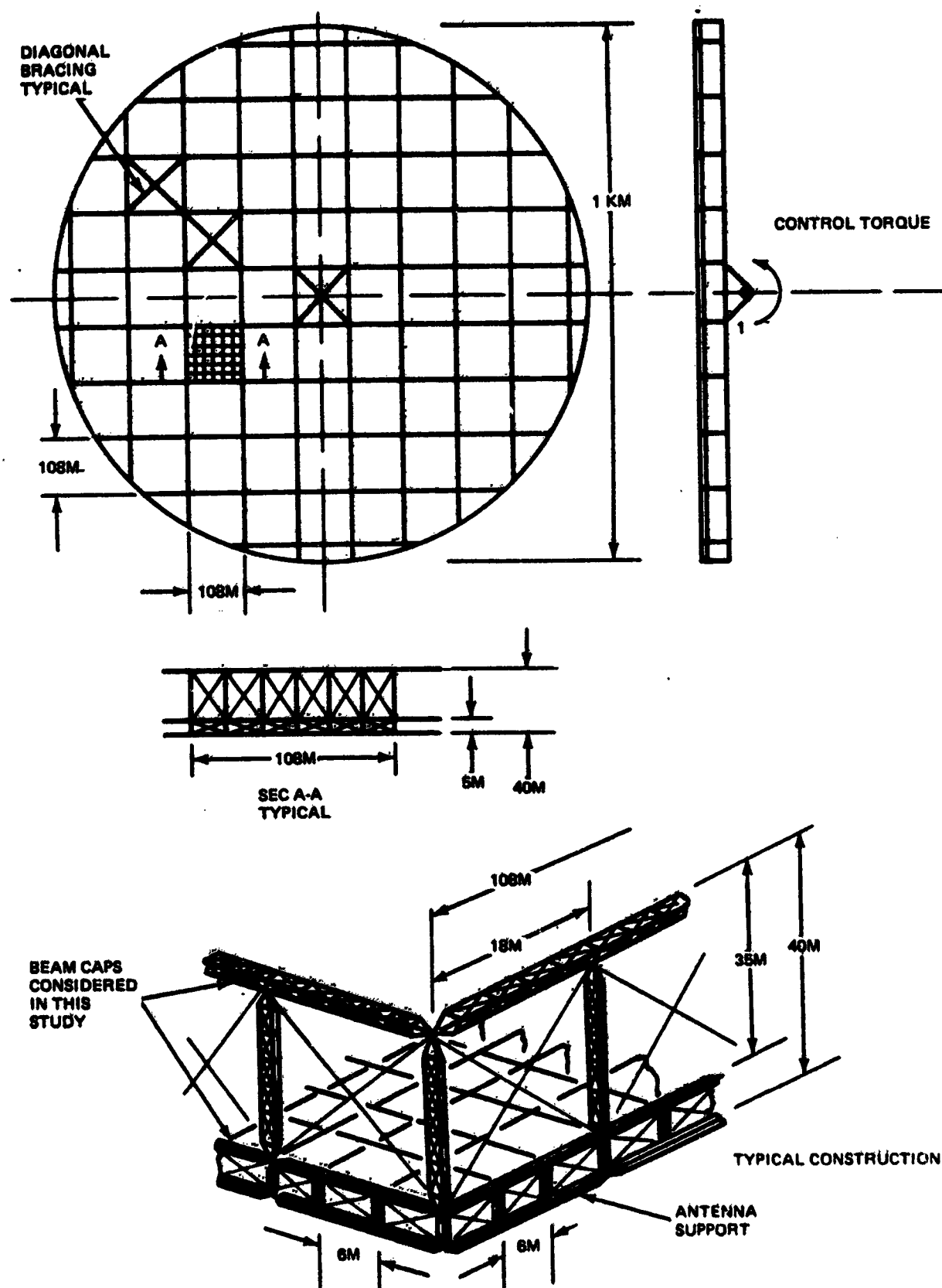
Fig. 3.3-11 Microwave Power Transmission System Structure

TUBE

HIGH
HAT

TRIANGLE
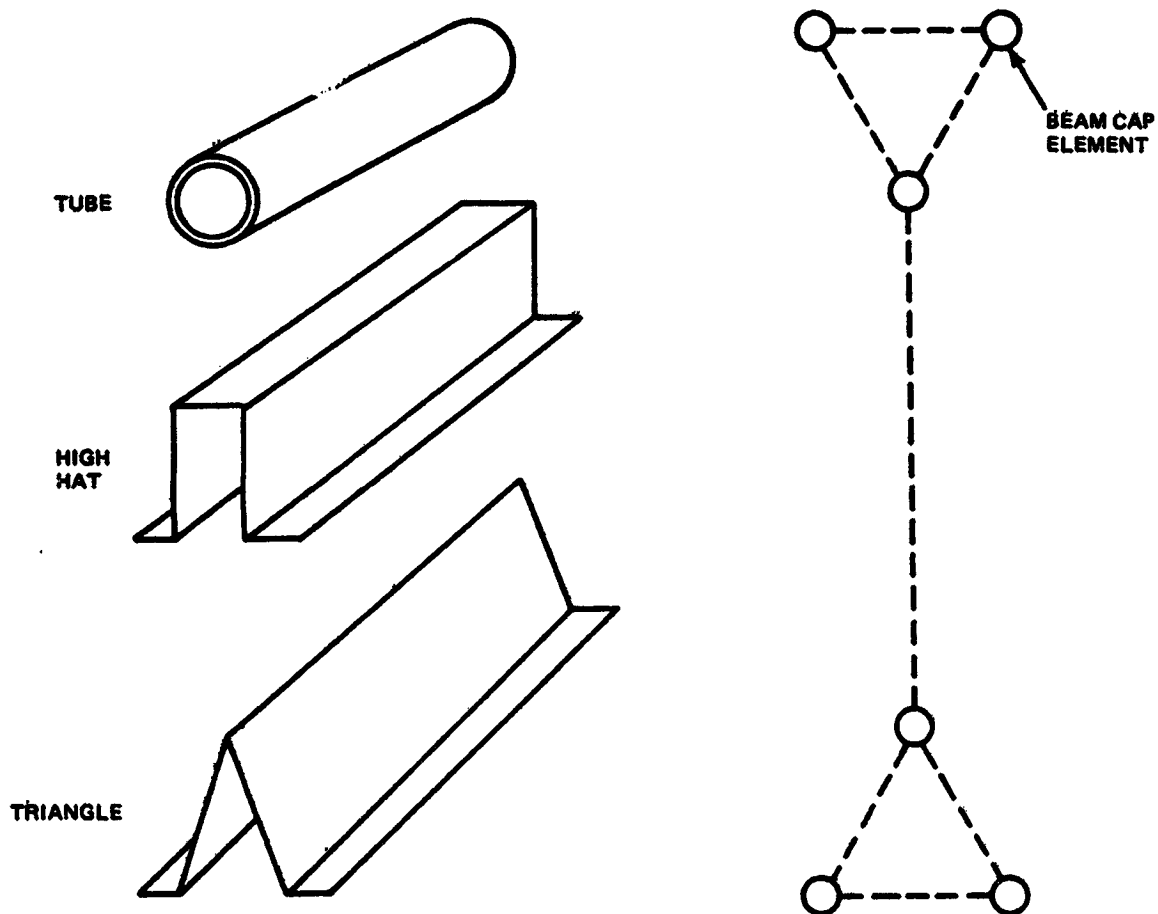
BEAM CAP
ELEMENT

Fig. 3.3-12 Beam Cap Element Geometries
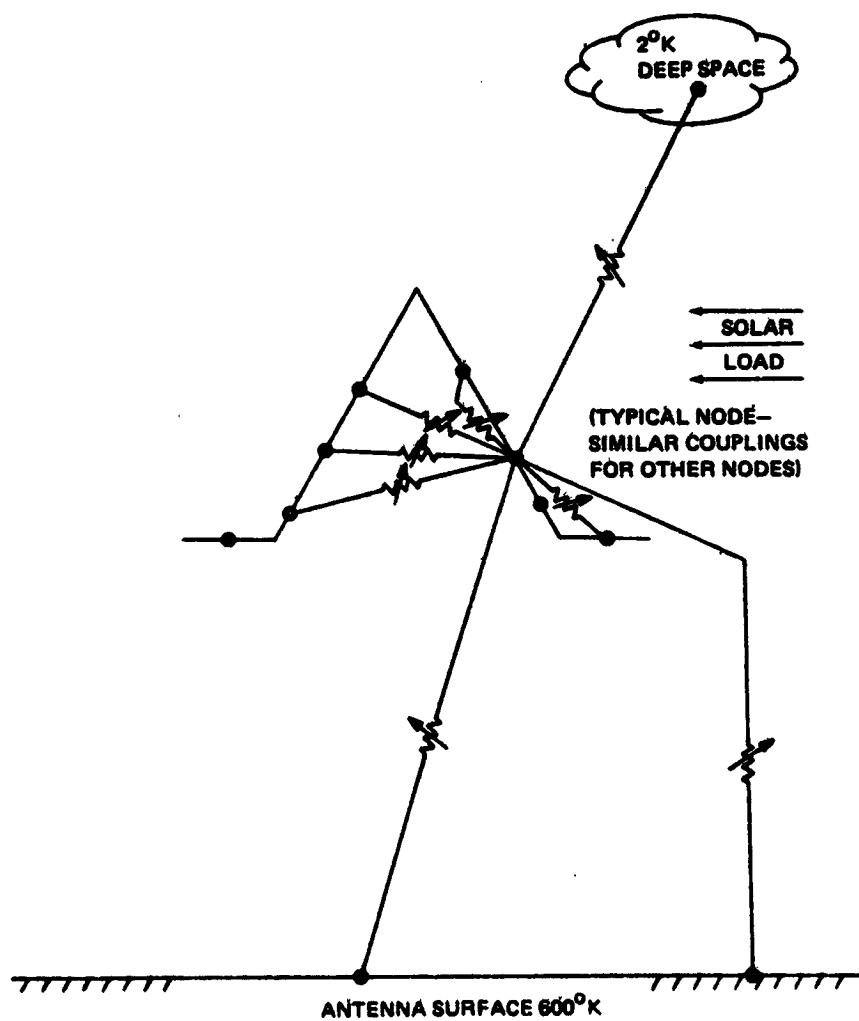
Fig. 3.3-13 Typical Thermal Model for Structural Member
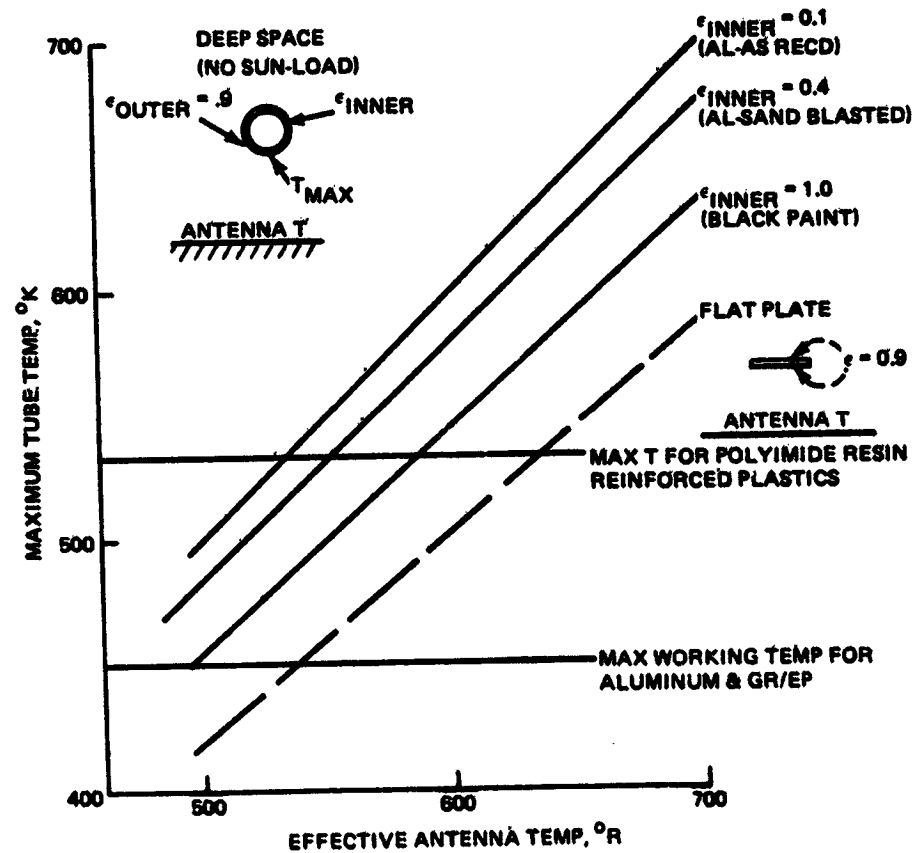
Fig. 3.3-14 Maximum Tube Temperature as a Function of Antenna Surface Temperature with Tube Inner Wall Emissivity as a Parameter

temperature. The tube outer surface was taken to have an emissivity of 0.9 (e.g. white paint). Three values, 0.1, 0.4 and 1.0, were used for the emissivity of the inner wall, and as expected, the higher the emissivity of the inner wall, the lower the maximum temperature. This is due to the increased thermal communication between the hot bottom and the cool top afforded by the higher inner wall emissivity. Figure 3.3-15 shows the temperature difference between the bottom and top of the tube for the three interior emissivities. These temperature differences induce bending stresses within the tubes. To sustain these induced stresses, the tube wall must have a minimum thickness. Based on Fig. 6 of Ref 22, Fig. 3.3-16 was generated. It is apparent from this figure that stresses induced in aluminium are considerable and that the required tube wall thickness would have to be an order of magnitude greater than that required for a graphite/epoxy tube. Furthermore, the need to paint the inside of aluminum tubes black is obvious, otherwise the required tube wall thickness will lead to an excessively heavy beam. For example, a tube diameter of 0.1 meter requires a minimum tube wall thickness of 1 mm (0.039 inch) to sustain the induced bending stress associated with a temperature difference of $235°K$. Painting the inside surface black will reduce the required thickness to 0.43 mm (0.017 inch), a greater than 50% reduction in weight. An alternate approach to painting the inside of the tubes black is to manufacture the tubes with holes in the walls. This may prove even more effective than the black paint in reducing the maximum temperature and temperature gradient.

A review of Fig. 3.3-14 shows that neither aluminum nor graphite/epoxy can be used in a tubular geometry in locations where the effective surface temperature is greater than $500°K$ because the maximum working temperature of these materials will be exceeded. Insulating the bottom half of the tube with layers of aluminized Kapton will lower the temperature sufficiently so that they can be used. Note, however, that the temperature gradient will not be significantly reduced. This is apparent from Fig. 3.3-15 which shows the temperature difference to be a weak function of effective antenna temperature. (Insulating the bottom half of the tube can be viewed as reducing the effective antenna temperature). Wrapping the entire tube with insulation will result in smaller temperature gradients but higher temperatures.

In conclusion, a tube is considered a poor geometry for a structural member that is parallel to the antenna surface due to the high temperature and gradient that will exist within the tube.
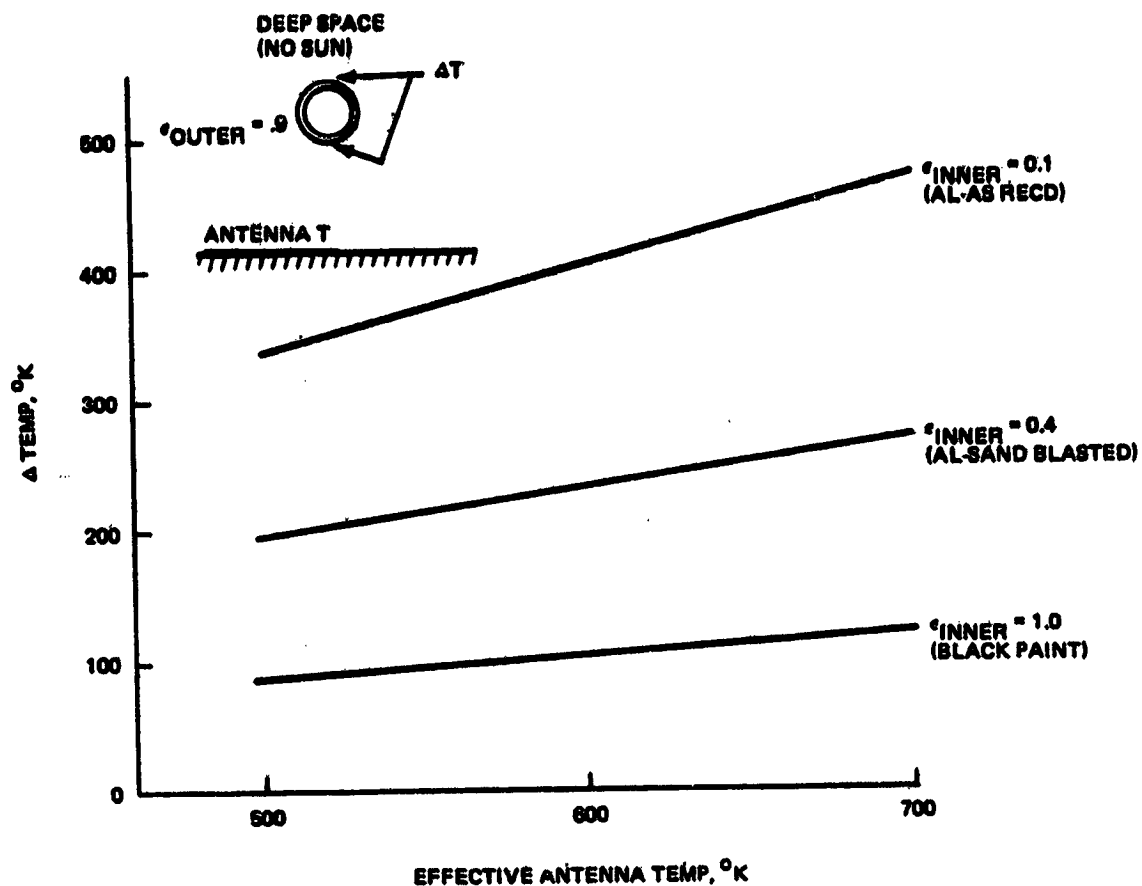
Fig. 3.3-15 Maximum Temperature Difference Across a Tubular Structural Member as a Function of Antenna Surface Temperature with Tube Inner Wall Emissivity as a Parameter

ΔT, °K (εINNER WALL)	ALUMINUM		GRAPHITE/EPOXY	
	INDUCED BENDING STRESS, n/m² (KSI)	MIN TUBE WALL TO RADIUS RATIO	INDUCED BENDING STRESS n/m² (KSI)	MIN TUBE WALL TO RADIUS RATIO
100°K (ε = 1.0)	103 X 10⁸ n/m² (15 KSI)	0.0085	14 X 10⁶ n/m² (2 KSI)	0.0009
238°K (ε = 0.4)	248 X 10⁶ n/m² (36 KSI)	0.020	31 X 10⁶ n/m² (4.5 KSI)	0.0025
400°K (ε = 0.1)	414 X 10⁶ n/m² (60 KSI)	0.034	50 X 10⁶ n/m² (7.3 KSI)	0.004

Fig. 3.3-16 Thermally Induced Stresses and Minimum Wall-to-Radius Ratios for Tubes

3.3.2.3 High-Hat Section

The high temperature and gradients within the tube geometry are caused basically by the bottom segment of the tube not being able to radiate directly to deep space and the top segment not receiving radiant energy directly from the antenna surface. A "high-hat" geometry does not have this disadvantage. Instead each segment has some view of both the antenna surface and deep space; albeit the fractional view of each varies from segment to segment.

Figure 3.3-17 shows the temperature distribution in a high-hat section that is dimensioned L x 6L x 4L. Two cases are shown: One where both sides of the member are painted white, and the other case where the side towards the antenna surface has a low emissivity coating ($\epsilon = 0.1$) or, if aluminum were used, the side towards the antenna surface is left untreated.

A solar load of 1356 watts/meter^2 was applied to the right side of the high-hat to obtain the maximum temperature gradient. The following conclusions can be drawn from Fig. 3.3-17:

- The high-hat section runs cooler than the tubular cross-section

- Temperature gradients are smaller in the high-hat than in the tube

- Both sides of the high-hat should be painted white as this reduces the maximum temperature difference from 196°K to 76°K

- Aluminum or graphite/epoxy cannot be used without some insulation between the member and the antenna surface.

3.3.2.4 Triangular Cross-Section

The next geometry considered was that of a triangle. In this geometry each segment of the triangle has a good view of cold space. Figure 3.3-18 shows the temperature distribution within such a member with and without a solar load. Of great significance here is the low maximum temperature of 439°K (330°F) which permits aluminum or graphite/epoxy to be used. This geometry can be easily manufactured with one side of the aluminum sheet left untreated and the other side painted white or given an alzac finish. Graphite/epoxy would have the top painted white and the side facing the antenna would be aluminum foil bonded into the epoxy.

The maximum temperature differences in the triangular shaped member are seen to be 73°K with a side solar load and 56°K without a solar load. The two side tabs are running
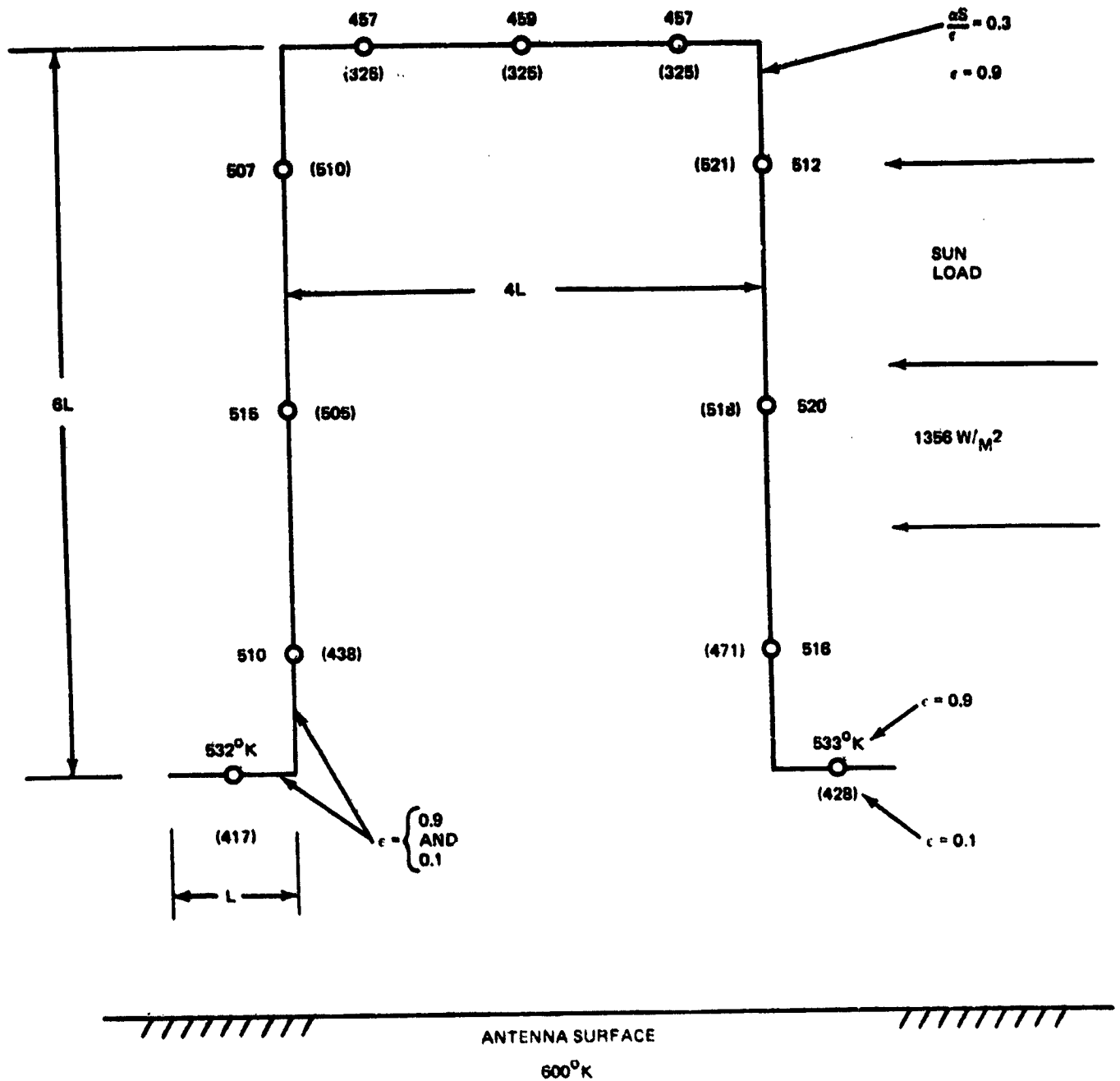
Fig. 3.3-17 Comparison of Temperature Profiles in High-Hat Section for ϵ_{Inside} = 0.9 vs 0.1

Fig. 3.3-18 Temperature Distribution within Triangular Shaped Structural Member
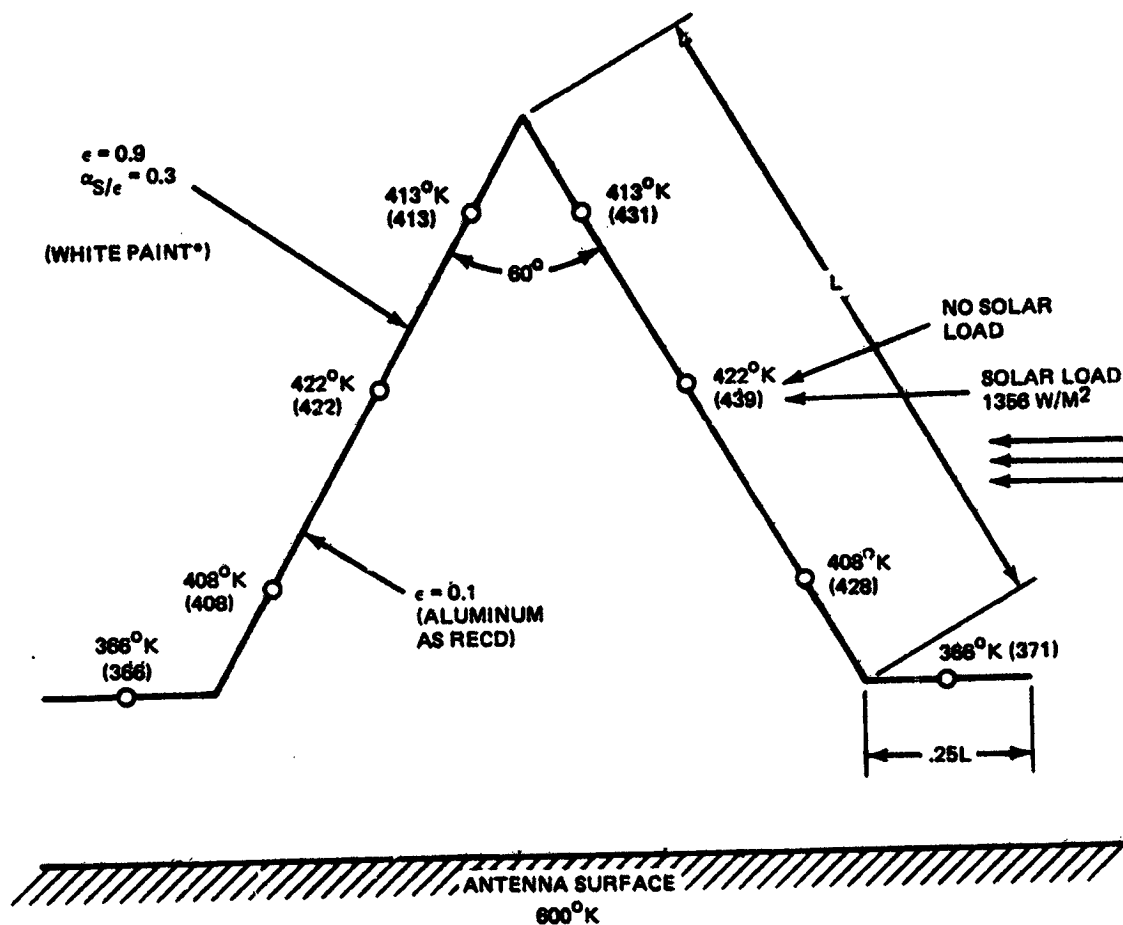
*FOR ALZAK FINISH, WITH ϵ = 0.75, TEMPERATURES WILL BE APPROXIMATELY 20°K HIGHER

• CONDUCTION EFFECTS WILL REDUCE THE TEMPERATURE GRADIENT

cooler than the triangle proper. Increasing the emissivity of the tabs on the side facing the antenna surface results in higher tab temperatures. Therefore, it is possible to reduce the temperature gradient within the member by proper selection of the emissivity of the tabs. Although applying a coating to the tabs will increase manufacturing costs, the smaller temperature gradient will permit a thinner, and hence lighter, structural member to be used. The net effect may be a reduction in the total system cost.

Figure 3.3-19 presents the maximum temperature and temperature difference that Figure 3.3-19 exists in triangular members. The results are shown with and without a side solar load for two different size tabs with various emissivity values on the tabs. The emissivity value that minimizes the temperature difference is in the neighborhood of 0.2, which can be achieved by applying an anodized coating 0.1 microns in thickness (Ref 23). The maximum temperature difference is reduced to 30°K with solar load and 12°K without solar load.

Figure 3.3-19 also shows that there is no thermal advantage to the larger tabs. However, opening the triangle beyond the 60° angle considered in the study will reduce both the maximum temperature and the temperature difference within the member. In the limit, opening the triangle completely to a flat plate produces the lowest possible temperature, 337°K (147°F), for white paint on the top ($\epsilon = 0.9$) and unfinished aluminum($\epsilon = 0.1$) on the bottom. This is, of course, at the complete expense of the member strength. No doubt there is an optimum angle.

The following conclusions can be drawn from this study of candidate beam geometries:

- Tube geometry is the worst from a thermal standpoint. The highest temperatures and largest temperature differences are achieved with this geometry. The use of aluminum or graphite/epoxy tubing near the center of the antenna will not be possible without the use of some insulation between the tubing and the antenna surface. (The insulation should not encapsulate the tubing.)

- The high-hat section is not an attractive geometry although the temperature picture is somewhat better than the tubular geometry. The tube with its greater rigidity is preferred over the high-hat.

- The triangular section is the best geometry of those studied. It has the lowest temperature and the smallest temperature differences. It can be easily manufactured and made of aluminum. Whether it is economically justifiable to anodize the bottom of the side tabs remains to be investigated.
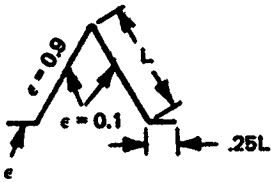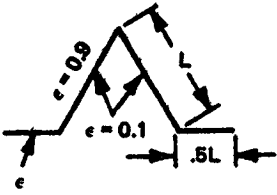
EMISSIVITY ON BOTTOM OF TABS	T_{MAX}, °K	ΔT_{MAX}, °K	T_{MAX}, °K	ΔT_{MAX}, °K
0.1 NO SUN	422	56	420	61
0.2 NO SUN	422	12	422	16
0.3 NO SUN	438	23	436	21
0.4 NO SUN	458	44	NC	NC
0.1 SUN	439	73	NC	NC
0.2 SUN	440	30	439	33
0.4 SUN	461	51	NC	NC

NC = NOT COMPUTED

Fig. 3.3-19 Maximum Temperature and Temperature Difference in Triangular Member

Figure 3.3-20 and 3.3-21 summarize the results of the study and show clearly the thermally superior performance of the triangular geometry, both from the standpoint of lower maximum temperature and smaller temperature difference.

3.3.2.5 Temperature Profile

Temperature profiles along the beam cap elements were calculated for the MPTS in various orbital positions during the equinoxes and solstices. Orbital variations in the temperature profiles are caused by the varying angle, normal to the structure made with the sun vector, as a result of the antenna being earth oriented. The "North-South" and "East-West" beam caps have been assumed to be oriented at 45° to the sun line to minimize differential solar inputs. The temperature profiles change during the year as a result of the solar load on the structure varying with the changes in Earth-Sun distance and the inclination of the solar vector to the orbital plane.

Figure 3.3-22 shows three temperature profiles for a beam cap member located one meter above the antenna surface. Two profiles are for the extremes of the full sun condition, that is, when the structure is located at the sub-solar point of the orbit during the equinoxes and the summer solstice. It is observed that the yearly variation in the temperature profile of a beam cap element is only a few degrees. This is contrasted with the orbital variation which is much greater. Figure 3.3-22 shows that as the structure near the center of the antenna goes around an orbit its temperature will change approximately 50°K. Near the perimeter of the structure, where the sun's load represents a greater fraction of the total heat load on the structure, the temperature of the beam elements shifts roughly 150°K as the MPTS moves around an orbit. This swing in temperature may be significant when one considers that there will be over 10,000 such cycles during the 30-year life of the MPTS.

The temperature swing near the structure perimeter is reduced when a more nearly uniform microwave converter spacing is used. The temperature profiles shown in Fig. 3.3-22 are those associated with a scale factor $\rho = 466$ meters* which produces a 10 to 1 power ratio from the center to the antenna tip. With a scale factor of $\rho = 557$ meters the power ratio is reduced to 5 to 1 and, as Fig. 3.3-23 shows, the temperature shift near the perimeter is reduced from its previous value of 150° to 120°K. The swing near the center, however, has increased from 50° to 60°K.

- - - - - - -

*Microwave Converter Spacing = $L_{min} \times Exp ((r/\rho)^2)$
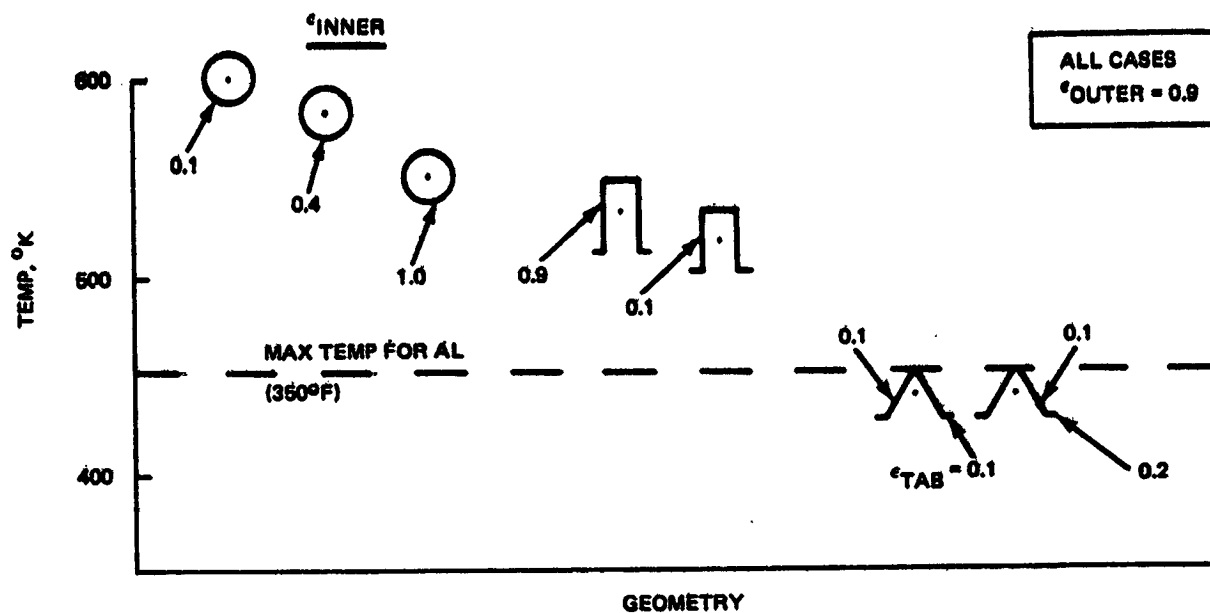
Fig. 3.3-20 Comparison of Maximum Temperature for Different Beam Cap Element Geometries
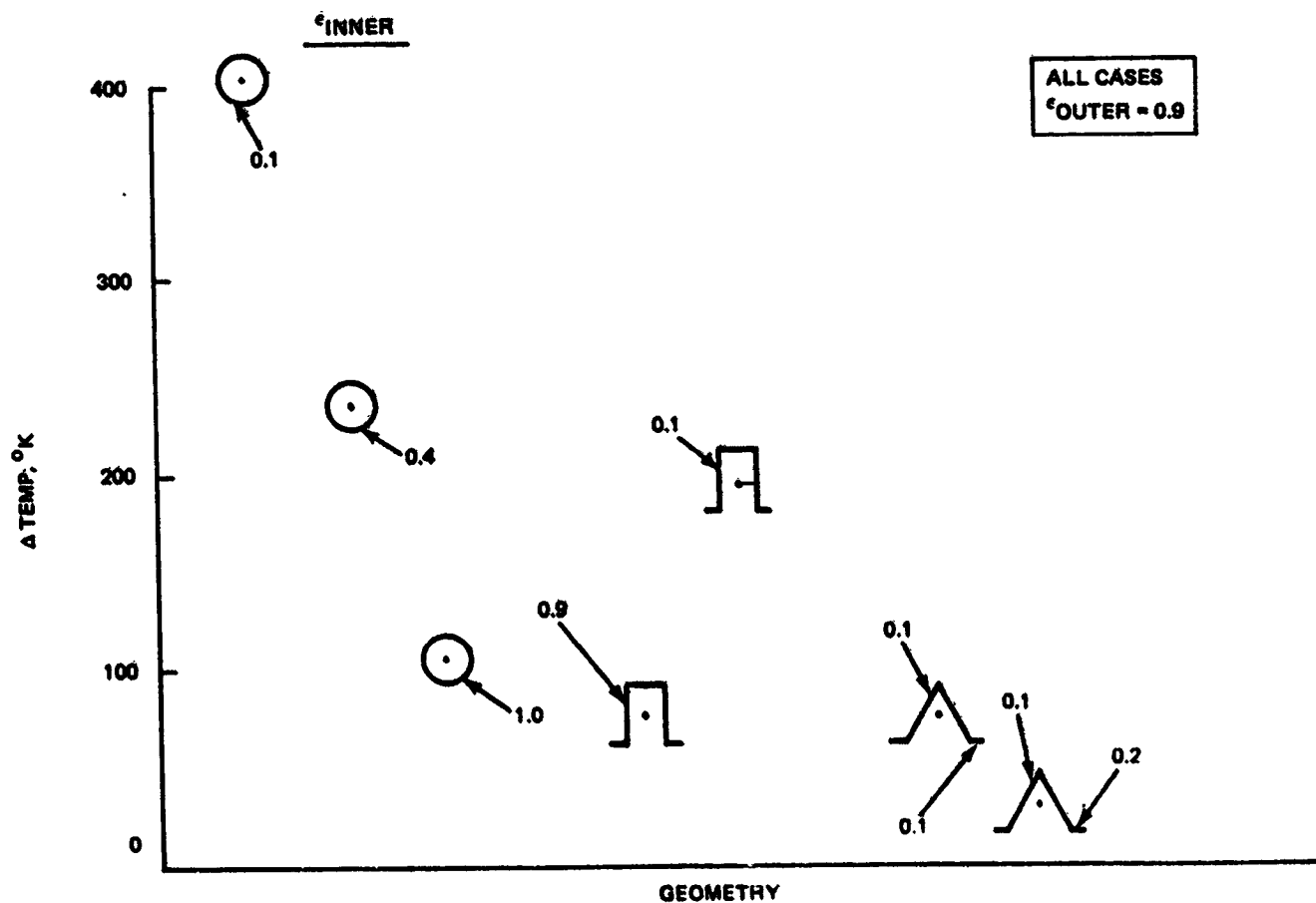
Fig. 3.3-21 Comparison of Maximum Temperature Difference for Various Geometries
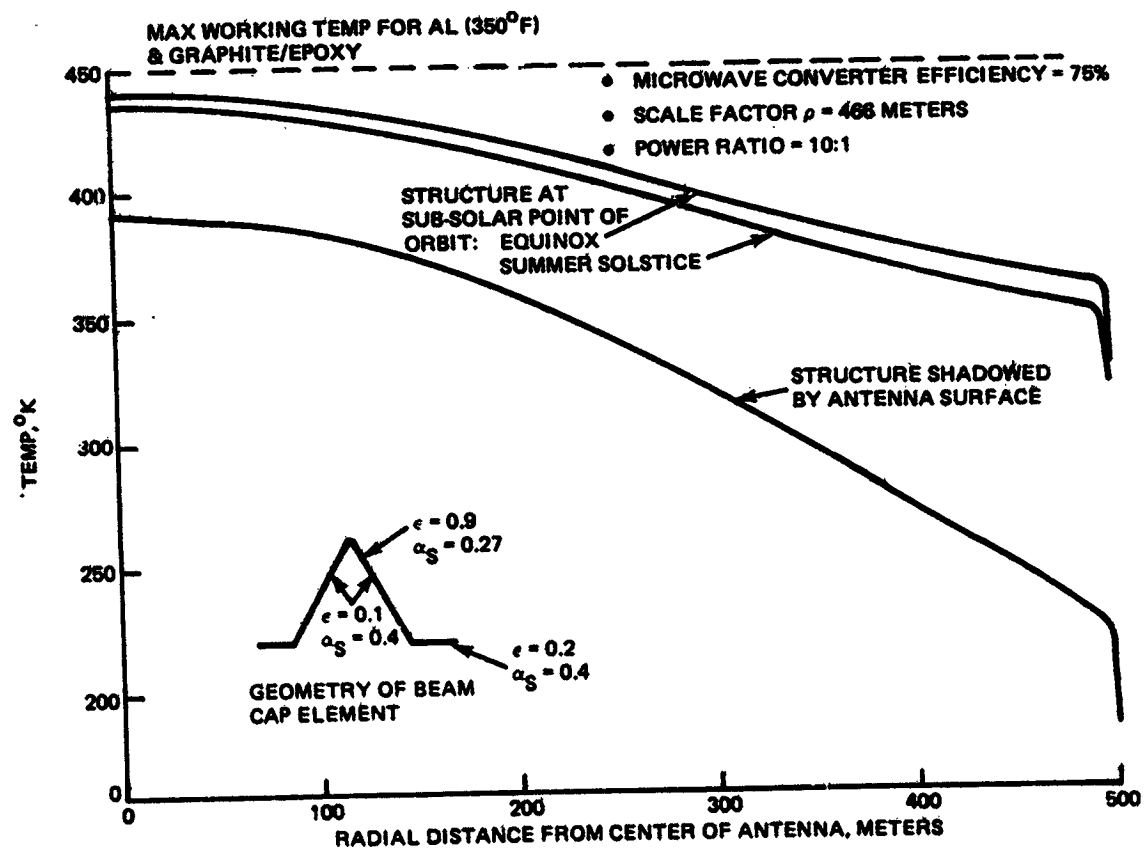
Fig. 3.3-22 Temperature Distribution in a Beam Cap Member Located 1 Meter Above Antenna Surface
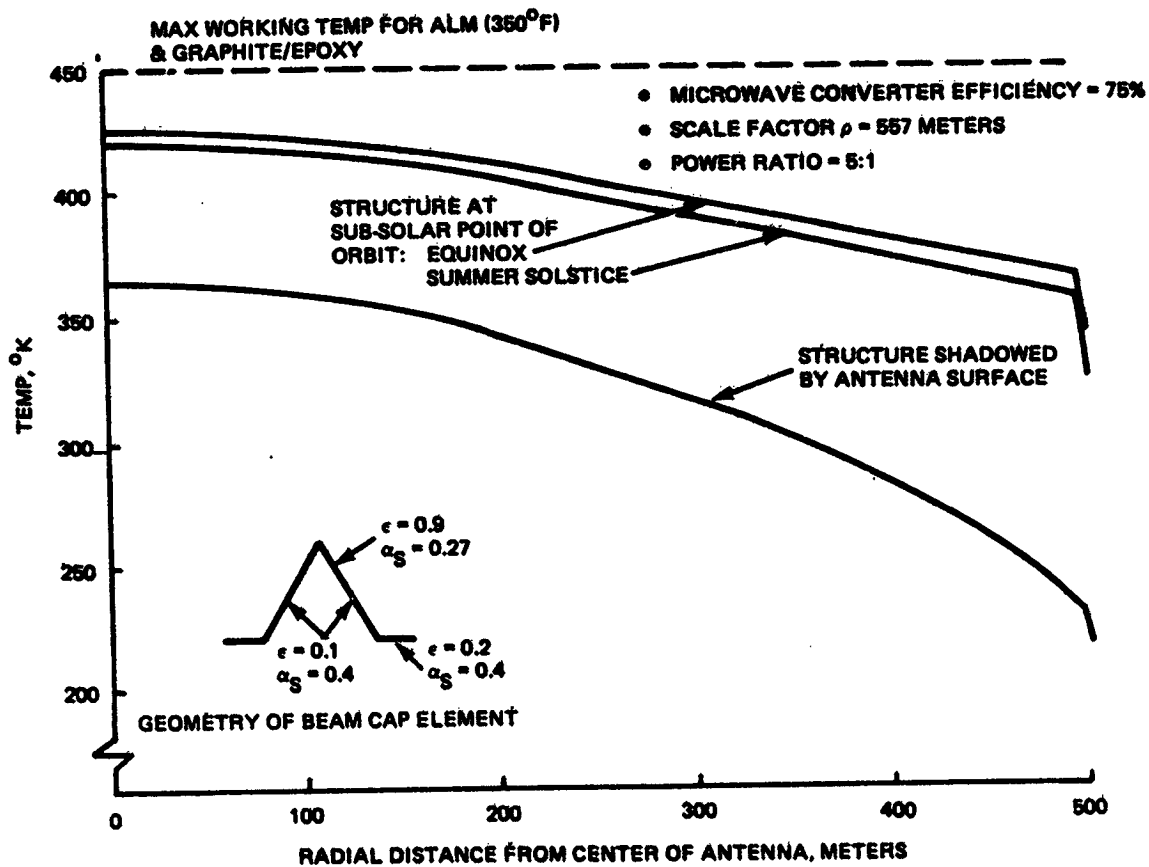
Fig. 3.3-23 Temperature Distribution in a Beam Cap Member Located 1 Meter Above Antenna Surface

Another significant item shown in Fig. 3.3-23 is that the maximum temperature has been reduced from the 440°K shown in Fig. 3.3-22 to 425°K. This is an important reduction in temperature as it provides some margin for an aluminum or graphite/epoxy structure. (The maximum recommended service temperature for these materials is 450°K.)

3.3.2.6 Temperature Difference Between Beam Cap Elements

The temperature gradients within the antenna support structure will pose the most severe design condition for maintaining structural flatness. The severity of the problem is indicated by Ref 12 which states that to limit antenna tip deflections to less than 1 arc-min, the temperature difference between the upper and lower caps must be less than 3°K. Some of the temperature gradients and their causes that can exist within the structure are given next.

A temperature gradient through the cross section of a standard member will exist tending to give the member a banana shape. Such a gradient is caused by non-uniform heating around the surface of a member. The magnitude of the gradient depends on the material, surface radiation properties and geometry of the element. Figure 3.3-21 shows the triangular shaped geometry to have the smallest temperature difference (20°K versus 400°K for the tubular geometry with low inner wall emissivity).

However, a much more significant temperature difference that can exist within the structure is between corresponding elements on the upper and lower caps. The cause of the temperature difference is the different views that the two corresponding elements will have of the radiating antenna surface, with the element furthest away effectively receiving radiant energy from a larger portion of the antenna surface below it. For example, 90% of the radiation flux that impinges on a structural element located a distance d above the antenna surface comes from within an imaginary disc of radius 3d on the surface below it. Because the surface has a Gaussian rather than a uniform distribution, the further element will receive a different amount of energy than the closer element. The amount of radiant energy received by the further element may be more or less than that received by the closer element depending on the location of the elements with respect to the center of the antenna. Near the center, the further element will receive less energy, while near the edge it will receive more. The exact amount of energy received by an element and its resulting temperature were calculated using a computer program that was developed to account for the Gaussian waste heat distribution on the antenna surface.

As a result of this type of temperature difference, the elements on the lower cap will expand more than those on the upper cap and the antenna will tend to "dish." Naturally if a

constant temperature difference existed between upper and lower caps, the structure could be built with members prestressed such that when the temperature difference was applied the antenna would straighten out and become flat. However as the MPTS travels around an orbit the temperature difference between beam caps will vary.

An analysis was performed to assess the temperature difference between beam caps, both on a daily and yearly basis. Figure 3.3-24 presents results of the analysis and shows several things. The first is that the greater the separation distance between elements, the greater the temperature difference between them. There is virtually no temperature difference between elements located 6 meters and 1 meter above the antenna surface, except near the perimeter where the difference is approximately $3°K$. The difference in temperature between elements at 41 meters and 1 meter varys from about $5°K$ near the center to nearly zero and then over $14°K$ at the perimeter. (Note that calculations for temperatures did not include the effects of partial shading that will occur during parts of an orbit and lead to an asymmetrical temperature profile about the center of the antenna.)

Another item of importance shown in Fig. 3.3-24 is that the orbital variation in the temperature difference between the 41 and 1 meter locations is for the most part less than $2°K$; and this is true any time of the year. The orbital variation in the temperature difference between the 6 and 1 meter locations is insignificant - it is lost in the thickness of the line. It is now apparent that the orbital variations in temperature difference are not large and therefore by properly rigging the structure the thermally induced deflections can be nulled out on an orbital average basis. The additional time varying deflections may prove negligible, especially if organic matrices are used, if not it may be possible to electronically compensate for them by "phasing" the microwave converters several times a day.

It is instructive to consider the temperature differences that are produced by a more uniform waste heat distribution. Figure 3.3-25 shows the situation for the scale factor $\rho = 557$ meters which yields a power ratio of 5 to 1 in comparison with the 10 to 1 of Figure 3.3-24. A comparison of the two figures shows that the more nearly uniform the distribution, the smaller the temperature difference between beam caps. This is a second advantage to having a large scale factor; the first advantage of yielding a lower maximum temperature was mentioned earlier.

3.3.2.7 Column Temperatures

Temperature predictions for the columns or vertical members tying the beam caps together as well as the antenna surface to the beams are shown in Fig. 3.3-26. (Columns not shown will have temperatures intermediate to the center and perimeter column

- MICROWAVE CONVERTER EFFICIENCY = 75%
- SCALE FACTOR ρ = 466 METERS
- POWER RATIO = 10:1

RADIAL DISTANCE FROM CENTER OF ANTENNA, METERS

Δ TEMP, $^\circ$K

ORBITAL VARIATION (ANY SEASON)

PRIMARY STRUCTURE

SECONDARY STRUCTURE

$(T_6 \text{ METER} - T_1 \text{ METER})$

TEMP OF MEMBER LOCATED 41 METERS ABOVE ANT. MINUS TEMP OF MEMBER AT 1 METER $(T_{41} - T_1)$
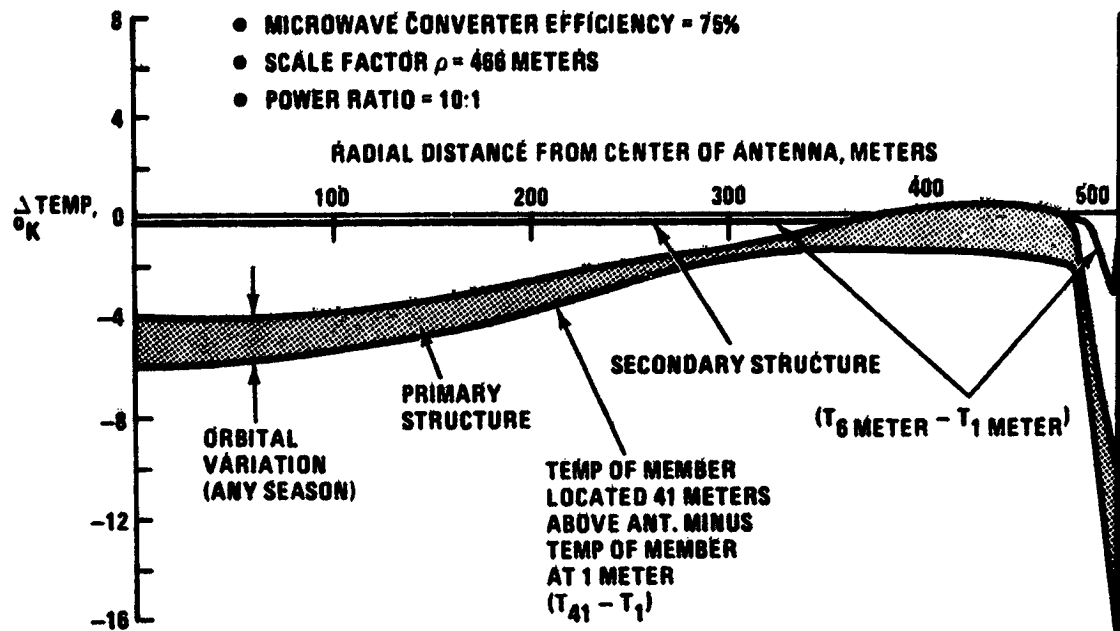
Fig. 3.3-24 Temperature Difference between Beam Cap Members Located Different Distances Above Antenna Surface

- MICROWAVE CONVERTER EFFICIENCY = 75%
- SCALE FACTOR ρ = 557 METERS
- POWER RATIO = 5:1

RADIAL DISTANCE FROM CENTER OF ANTENNA, METERS

ΔTEMP, $^\circ$K

PRIMARY STRUCTURE

SECONDARY STRUCTURE
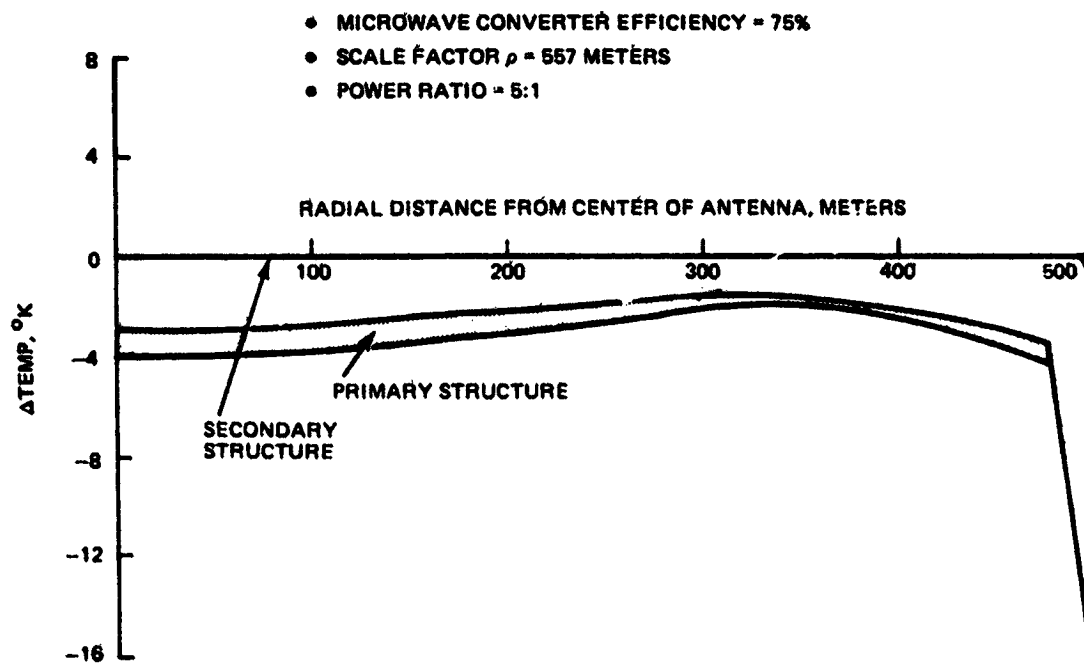
Fig. 3.3-25 Temperature Difference Between Beam Cap Members Located Different Distances Above Antenna Surface

temperatures.) It is seen that there is well over a 200°K temperature difference between a column at the perimeter of the structure and the one at the center. This large temperature difference does not pose a deflection problem provided the sizing of the vertical members reflects the different operating temperatures. However, careful design consideration will have to be given to the vertical members to minimize deflections induced by the different temperature swings (viz., 18°K for a member located near the center, 61°K for a member near the perimeter) caused by the varying sun load. Use of a low solar absorptance coating on vertical members will diminish the Sun's influence so far as a direct solar load on the members is concerned. ($\alpha_s = 0.27$ corresponding to white paint was used in the present study.) However, since the sun's energy is absorbed by the antenna surface and then re-radiated as energy in the infrared region, it is seen that the low α_s coating will not eliminate entirely the difference in temperature swings between columns. Organic matrices with their low thermal expansion coefficients may well be the answer.

The columns near the perimeter are prone to having large temperature gradients along their length and through their cross-section and therefore will probably not be tubular in cross-section. The gradients tend to exist because of the different views elements on the column have of the antenna surface and space. This contrasted with the columns near the center. Every element along these columns, regardless of orientation or position, has the same view of the antenna surface and space, 0.5 each. Consequently, columns near the center will be essentially uniform in temperature but rather hot (viz. 482 - 500°K). Coatings, insulation or geometry selections will not yield any significant reduction in these column temperatures. Near the center of the antenna, the columns will have to be made from a material such as polyimide that can sustain the temperature level of 500°K. If aluminum or graphite/epoxy is to be used for these vertical members, waste heat flux at the center of the antenna must be reduced. One way of accomplishing this reduction while maintaining the total power level of the MPTS is to space the microwave converters differently which can be achieved by increasing the scale factor ρ. Increasing ρ has the effect of reducing the power transmitted from the center of the antenna and increasing it at the perimeter. A discussion of the effects of varying ρ are given next.

3.3.2.8 Effect of Microwave Converter Spacing

Maximum structural temperatures are dictated by the maximum waste heat flux. These maximum values occur at the center of the antenna where the microwave converters are most densely packed. The microwave converter spacing is given by $L = L_{min} \cdot EXP$ $((r/\rho)^2)$ meters where L_{min} = the converter spacing at the center of the antenna in meters,

r = distance from antenna center in meters, and ρ = scale factor in meters. It follows that the waste heat flux radiated towards the structure at the center of the antenna is given by:

$$Q_{max} = \frac{2 * F * (1 - \eta) * P}{\pi * \eta * \rho^2 \left[1 - EXP\ (2(r_0/\rho)^2\right]} \qquad \frac{watts}{m^2}$$

where

F = fraction of waste heat radiated toward the structure, the remainder being radiated toward earth

η = efficiency of microwave converter

P = power transmitted by antenna watts

ρ = scale factor, meters

r_0 = radius of antenna, meters

It is interesting to observe that for a given power transmission the maximum waste heat flux is independent of L_{min}. This can be attributed to the fact that increasing L_{min} requires increasing the power level per converter. The end result being that the waste heat per unit area remains constant (assuming constant converter efficiency).

Figure 3.3-27 presents the waste heat flux at the center of the antenna as a function of the scale factor ρ. Two curves are shown: one for a microwave converter efficiency of 85% and the other for an efficiency of 70% which is now considered representative of the klystron performance rather than 75%. For values up to about 600 meters, ρ exhibits a strong influence on the maximum waste heat flux. The maximum flux values that can be tolerated by three candidate materials are shown as 3600, 3600, and 8100 w/m^2 for aluminum, graphite/epoxy and polyimide composites, respectively. These values establish minimum values for the scale factor ρ, i.e., they impose a constraint on the shape of the Gaussian distribution. For example, considering an efficiency of 70% and an aluminum structure, Fig. 3.3-27 shows that the microwave converters will have to be spaced according to $\rho \geqq 1100$ meters, which produces a fairly flat Gaussian distribution, nearly a uniform distribution. Figure 3.3-28 shows the waste heat profile across the antenna surface for three values of ρ. It clearly illustrates the effect that ρ has on the waste heat profile; smaller values of ρ producing profiles with greater waste heat concentrations at the center and lower waste heat concentrations at the perimeter, which in turn leads to greater differences in column and beam temperatures between the center and the perimeter.

289°K (60°F) FULL SUN

228°K (–50°F) NO SUN
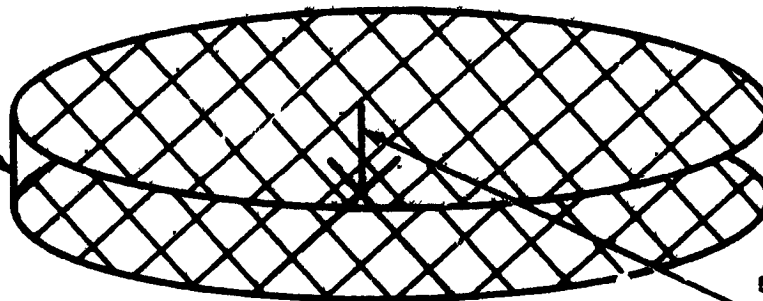
500°K (440°F) FULL SUN

482°K (408°F) NO SUN

Fig. 3.3-26 Column Temperatures

- MICROWAVE CONVERTER SPACING = $L_{MIN} \cdot EXP((R/\rho)^2)$
- ANTENNA DIAMETER = 1 Km
- WASTE HEAT TOWARD STRUCTURE = 87.5%

WASTE HEAT FLUX, KW/M²

MAX FOR POLYIMIDE

MAX FOR ALUMINUM GR/EP

MICROWAVE CONVERTER EFFICIENCY

70%

85%

SCALE FACTOR ρ, METERS
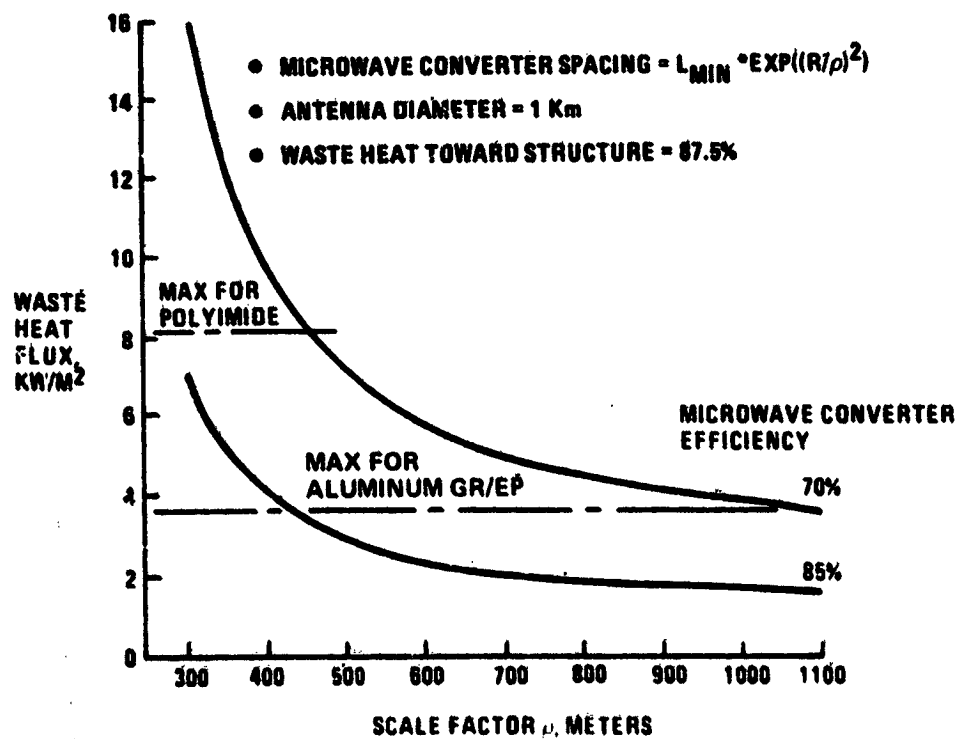
Fig. 3.3-27 Waste Heat Flux at Center of Antenna as Function of the Scale Factor
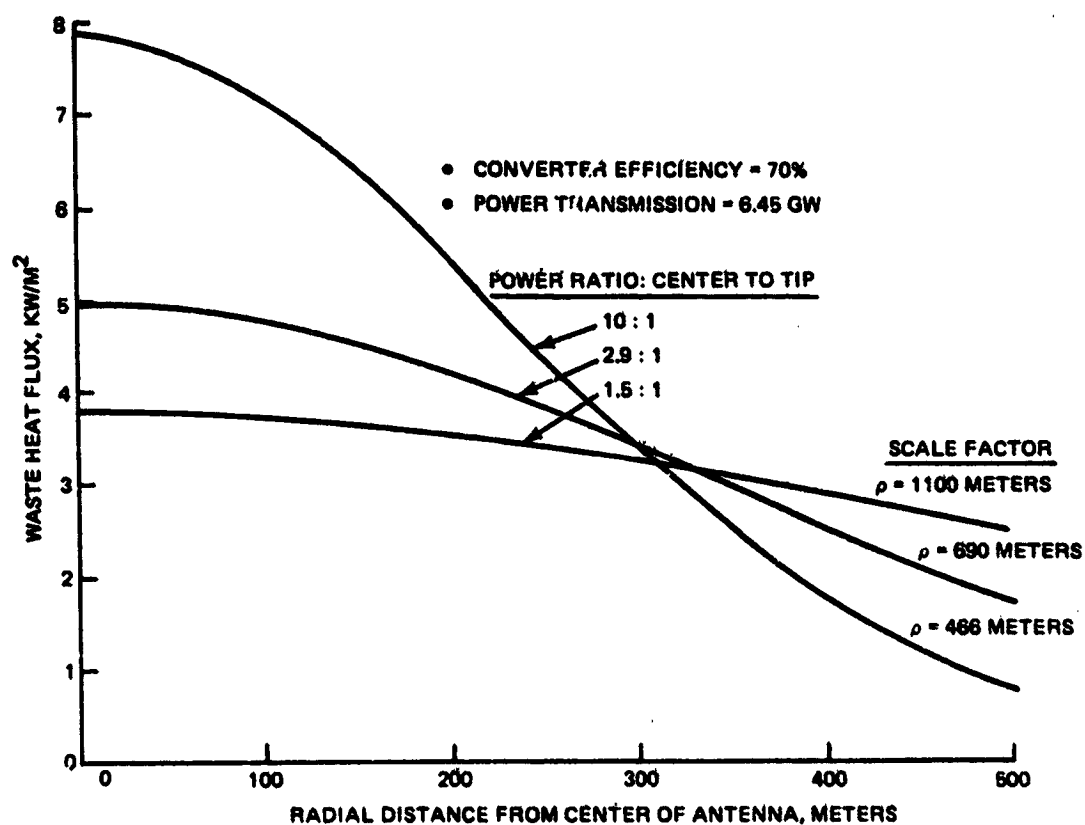
Fig. 3.3-28 Waste Heat Profile for Various Values of the Scale Factor

The effect of ρ on the maximum structural temperatures is shown in Fig. 3.3-29 for two efficiencies, 70 and 85%, and two types of members, vertical and horizontal. Figure 3.3-29 reinforces what was mentioned early that a vertical member or column will run hotter than a horizontal beam at the center of the antenna. But more to the relevancy of ρ is the trend shown of decreasing temperature with increasing ρ. It is obvious that the choice of ρ may well impose a constraint on material selection. It is recognized that ρ will influence the microwave transmission efficiency and the total power that can be handled by the MPTS. It should now be obvious that ρ has a strong effect on structural temperatures and material selection which must be accounted for in any studies to optimize the power received on Earth.

Before closing this section it should be noted that there are other ways of reducing the maximum structural temperature than by increasing ρ; some of the methods are:

● Alter the microwave converter radiator design so that more of the waste heat is rejected in the transmission direction of the microwaves (toward Earth) and less is radiated towards the antenna support structure. In the present study, 87.5% of the microwave converter waste heat is being radiated towards the structure and 12.5% toward Earth.

● Employ heat pipes to smooth out the heat rejection profile so as to produce a nearly uniform profile across the surface of the antenna (see Fig. 3.3-30).

● Design the microwave converter radiator surfaces to be geometrically and spectrally selective so as to reduce the amount of solar energy that is absorbed and to alter the distribution of radiant flux emanating from the antenna to a more nearly uniform one.

● Use special coatings on the structural members. For the present study white paint ($\alpha_s/\epsilon = 0.3$) was used on the side of members facing space and an aluminum finish ($\epsilon = 0.1$ and $\epsilon = 0.2$, lightly anodized) for the side facing the antenna surface. Coatings such as silver teflon ($\alpha_s/\epsilon = 0.1$) and gold ($\epsilon = 0.05$), respectively could be substituted for the white paint and aluminum.

It must be noted that most coatings degrade as a result of exposure to ultraviolet radiation and particulate radiation emanating from galactic sources and the Van Allen belt. The 30-year MPTS design life demands that serious consideration be given to establishing the extent of degradation. At the present time there is a dearth of data for ultraviolet exposures greater than 10^4 sun-hours; the MPTS will have an exposure of approximately 2.6 x 10^5 sun-hours.
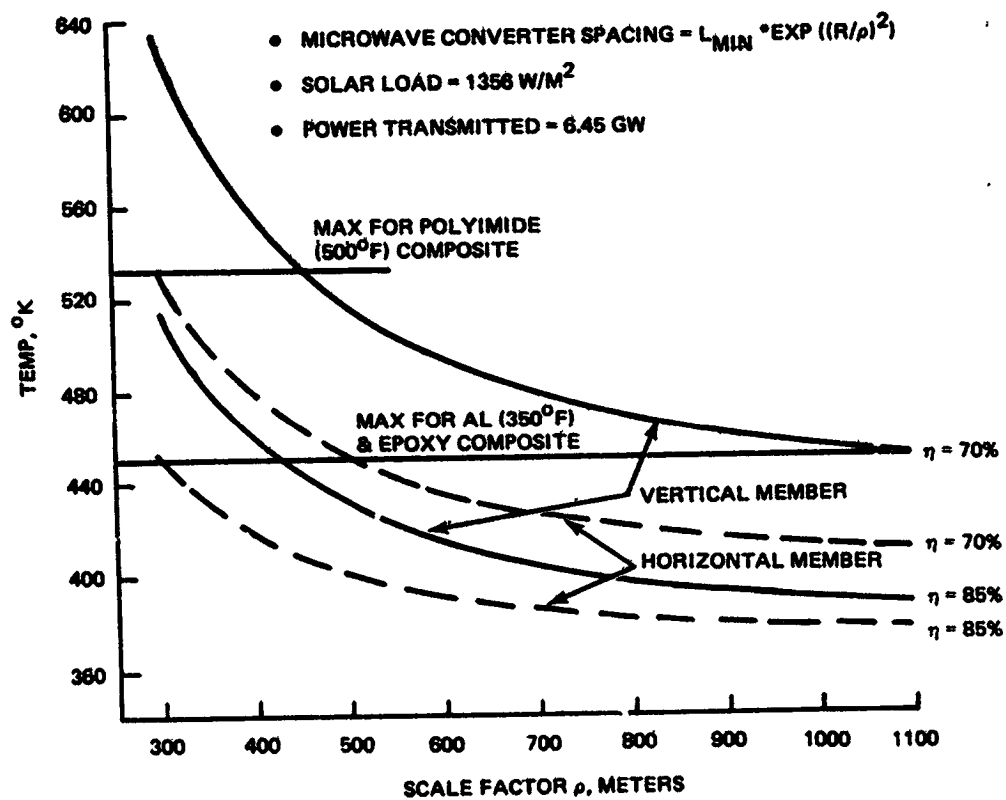
Fig. 3.3-29 Maximum Temperatures as a Function of Scale Factor
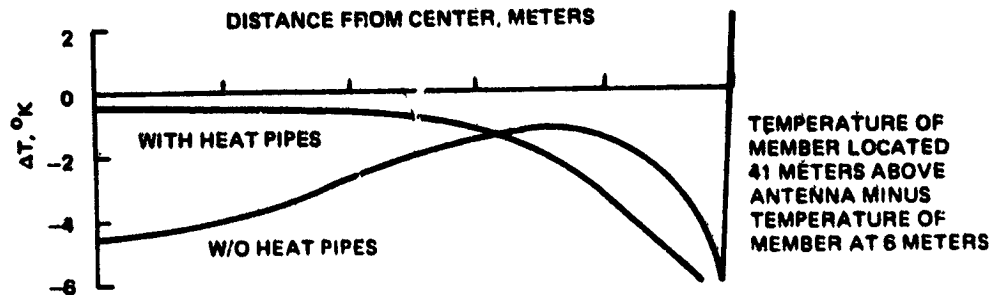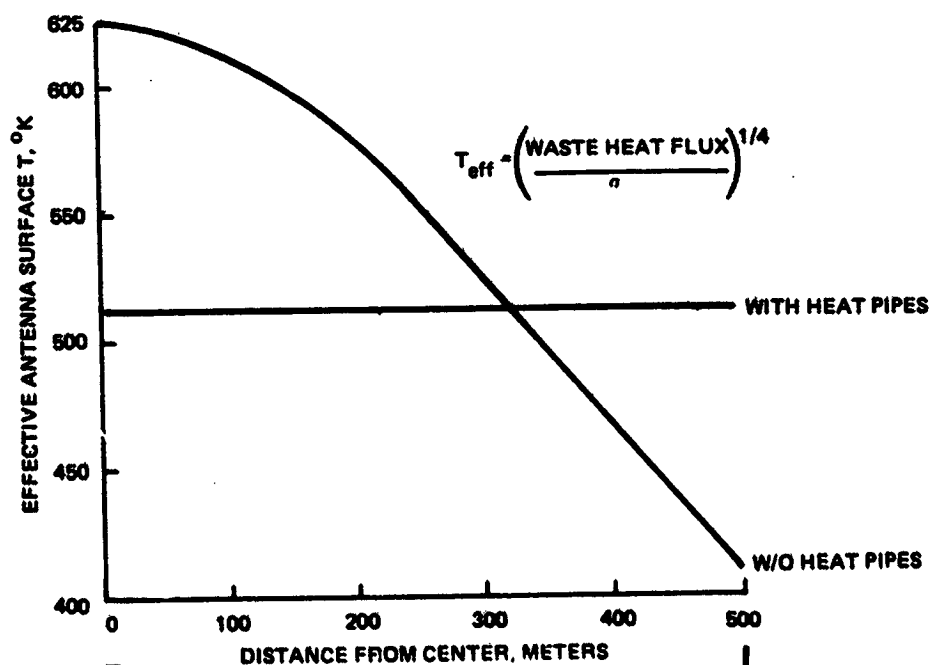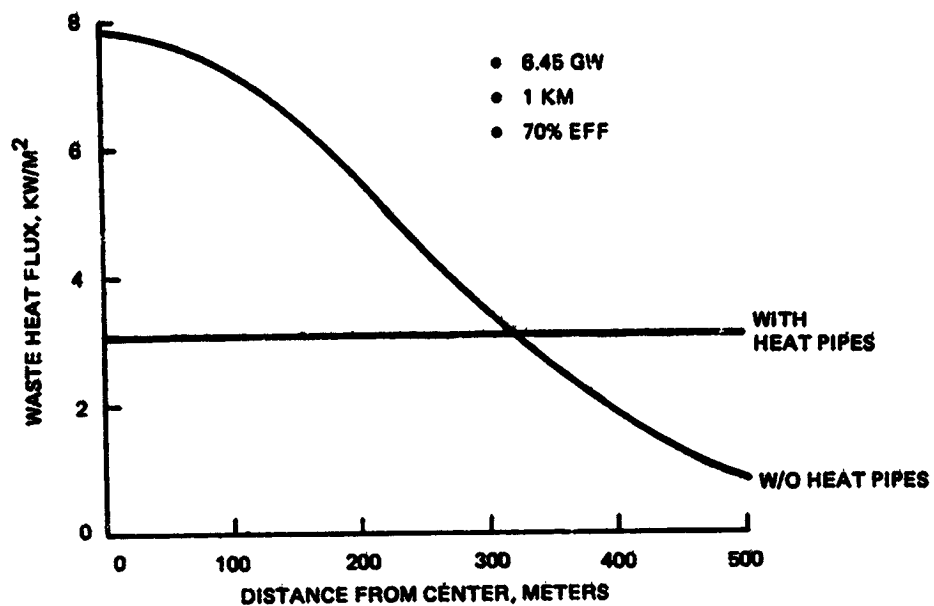
Fig. 3.3-30 Thermal Performance of MPTS With and Without Heat Pipes

The chart labels and values:

Top graph:
- Y-axis: WASTE HEAT FLUX, KW/M²
- X-axis: DISTANCE FROM CENTER, METERS
- • 6.45 GW
- • 1 KM
- • 70% EFF
- WITH HEAT PIPES
- W/O HEAT PIPES

Middle graph:
- Y-axis: EFFECTIVE ANTENNA SURFACE T, °K
- X-axis: DISTANCE FROM CENTER, METERS
- $T_{eff} = \left(\dfrac{WASTE\ HEAT\ FLUX}{\sigma}\right)^{1/4}$
- WITH HEAT PIPES
- W/O HEAT PIPES

Bottom graph:
- Y-axis: ΔT, °K
- WITH HEAT PIPES
- W/O HEAT PIPES
- TEMPERATURE OF MEMBER LOCATED 41 METERS ABOVE ANTENNA MINUS TEMPERATURE OF MEMBER AT 6 METERS

3.3.3 Structural Analysis

The following is a summary assessment of preliminary structural design options:

- Structural arrangements of the antenna primary structure leads to selection based on light weight of a rectangular grid beam arrangement, which is 15% to 30% lighter than either a triangular or radial arrangement.

- Primary structural member evaluation considering columns of 5, 25 and 100 meter lengths concludes that primary structure caps should be built up as triangular girders. 18 meter long girders made up of 3 meter bays has been selected for cap members.

- A determination was made that inertially induced deflections are insignificant, but thermal gradients must be kept low, in the order $2°$ to $4°C$ between the upper and lower caps of the primary structure.

- Composites offer attractive features in terms of weight savings and thermal properties.

- Other factors for future study are the integration of power lines and structure.

3.3.3.1 Antenna Structural Design Arrangements

Three structural arrangements were considered as candidates for the baseline design (see Fig. 3.3-31).

- Rectangular Grid Beams - Primary beams at right angles to each other

- Triangular Grid Beams - Primary beams arranged in such a manner as to produce geodetic structure

- Radial spoke beams - Primary beams emanating from a central core and extending to the periphery as spokes in a bicycle wheel.

The inertial loads applied to the antenna are relatively low, therefore the total structural weight is a direct function of total beam length. Assuming equal lengths of unsupported beams in each case, the total beam length for the three arrangements were generated. The ratio of their respective total lengths are shown in Fig. 3.3-32. The respective total lengths are approximately 15.760 meters for the rectangular grid, 23,300 meters for the triangular and 21,330 meters for the radial. Figure 3.3-32 was generated to demonstrate weight relationships using an L/D (length of member/dia. of member) of 20 to 100. In each case aluminum with a thickness of 0.02 in. (0.05 cm) and a height between caps of 40 meters was assumed.
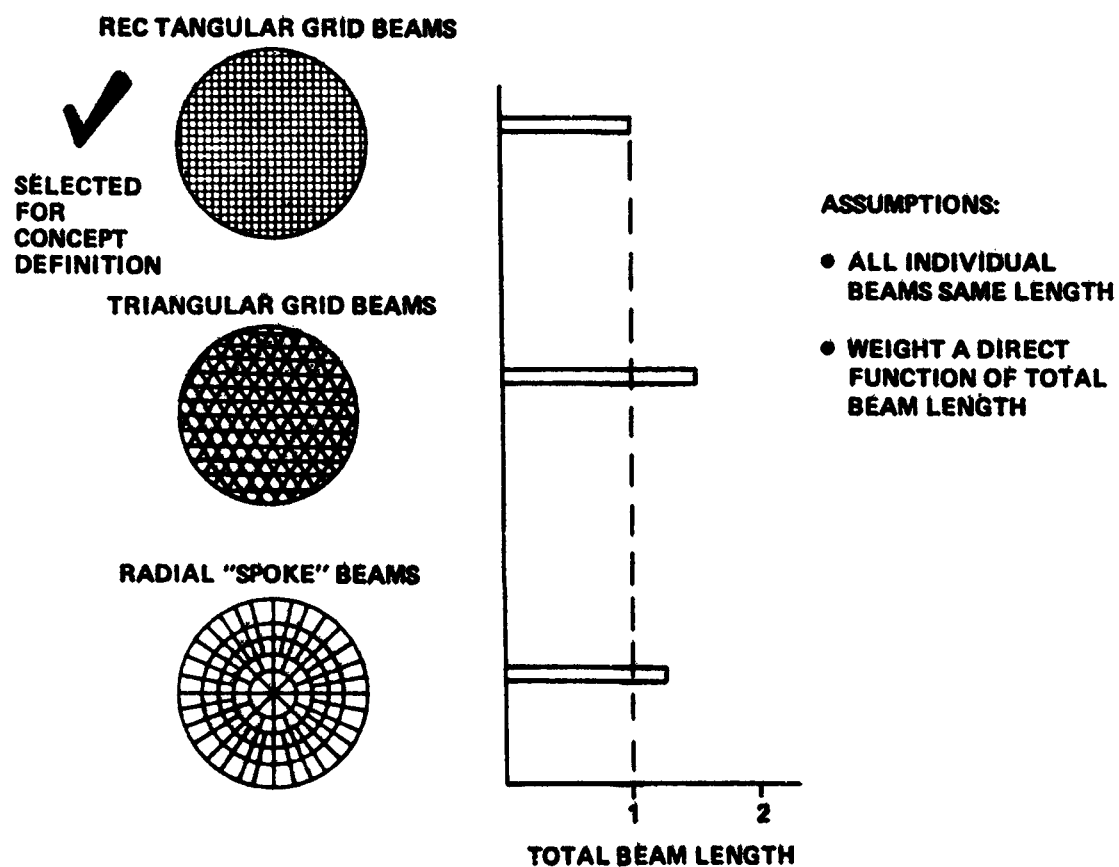
Fig. 3.3-31 Alternate Structural Arrangements
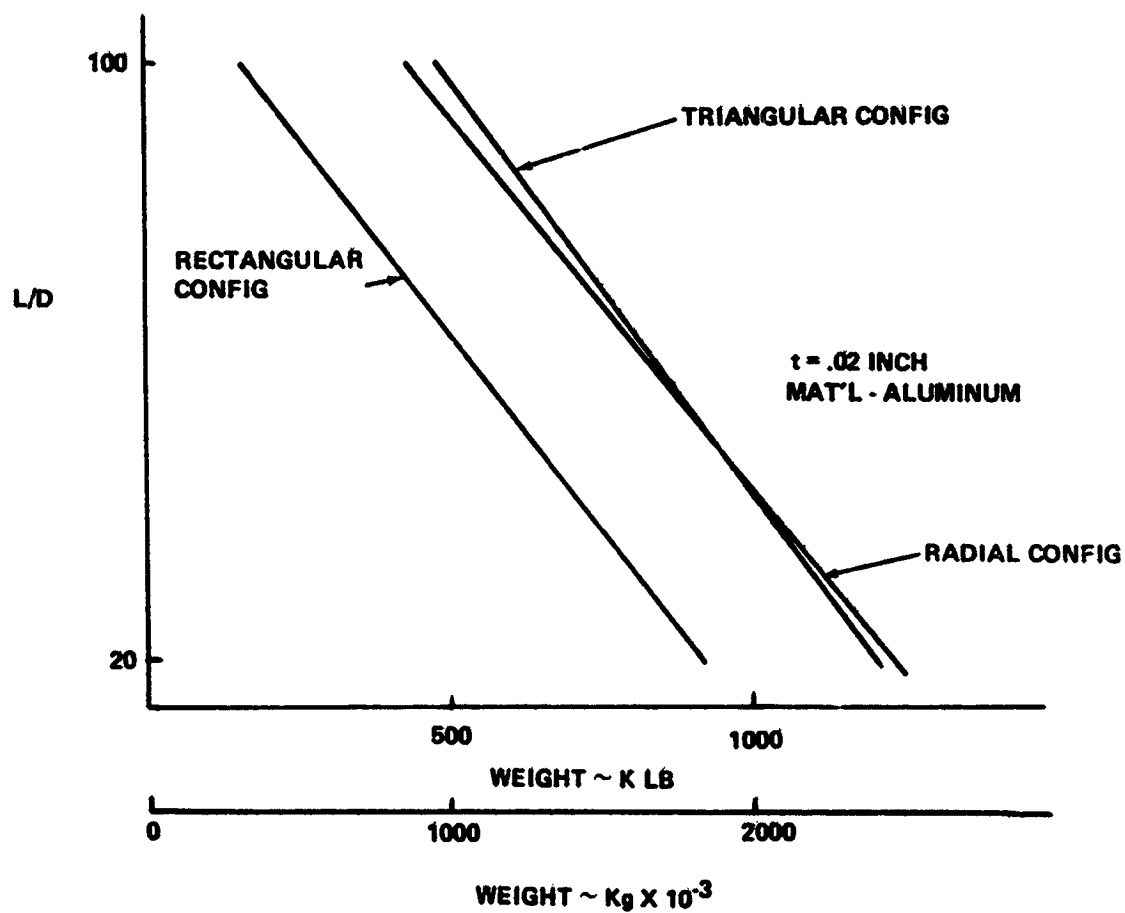
Fig. 3.3-32 Weight Relationship for Different L/D (Length Tube/Diameters)

3.3.3.2 Structural Member Evaluation

Structural member analyses were carried out to establish a feasible structural arrangement and to calculate member sizes to arrive at the lowest weight compatible with the existing thermal environment. It should be noted that this study did not include overall structural geometry optimization and the general arrangement, Fig. 3.2-1 and 3.2-2 was used to determine member loads and sizes. The previously used applied loads based on gravity gradient induced torques, have been superseded by torques generated by slip ring/brush pressure and result in an average of 100 lb force compression loads in the upper and lower bending members.

Our Task 1 sizing effort was based on aluminum tubular members to form the baseline triangular girder. The selection was based on the comparison of (1) a single circular tube 100 meters long and (2) a triangular girder with a tubular member at each apex with cross tubes and diagonal bracing. The later section was also assumed as an Euler column 100 meters long, since this member, while braced at 25 meter intervals by vertical members, can fail in the lateral column buckling mode. Figure 3.3-33 and 3.3-34 show the wall thickness vs diameter at various compression loads for the Euler failure mode and were calculated for 5, 25 and 100 meter lengths.

After the thermal profile was generated, it became evident that the tubular elements, particularly aluminum, could not be used. Considering that, plus the new loads, selection of a new shape and material was initiated, resulting in the "modified V" fabricated from graphite/epoxy or graphite/polyimide. Analysis of this section, Fig. 3.3-35 shows that it is capable of balancing a compressive load of 127 lb at 450°K. Local crippling does not appear to be critical. The current investigation did not include loads induced by preloads in cable cross bracing required to overcome cable slack or tension caused by thermal expansion. Further study is required for this investigation.

3.3.3.3 Structural Deflection

The primary load which the antenna is subjected to is due to the torques generated by slip ring brush pressure. A bending moment curve Fig. 3.3-36 was generated and resulting deflections calculated. As shown in Fig. 3.3-37 these deflections are within the allowable 1 arc-min.

Initially a simplified thermal model was used to arrive at the deflections shown in Fig. 3.3-37. With the selection of the 1 km diameter baseline, a more extensive thermal profile, Fig. 3.3-24, was generated and new deflections calculated. These calculations

Fig. 3.3-33 Strength of Circular Tubes for Various Axial Compression
Loads as Function of Wall Thickness and Diameter
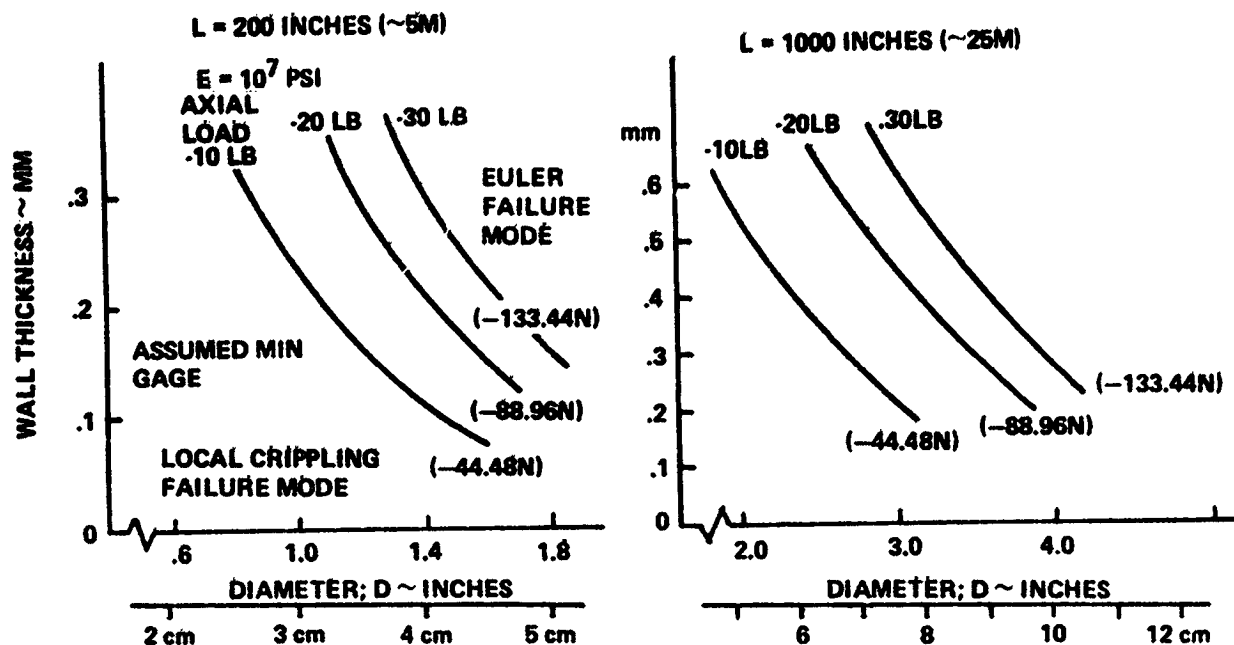
LOCAL CRIPPLING SHOWN AS INDEPENDENT OF
D SINCE LOW VALUE OF C IS USED IN BUCKLING

RELATION $F = CE \frac{t}{r}$ C = .06 WAS USED TO ACCOUNT FOR INITIAL IMPERFECTIONS
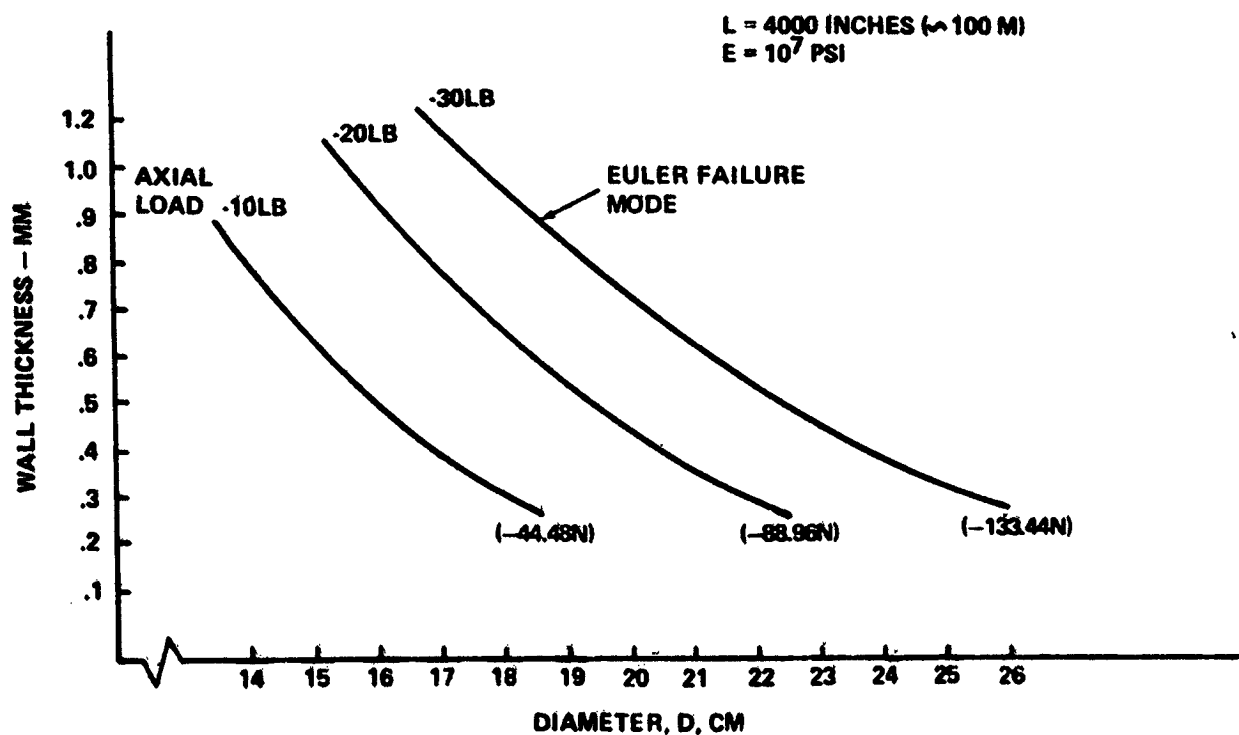
Fig. 3.3-34 Strength of Circular Tubes for Various Axial Compression
Loads as Function of Wall Thickness

DESIGN CONDITIONS

- $T = 450^\circ K$
- END LOAD = 440 NEWTON
- SUPPORT EVERY 3M
- MINIMUM 5 PLY COMPOSITE

3/16 R

.02

60°

1.78 IN.

1/8 R.

.436 TYP.

3M (118")
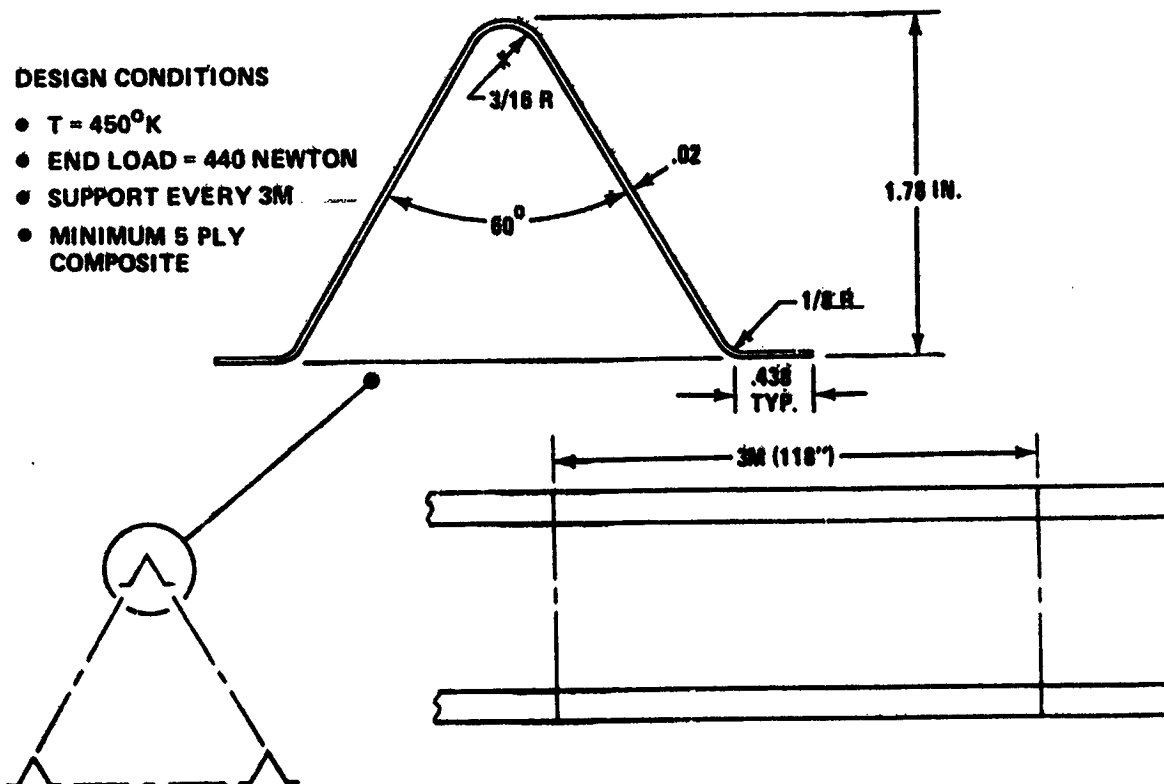
Fig. 3.3-35 Tri Beam Cap Cross-Sections (Graphite/Epoxy)

ULTIMATE BENDING MOMENT
FOR .75 KM, 1.0 KM, 1.5 KM,
DIAMETERS

FACTOR OF
SAFETY = 1.25

1.5 KM

1 KM

.75 KM

.5 KM

NEWTON-METERS X 10^3

Fig. 3.3-36 Design Loads

A. LOAD INDUCED

B. THERMALLY INDUCED
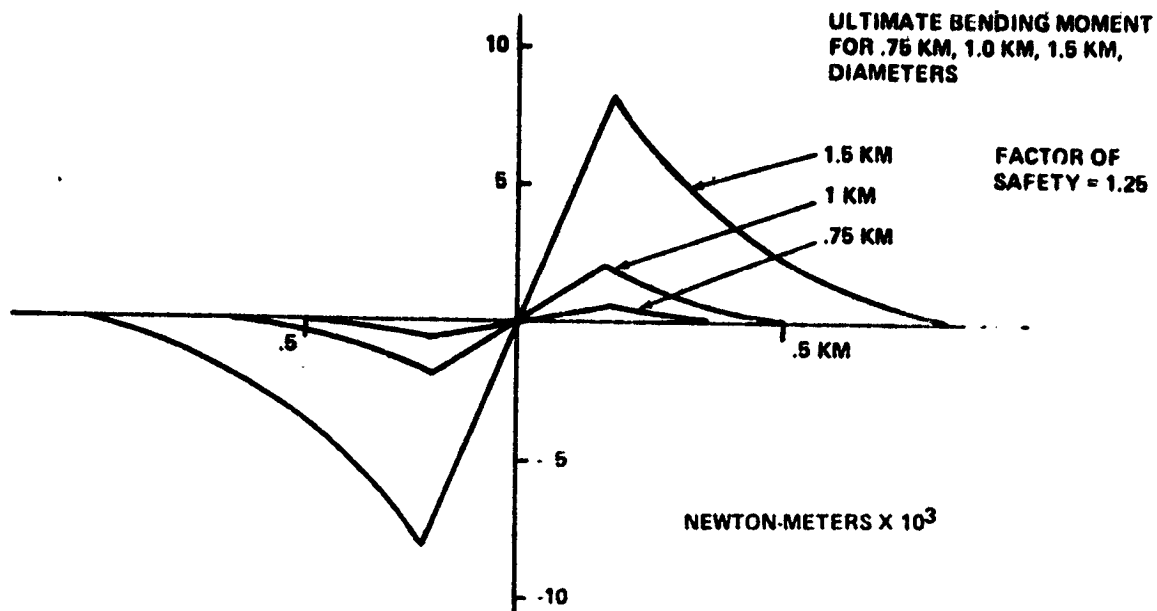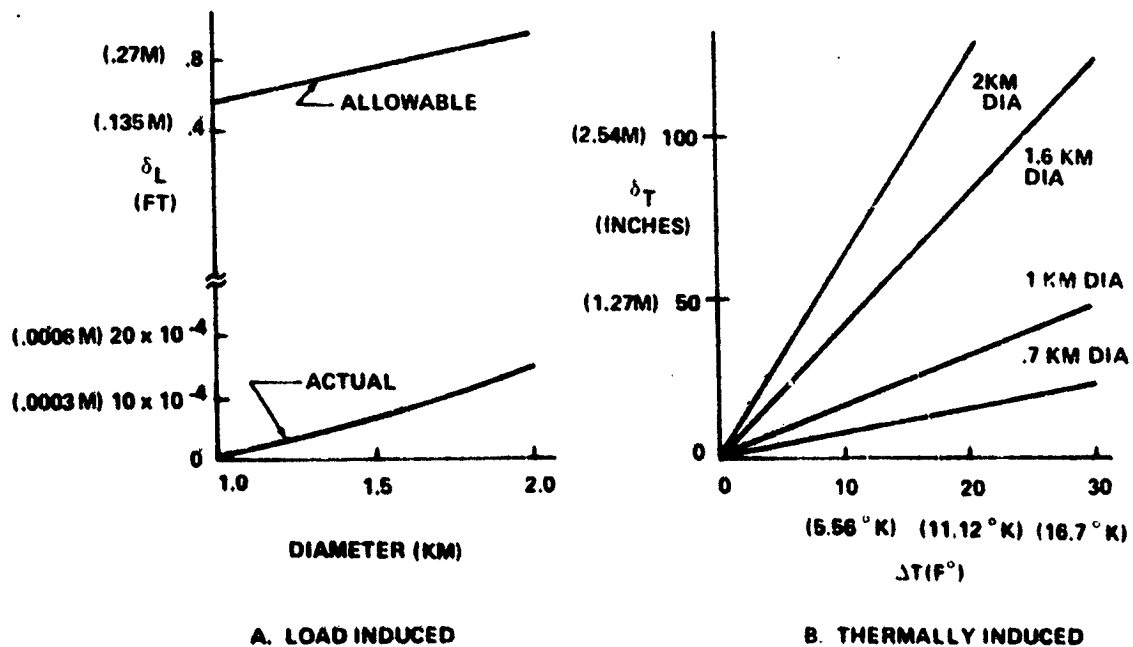
Fig. 3.3-37 Deflections — Preliminary Assessment

3.3-47

were performed with the use of an in-house "3-dimensional frame" computer program. The resulting deflections curve and slopes are shown in Fig. 3.3-38 and 3.3-39 for the primary structure.

To evaluate the effects of secondary structural deflection on the overall deflection, a section of structure farthese from the antenna center was chosen for examination. This particular area was chosen because (1) it is the area that the primary structure experiences its largest deflection and (2) the temperature gradients are highest. Figure 3.3-40 reflects the deflections and slopes calculated for the secondary structure, and as can be seen, the magnitudes will contribute very little to the overall deflections.

Note that Fig. 3.3-38 and 3.3-39 show the deflections and slopes calculated for temperature deviations that occur during different seasonal and orbital positions. The mean ΔT curves represent the location and angle that the respective waveguide arrays would be assembled to the secondary structure. The waveguide assemblies within approximately the 16,000 in. (406 M) radius can be preset or "tuned" once and left alone. Those located beyond this radius must be adjustable in flight by use of screw jacks or similar devices. Further elimination of adjustable devices can be achieved by judicious design procedures to reduce deflections at the antenna periphery. Close manufacturing tolerances will have to be augmented by an adjustment or "tuning" technique in order to minimize built-in waviness and deflections. A study of tolerances, both manufacturing and assembly would determine the extent and type of adjustment that would be necessary. A typical girder 18 meters long has the following tolerances:

Length	± 2 in. (50.8 mm)
Coupling fitting	± .25 in. (6.35 mm) (mechanical or weldment)
Straightness	± 1/2 in. (12.7 mm)
RSS	± 2.076 in. (52.73 mm)

The RSS over a 1000-meter length of 40 beam element is:

$$\delta = \sqrt{N\sigma_n} \qquad \text{where} \qquad \sigma_N = \sqrt{\sigma_1^2 + \sigma_2^2 + \cdots \sigma_n^2}$$

The worst case angle of curvature is defined by:

$$\ominus = \frac{(\ell/2 + \delta/2) \; (1 - \frac{\ell/2 - \delta/2}{\ell/2 + \delta/2})}{H}$$

where H = 35 meters

$\ell/2$ = 500 meters

$\delta/2 = .\dfrac{10540}{2} = .05275$

= 0.003 radians or 0.1723°
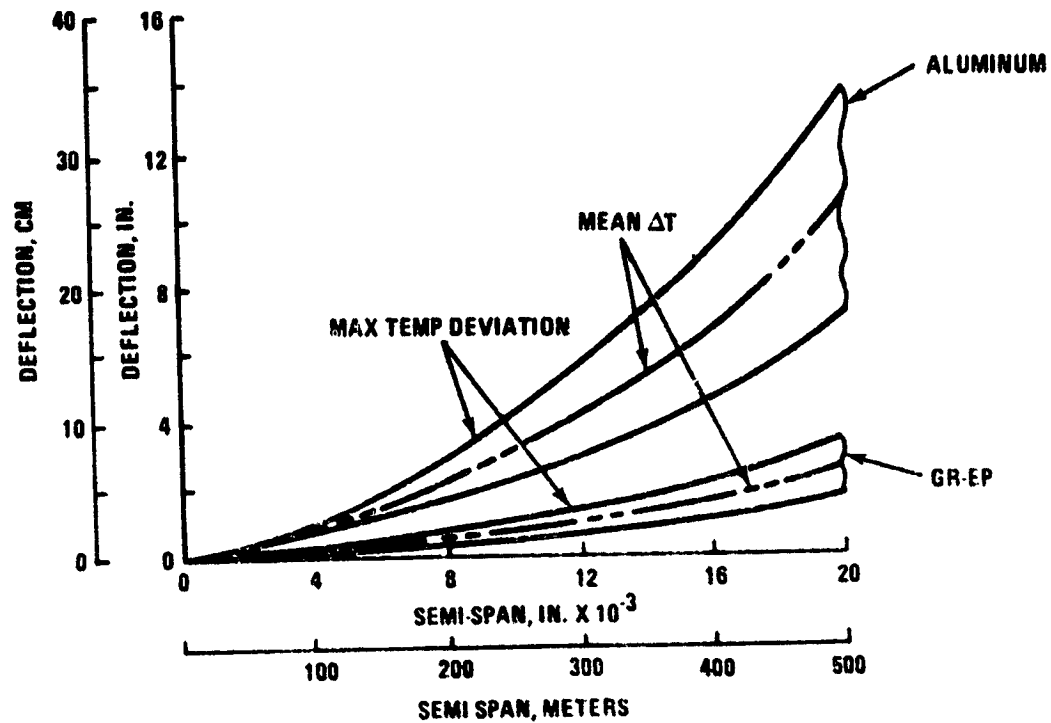
Fig. 3.3-38 Typical Antenna Deflections Due to Thermal Gradients (40 Meter Beam Depth)
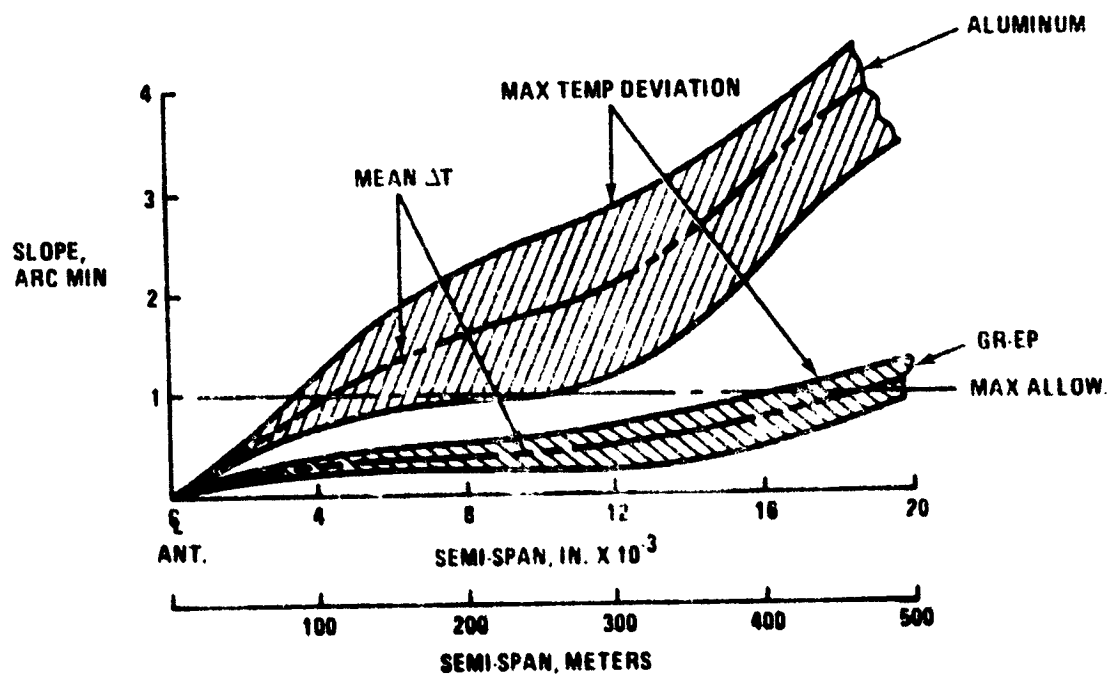
Fig. 3.3-39 Typical Slopes of Structure Due to Thermal Gradients
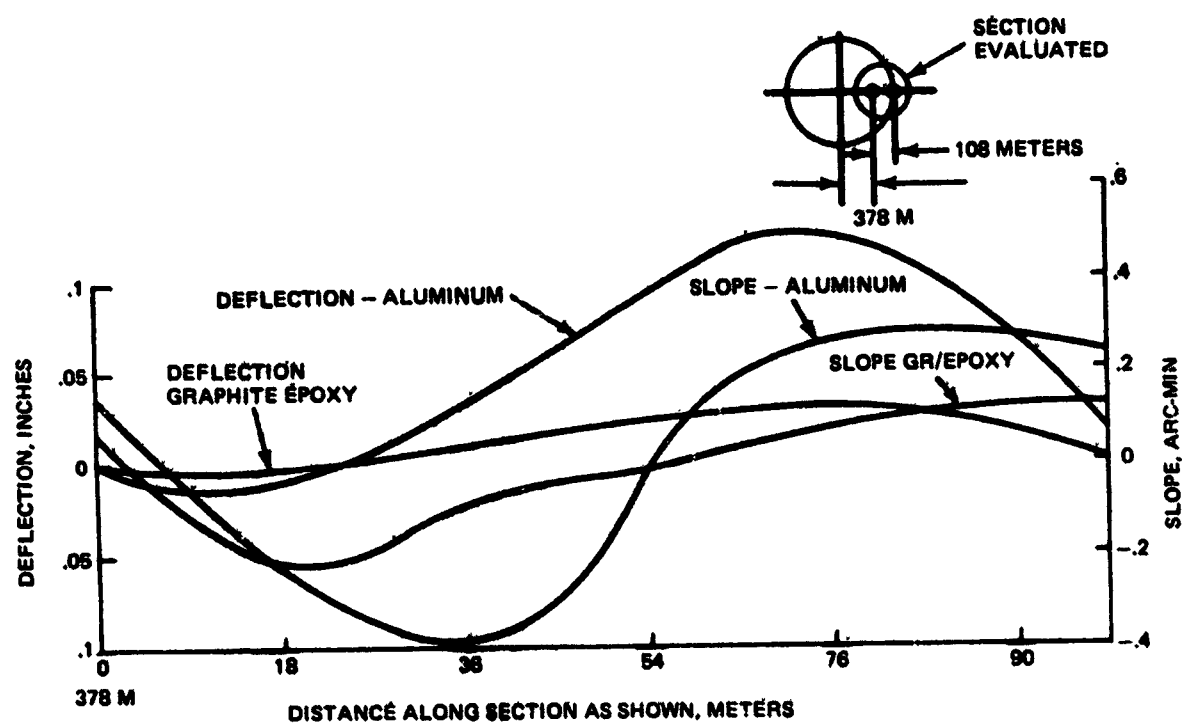
Fig. 3.3-40 "Egg Crate" Secondary Structure Deflection Slopes (108 Meter Section)

As the limit of curvature must be held to 1 arc-min or 0.0166°, a further analysis is required to determine probability of this worst case occurring.

3.3.3.4 Materials

Three materials have been considered for the antenna structure: aluminum, graphite/epoxy and polyimide composites. Each material has its advantages and disadvantages. Aluminum offers low material cost and established processing, manufacturing and assembly techniques but suffers from relatively high coefficient of thermal expansion. Graphite/epoxy, an organic composite that Grumman is developing extensive experience with, exhibits the attractive properties of a low coefficient of thermal expansion and a high strength-to-weight ratio. On the debit side, the material cost of graphite/epoxy runs 25 to 200 times that of aluminum. Also on the debit side is the relatively low maximum recommended service temperature for graphite/epoxy (conservative designers limit graphite/epoxy to 450°K, i.e., 350°F, the same as aluminum). Based on the temperature predictions of Subsection 3.3.2, the use of either aluminum or graphite/epoxy for the columns near the center of the antenna is precluded (see Fig. 3.3-26); the use of these materials for the beam cap elements near the center is marginally satisfactory.

Polyimide composites such as graphite/polyimide or Kevlar/polyimide offer relief to the temperature problem as they have maximum recommended service temperatures in the range 530 to 645°K (500 to 700°F). In addition to the higher allowable temperature, graphite/polyimide offers the same main advantages of a graphite/epoxy matrix, namely high strength-to-weight ratio and low coefficient of thermal expansion. Figure 3.3-41 shows these properties for various graphite composite systems. Little data exists for the strength characteristics of epoxy and polyimide composites at elevated temperatures. However, Fig. 3.3-42 sheds light on the performance of these materials when used as adhesives. The superiority of polyimide over epoxy at 533°K (500°F) is obvious. But concern exists as to what the performance of polyimide will be after 30 years (2.6×10^{5} hrs) of operation at 533°K. Figure 3.3-42 shows that after 4×10^{4} hours (4.6 years) the lap shear strength is only 65% of its value after 10 hours. Suitable tests and extrapolation procedures are required to resolve this concern.

On the debit side, the material and processing costs for polyimides are considerable in comparison with epoxy. Futhermore, as Fig. 3.3-43 shows, polyimides have a high volatile content. More than likely the polyimides will be processed in space and, therefore, a suitable bleeder system must be provided to prevent contaminating items such as microwave converters and parts that have been thermally coated.

| GRAPHITE & COMPOSITE | FIBER LAYOUT (3-PLY) | RESIN | 3 PLY PROPERTIES | | | | | | MAX TEMP, °K |
| | | | THICKNESS (mm) | DENSITY (Kg/m³) | TENSILE STRENGTH (10^6n/m²) | TENSILE MODULUS (10^9n/m) | THERMAL COEF 10^{-6} m/m/°K | | |
							LONG.	TRANSVERSE	
T300/5208 (EPOXY)	$(0 \pm 60)_T$	5208	0.17	1600	345-415	48-76	0.36-0.63	1.1-4.5	450
HT-S/710 (POLYIMIDE)	$(0 \pm 60)_T$	SKYBOND 710	0.17 (1)	1550	275-310	48-69	0.36-0.63	1.1-4.5	590
HT-S/710 (POLYIMIDE)	$(0 \pm 45)_T$	SKYBOND 710	0.17 (1)	1550	345-415	69-83	0.36-0.90	1.2-3.6	645
AS/3501 (EPOXY)	(0 ± 60)	3501	0.17	1520	275-310	58-69	0.36-0.63	1.1-4.5	450
HH-S/3501 (EPOXY)	(0 ± 60)	3501	0.17 (1)	1745	195-240	83-103	0.18-0.40	0.7-1.8	450

NOTE: AT PRESENT NO SOURCE IS AVAILABLE FOR THIN PLY GR/PI, OR HM-S/3501. THESE ESTIMATES ARE BASED ON LIMITED DATA AVAILABLE ON COMPOSITE LAMINATES SUCH AS $(0/\pm 60)_S$ OF CONVENTIONAL THICKNESS.

Fig. 3.3-41 Estimated Graphite Composite Properties
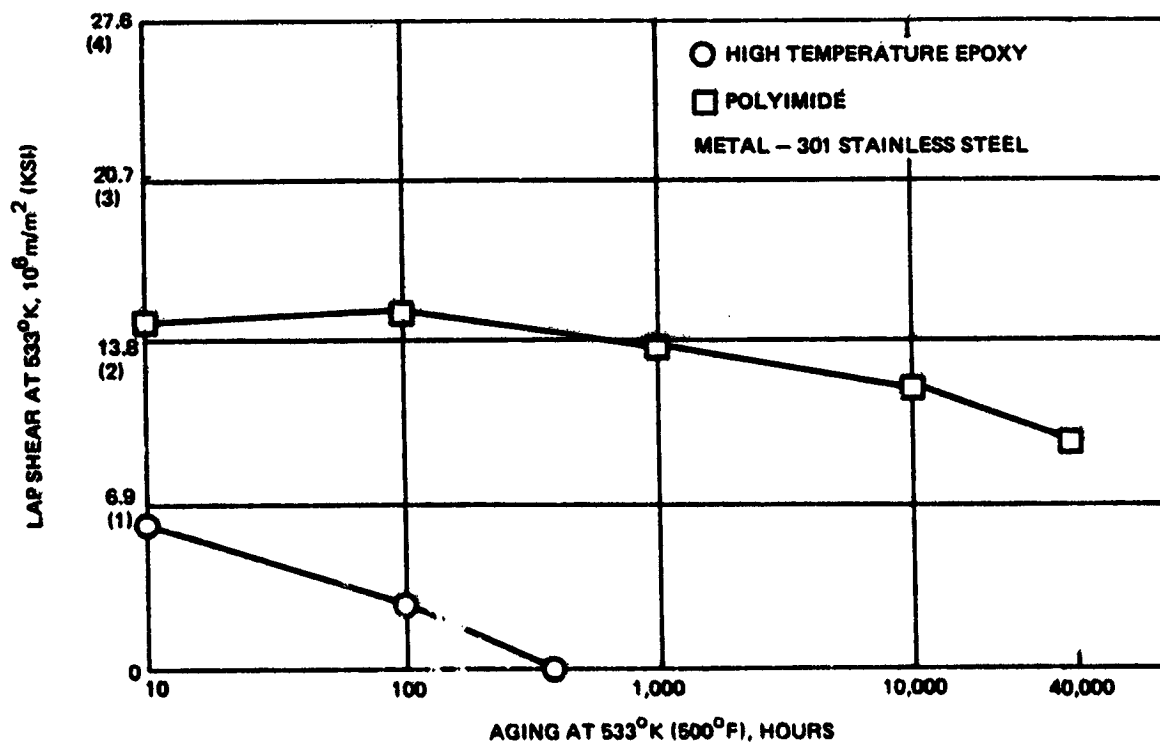
Fig. 3.3-42 Thermal Stability of Various Adhesives at 533°K

With any of the composites, the question of outgassing naturally arises. Tests run at Grumman on graphite/epoxy laminates showed essentially no outgassing when the specimens were exposed to high vacuum at room temperature for 72 hours. Tests at elevated temperatures need to be run. Polyimides, not being free of volatiles as are epoxys, may present an outgassing problem. The vapors given off by a polyimide composite structure may inhibit proper operation of the microwave converters. Tests are required to establish the vapor pressure characteristics of candidate composites at elevated temperatures and then, if necessary, suitable coatings to minimize the outgassing must be found.

Up to this point, any reference to temperature has always been along the lines of high temperature. The MPTS, however, will experience cold temperatures around the time of the two equinoxes each year. The structure will cool down to temperatures in the neighborhood of $75^\circ K$ ($-325^\circ F$). This cold temperature will not present any problem to aluminum which has been used to virtually $0^\circ K$. How the composites hold up is an unknown. Tests to establish their cold temperature performance and their response to temperature cycling (from 75 to say $600^\circ K$) are required.

Structural members manufactured from composite materials will have a white thermal control paint applied to the side of the member that faces space while the opposite side which faces the hot antenna surface will have an aluminum foil bonded into it to provide a good heat reflector. Thus, the composite materials will not be directly subjected to ultraviolet radiation. However, tests to establish the ultraviolet degradation that the white paint and aluminum foil will undergo during the 30-year MPTS life are required.

Figure 3.3-44 summarizes pertinent properties of the three materials: aluminum, graphite/epoxy and graphite/polyimide. At the risk of over simplification, the material to use for the antenna support structure should have the best available strength-to-weight ratio and be capable of operating at $600^\circ K$ for 30 years. This statement can be made because material and processing costs should play a secondary role in material selection since transportation costs dominate the overall cost picture. Furthermore, it can be assumed that any tendancy towards outgassing or ultraviolet degradation will be aptly prevented by application of suitable coatings. A low thermal expansion coefficient is desirable but should never play a dominant role in the material selection process since a mechanical adjustment device will most likely be utilized to remove manufacturing tolerances. This same device, properly controlled can remove deflections caused by differential thermal expansions.

In conclusion, the polyimide matrices have much to offer but appropriate test data for a 30-year life are required on their low and high temperature performance as well as their vapor pressure characteristics.

ADHESIVE TYPE	CURE TEMP, $^{\circ}K$	VOLATILES	MATERIAL COST	PROCESSING COST
EPOXY	450°	NONE	LOW	LOW
EPOXY-PHENOLIC	450°	5%	LOW	LOW TO MODERATE
POLYBENZIMIDAZOLE	$530 - 645^{\circ}$	10 – 15%	HIGH	VERY HIGH
POLYIMIDE	$530 - 645^{\circ}$	10 – 15%	HIGH	VERY HIGH

Fig. 3.3-43 Cost and Processing Characteristics of Various Types of Adhesives

PROPERTY	ALUMINUM	GRAPHITE/ EPOXY	GRAPHITE/ POLYIMIDE
APPROXIMATE STRENGTH TO WEIGHT* (10^3 M)	23	28	28
TENSILE STRENGTH 10^6 N/M^2	241-600	195-415	275-415
DENSITY (Kg/M^3)	2570-2960	1500-2000	1500-2000
COEFFICIENT OF THERMAL EXPANSION (10^{-6} M/M PER $^{\circ}$K)	23.4	0.1-0.7	0.3-1.0
MAXIMUM RECOMMENDED SERVICE TEMPERATURE ($^{\circ}$K)	450	450	530-645
MOD. OF ELAST. 10^9N/M^2	73	48-105	48-83
SPECIFIC HEAT (j/kg-$^{\circ}$K)	920-962	870-1000	–
THERMAL CONDUCTIVITY W/(M-$^{\circ}$K)	117-234	0.2-4.5	5-10
REQUIRED THERMAL COATING – SPACE SIDE	ANODIZED E.G. ALZAC OR WHITE PAINT	WHITE PAINT	WHITE PAINT
REQUIRED THERMAL COATING-ANTENNA SIDE	NONE	ALUMINUM FOIL BONDED IN	ALUMINUM FOIL BONDED IN

*TITANIUM AND ITS ALLOYS HAVE A STRENGTH TO WEIGHT RATIO OF 36

Fig. 3.3-44 Comparison of Material Properties

3.3.3.5 Other Factors

At this time no attempt has been made to integrate power transmission lines and structural elements. The large current flow in this network requires large conductors and it is possible, perhaps necessary, to utilize the structure as an integral part of the power system. For example, if we assume a Gaussian distribution, the mean distance from the center would be approximated by $d = 1.77\sigma$, where 3σ = radius of the antenna. Assuming a total power of 5 gigawatts and 1600 areas of equal power, it follows that the power from each area = 5×10^9 watts/1600 = 3.1×10^6 watts. The current at 20 KV, to each of these areas would be $I = P/E = 3.1 \times 10^6/2 \times 10^4 = 156$ amp. The mean conductor length is (1.777) (500/3)=195M (640 ft) long. Neglecting temperature, a No. 2 size copper conductor (AN-J-C-48) or an equivalent No. 0 aluminum conductor can carry that load. The weight of the aluminum conductor is $\sim$.1/ft and results in a total weight of (.1) (640) (1600) = 102,400 lb (225,280 kg). Weights of this magnitude should be integrated into the basic structure.

3.4 ASSEMBLY AND PACKAGING

3.4.1 Detail Parts

A study of packaging structural members/elements was initiated to determine the optimum arrangement within Shuttle constraints, and to determine the sensitivity of various levels of ground prefabrication compared to corresponding levels of orbital assembly. The options selected for evaluation, shown in Fig. 3.4-1, span the potential split up of fabrication methods between ground based and space based operations. These cases are as follows:

- Case I - Assemble collapsible beam members on earth which will provide the most efficient Shuttle packing density and deploy when in space

- Case II - Prefabricate structural elements of tri-beams and manually assemble in space

- Case III - Prefabricate flat stock on ground with required thermal coatings and autc assemble in space.

Assembly of structural members on the ground requires that these members be stowed in a folded or compressed manner to achieve as high a density as possible. Efficient Shuttle utilization requires a cargo density of at least 6 lb/ft^3. A survey of existing stowable structural members (astromast, articulated lattice) suggest that an order of magnitude less is the best that can be achieved. Figure 3.4-2 was generated for typical articulated lattice girder members and, as can be seen, the densities are in the order of 0.01 to 0.02 lb/ft^3. This represents a Shuttle load factor of 1% and it is obvious that even with improved design techniques, the net gain would still fall far short of the desired goal. The attractive facet of this approach is that most of the subassembly work is done on the ground, not at the orbital site. If advanced launch systems were not as volume restricted as the Shuttle, this approach could become the preferred choice.

Detail component fabrication on the ground and assembly at the orbital site offers opportunity for a much more efficient packaging density. The first step in this approach is to substitute very thin solid elements for the "Baseline" approach of thin walled tubes (Fig. 3.4-3). This immediately achieves a packaging density far in excess of the minimum 6 lb per cubic foot, but as the following example shows, also results in a weight increase. To balance a 100 lb load in a thin walled, 2.5 in. diameter graphite/epoxy tube, supported at six meter intervals, the wall thickness would be 0.0075 in. The resulting weight is 0.039 lb/ft. By

EARTH

TRANSPORT

ON ORBIT

CASE I → ASSEMBLE ARTICULATED LATTICE BEAMS ON GROUND → PACKAGE IN ORBITER → DEPLOY BEAMS IN ORBIT

CASE II → FABRICATE BEAM ELEMENTS ON GROUND → PACKAGE IN ORBITER → ASSEMBLE INTO TRI BEAMS AT SPACE STATION

CASE III → PRE FAB FLAT STOCK ON GROUND → PACKAGE IN ORBITER → AUTO MANUFACTURE ON ORBIT
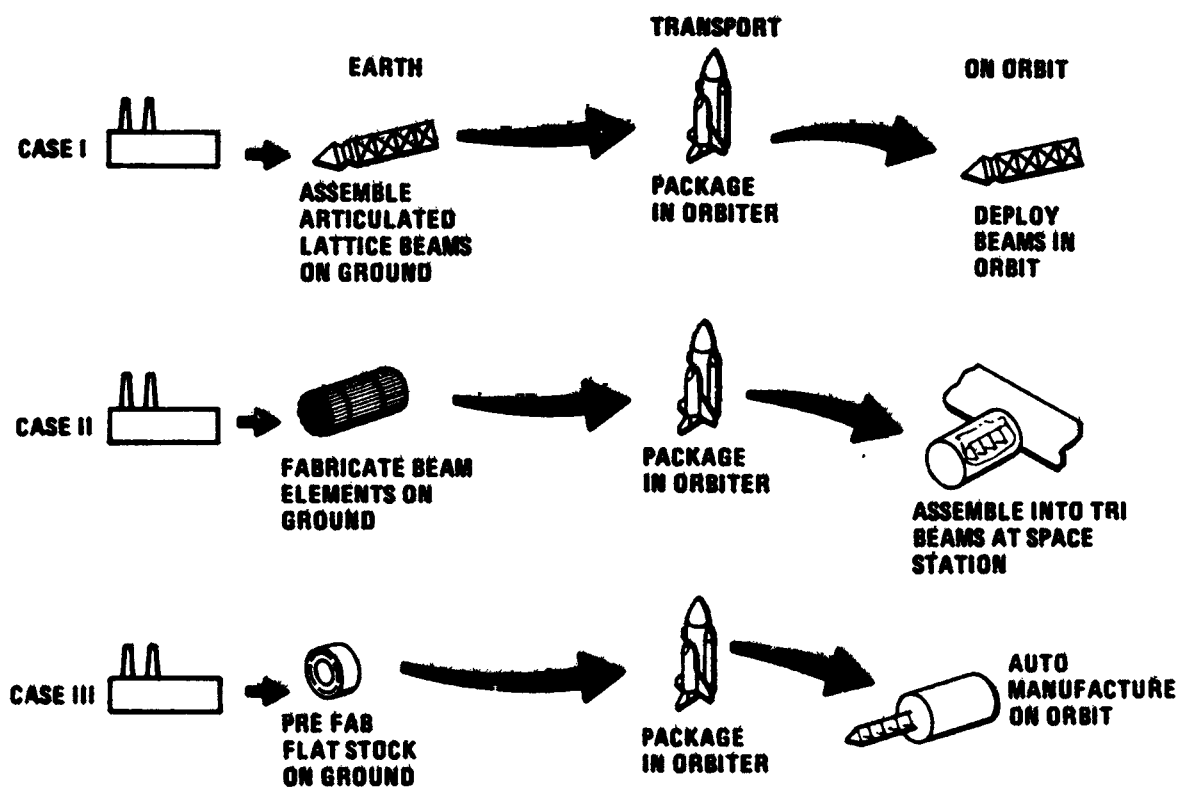
Fig. 3.4-1 Structural Detail Parts Assembly Options

3.4-2
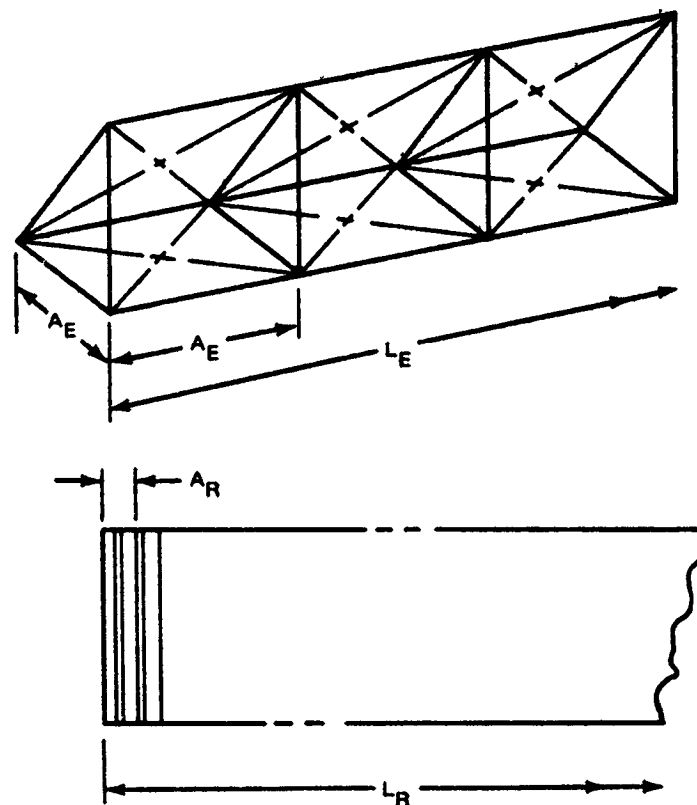
DIAMETER-MEMBER, IN.	2	3	4	5	6
ALLOWANCE FOR CABLES & FITTINGS, IN.	1	1.5	2	2.5	3
A_E – BAY LENGTH EXTENDED, FT	4.9	4.9	9.85	9.85	9.85
A_R – BAY LENGTH RETRACTED, IN.	5	7.5	10	12.5	15
NO. OF BAYS (RETRACTED IN 60 FT)	144	96	72	57.5	48
L_E – EXTENDED LENGTH, FT	700	470	710	570	475
ESTIMATED WT OF FITTINGS, LB	(.2) 86	(.3) 86	(.4) 86	(.5) 86	(.6) 86
ESTIMATED STRUCTURE, WT, LB (0.0075 GRAPHITE EPOXY)	22	22	44	44	44
NO. OF BIRDERS THAT CAN BE PACKAGED IN SHUTTLE BAY	7	7	1	1	1
TOTAL WT PACKAGED IN SHUTTLE, LB	756	756	130	130	130
PACKAGING DENSITY IN SHUTTLE, LB/FT^3	0.071	0.071	0.012	0.012	0.012

Fig. 3.4-2 Characteristics of Articulated Lattice Beam

2.5 IN. DIA X .0075
WALL GRAPHITE EPOXY

THIN WALLED TUBING

INTERMEDIATE SUPPORTS

12" TYP.

6 METERS
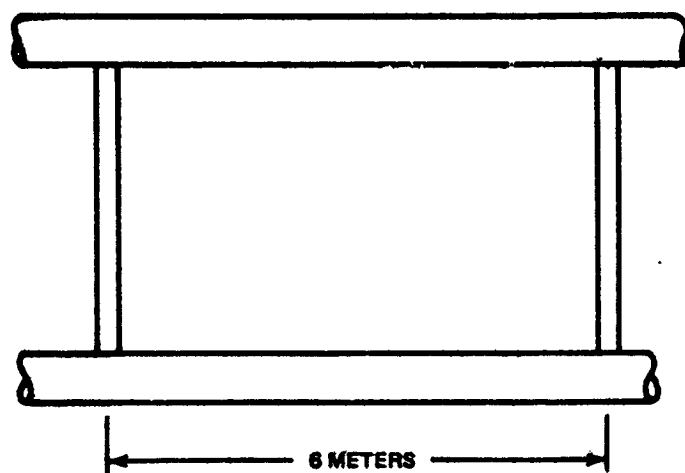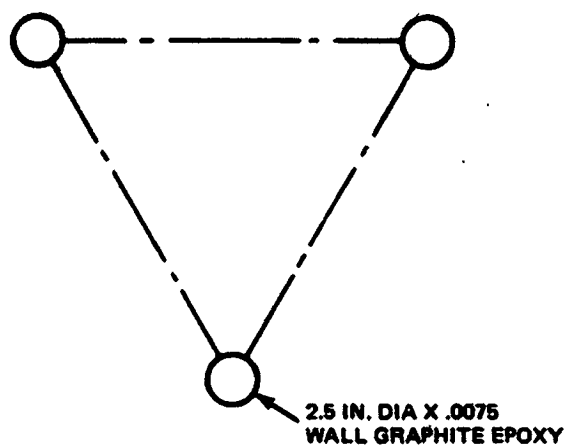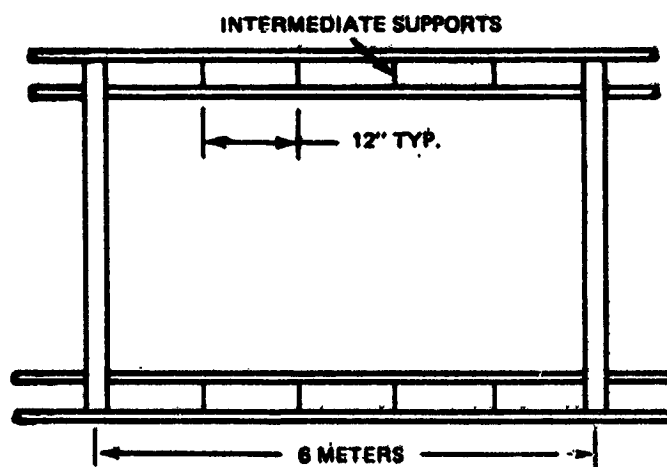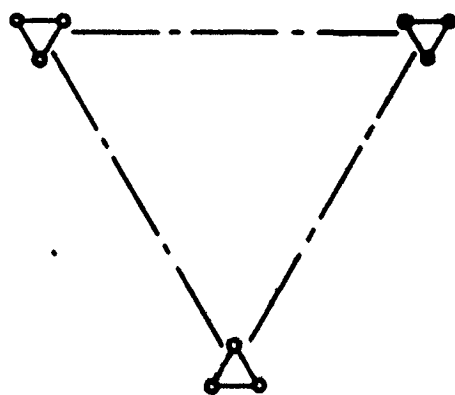
SOLID ELEMENT MEMBERS

Fig. 3.4-3 Tri-Beam Layout Using Tubular and Solid Element Caps

3.4-4

substituting three solid elements, arbitrarily adding supports every 12 inches to balance 33 lb each, the weight is 0.0429 lb/ft (0.0143 x 3) Fig. 3.4-4. Assuming the 12 in. supports add an additional 50% weight penalty, the total weight would be 0.0643 lb/ft. Figure 3.4-5 shows the limitations of both structural elements with respect to the Shuttle cargo bay, and it is clear that further optimization can result in less weight penalty while yielding an efficient packaging density.

This assembly concept would require the largest work force in orbit of any of the options considered. When the cost of the required Space Station, crew rotation and materials and life support logistics is factored into the equation, this approach does not appear desirable. Figure 3.4-6 summarizes an estimate of the rate of assembly of a typical structural tri-beam in which the caps and intercostal members have been shipped in an efficient Shuttle packaging arrangement to a Space Station. Skylab 3 data on the rate of assembly of the twin pole sunshade was used to establish the degree of human skills in space environment. In the Skylab 3 mission, a single man assembled two 55 ft poles in 5 ft sections in 137 minutes. This represents an assembly rate of 6.2 min/operation. A typical MPTS 18 meter structural member would require 78 operations. Assuming a 90% learning curve improvement in skills relative to Skylab performance, a 2.5 min/operation could be considered plausible. At this rate 5.7 lb/m-hr rate of assembly could be achieved. Twenty-four 12-man Space Stations would be required to support the assembly crew at 5.7 lb/m-hr. A total of 470 klb of MPTS antenna structure could be fabricated using a crew of 275 in the allotted 2-month period. This high manpower requirement with associated Space Station support equipment tends to eliminate this approach as a viable detailed assembly approach (Fig. 3.4-7).

Complete fabrication and assembly in orbit can achieve 100% Shuttle load factor by transportation of raw materials to the fabrication/assembly site. This concept requires a free flying "factory". It is not unreasonable to assume that one could be designed and built with little technical risk. Figure 3.4-8 shows a concept for in-orbit fabrication and assembly of a typical girder. Considering the factors involved, that is, volume limitations of the Shuttle and the desire to minimize on-orbit personnel, this approach appears to be the most promising. An operations analysis of this process has tentatively established a rate of assembly of 420 lb/hr for the MPTS structural elements. At this rate, eight manufacturing modules would be required to meet assembly time tables.
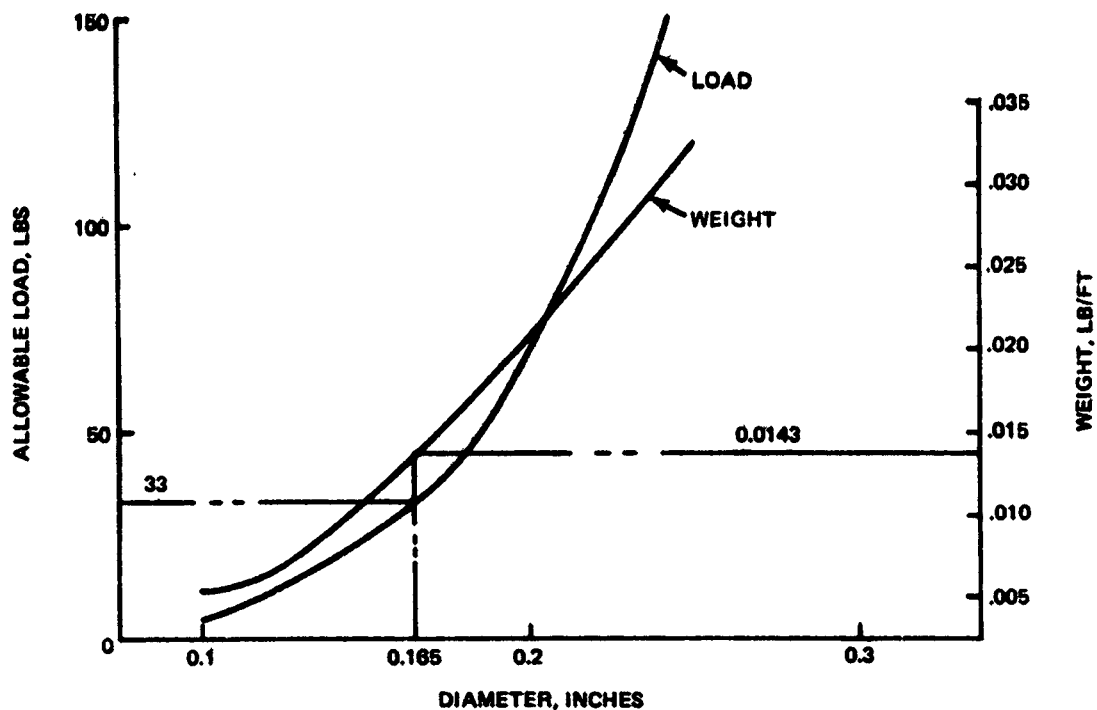
Fig. 3.4-4 Allowable Column Load vs Diameter (Solid Graphite Epoxy E = 13×10^6 PSI, 12" Long).

POOR PACKAGING DENSITY
VOLUME LIMITED CAPACITY OF
4000 TUBES, 9300 LB

GOOD PACKAGING DENSITY
WEIGHT LIMITED TO 65,000 LB
APPROX 16,000 ELEMENTS
REQUIRE THREE TIMES AS
MANY ELEMENTS AS TUBES TO
BUILD UP EQUAL AMOUNT OF
STRUCTURE
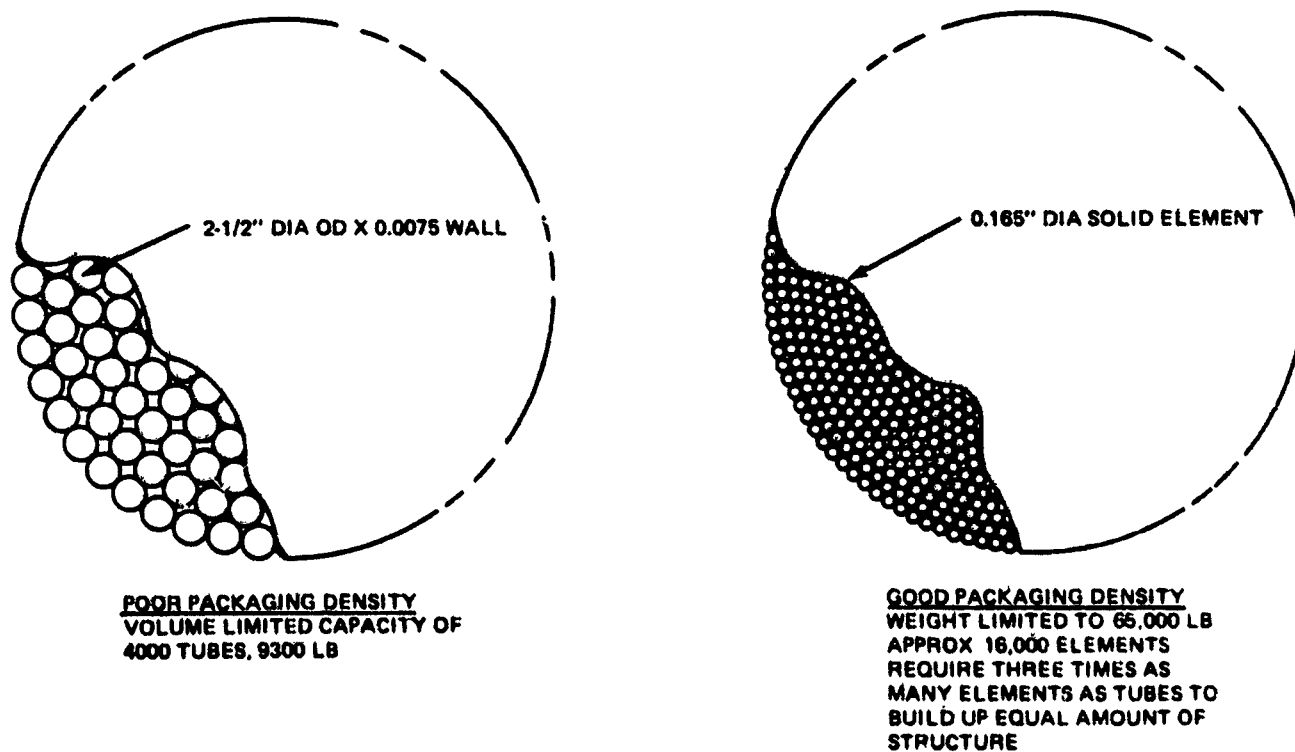
Fig. 3.4-5 Shuttle Compatibility Packaging

3.4-6

SPACE STATION

ASSY MODULE (60' X 14')

HATCH

ASSEMBLY RATE

SKYLAB 3

90% LEARNING CURVE

ASSY RATE MIN/OPERATION
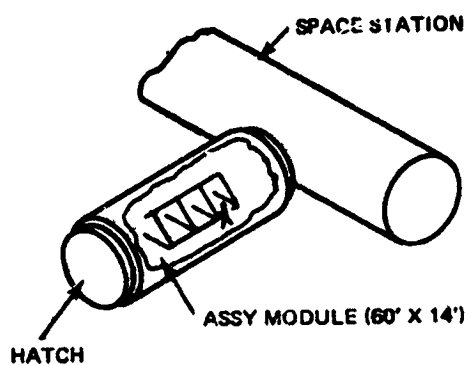
NO. OF OPERATIONS

TYPICAL TRIBEAM

— WEIGHT = 21.4 LB (AL. ALLOY)
— NO OF OPERATIONS = 78
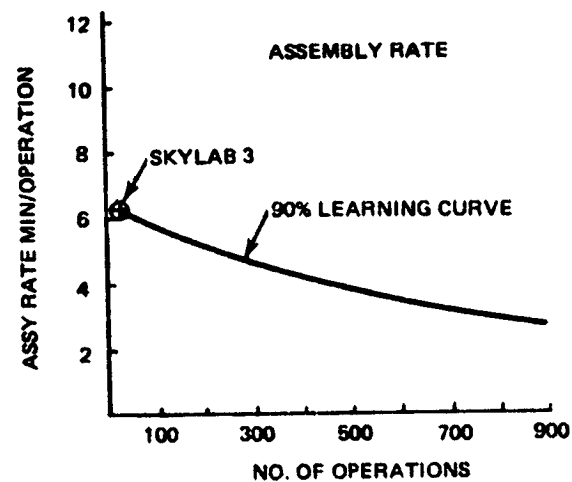
2.5 MIN/OPERATION

TIMELINE (ONE BEAM ASSY)

TASK	TIME
1. SET UP EQUIPMENT/MATERIALS	15 MIN
2. ASSEMBLE BEAM	195 MIN
3. RETURN TO SPACE STATION OPEN HATCH & REMOVE BEAM FROM ASSEMBLY MODULE	15 MIN
TOTAL TIME	225 MIN

BEAM ASSEMBLY RATE = 0.095 LB/MIN
= 5.7 LB/M-HR (2.6 Kg/M-HR)

Fig. 3.4-6 Inflight Detail Parts Assembly

- ANTENNA STRUCTURAL WT = 470 KLB ALUMINUM
- ASSIGNED ASSEMBLY TIME = 1.9 MONTHS
- STRUCTURAL DETAIL PART MANPOWER = 82,500 M-HRS
- NO. OF PERSONNEL = 280

(24) 12-MAN SPACE STATIONS

(WT INFORMATION: SEE NAS 9-9953 MSC-02464; SD 70-546-1)

12 MAN SPACE STATION

SPACE STATION WT, 1000 Kg
SPACE STATION WT, KLB
NO. OF CREWMAN
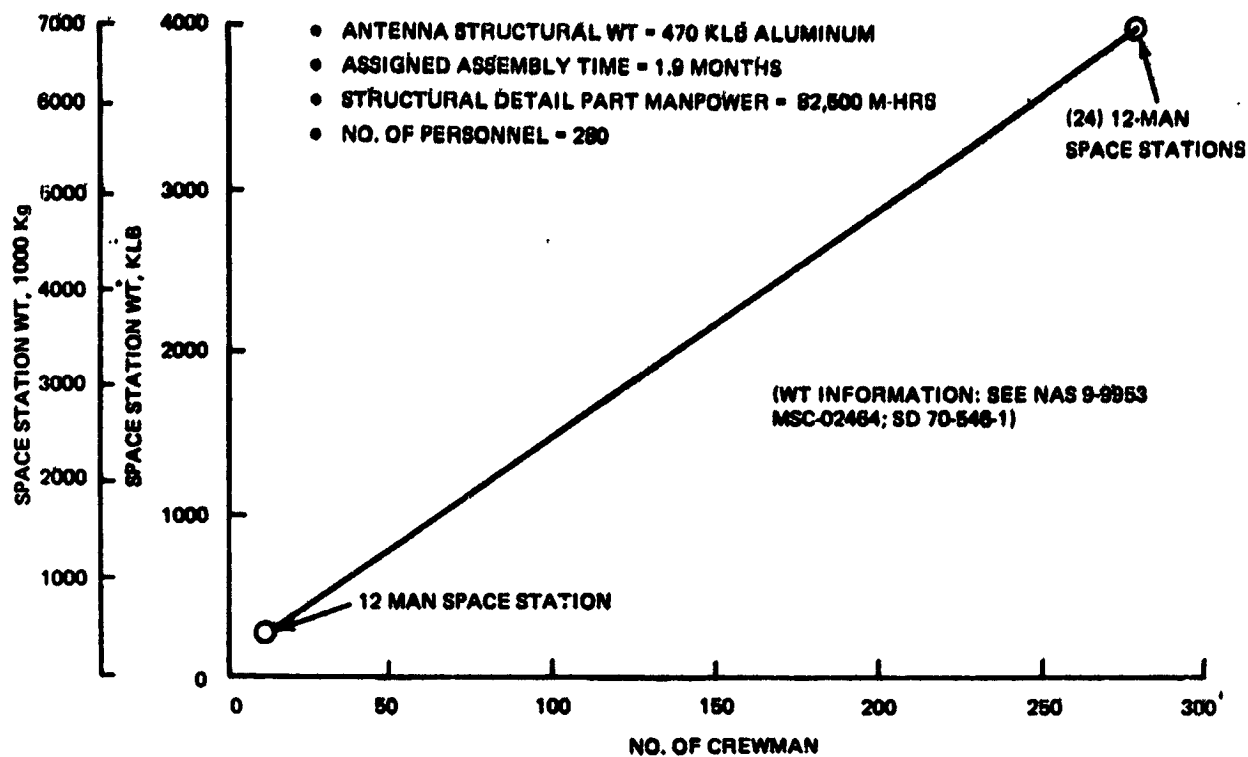
Fig. 3.4-7 Support Equipment Requirements for In-Flight Assembly of Tri Beams

STACKS OF EDGE STRIP FEED DRUMS

CROPPING HEADS

CROSS STRIP FEED DRUM

GUIDE ROLLERS

HARVESTING ARMS

WELDING HEADS

WELD CURRENT CONDITIONER SEQUENCER FOR:
- FEED
- CROP
- WELD

TYPICAL BEAM 10 – 15 FT LONG

POWER SUPPLY

AL STRIP 1" WIDE
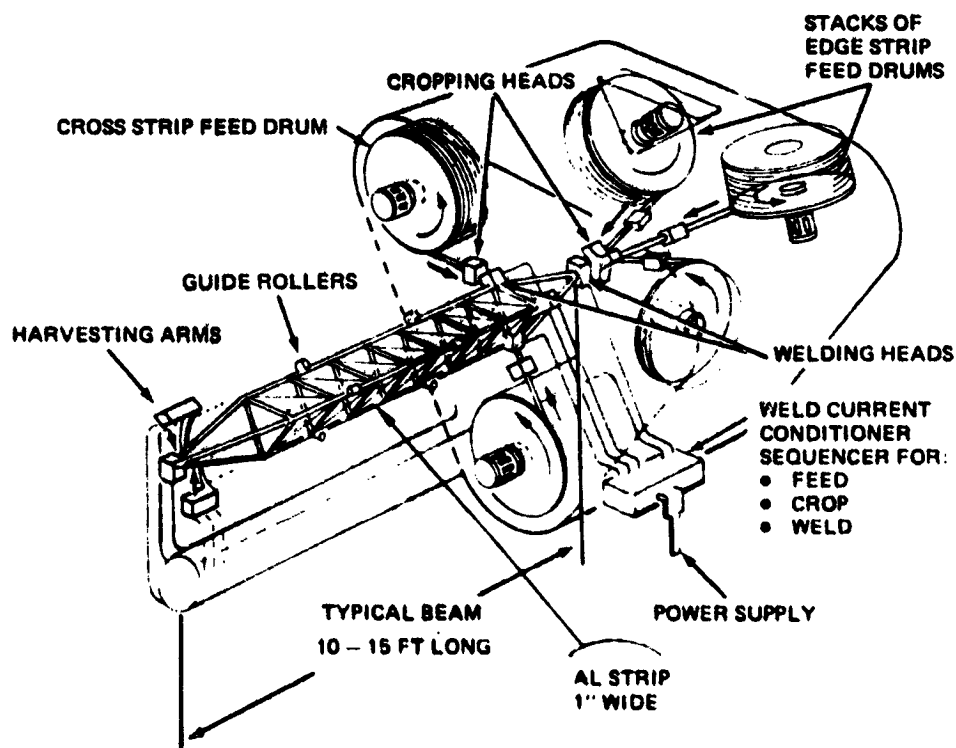
Fig. 3.4-8 Auto In-Orbit Manufacture (Aluminum)

3.4-8

3.4.2 Structural Assembly

A preliminary assembly sequence for the MPTS antenna follows. This assembly flow is based on the rectangular grid general arrangement, (see Fig. 3.2-1). Major functional blocks are identified in the order in which they are assembled.

A top level operations analysis is presented for the following structure assembly methods:

- Using manned free flying manipulator modules
- Using remote controlled free flying manipulator modules
- EVA using remote controlled logistics modules.

The analysis has led to the following indicators:

- Assembly using remote controlled manipulator modules offers the most cost effective approach
- EVA assembly with remote controlled logistics modules could be cost competitive
- Manned manipulator assembly tends not to be effective because of the high propellant consumption of the free flyers.

3.4.2.1 MPTS Assembly Functional Flow

3.4.2.1.1 Level 2 Assembly Flow - Figure 3.4-9 is a breakdown of the assembly steps for the MPTS antenna structure. Assembly starts with installation of the rotary joint using the SSPS central mast as a point of departure. The rotary joint to antenna interface structure assembly follows using the elevation rotary joint structure as an assembly base. Assembly of the primary and secondary structure is performed working radially from the center of the antenna. Installation of the waveguides and electronics follows.

3.4.2.1.2 Level 3 Assembly Flow - Figures 3.4-10 through 3.4-12 are more detailed definition of sequences for assembly of the rotary joints, interface structure, and antenna primary and secondary structure. Assembly of the rotary joints appears to represent the most complex assembly operation due to the number of unique installations (gears, flex harnesses, etc.). Assembly of the antenna itself along with waveguides and electronics, is a repetitive operation and should not pose difficult problems.
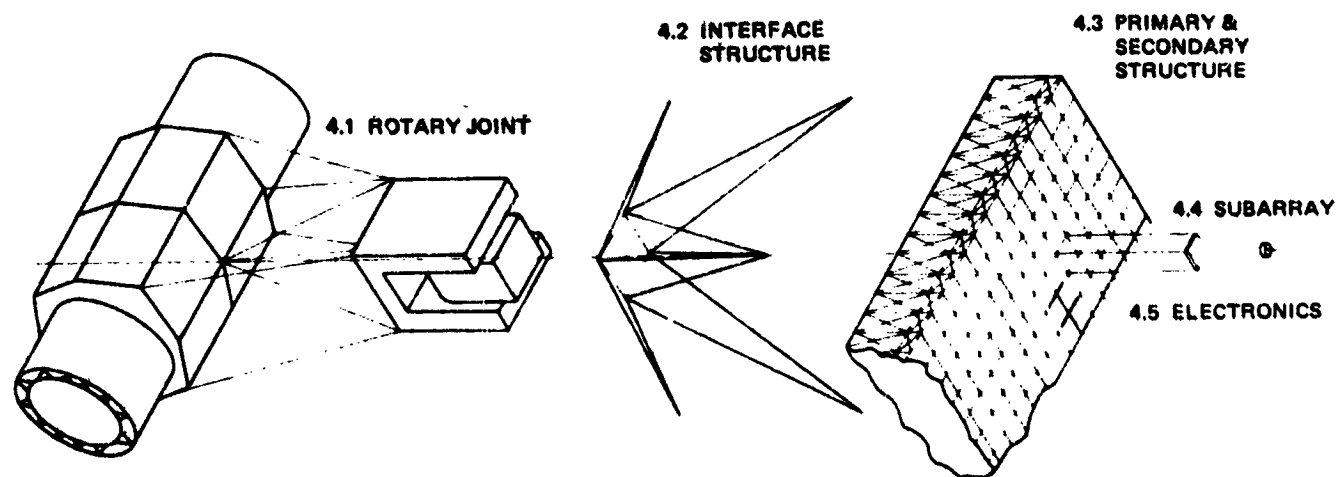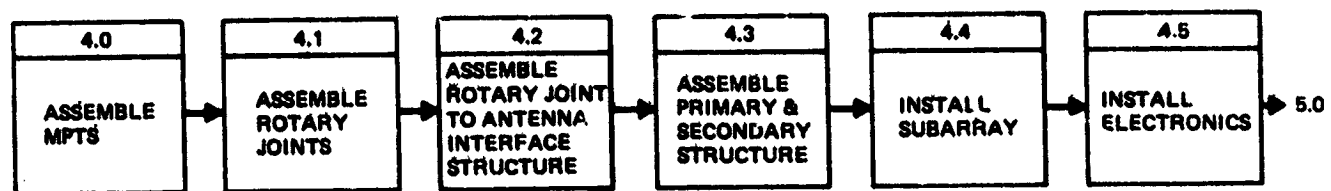
Fig. 3.4-9 Level 2 Functional Flow : Assemble MPTS
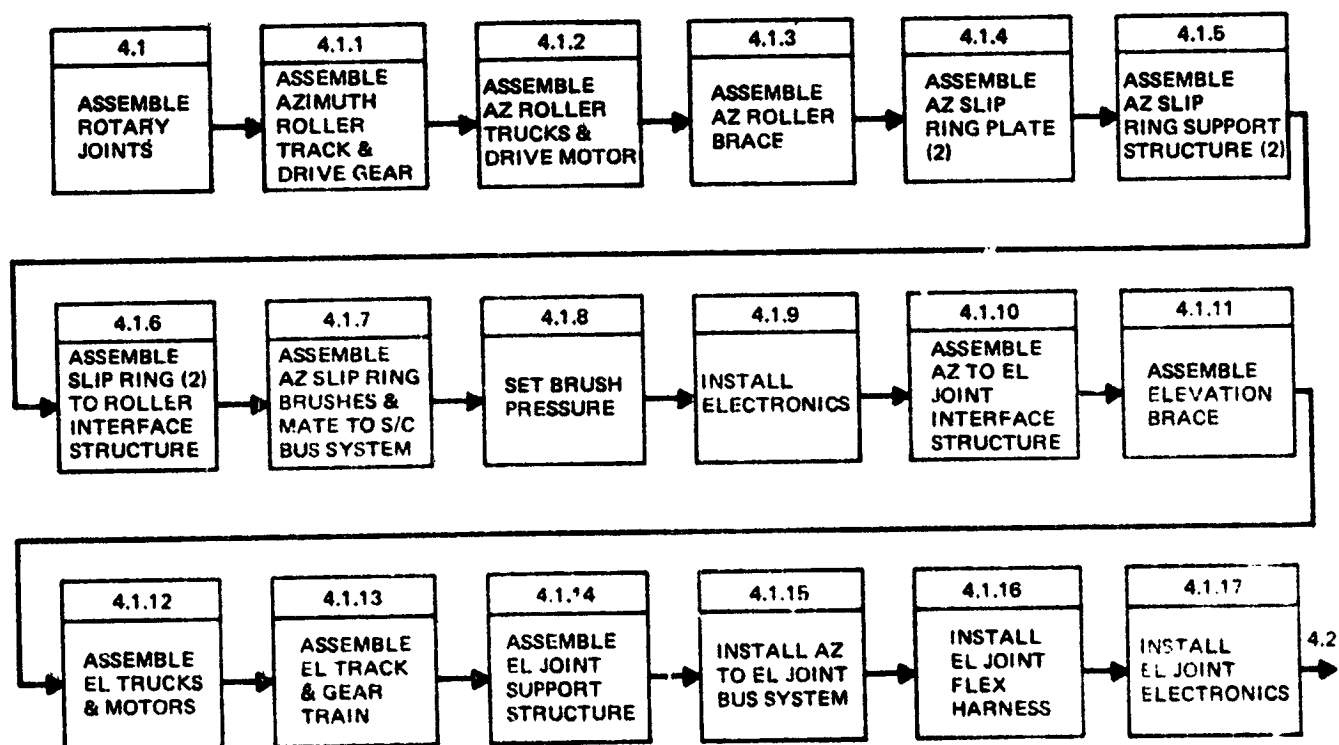
Fig. 3.4-10 Level 3 Functional Flow: Assemble Rotary Joints (Sheet 1 of 3)
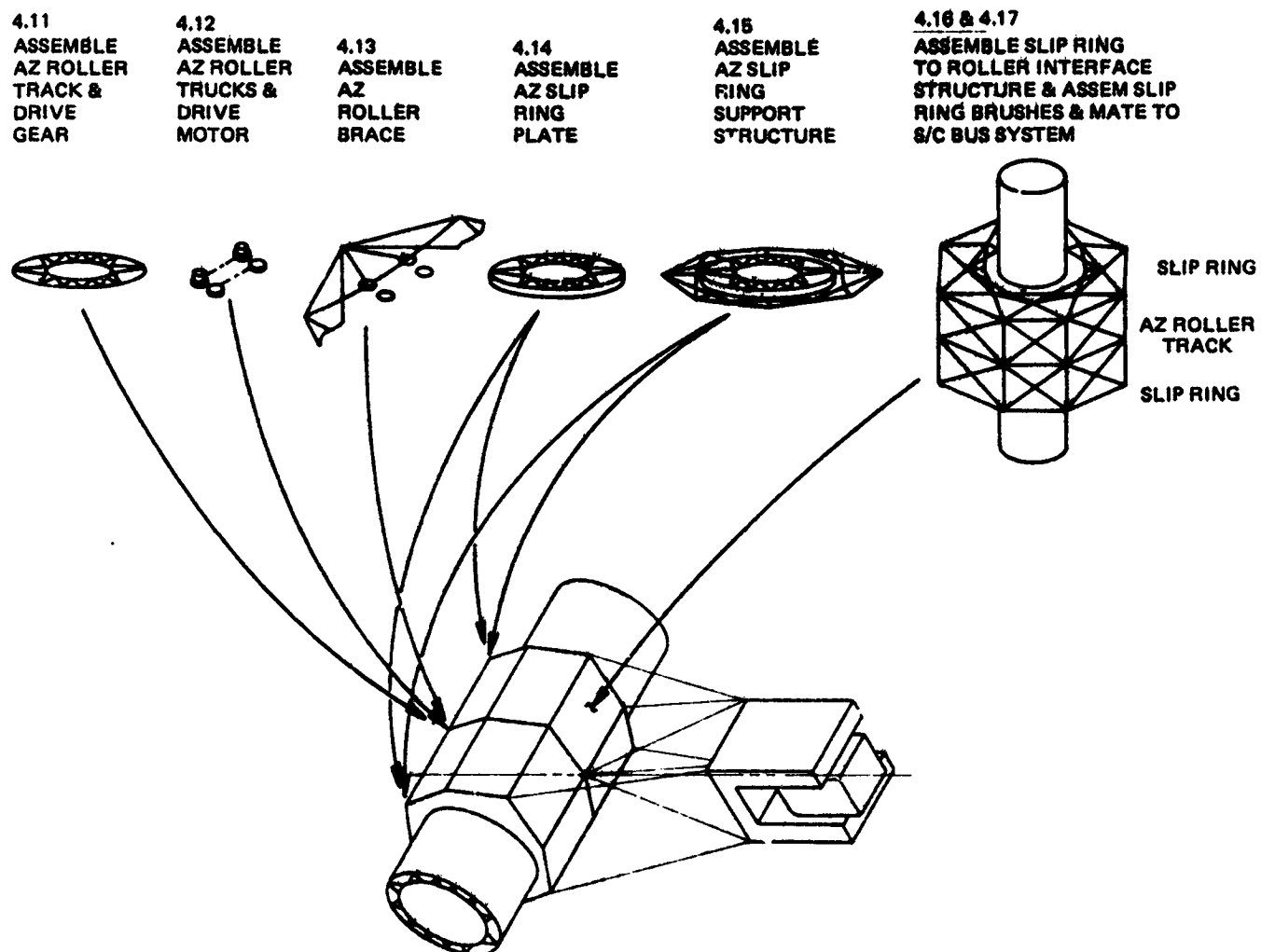
4.11
ASSEMBLE
AZ ROLLER
TRACK &
DRIVE
GEAR

4.12
ASSEMBLE
AZ ROLLER
TRUCKS &
DRIVE
MOTOR

4.13
ASSEMBLE
AZ
ROLLER
BRACE

4.14
ASSEMBLE
AZ SLIP
RING
PLATE

4.15
ASSEMBLE
AZ SLIP
RING
SUPPORT
STRUCTURE

4.16 & 4.17
ASSEMBLE SLIP RING
TO ROLLER INTERFACE
STRUCTURE & ASSEM SLIP
RING BRUSHES & MATE TO
S/C BUS SYSTEM

SLIP RING

AZ ROLLER
TRACK

SLIP RING

Fig. 3.4-10 Level 3 Functional Flow: Assemble Rotary Joints (Sheet 2 of 3)

3.4-12

4.1.10
ASSEMBLE AZ
TO EL JOINT
INTERFACE STRUCTURE

4.1.11
ASSEMBLE
ELEVATION BRACE

4.1.12
ASSEMBLE
EL TRUCKS & MOTORS

4.1.13
ASSEMBLE
EL TRACK &
GEAR TRAIN

4.1.14
ASSEMBLE
EL JOINT
SUPPORT STRUCTURE
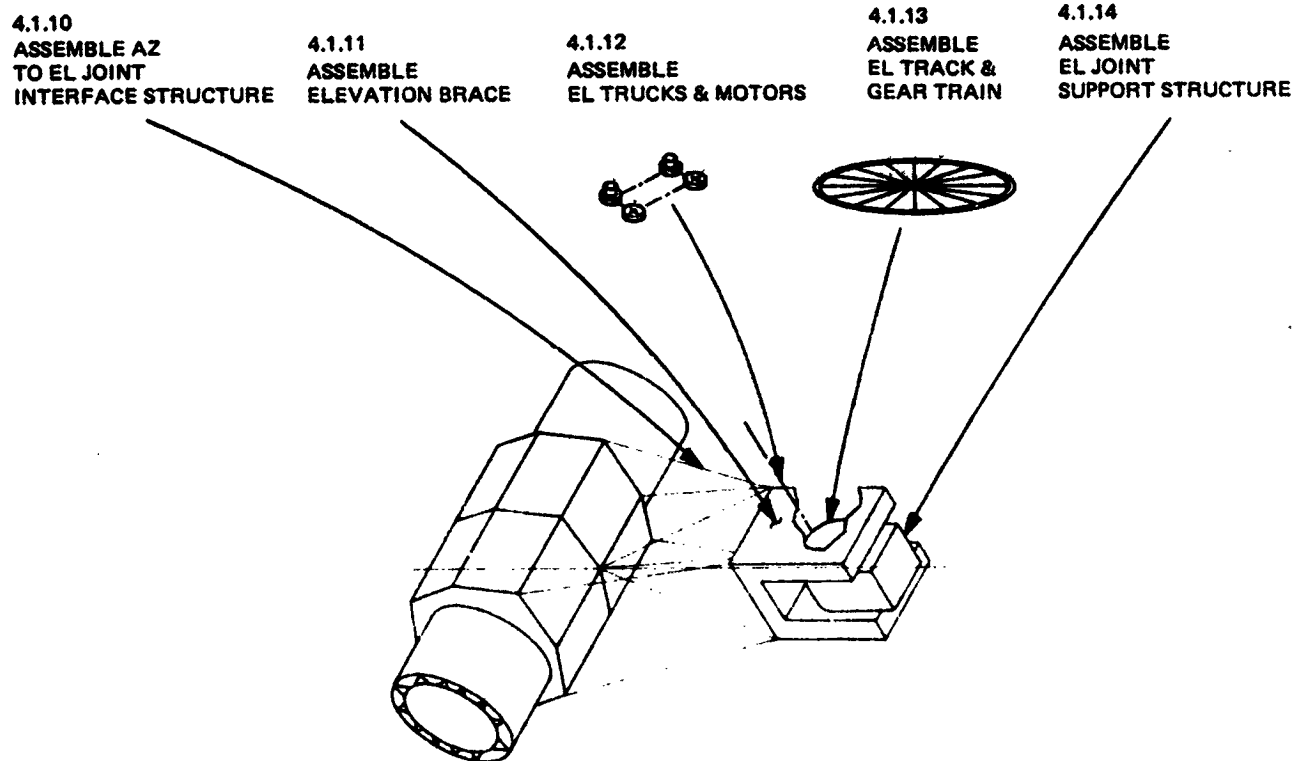
Fig. 3.4-10 Level 3 Functional Flow: Assemble Rotary Joints (Sheet 3 of 3)
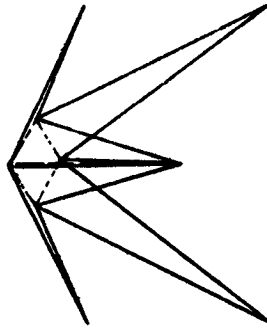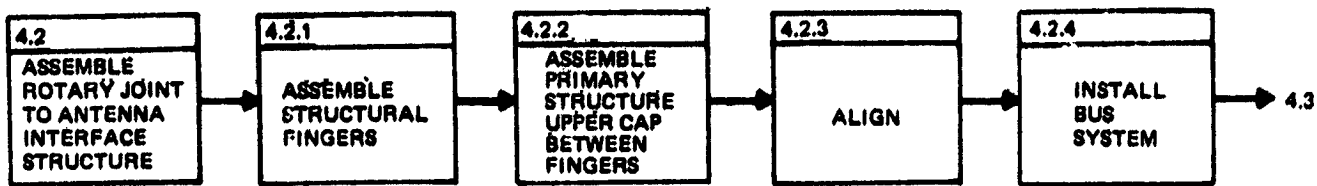
Fig. 3.4-11 Level 3 Functional Flow: Assemble Rotary Joint to Antenna Interface Structure

NOTE: FUNCTIONAL FLOW FOR TYPICAL 108 X 108 m STRUCTURAL BAY
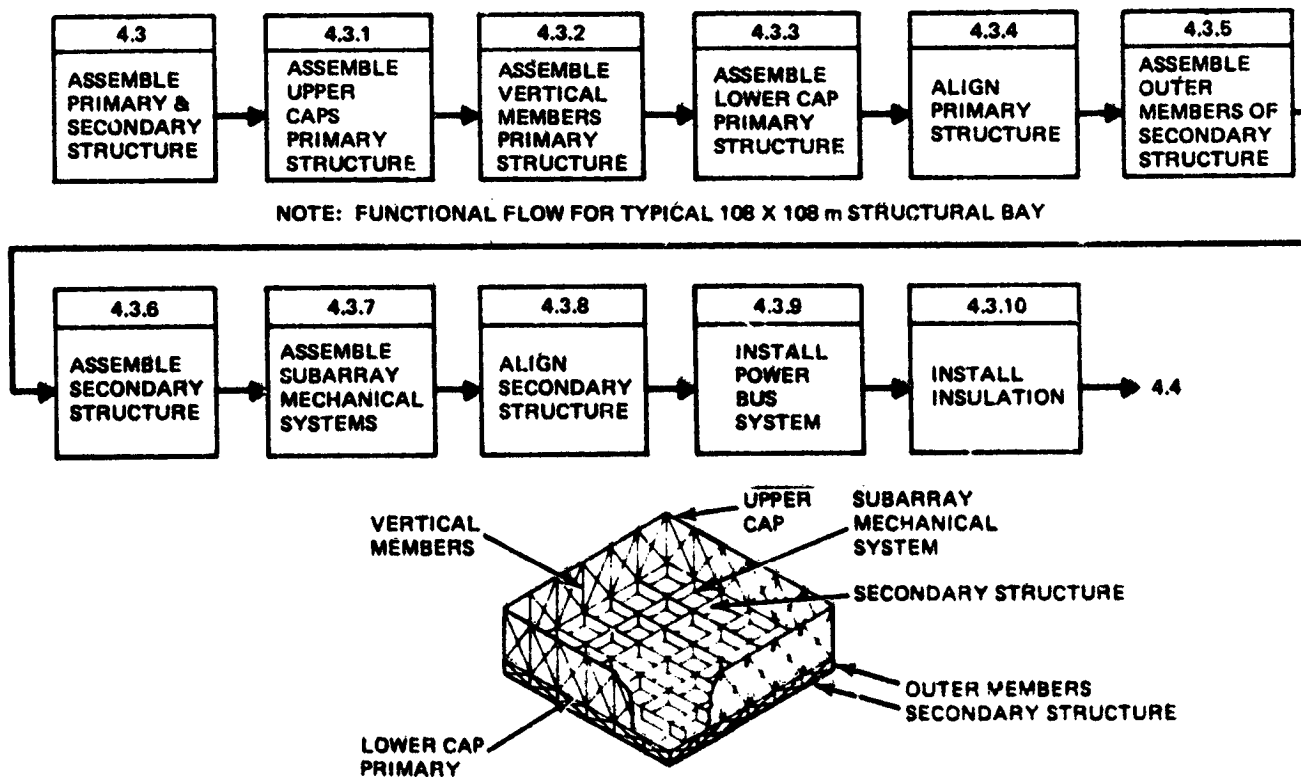
Fig. 3.4-12 Level 3 Functional Flow: Assemble Primary/Secondary Structure

3.4.2.1.3 Assembly Using Manipulator Modules - Figure 3.4-13 is a representative plan for assembling beams for the primary/secondary structure of the antenna. This operation is selected for detailed analysis because it represents the most frequently used operation in the buildup of structure. Manhour requirements to perform this operation represents 40 to 50% of the assembly cost of the antenna. Statistical data on aircraft assembly indicates that structural assembly accounts for 20% of the total cost to produce.

The assembly sequence presented in Fig. 3.4-13 assumes the use of a free flying manipulator module which could be manned or remotely controlled from the ground. Astromast beams are assumed stored in a logistics area in the retracted condition. The astromast storage area is also representative of the location of an auto beam manufacturing unit. The assembly joint is assumed to be a mechanical locking device similar to a docking drogue.

The objectives of the operations analysis are as follows:

- Establish a rough order of magnitude range of time required to assemble the structure

- Establish a level of complexity between performing assembly from the ground and manually in orbit

- Establish typical consumables requirements for ancillary equipments used in assembly.

Figure 3.4-14 summarizes the maximum and minimum time required to acquire a beam from storage, transport to the assembly area, join the beam to the structure and return to the storage area. A minimum time of 23.5 minutes and a maximum time of 40 minutes has been established assuming a manipulator design similar to the Shuttle RMS. The minimum time represents the potential of a manipulator to perform the required tasks assuming perfect accuracy and totally static conditions. The maximum time was established utilizing the parametric data in Ref 24 which relates the ratio of performing a basic task in a static environment to the time required to perform the task in a dynamic environment. The parameters considered in establishing complexity factors include:

- Control system frequency of the manipulator and target
- Attitude limit cycle amplitude of the target
- The distance between the target attachment point and the target cg
- The position and velocity accuracy during stationkeeping
- Manipulator time delay.
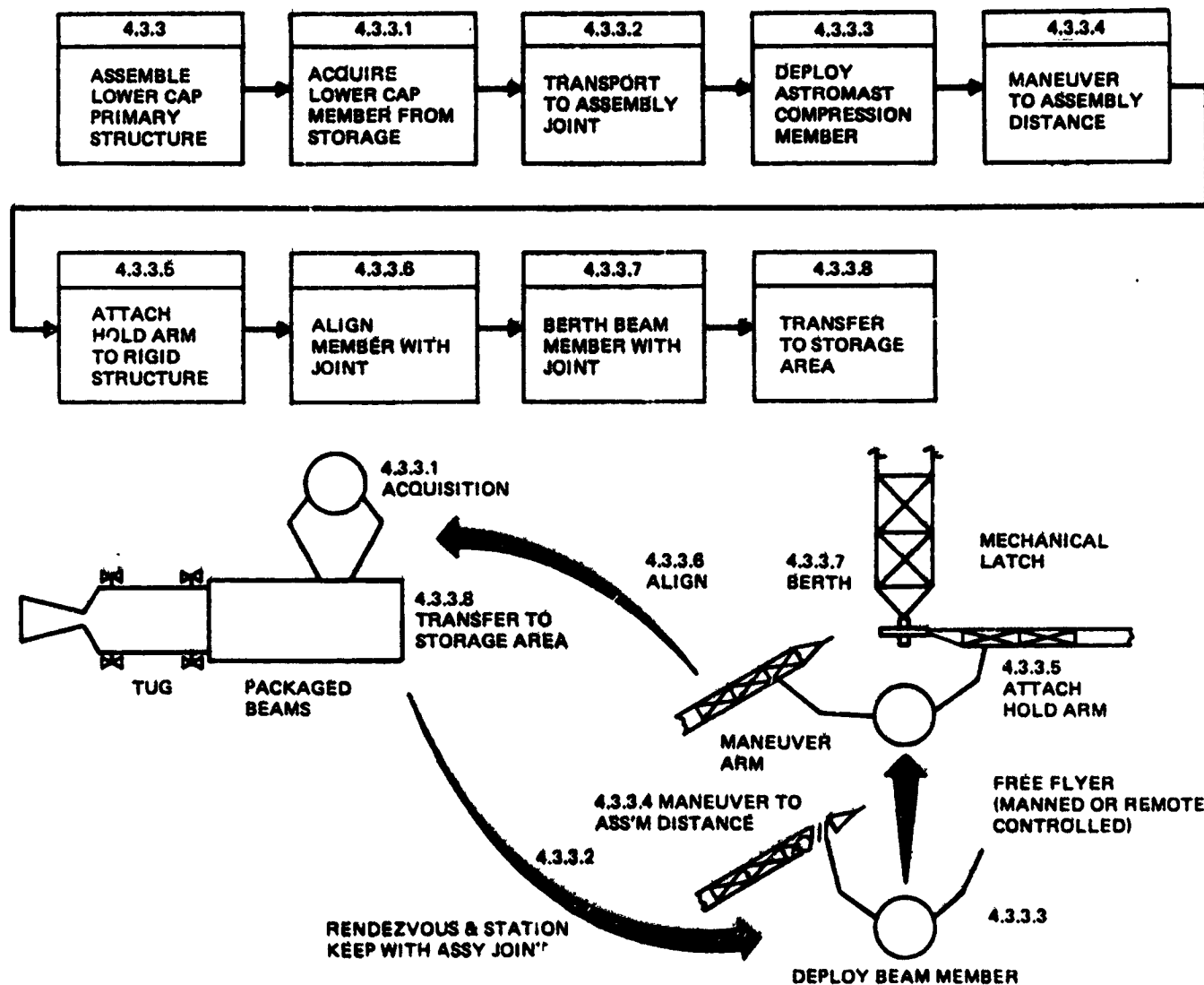
Fig. 3.4-13 Level 4 Functional Flow: Manipulator Module Assembly of Lower Cap; Primary Structure

EVENT		TIME, MIN.				CONSUMABLES, LB			
		MINIMUM		MAXIMUM		PROPELLANT		ECS	
		ΔT	T	ΔT	T	MIN	MAX	MIN	MAX
4.3.3.1	ACQUIRE LOWER CAP FROM STORAGE	3.0	3.0	10.5	10.5	0.36	1.20		
4.3.3.2	TRANSPORT TO ASSEMBLY JOINT	6.0	9.0	6.0	16.5	4.72	4.72		
4.3.3.3	DEPLOY ASTROMAST	2.0	11.0	2.0	18.5	0.24	0.24	1.17	2.3
4.3.3.4	MANEUVER TO ASSEMBLY DISTANCE	0.5	11.5	0.5	19.0	3.0	3.0		
4.3.3.5	ATTACH HOLD ARM	3.0	14.5	10.5	29.5	0.36	1.20		
4.3.3.6	ALIGN MEMBER WITH ATTACH JOINT	3.0	17.5	10.5	40.0	0.36	1.20		
4.3.3.7	BERTH BEAM MEMBER WITH JOINT	1.0	18.5	1.0	41.0	0.12	0.12		
4.3.3.8	TRANSFER TO STORAGE AREA	5.0	23.5	5.0	46.0	4.72	4.72		
	TOTAL LB					13.88	16.40	1.17	2.3
	TOTAL Kg					6.29	7.43	0.53	1 04

Fig. 3.4-14 Assembly Timeline and Consumables Requirement

Time delay effects can be used to establish the penalty for performing assembly remotely from the ground. The range of time delays considered in Ref 24 was between zero and two seconds. If it is assumed that a manned manipulator will perform with time delay near zero and remote controlled manipulators will perform with time delays near two seconds, little difference in total time to perform the assembly tasks can be identified.

Figure 3.4-15 presents the variation in complexity factor (time in dynamic environment/time in static environment) for variations in target limit cycle deadband, manipulator characteristic frequency and the distance between the target cg and manipulator attach point for a system with a two second time delay. A similar plot for a system with zero time delay shows little variation in complexity factor for target limit cycle amplitudes of less than 1° and low manipulator characteristic frequencies.

Manned free flyer module propellant consumption will vary between 14 and 16 lb (3.3 to 7.2 Kg) for the minimum and maximum time case, respectively. This quantity per trip includes limit cycle control and translational propellants. These estimates assume a 3000 lb (1359 Kg) vehicle with inertia and jet geometries similar to the Lunar Module (LM) ascent stage at docking. The ECS consumables required for life support will be approximately 0.2 to 0.3 lb (0.1 Kg) per trip. This estimate is based on the LM configured for one man.

An unmanned manipulator module could be configured at 400 lb (181 Kg). This lower weight reduces propellant consumption to reasonable levels, 1.8 to 2.1 lb (0.9 Kg) per trip. The order of magnitude difference in propellant consumption for the unmanned, relative to a manned free flyer, is a strong factor in favor of remote controlled assembly approaches.

Figure 3.4-16 presents assembly cost factors which utilize the operations time line analysis results. The overall structure can be assembled at a rate of 13 to 26 lb/m-hr (6 to 12 Kg/m-hr). This range of cost was established by determining the number of joints in a typical 108m x 108m primary/secondary structural bay (394) and the time to assemble, established in Fig. 3.4-14, for each joint. The rate in units of lb/m-hr is established by dividing the weight of a typical structural bay by the total time. These assembly rates are in line with that assumed during Task 1, 11 lb/m-hr. This is the rate at which steel workers can construct a major building on the ground assuming aluminum girders.

3.4.2.1.4 Assembly Using EVA Operations - Little or no data exist concerning large scale EVA assembly operations from which an extrapolation of task and time estimates can be made. This was determined after a survey of the literature and conversations with NASA personnel. However, actual EVA performance on Skylab equaled or exceeded expectations
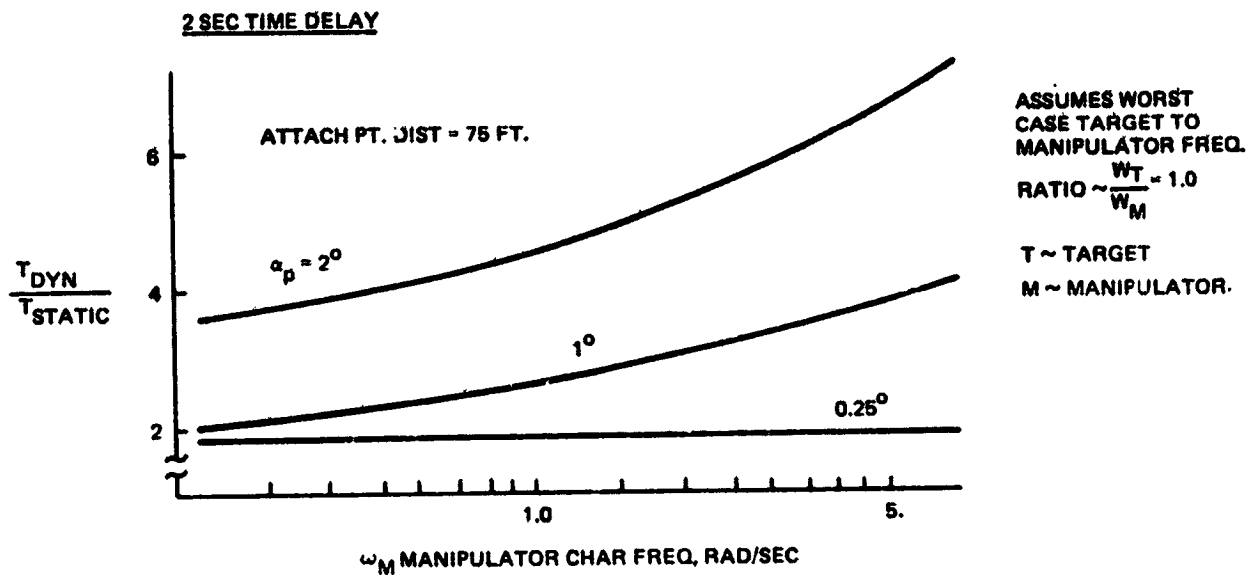
Fig. 3.4-15 Manipulator Performance Complexity Factor

Fig. 3.4-16 Manipulator Module Assembly Operations Summary

or simulation results of the same performance in neutral buoyancy procedures/proficiency development operations. It can be expected that, given proper restraints and life support systems, man can perform as well in space as he does on earth. It is felt that a degree of confidence can be achieved by relating MPTS structural assembly time estimates to that of the Twin-Pole Sunshade assembly using EVA techniques on Skylab 3.

Figure 3.4-17 shows the MPTS structural assembly plan utilizing EVA operations in conjunction with a remote controlled logistics module for transport of beam sections from storage to the assembly area. A two-man operation is assumed. A work platform with the appropriate foot and hand restraints is utilized. The first crew test (Operation 4.3.3.6) is to move the work platform to the next assembly point. The logistics module delivers three beams which are temporarily lashed to the work platform. The crew preassembles the three beams and tension wires to form the structural quad at the work platform. The crew unfolds the beams (total beam weight = 65 lb) (29.4 Kg) orients the unfolded section for mating to the structure.

Figure 3.4-18 is a task description of Skylab 3 Twin-Pole Sunshade deployment. The related operations used to define the time required to assemble the MPTS structure are steps 2, 4, and 5 which are similar to establishing the work station at the new assembly point, prefabrication of the delivered beams and deployment and mating of the structural quad. A learning advantage has been assumed in establishing the time estimates shown in Fig. 3.4-17.

Figure 3.4-19 summarizes the rate of assembly, rate of free flyer propellant expenditure and the required Space Station support requirement to house the needed crew size for MPTS structural assembly in approximately two months. The assembly rate in this case was not constrained by crew performance but rather by performance of the free flyer. This could in fact have validity in that even in earth construction of large structure, the supply of materials to the immediate assembly point is often the time constraining element. A Space Station at a projected weight of 500,000 lb would be required to support the 30-man crew necessary to assemble the 470 klb of antenna structure.

The assembly rate using EVA operations tends to be twice that using remote controlled manipulator operations. This agrees with intuition even though the operations analysis presented here is based on very limited data. Because of the potential increase in assembly rate using EVA operations, which could offset the cost of the Space Station, this approach should be retained as a potential option needing further technology study.
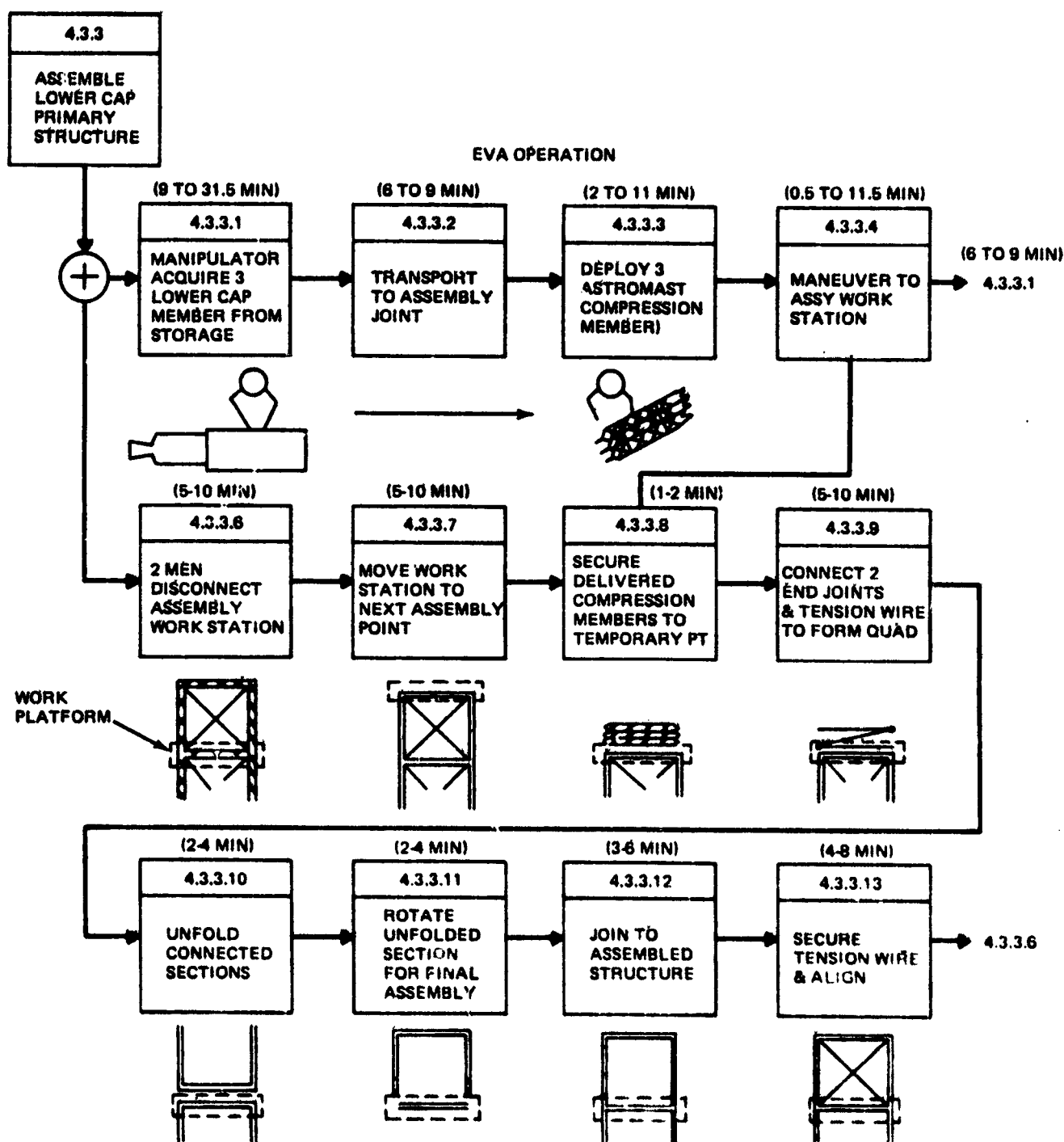
Fig. 3.4-17 Level 4 Functional Flow: EVA Assemble Lower Cap; Primary Structure

TASK DESCRIPTION	DETAILS	ACTUAL TIME WITH PROBLEMS (MINUTES)	ESTIMATED TIME WITHOUT PROBLEMS (MINUTES)
1. SETUP OF SAIL EQUIPMENT IN THE FIXED AIRLOCK SHROUD AREA	COLLECT POLES, RODS, SAIL, BASE PLATE, CLOTHES LINES, ETC.	25	25
2. SETUP DUAL HAND RAIL WORK STATION	INSTALL FOOT RESTRAINTS INSTALL BASE PLATE INSTALL SAIL BAG	18	18
3. ASSEMBLE TWO 55 FT POLES & INSTALL IN BASE PLATE	CONNECT 5 FOOT SECTION, ETC. NOTE: UNACCOUNTED FOR CONDITIONS RESULTED IN ASSEMBLY PROBLEMS	137	45
4. REMOVAL OF SAIL OUT OF BAG & DEPLOYMENT	STRETCH SAIL TO ITS 22 FOOT x 24 FOOT FULLY EXTENDED LENGTH NOTE: UNACCOUNTED FOR CONDITIONS RESULTED IN DEPLOYMENT PROBLEMS	25	15
5. INSTALL CLIPS ON CLOTHES LINE & PUSH SAIL POLES AGAINST WORKSHOP	FIRST STEP IN SECURING SAIL	9	9
6. DEPLOYMENT OF REEFING LINES	LAST STEP IN FLATTENING SAIL AGAINST WORKSHOPS	16	16
7. CLEAN-UP	RETRIEVE CONTAINERS & RESTRAINTS	8	8
		238	136
		(3 HR, 58 MIN.)	(2 HR., 16 MIN.)

*DATA SUPPLIED BY R. KAIN TELEPHONE CONVERSATION AND AS DERIVED, FROM ACTUAL SKYLAB 3 MISSION EVENTS TIMELINE

Fig. 3.4-18 Detailed Task Sequence and Performance Times for Two-Man Skylab 3 Twin-Pole Sunshade EVA Deployment*

- ASSUMPTIONS FOR TYPICAL 18X18m SUBARRAY BAY

  MATERIAL   — ALUMINUM
  WEIGHT   — 65.1 LB

  FREE FLYER

  WEIGHT   — 300 LB
  I_{SP} — 300 SEC

- ASSEMBLY ROM UNIT MODEL RELATIONSHIPS

  ASSEMBLY TIME   = 27 LB/M-HR (LONGEST)
                      50 LB/M-HR (FASTEST)

  FREE-FLYER PROPELLANT = 0.021 LB/LB STRUCTURE

- SUPPORT EQUIPMENT REQUIREMENT FOR ASSEMBLY OF MPTS STRUCTURE

  WEIGHT = 470 KLB
  ASSIGNED ASSEMBLY TIME = 2.9 MONTHS
  ASSY MANPOWER REQD = 9,400 MAN-HR
  NO OF PERSONNEL = 30

Fig. 3.4-19 EVA Assembly Operations Summary

3.4.2.2 On-Orbit Support System Requirements

Preliminary definition of support system requirements have been established for the low altitude and high altitude assembly sites using data generated during the studies of Space Stations, research application modules and remote teleoperator vehicles (Ref 25 through 28). The major support equipment requirements are summarized for the alternate assembly sites as follows:

Low Altitude (190 N Mi)

- Remote controlled manipulators
- Shuttle crew accommodations
  - Crew support module
  - Communications module
- Manufacturing modules

High Altitude (7000 N Mi)

- Remote controlled manipulators
- Manufacturing module
- Space station
- Crew transportation module.

3.4.2.2.1 Remote Controlled Manipulator Module - The RMM is a free-flying teleoperated vehicle which serves to extend and enhance the natural sensory, manipulative, locomotive and cognitive capabilities of a man from a remote location. Figure 3.4-20 is a sketch of the Free-Flying Teleoperator (FFTO), identified in the preliminary Payload Descriptions Level B Data package for potential Shuttle sortie payloads (Payload No. LS-04-S). The FFTO weighs 183 Kg dry and has 33 Kg of hydrazine for propulsive maneuvers. Although more detailed definition of a remote controlled manipulator system for use in assembly of the MPTS is required, the functional capabilities of the FFTO is sufficiently close to what is needed to use it as a strawman in overall system assessment of the assembly operation.

3.4.2.2.2 Crew Support Module - A RAM Support Module (RSM) is used in the study as being representative of the support equipment necessary to house the crew for monitoring the assembly operation. The RSM is a pressurized vehicle which will accommodate up to four additional crewmen over the number transported in the Orbiter. Figure 3.4-21 is a

GROUND CONTROLLER
STATION

- WEIGHT = 405 LB (183 Kg)
- COST
  - NON RECURRING = $4.75M
  - RECURRING = $0.99M/UNIT
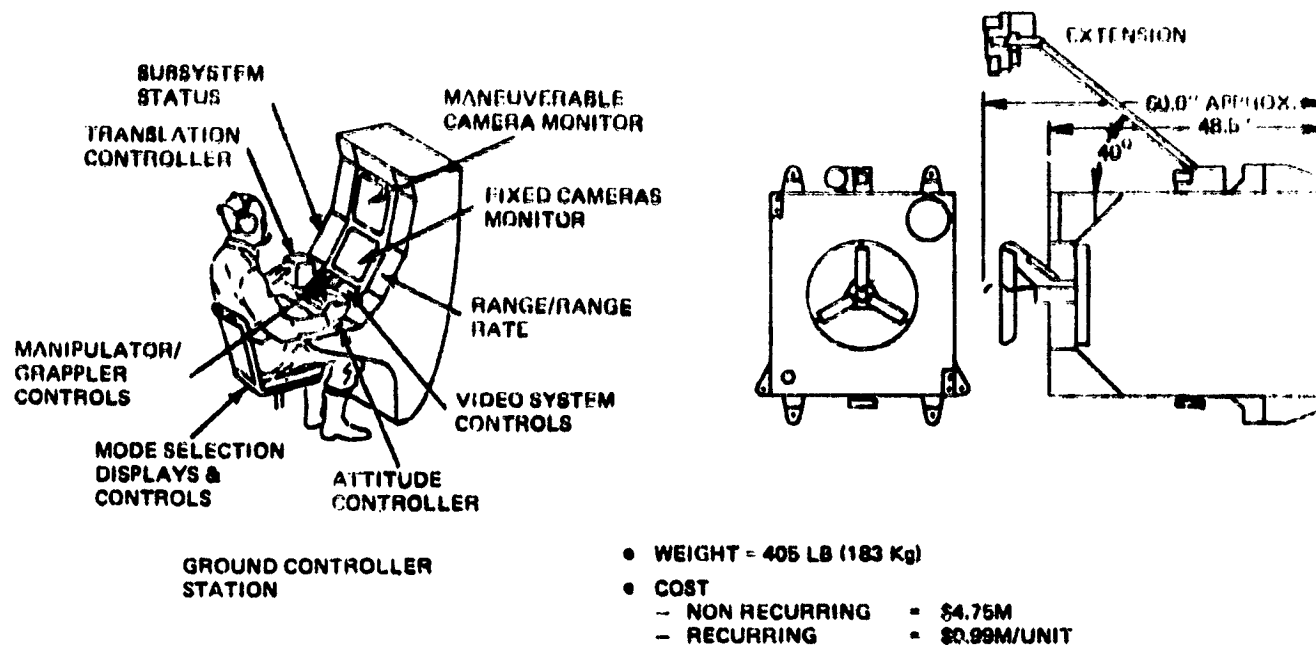
Fig. 3.4-20 Free-Flying Teleoperator Concept
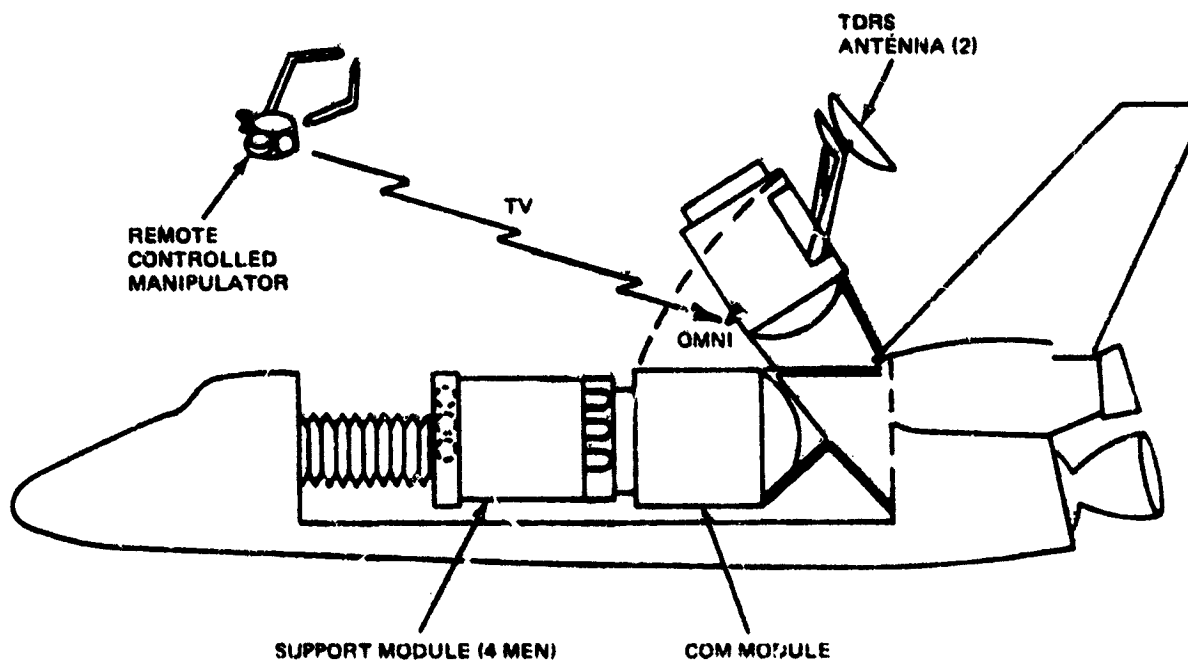
SUPPORT MODULE

- WEIGHT = 10,887 LB
- COST (1970$)
  - NON RECURRING = $174M
  - RECURRING = $32M/UNIT

COM MODULE

- WEIGHT = 19,230
- COST (1970$)
  - NON RECURRING = $226M
  - RECURRING = $47M/UNIT

Fig. 3.4-21 Low Altitude Assembly Support Equipment Weight and Cost Estimates

sketch of the RSM configured (see Ref 26) in the Orbiter for support of the MPTS assembly mission. The interior arrangement is based on a longitudinal floor arrangement between the end bulkheads. Interior secondary structure includes four overhead sleep compartments, storage volume, air ducting, and utilities runs. Sufficient room exists in the main platform of the interior for mounting controls and displays consoles for monitoring assembly operations. Consumables and other life support items necessary for a 30-day mission are considered an integral part of the module.

3.4.2.2.3 Communications Module - A communications module, Fig. 3.4-21, is used as a center to transmit television data via TDRS to the ground and to receive command data from ground controllers for operation of the remote manipulators. A potential need for as much as 190 simultaneous TV pictures would be required. The communications module would receive TV signals from the manipulator modules via omni antennas and condition the signals for Ku-band transmission.

A total bandwidth of 5700 MHz would be required for black and white pictures (no data compaction) if assembly is performed in one year. The planned TDRS has a bandwidth of only 225 MHz which can simultaneously support 7 RMM's.

Several observations for remote operations can be identified:

- A dedicated high bandwidth communications satellite system is needed similar to TDRS

- Slow scan TV (1MHz) could be used if it can be shown that the RMM's can adequately be controlled with this quality picture. Only 25 RMM's could be serviced at one time with the current TDRS concept

- A high degree of operations coordination is needed if TV operations are to be limited to 25 at a time - this assumes TV is used for only close-in assembly tasks

- If assembly time were increased from 1 to 4 years, 45 manipulator modules would be needed with 7 in a TV operations mode at a time and hence would be more compatible with a dedicated TDRS system (three satellites).

The weight estimates shown in Fig. 3.4-21 are based on an 18-ft Sortie RAM (Ref 26) with 1310 lb of antenna and communication equipment added. The 1310 lb is the estimated weight for the dual Shuttle communications system.

It is recommended that two dedicated TDRS (3 satellites each) be utilized in a support role.

C.3

3.4-25

3.4.2.2.4 Manufacturing Module - The manufacturing module processes flat stock into basic structural element tri-beams. Figure 3.4-8 shows the application of these modules for manufacture of beams using aluminum. The basic operations for aluminum beam manufacture include roll forming the flat strip stock into the required longeron and intercostal elements of the beam. Feed and cropping mechanisms ensure proper member lengths. Spot welding is used to join longerons and intercostals. Harvesting arms and associated mechanisms are used to assemble the end fittings.

Beam manufacture using graphite/epoxy could utilize rolled strips of partially cured composite materials. A series of hot and cold rollers would be used to finalize the setting process. Bonding devices are used to join elements.

A preliminary operations analysis of the manufacturing steps indicates that beams can roughly be manufactured at the rate of 420 lb/hr. The weight estimate shown in Fig. 3.4-8 uses the RAM free flying payload module for the basic spacecraft and a 100% wrap around factor to account for manufacturing equipments. Significantly more study is required to define the module concept for a more realistic estimate.

3.4.2.2.5 Space Station - Figure 3.4-22 is a schematic of a basic six-man Space Station needed to support assembly operations at a 7000 n mi altitude site. Information presented in Ref 25 was used to establish weight and cost estimates. To achieve consistency of data, the $/lb non-recurring and recurring cost estimates for the Space Station established in Ref 25 has been applied to the cost of all support equipment (RMM, RAM, Support Modules, etc.). Figure 3.4-23 is the weight and cost estimates for a 12-man support Space Station, and has been used to establish the weight and cost trends as a function of number of crew members.

3.4.2.2.6 Crew Transport Module - Reference 27 was used to establish a strawman for the crew transport module, Fig. 3.4-24. The conceptual design of this module can be used to transport crews between the Shuttle and the support Space Station at 7000 n mi using the Space Tug as a propulsion stage. It also has the operational capability for servicing the manufacturing modules and remote manipulator modules.
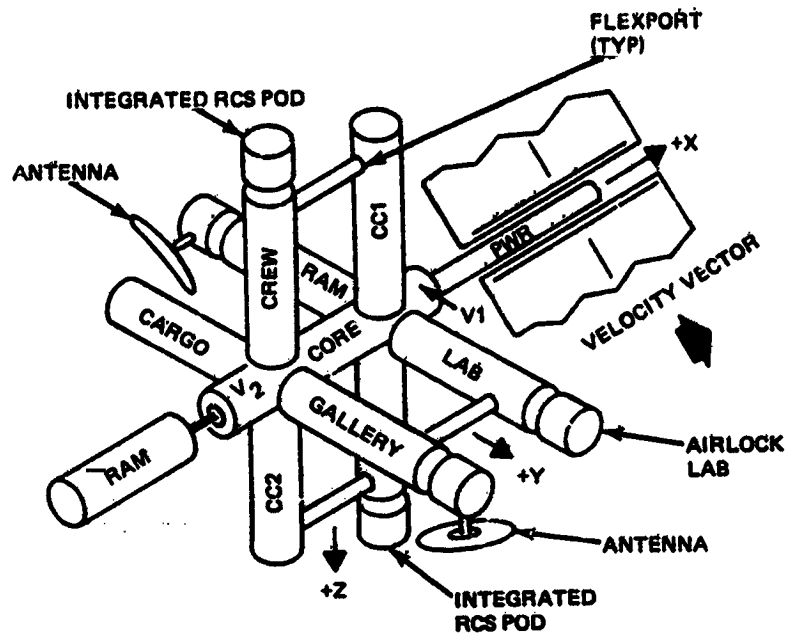
- WEIGHT = 168,400 LB
- COST
  - NON RECURRING = $2097.8M
  - RECURRING = $ 487.8M

Fig. 3.4-22 High Altitude Assembly, Typical 6-Man Support Space Station Concept
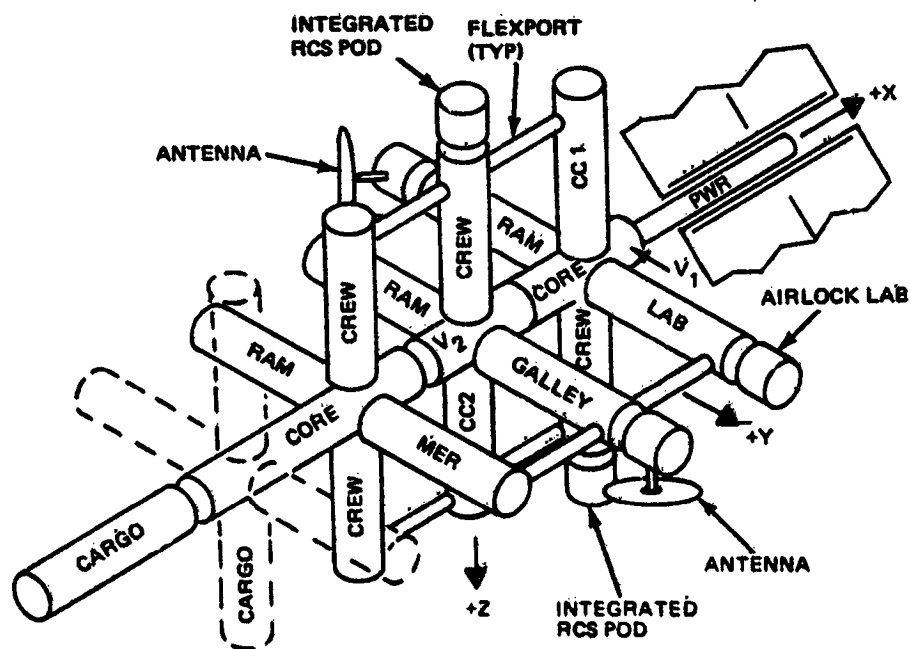
- WEIGHT = 243,620 LB
- COST
  - NON-RECURRING = $2309.9M
  - RECURRING = 759.1M

Fig. 3.4-23 High Altitude Assembly, Typical 12-Man Support Space Station Concept

HYGIENE, WASTE & H₂O MGMT

CABIN FAN, H-X, ECS

BUNK

15 FT. DIA.

CONTROL STA.

A-A

N₂

O₂

H₂O

A

A

N₂H₄   WORKSHOP & CARGO

COMMON MODULE CM-1

28 FT.

HALF AREA SOLAR CELL ARRAY

BLK.

	WEIGHT (LB)
GROSS	22,740
STRUCTURE	12,300
SUBSYSTEMS	6,940
EXPENDABLES	800
PROPELLANT	2,700

REF: NAS 8-25051
REPORT NO XM-TN-160
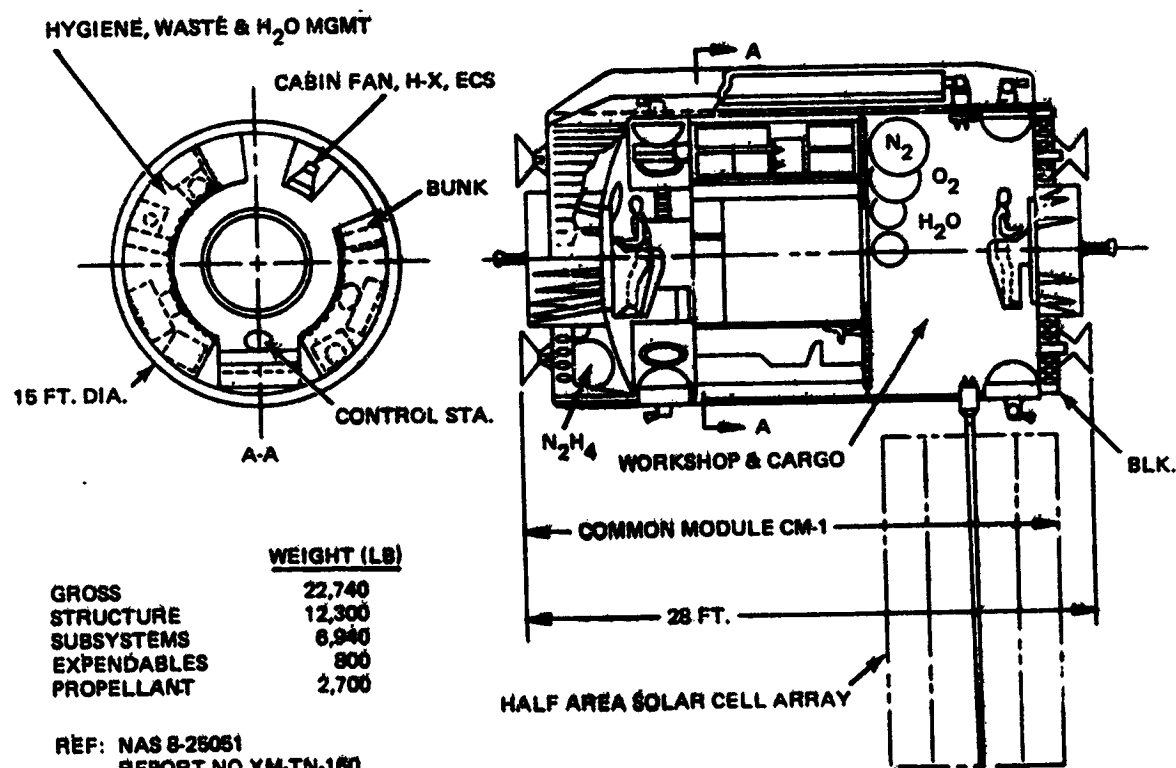
Fig. 3.4-24 Typical Manned Transport Module Concept

3.5 COST

This subsection contains cost parametrics for mechanical systems and flight operations. Flight operations cost estimates are made for the entire SSPS including the recurring costs for suppport equipment. Mechanical System costs are estimated for the MPTS antenna and include the following cost elements:

- Primary and secondary structure

    - Materials

    - Manufacturing

- Materials transportation

- Assembly.

3.5.1 Task 1 – Preliminary Design Results

The following summarizes the significant outputs of this initial activity:

- The performance of the Interim Upper Stage (Transtage) is insufficient to transport assembly crews to the prime assembly site above the Van Allen belt

- Assembly at low altitude results in a significant reduction in total structural system cost relative to assembly at the prime site

- Kevlar/polyimide is the low cost material for assembly at 7000 n mi altitude

- Aluminim structures would result in lowest cost structure for low altitude assembly

- A 1.4 km diameter aluminum antenna is four times the cost of a 0.7 km diameter antenna.

The top level alternate concepts assessed during Task 1 are summarized in Fig. 1-1. Four transportation modes, three structural materials, two structural arrangements and three antenna diameters were included in the preliminary matrix of options. The four transportation modes included:

- Shuttle/Expendable Transtage (1980 IOC)

- Shuttle/Reusable Transtage (1980 IOC)

- Shuttle/Cryo Tug (1984 IOC)

- Shuttle/Low Orbit Assembly (1980)

The materials considered in this initial assessment included:

- Aluminum (Alzac coating)
- Graphite/epoxy (white paint coating)
- Kevlar polyimide (white paint coating)

The two structural arrangements evaluated were the "rectangular grid" and "radial spike" designs discussed in Reference 16. Antenna diameters of 1.4, 1.0 and 0.7 km were assessed.

Figure 3.5-1 and 3.5-2 summarize the Task 1 preliminary estimates of weights and costs for the "rectangular grid" and "radial spike" design options. Figure 3.5-1 shows weight and cost variations for antenna diameters between 0.7 and 1.4 km and for aluminum, graphite/epoxy and Kevlar/polyimide. Figure 3.5-2 shows the radial spike design for a 1 km diameter antenna using the same three materials. Only two of the four flight modes (e.g., Cryo Tug, Mode III and Shuttle/low orbit assembly, Mode IV) are presented. The performance of the Transtage IUS was found to be insufficient to deliver assembly crews to a site of 7000 n mi altitude. Assembly at low altitude shows a significant cost benefit over assembly at 7000 n mi. On the average, a 40 to 60% decrease in costs can be achieved with the lower altitude assembly site.

Kevlar/polyimide is potentially the low cost material for assembly at 7000 n mi altitude. This cost advantage over aluminum or graphite/epoxy will be greater if it can be shown that the thermal variation of polyimide would be sufficient to withstand the expected environment without coatings. Aluminum is the low cost material for low altitude assembly, with Kevlar polyimide the second choice. Aluminum structure will be approximately 25% less costly than graphite/epoxy and 20% less than Kevlar for the low altitude case.

The rectangular grid (1 km) antenna was selected for concept definition during Task 2. Aluminum and graphite/epoxy or polyimide was selected for more in-depth assessment. Further evaluation of the assembly altitude selection was recommended to determine the impact on cost:

- Support Equipments
- SEPS transportation costs
- Asse .bly costs of the entire SSPS.

Fig. 3.5-1 Task I – Preliminary MPTS Design Data Sheet, Rectangular Grid

PARAMETER	DESIGN OPTION		
		1.0 KM	
• DIAMETER			
• MATERIAL	ALUM	GRAPHITE/ EPOXY	KEVLAR POLYIMIDE
• COATING	ALZAC	WHITE PAINT & ALUMINUM FOIL	WHITE PAINT & ALUMINUM FOIL
• LIMIT TRANSMITTED POWER	1.5GW (90%) 3.8GW (79%)	1EGW (90%) 3.8GW (70%)	20GW (90%) 17GW (70%)
• WEIGHTS KLB (1000 Kg) – PRIMARY STRUCT – SECONDARY – COATINGS – ATTACHMENTS	112.0 (50.7) 289.3 (131.2) 7.0 (3.2) 184.0 (83.4)	74.6 (33.8) 159.2 (72.2) 59.1 (26.8) 131.7 (59.7)	77.8 (35.3) 144.6 (65.6) 61.9 (28.1) 128.0 (58.0)
TOTAL KLB (1000 Kg)	592.3 (268.6)	424.6 (192.6)	412.3)186.9)
• COSTS – MATERIAL – PROCESSING	0.74 35.5	8.5 83.0	5.5 49.5
SUB TOTAL	35.974	91.5	55.0
SHUTTLE/CRYO TUG			
– MATERIALS TRANS – ASSEMBLY – FLT SUPPORT	458.0M 205.0M 21.1M	329.0 266.0 24.4	319.5 307.0 26.2
TOTAL	720.074	710.9	707.7
SHUTTLE/FLOW ORBIT ASSEM			
– MATERIALS TRANS – ASSEMBLY – FLT SUPPORT	98.0 132.0M 13.4M	70.4 170.0 17.0	68.0 18.7 18.7
TOTAL	279.374	348.9	324.7

Fig. 3.5-2 Task I, Preliminary MPTS Design Data Sheet — Radial Spoke

3.5.2 Task 2 - Concept Definition Results

The Task 2 findings are summarized as follows:

- Low altitude assembly (190 nmi) is significantly lower in cost than assembly above the Van-Allen belt.

- The major cost driver is the Shuttle operations cost. The most payoff for reduction of overall assembly and transportation costs would be the reduction of the per flight STS costs by introducing the Fly-Back Booster and/or heavy lift vehicle.

- Recurring unit costs for Shuttles, Tugs, Space Stations, etc. represents 1/6 of the total costs for assembly.

- Aluminum is the low cost material for the antenna. Composites increase cost 4 to 5%.

3.5.2.1 Transportation and Assembly

The assembly and transportation system elements assumed for the low altitude and high altitude assembly site Task 2 cost estimates are presented in Fig. 3.5-3. The low altitude assembly site uses the Shuttle for transportation of materials and consumables. The Shuttle, augmented by support modules in the payload bay, are used for crew accommodations. Detailed parts are fabricated in orbit using automated manufacturing modules. Assembly is performed using remote controlled manipulators. Solar Electric Propulsion is used for transport of the assembled SSPS to the geosynchronous orbital position. The high altitude site requires the addition of the Full Capability Tug for transport of materials and must be augmented by a crew transport module for rotation of assembly crews. A six-man space station is assumed required for crew accommodations at the high altitude site.

3.5.2.2 Fleet Size and Traffic Assessment

Both fleet size calculations and the assessment of vehicle traffic are directly affected by the total weight that is transported to orbit, the assembly altitude, and the assembly time in orbit. This subsection presents the effect that these elements have on traffic rate and fleet size for three representative flight plans. All three flight plans considered in-orbit manufacture of all SSPS structural components by manufacturing modules. The three flight plans are:

- Flight Plan 1 - One year assembly at 190 n mi
- Flight Plan 2 - One year assembly at 7000 n mi
- Flight Plan 3 - Two year assembly at 190 n mi.

Figure 3.5-4 summarizes the SSPS component weights for the three flight plans listed above.

ASSEMBLY ALTITUDE	TRANSPORT MODE (MATERIALS)	TRANSPORT CREWS	CREW ACCOMMODATIONS	DETAIL PARTS ASSEMBLY	ASSEMBLY METHOD	TRANSPORT TO GEOSYNCH

LOW ORBIT
• 190 N MI
• 28.5° INCL
	• SHUTTLE	• SHUTTLE	• SHUTTLE
			  – 6 MEN
			  – 30 DAYS
				• AUTOMATIC IN-ORBIT MANUFACTURE	• REMOTE MANIPULATOR	• SEPS

HIGH ORBIT
• 7000 N MI
• 28.5° INCL
	• SHUTTLE
	• FULL CAP. TUG
		• SHUTTLE
		• FULL CAP.
		• CREW TRANSPORT MODULE
			• SPACE STATION
			  – 6 MEN
			  – 180 DAYS
				• AUTOMATIC IN-ORBIT MANUFACTURE	• REMOTE MANIPULATOR	• SEPS

Fig. 3.5-3 Transportation and Assembly Cost Comparison Cases

		FLIGHT PLAN		
		1	2	3
STAT. KEEP MOD. STRUCTURE	KLB (10^3 Kg)	45.0 (20.4)	NOT REQD	45.0 (20.4)
STAT. KEEP CONSUMABLES	KLB (10^3 Kg)	44.0 (19.9)	NOT REQD	88.0 (39.9)
SSPS STRUCTURE	MLB (10^6 Kg)	21.1 (9.6)	21.1 (9.6)	21.1 (9.6)
MPTS ANTENNA	MLB (10^6 Kg)	4.12 (1.9)	4.12 (1.9)	4.12 (1.9)
SEPS STRUCTURE[1]	MLB (10^6 Kg)	1.77 (0.8)	0.32 (0.14)	1.06 (0.48)
SEPS CONSUMABLES[1]	MLB (10^6 Kg)	1.78 (0.8)	0.90 (0.41)	1.67 (0.76)
TOTAL MLB	MLB (10^6 Kg)	28.86 (13.1)	26.44 (11.97)	27.98 (12.67)

Fig. 3.5-4 SSPS Weights

The assumptions used for fleet sizing are divided into three groups as follows:

Shuttle and Tug Performance

- 65K lb Shuttle capability to 190 n mi orbit
- 36.8K Tug payload capability from 190 to 7000 n mi
- 23 Shuttle flts/yr for each Shuttle vehicle
- 23 Tug flts/yr for each Tug vehicle

Support Equipment

- Each manufacturing module processes 420 lb/hr
- Manufacturing modules operate 24 hr/day
- Remote manipulator modules (RMM) assembles at 26 lb/man-hour
- One ground controller for each RMM
- Each ground controller works 155 mhr/month
- RMM's are used three shifts/day
- RMM's require 5% consumables for each 1 lb moved

Crew Requirements

7000 N Mi site

- Six men needed in 7000 n mi orbit for 1 yr
- Crew change every 180 days at high altitude site

190 N Mi site

- Shuttle crew quarters
- Six men
- 30-day missions

Figure 3.5-5 and 3.5-6 present a detailed breakdown by assembly phase
(see Fig. 3.5-7) of the number of Shuttles used during each phase of assembly for Flight
Plan 1 (1 year assembly 190 n mi), and Flight Plan 3 (2 year assembly at 190 n mi). Also
listed are the approximate assembly times based on the material delivery and manufacturing
assumptions. Both of these flight plans have assumed that a separate solar array is avail-
able to power the SEPS during the trip to geosynchronous orbit. An investigation of the

- **FLT PLAN 1 – LOW ALTITUDE ASSY**
- **DETAILED ASSEMBLY – IN-ORBIT MANUFACTURE**
- **ASSEMBLY – REMOTE MANIPULATOR MODULE**
- **ANTENNA MATERIAL – ALUMINUM**
- **ASSEMBLY TIME – 1 YR.**

- **PHASE 1 – ASSEMBLE STATION KEEP/CONTROL MODULE**
  - SHUTTLE FLTS (MATERIALS) — 2
  - SHUTTLE FLTS (MANUFAC. MODULES & RMM'S) – 9
  - SHUTTLE FLTS (CONSUMABLES) – 1

- **PHASE 2 – ASSEMBLE CREW SPACE STATION – N/A**

- **PHASE 3 – ASSEMBLE SSPS**   (9.6 MONTHS TO ASSEMBLE)
  - SHUTTLE FLTS (MATERIALS) — 325
  - SHUTTLE FLTS (PERSONNEL) — 10
  - SHUTTLE FLTS (CONSUMABLES) — 17

- **PHASE 4 – ASSEMBLE MPTS**   (1.9 MONTHS TO ASSEMBLE)
  - SHUTTLE FLTS (MATERIALS) — 64
  - SHUTTLE FLTS (PERSONNEL) — 2
  - SHUTTLE FLTS (CONSUMABLES) — 4

- **PHASE 5 – ASSEMBLE SEPS**   (0.5 MONTHS TO ASSEMBLE)
  - SHUTTLE FLTS (MATERIAL) — 27
  - SHUTTLE FLTS (CONSUMABLES) — 31

- **PHASE 6 – TRANSPORT TO GEOSYNCH – N/A**

- **PHASE 7 – CHECKOUT – N/A**

                    TOTAL SHUTTLE FLTS   492

Fig. 3.5-5 Traffic Model Assessment, Flight Plan 1

- FLT PLAN 3 – LOW ALTITUDE ASSY
- DETAILED ASSEMBLY – IN-ORBIT MANUFACTURE
- ASSEMBLY – REMOTE MANIPULATOR MODULE
- ANTENNA MATERIAL – ALUMINUM
- ASSEMBLY TIME – 2 YR.

PHASE 1 – ASSEMBLE STN KEEP/CONTROL MODULE

– SHUTTLE FLTS (MATERIALS) –	2
– SHUTTLE FLTS (MFR. MODULES & RMM'S) –	6
– SHUTTLE FLTS (CONSUMABLES)	7

PHASE 2 – ASSEMBLE CREW SPACE STATION – N/A

PHASE 3 – ASSEMBLE SSPS   (19.2 MONTHS TO ASSEMBLE)

– SHUTTLE FLTS (MATERIALS)	325
– SHUTTLE FLTS (PERSONNEL)	20
– SHUTTLE FLTS (CONSUMABLES)	17

PHASE 4 – ASSEMBLE MPTS   (3.8 MONTHS TO ASSEMBLE)

– SHUTTLE FLTS (MATERIALS)	
– SHUTTLE FLTS (PERSONNEL)	
– SHUTTLE FLTS (CONSUMABLES)	

PHASE 5 – ASSEMBLE SEPS   (0.5 MON. TO ASLE.)

– SHUTTLE FLTS (MATERIALS)	27
– SHUTTLE FLTS (CONSUMABLES)	31

PHASE 6 – TRANSPORT TO GEOSYNCH – N/A

PHASE 7 CHECKOUT – N/A

TOTAL SHUTTLE FLTS • 501

Fig. 3.5-6 Traffic Model Assessment, Flight Plan 3

- SSPS: – SATELLITE SOLAR POWER STATION
- MPTS: – MICROWAVE POWER TRANSMISSION SYSTEM
- SEPS: – SOLAR ELECTRONIC PROPULSION SYSTEM
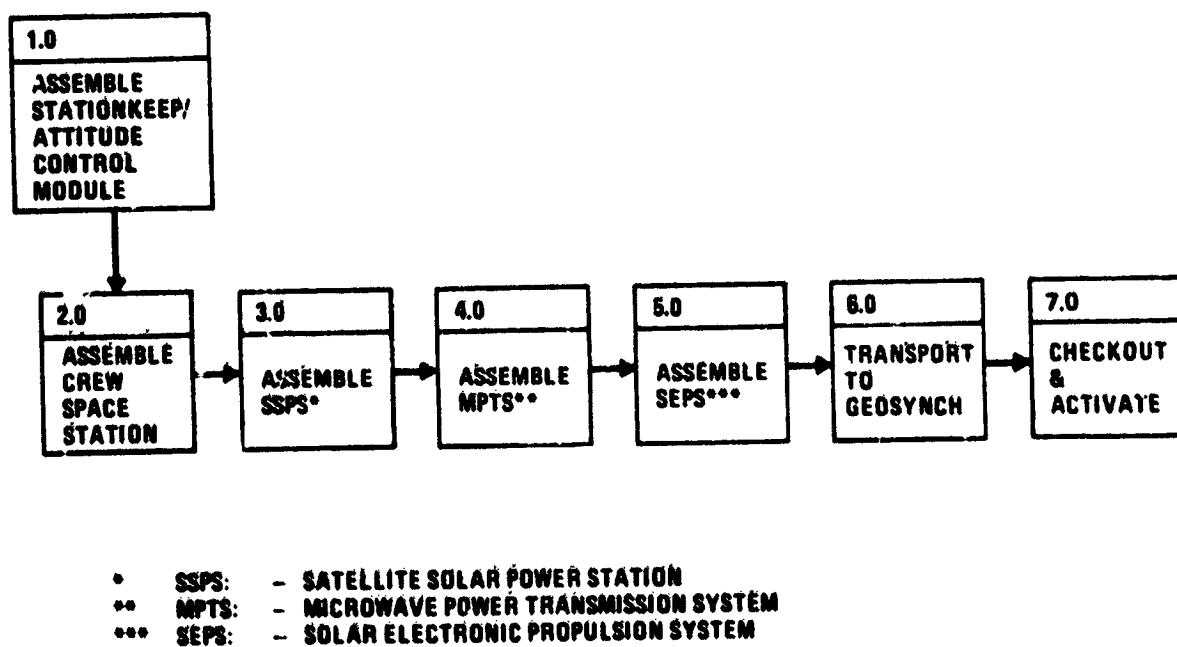
Fig. 3.5-7 Level I Functional Flow: Assembly

feasibility of using the SSPS for this purpose and reconfiguring it once in geosynchronous orbit, proved to be extremely costly because of the additional hardware required to support reconfiguration. Manned Space Stations in geosynchronous orbit would be necessary to support the reconfiguration crew; this would impose a requirement for a Tug fleet and additional Shuttle flights to effect deployment of hardware, consumables, personnel, and Tugs. Secondly, a delay in the start of SSPS operation would be required. A separate SEPS array avoids the reconfiguration step and results in lower total program cost and a SSPS which becomes operational earlier.

Results of the fleet size analyses show that 24 Shuttles are required for the one year assembly plan (Flight Plan 1) and 15 Shuttles are needed to support the two year assembly plan (Flight Plan 3). In both cases, two crew support modules are required to support the six-man crew. Eight manufacturing modules and 182 manipulator modules are needed for Flight Plan 1 and half that number for Flight Plan 2.

Figure 3.5-8 presents the detailed Shuttle/Tug flight requirements necessary to support Flight Plan 2, i.e., one year assembly at 7000 n mi. Since atmospheric drag is not a consideration at 7000 n mi, the stationkeeping module has been eliminated. The figure shows that the Shuttle is required to make approximately 1300 flights in a year. The dramatic use over the LEO assembly requirement of approximately 500 Shuttle flights can be explained by the fact that additional flights are required (at less than 100% load factor, i.e., 65000 lb payload) to get Tugs into orbit. The result is that 59 Shuttles and 37 Tugs are needed to support Flight Plan 3.

3.5.2.3 Launch Opportunity Sensitivity to Traffic Rate

The Shuttle has an ETR launch opportunity every 23.5 hours to a 190 n mi 28.5 inclined orbit assembly site. A glance at the total number of Shuttle launches required for either of the one year assemblies (see Fig. 3.5-9) indicates that from one to four Shuttle launches per day are required if orbit phasing is neglected. Worst case phasing conditions can exist on some of these days; this only serves to aggrevate the launch/day situation. This situation arises from the fact that under worst case phasing conditions, it is optimum to delay launch a day, and spend 16 hours phasing with the assembly area at 190 n mi. The alternative is to launch on the first opportunity, spend 40 hours phasing, and arrive at the assembly point at the same time as a vehicle that delayed launch for 1 day. Obviously, it is more advantageous to delay launch for the day and wait on the ground for better relative launch site/assembly point phasing to exist. This waiting would mean that the ETR launch rate would double on some days during the year and that from 2 to 8 vehicles would have to

- FLT PLAN 2 – HIGH ALTITUDE ASSY (7000 N MI)
- IN-ORBIT MANUFACTURE AT 7000 N MI
- REMOTE MANIPULATOR ASSEMBLY
- 1 YEAR MANUFACTURE & ASSEMBLY
- ANTENNA MATERIAL – ALUMINUM

- PHASE 1 – EQUIPMENT DEPLOYMENT
  - SHUTTLE FLTS TO LOW EARTH ORBIT (MFR. MOD)   8
  - SHUTTLE FLTS TO LOW EARTH ORBIT (RMM'S)   1
  - SHUTTLE FLTS FOR TUG DEPLOYMENT   10
  - TUG FLTS   10

- PHASE 2 – CREW SPACE STATION DEPLOYMENT
  - SHUTTLE FLTS TO LOW EARTH ORBIT (SPACE STATION) 8
  - SHUTTLE FLTS FOR TUG DEPLOYMENT   8
  - TUG FLTS   8

- PHASE 3 – SSPS MANUFACTURE
  - SHUTTLE FLTS TO LOW EARTH ORBIT (MATERIAL)   325
  - SHUTTLE FLTS FOR TUG DEPLOYMENT   574
  - TUG FLTS   574

- PHASE 4 – MPTS MANUFACTURE
  - SHUTTLE FLTS TO LOW EARTH ORBIT (MATERIAL)   64
  - SHUTTLE FLTS FOR TUG DEPLOYMENT   112
  - TUG FLTS   112

- PHASE 5 – SEPS MANUFACTURE
  - SHUTTLE FLTS TO LOW EARTH ORBIT (MATERIAL)   50
  - SHUTTLE FLTS FOR TUG DEPLOYMENT   88
  - TUG FLTS   88

- PHASE 6 – TRANSPORT TO GEOSYNCH
  - SHUTTLE FLTS TO LOW EARTH ORBIT (SEPS PROPELLANT) 14
  - SHUTTLE FLTS FOR TUG DEPLOYMENT   25
  - TUG FLTS   25

- MISC.
  - SHUTTLE FLTS TO LOW EARTH ORBIT (RMM CONSUMABLES) 21
  - SHUTTLE FLTS FOR TUG DEPLOYMENT   36
  - TUG FLTS   36
  - SHUTTLE FLTS TO LOW EARTH ORBIT (CREW + RSM)   2
  - SHUTTLE FLTS FOR TUG DEPLOYMENT   2
  - TUG FLTS   2

                          TOTAL SHUTTLE FLTS   1348
                          TOTAL TUG FLTS   8?5

Fig. 3.5-8 Traffic Model and Fleet Size Assessment, Flight Plan 2

launched within the launch window (~ 15 minutes). Based on current launch operating techniques this seems to be an unacceptable traffic rate.

It is interesting to note that if an assembly altitude of 255 n mi were chosen, proper phasing with the assembly point would exist on a daily basis and the launch overflow from one day to the next would be avoided.

3.5.2.4 Fleet Size/Traffic Recommendations

Figure 3.5-9 presents a summary of the fleet size/traffic requirements of the three flight plans. Based on strictly fleet size consideration a two year assembly at LEO is recommended. From a launch opportunity point of view, a 255 n mi assembly altitude is recommended. This altitude also offers orbit decay advantages.

3.5.2.4.1 Concept Cost Comparison - Cost compilations were prepared for the following three cases: —

- Flight Plan 1 - Low altitude assembly, one year assembly period (Fig. 3.5-10)

- Flight Plan 2 - High altitude assembly, one year assembly period (Fig. 3.5-11)

- Flight Plan 3 - Low altitude assembly, two year assembly period (Fig. 3.5-12).

The recurring and nonrecurring cost estimates for support equipments assumed in this concept comparison are outlined in Fig. 3.5-13. Previous cost data on Space Station (NAS 9-9953) were updated to 1974 dollars and applied as a unit cost factor ($/Kg) to space station, Shuttle Support modules, remote manipulators and auto manufacturing modules. Weight estimates were taken from Ref. 25 and 26 for the Modular Space Station and Shuttle Support Modules, respectively. Cost estimates for Shuttle were taken from Grumman Phase A study results while Tug estimates were based on recent Tug System Studies. The cost of SEPS and the control modules were assumed at $1M/lb of thrust, Ref. 29. All equipments used in the cost comparison were amortized over the assembly of five SSPS.

Figure 3.5-10 through 3.5-12 summarize the transportation and assembly costs for the three flight plans cited above. An assembly cost of 1323/kw (5 GW system) can be achieved at a low altitude site with a one year assembly time (Flight Plan 1, Fig. 3.5-10). These costs can be reduced slightly, $1300/kw, if the assembly time is increased to two years. (Flight Plan 3, Fig. 3.5-12). Assembly at high altitude would cost 350/kw (Flight Plan 2, Fig. 3.5-11), an unacceptable cost level, if space based power generation is to be competitive with ground generated power.

CONDITION	FLT PLAN 1	FLT PLAN 2	FLT PLAN 3
— ASSEMBLY ALT	190 N.M	7000 N.M	190 N M
— ASSEMBLY TIME	1 YR	1 YR	2 YR
— DETAIL PARTS	AUTO IN-ORBIT	AUTO IN-ORBIT	AUTO IN-ORBIT
— ASSEMBLY	REMOTE	REMOTE	REMOTE
FLTS			
— SHUTTLE	491	1348	501
— TUG	—	855	—
— AVG SHUTTLE FLTS/DAY	1.37	3.68	0.7
— AVG TUG FLTS/DAY	—	2.34	—
FLEET SIZE			
— SHUTTLE	24	59	18
— MANUFACTURE MODULES	8	8	4
— MANIPULATOR MODULES	182	176	91
— CREW SUPPORT MODULES	2	—	2
— TUGS	—	37	—
— SPACE STATION	—	1	—
— CREW TRANSPORT MODULE	—	2	—

RECOMMENDED

Fig. 3.5-9 Traffic Analysis Summary

ELEMENT	NON-RECURRING, $M	FLEET SIZE	RECURRING AMORTIZED OVER 5 SSPS, $M	NO. FLTS	NO. PERSONNEL	OPS COST, $M
SHUTTLE	N/A	24	864	492	—	5,166
RAM SUPPORT MODULE	218	2	16	12	—	12
RAM COM MODULE	283	2	23.5	12-	—	12
MANUFACTURE MODULE	288	8	100	—	—	12
FREE-FLYING TELEOPERATOR	5.95	182	45.2	—	546	21.7
CONTROL MODULE	TBD	1	3.2	—	—	1.4
TDRS	230	6	60	—	—	9
SEPS	TBD	1	400	1	—	15.7
TOTAL			1,511.9			5,240

- TOTAL COST (RECUR + OPS) = $6,761.7M
- COST/LB = $270/LB ($594/Kg)
- $/KW = $1352/KW

*ASSUMES $1M/MONTH OVER 1 YR PERIOD FOR FLT OPS SUPPORT

Fig. 3.5-10 Transportation and Assembly Cost, Flight Plan 1

	NON-RECURRING, $M	FLEET SIZE	RECURRING AMORTIZED OVER 5 SSPS, $M	NO. FLTS	NO. PERSONNEL	OPS COST, $M
SHUTTLE	N/A	59	2,120	1348	—	14,154
TUG	N/A	37	89	855	—	855
SPACE STATION (6-MAN)	2097	1	97.5	—	—	12
CREW TRANSFER MODULE	328	1	14.2	—	—	12
MANUFACTURE MODULE	288	8	100	—	—	12
FREE-FLYING TELEOPERATOR	5.95	178	43.6	—	528	20.9
CONTROL MODULE	TBD	1	3.2	—	—	1.4
TDRS	230	6	60	—	—	9
SEPS	TBD	1	70	—	—	9.0
SUB TOTALS			2597.5			15,085.3

- TOTAL (RECURRING + OPS) = $17,682.8M
- COST/LB $707/LB (1554 $/Kg)
- COST/KW = $3537/KW

*ASSUMES $1M/MONTH OVER 1 YR PERIOD FOR FLT OPS SUPPORT

Fig. 3.5-11 Transportation and Assembly Cost, Flight Plan 2

ELEMENT	NON-RECURRING, $M	FLEET SIZE	RECURRING AMORTIZED OVER 5 SSPS, $M	NO. FLTS	NO. PERSONNEL	OPS COST, $M
SHUTTLE	N/A	15	540	501	—	5260.5
RAM SUPPORT MODULE	218	2	16	24	—	24
RAM COM. MODULE	283	2	23.5	24	—	24
MANUFACTURE MODULE	288	4	50.0	—	—	24
FREE-FLYING TELEOPERATOR	5.95	91	22.60	—	273	21.6
CONTROL MODULE	TBD	1	3.2	—	—	2.8
TDRS	230	6	60	—	—	18
SEP	TBD	1	400	1	—	15.7
TOTAL			1115.3			5390.6

- TOTAL COST (RECURR + OPS) = $6427.9M
- COST/LB = $260/LB (571.9 $/Kg)
- $/KW = $1301/KW

*ASSUMES $1M/MONTH OVER 2 YR PERIOD FOR FLT OPS SUPPORT

Fig. 3.5-12 Transportation and Assembly Cost, Flight Plan 3

ELEMENT	PERFORMANCE	WEIGHT	COST/FLT	NON-RECURRING	RECURRING UNIT	SOURCE
SHUTTLE	65K TO 190 N M 100 FLT LIFE	N/A	$10.5M	N/A	$180M	GAC SHUTTLE STUDY
CRYO TUG	36.8 K LB TO 7000 N M 100 FLT LIFE	BURN OUT= 2680 Kg FULL = 24,900 Kg	$ 1.0M	N/A	$12M	MDAC TUG STUDY
FREE-FLYING TELE OPERATOR	5 YR LIFE	183 Kg	TBD	$5.95M	$1.24M	MSFC-PAYLOAD DESCRIPTION VOL II
RAM SUPPORT MODULE	30 DAY MISSION 5 YR LIFE	5000 Kg	$ 1.0M	$218M	$40M	WT DATA — NAS 8-27539 COST DATA — NAS 9-9953
RAM-COM MODULE	30 DAY MISSION 5 YR LIFE	8760 Kg	$ 1.0M	$283M	$59M	WT DATA — NAS 8-27539 COST DATA — NAS 9-9953
MANUFACTURE MODULE	5 YR LIFE	9100 Kg	TBD	$288M	$62.5M	SWAG
SEPS	1 YR TRIP TIME	FROM 190 N M = 1.18 X 10^6 Kg FROM 700 N M = .556 X 10^6 Kg	$15.7M $ 9.0M	TBD TBD	$400M $400M	GAC RPT NO. ASP 583-R-8
SPACE STATION 6 MAN	5 YR LIFE	76,700 Kg	TBD	$2097.6M	$487.8M	NAS 9-9953
12 MAN	5 YR LIFE	102,000 Kg	TBD	$2306.9M	$759.1M	NAS 9-25051
CREW TRANSFER MODULE (4)	100 FLT LIFE	10,300 Kg	TBD	$328M	$71.2M	
TDRS	N/A	2038 Kg	N/A	$210M	$30-50M	HUGHS REPORT 30096-3514

Fig. 3.5-13 Transportation and Assembly System Fleet and Support Equipment Characteristics and Cost Summary (1974 $'s)

STS operations cost is the major cost driver. Over 80% of the cost for assembly are related to STS per flight launch costs. These costs can be significantly reduced by introducing the Fly-Back Boosters. Data generated during the Shuttle Phase A studies indicated that launch costs could be reduced by a factor of two or three with a Fly-Back Booster. A heavy lift vehicle, which utilizes the current Shuttle system external tanks, SSME and solid rockets could be utilized in a deploy only flight mode and increase throw weight performance to $120,000 lb per flight without increasing launch costs. Launch cost of $25 to $50/lb could be achieved with these STS modifications.

Recurring costs for support equipments were found not to be as significant a cost driver as was expected. The unit costs to purchase the Space Stations, additional Shuttles, manufacturing modules, etc. represent only 1/6 the cost to assemble each SSPS.

The development cost of Space Stations, Shuttle payload bay support modules and free flying teleoperators can be shared or fully absorbed by programs which are more near term than SSPS. The function of the manufacturing modules and SEPS, may be so unique to SSPS that these elements may have to be accounted as part of the SSPS development costs.

3.5.2.4.2 Sensitivity To Shuttle Packaging Density - A review of packaging factors for all elements of the SSPS has shown that most components and/or subassemblies can utilize the full payload performance capability of the Shuttle. The exception is perhaps the antenna waveguides. Structural subassemblies, can be packages as flat stock and fabricated in space with relatively simple auto manufacturing modules. Solar cell blankets can be rolled into tightly packages bundles for transport. Electrical wiring and equipments can also be densely packaged. The waveguides, however, may require fabrication on earth where the tight dimensional tolerances necessary for efficient microwave performance can be closely controlled.

The design of close tolerance hinges and locking mechanisms as an integral part of the waveguide subarray offers a packaging approach with reasonable densities. Figure 3.5-14 is a parametric presentation of total waveguide weight and packaging density as a function of waveguide wall thickness. The final selection of thickness will be determined by analysis of the operational thermal requirements of the waveguides. An increase in thickness will increase conductivity of heat from the hot surface where the microwave conversion electronics are mounted to the cooler slotted face of the subarray. This thermal transfer is required to minimize the thermal gradients between the surfaces thereby minimizing thermal distortion. The packaging approach shown in Fig. 3.5-14 utilizes the
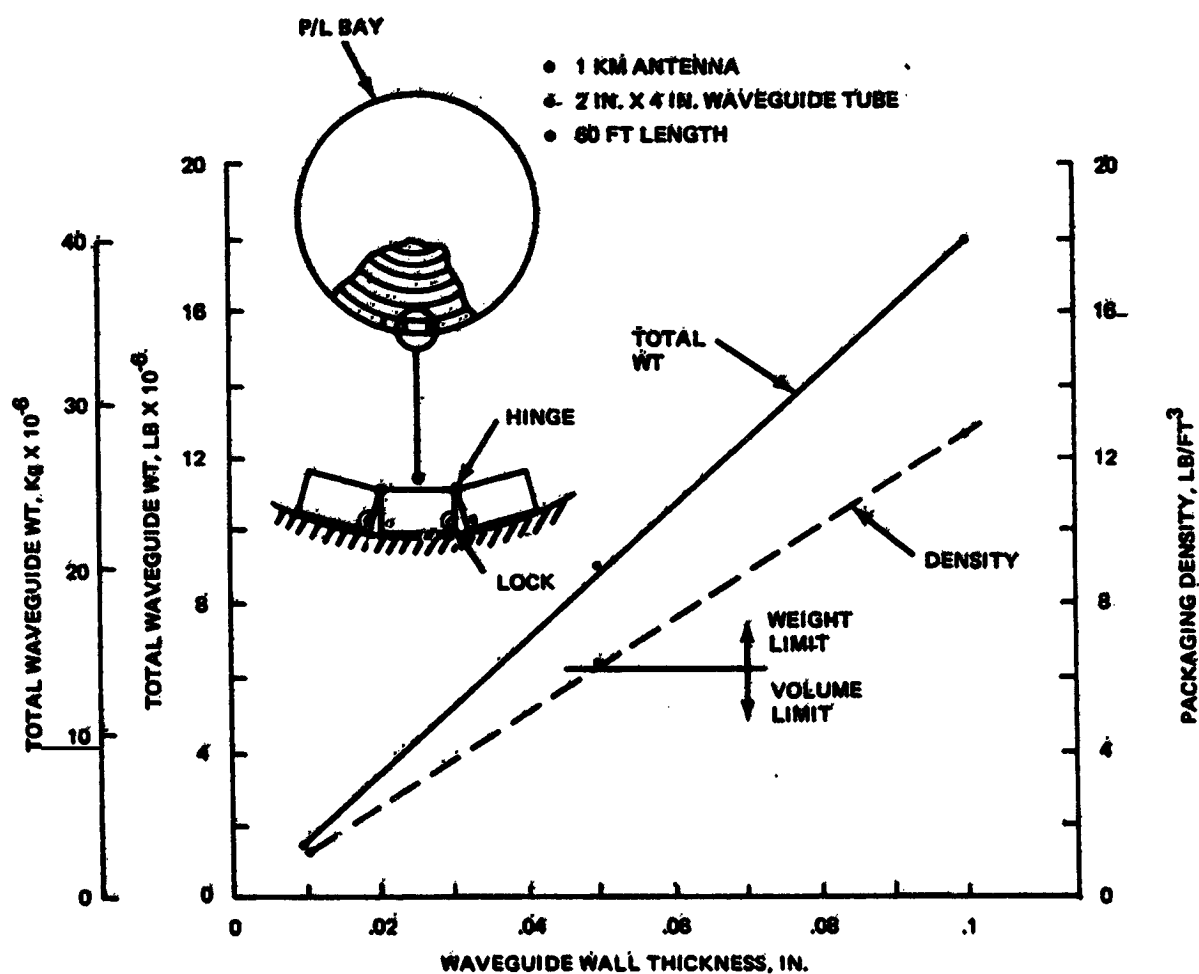
Fig. 3.5-14 Waveguide Weight and Packaging Density

hinges running the 18 meter length of the waveguide as a means of rolling the array into as tight a bundle as possible, without affecting the dimensional characteristics of individual waveguides within the subarray (similar packaging approach as used to stow snow fence). After delivery of the subarrays to orbit, locki᷄ᷟ mechanism on the face opposite the hinge lines are utilized to securely deploy the subarray to within the required flatness.

Figure 3.5-15 relates total waveguide system weight to packing density and number of Shuttle flights. The flight plans presented earlier in this section, assumed inflight fabrication of these units. A total of 25 flights was required to transport the 3.95 Kg of 10 mil aluminum stock for inflight manufacture. The number of flights increases to 140 if the waveguides are fabricated on the ground and transported in the packaging arrangement shown in Fig. 3.5-14. The number of required flights remain constant up to a waveguide wall thickness of 50 mil. Above this material thickness, the Shuttle performance limitations become the driving factor for establishing quantity of flights.

Transportation costs increase 20% from the baseline rate of 1301 $/kw to 1550 $/kw if space fabrication is not used for the waveguide. This 20% increase holds up to a waveguide wall thickness of 50 mil. At a thickness of 100 mil, the increase in cost is 50%. Figure 3.5-16 summarizes the cost delta's as a function of waveguide wall thickness.

3.5.3 MPTS Structural Costs

The cost elements for mechanical systems and flight operations have been broken down into the following subdivisions:

- Primary and secondary structure

  - Materials

  - Manufacturing

- Materials transportation

- Assembly.

Cost parametrics for the structure are in 1974 dollars and include the cost of materials and thermal coatings. The manufacturing processing costs for prelaunch forming of beam elements and application of thermal coatings are included. Cost relationships are in the form of $/Kg.
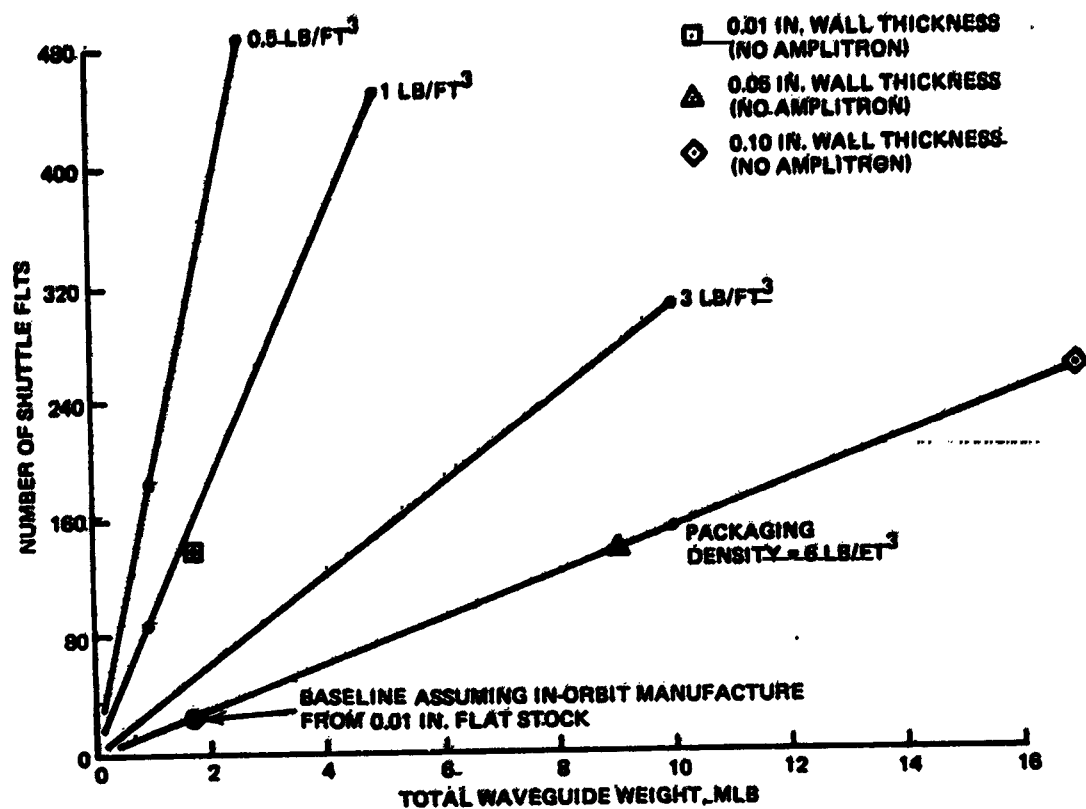
Fig. 3.5-15 Traffic Requirements as Function of Waveguide Weight and Packaging Density

	FLT PLAN 3 — LOW ALT ASSEMBLY — YR ASSEMBLY PERIOD		
	WAVEGUIDE WALL THICKNESS, IN. (ALUM.)		
	0.01	0.05	0.1
BASELINE SSPS COSTS, $M			
— RECURRING	1115.3	—	—
— OPS COST	5390.0	—	—
— TOTAL	6427.9		
COST, $/Kg	571.9	—	—
$/KW	1301		
DELTA COST DUE TO PACKAGING			
— DELTA FLTS	115	115	247
— DELTA SHUTTLE FLEET SIZE	4	4	7
— DELTA RECURRING COST, $M	144	144	262
— DELTA OPS COST, $M	1207.5	1207.5	2593.5
— TOTAL DELTA, $M	1351.5	1351.5	2845.5
TOTAL COST INCLUDING WAVEGUIDE PACKAGING PENALTIES, $M	7779.4	7779.4	9273.4
TOTAL SYSTEM WEIGHT, MLB (MKg)	25	32.2	41.2
COST RATE, $/Kg	683	530	494.6
$/KW	1555	1555	1854

Fig. 3.5-16 Transportation and Assembly Cost Sensitivity to Waveguide Packaging Density

7 Materials Transportation costs are evaluated for a low altitude assembly site only. The high altitude option was deopped because of the non-competitive costs (see Subsection 3.5.2). The cost of transporting assembly crews and in-flight processing modules are not included under this cost element.

Assembly costs for the structural materials (i.e., aluminum and graphite composites) options considered were assumed the same. The results of the assembly cost comparison (Subsection 3.5.2) were used to establish a proportionate cost for support equipments, SEP transportation cost, etc. based on antenna weight relative to the entire SSPS. The assembly cost of structure varies with the number of joints or pieces of material that must be assembled and is independent of the properties or weight of the material.

3.5.3.1 Materials and Manufacturing Costs

The microwave power transmission section of the orbiting solar energy collector can be designed from advanced composite material or aluminum to meet three criteria. These are (a) 30-year life, (b) low or zero thermal expansion and (c) operating temperature range between $450°K$ and $480°K$. This structure can be designed as thin-wall tubes, 3-6 inches in diameter, 18m (60 ft) or less in length, or as thin (0.010) slats which roll up to a helix 4.6m (15 ft) in diameter.

A summary of material and processing costs are given in Fig. 3.5-17 for several candidates. Thermal control coating costs are included.

Material costs were obtained during the week of August 19, 1974 from Grumman purchasing agents, who are in direct contact with vendors and who used most recent purchase orders and quotes as their basis. These costs are listed in Fig. 3.5-17 as "present material cost", and would be the price paid today for a large quantity order. The only exception is 2-mil-thick graphite/epoxy 3-inch-wide tape whose price would drop from 726 $/Kg ($330 per lb) (which is the small batch cost) to less than 210 $/Kg ($100 per lb) for large volume orders; a firm price could not be obtained from the vendors.

Minimum prices shown in Fig. 3.5-17 are generally the same as present prices or are based on recent prices (e.g. 236 $/Kg ($107/lb) for boron/epoxy in January 1974), projected near term lower costs (e.g. 44 $/Kg ($20/lb) for graphite/epoxy) or different forms of the material (e.g., Kevlar prices, aluminum alloy types).

OPTION	GRUMMAN SPEC.	STRUCTURAL MATERIAL COST			PROCESSING COST			TOTAL COST RANGE	
		PRESENT	MIN.	MAX.	PRESENT	MIN.	MAX.	MIN.	MAX.
Boron/epoxy 3" tape, 5-mil	GM3004-3	170.00 (374.0)	107.00 (235)	195.00 (429)	200 (441)	150 (330)	300 (661)	257 (566)	495 (1091)
Graphite/epoxy 3" tape, 5 mil	GM3012	47.00 (103)	20.00 (44)	60.00 (132)	200 (441)	150 (330)	275 (606)	150 (330)	335 (738)
Graphite/epoxy 3" tape, 2-mil	GM3012	330.00 (727)	140 (308)	420.00 (926)	300 (661)	195 (429)	425 (937)	335 (738)	845 (1863)
Quartz-polyimide 12" cloth, 8-mil	GC110BC	44.00 (97)	44.00 (97)	53.00 (116)	160 (352)	120 (264)	210 (463)	164 (361)	263 (579)
Glass-polyimide 44" cloth, 8-mil	GC110BBI	6.50 (14.3)	6.50 (14.3)	7.80 (17.2)	160 352	120 (264)	210 (463)	127 (280)	218 (480)
Glass-polyimide 44" cloth, 8-mil	GM4001G42	2.98 (6.57)	2.98 (6.57)	3.60 (7.93)	133 (293)	100 (220)	180 (396)	103 (227)	184 (405)
Kevlar-polyimide 50" cloth, 8-mil	-	22.50 (49.61) (2)	13.20 (29.11) (3)	37.10 (81.80) (4)	160 (132)	120 (264)	210 (463)	133 (293)	247 (544)
Kevlar-epoxy 50" cloth	-	19.00 (41.90)	9.70 (21.39)	33.60 (74.09)	133 (293)	100 (220)	180 (396)	110 (242)	224 (493)
Aluminum (5)		1.00 (2.20)	0.80 (1.76)	1.25 (2.75)	90 (198)	60 (132)	290 (639)	61 (134)	291 (641)

General Note: All composites cost include external white thermal control coatings at $3.00/lb wet cost, or approximately 16 sq ft per lb. This cost is included as part of processing.

(1) The cost depends on type of structure being fabricated.
(2) Style 181 8-mil fabric
(3) Style 281 special 1420 derrie.
(4) Style 120 4-mil fabric
(5) Includes Alzac coating for thermal control.

Fig. 3.5-17 Materials and Processing Costs, $/LB ($/Kg)

Maximum prices anticipate a 20-25% inflationary raise during the 1974-1975 time-span for most of the materials listed in Fig. 3.5-17 except for the Kevlar maximum price which is a more expensive form of this particular material. Kevlar prices may drop in the near future as usage of this man-made fiber increases.

Processing costs were based on a recent study for the VFAX airplane design in which an analysis considered metal and composite designs. These costs are based on the current $14-$15 per hour manufacturing rate. They reflect a 75-80% learning curve, with maximum cost taken at Ship No. 1 and minimum cost at Ship No. 150. It is understo that 150 ships may not be built, but that within each ship there exists sufficient repetitive structure such that mass production of identical items will tend to lower unit cost as more and more items are built.

For further in-depth reference the reader is directed to Ref 17.

3.5.3.2 Transportation and Assembly

Figure 3.5-18 summarizes the cost relationships used in comparing MPTS structur options. The cost of materials transportation assumes the Shuttle can deliver 29.4×10^3 (65 K/lb) to 190 n mi at a cost of $10.5M per flight. In the four month period allocated to the assembly of the antenna, eight flights were needed for transportation of consumables and personnel (see Subsection 3.5.2). It is assumed that the type of material used in the construction of the antenna does not affect this requirement. The cost of equipments for support of assembly and the cost of SEPS transportation to geosynchronous was allocated in proportion to the baseline antenna weight to solar array weight ratio used in the traffic model assessment and was assumed independent of structural material.

Figure 3.5-19 shows that aluminum is the low cost material for the antenna structu The three graphite/composite options evaluated are:

● Graphite/epoxy - 5 mil material

● Graphite/epoxy - 2 mil material

● Graphite/polyimide - 2 mil material.

The increased cost of the graphite composite materials and prelaunch processing relative to aluminum is greater than the transportation cost savings achieved with the lighter material. These composite cost estimates are based on projected costs of graphi material in quantities of a few thousand pounds. Vendor contacts have indicated, howeve that large quantity orders (millions of pounds) may significantly reduce these costs.

	ALUMINUM	GRAPHITE/EPOXY
MATERIALS TRANSPORT COST, $/LB ($/Kg)	162 (357)	182 (357)
TRANSPORT OF PERSONNEL, EQUIP & CONSUMABLES, $M	84	84
ASSEMBLY EQUIPMENT (0.2 OF TOTAL SATELLITE REQMTS), $M	275	276
FLT OPS (0.2 OF TOTAL SATELLITE REQMTS), $M	14.9	14.9

Fig. 3.5-18 MPTS Structural Cost Estimate Assumptions

MATERIAL	ALUMINUM		GRAPHITE/EPOXY		GRAPHITE/POLYIMIDE
			5-MIL LAYERS	2-MIL LAYERS	2-MIL LAYERS
DIAMETER km	1		1	1	1
COATING	ALZAC		WHITE PAINT	WHITE PAINT	WHITE PAINT
TRANSMITTED POWER	6.45		6.45	6.45	6.45
LIMIT WASTE HEAT @ ANTENNA CENTER w/m²	3600		3600	3600	8000
TRI BEAM CROSS SECTION	TRIANGULAR HAT		TRIANGULAR HAT	TRIANGULAR HAT	TRIANGULAR HAT
• WEIGHT, KLB (1000 Kg)					
PRIM STRUCTURE	300	(137)	207 (94)	207 (94)	207 (94)
SEC STRUCTURE	103	(47)	65 (30)	65 (30)	65 (30)
SUPPORT STRUCTURE	233	(106)	157 (71)	157 (71)	157 (71)
YOKE & MECHANISM	146	(66)	122 (56)	122 (56)	122 (56)
COATINGS	46	(21)	49 (22)	49 (22)	49 (22)
SUBARRAY ACTUATORS	268	(122)	268 (122)	268 (122)	268 (122)
SUBARRAY ATTACH STR	51	(23)	36 (16)	36 (16)	36 (16)
TOTAL	1147	(522)	904 (411)	904 (411)	904 (411)
RECURRING COST ($M)					
– MATERIAL	0.918		18.080	126.560	129.868
– PROCESSING	78.882		135.600	176.280	194.575
– MATERIALS TRANSPORT	185.814		146.448	146.448	146.448
SUB TOTAL	265.614		300.128	449.288	470.891
– ASSEMBLY & FLT OPS	373.900		373.900	373.900	373.900
TOTAL ($M)	629.514		674.028	823.188	844.791

Fig. 3.5-19 MPTS Structural Concept Comparison

Section 4

TECHNOLOGY ISSUES

This section includes an initial listing of MPTS technology issues. This listing identifies areas in technology where more work needs to be done and suggests approaches for accomplishing these tasks. No attempt has been made at this time to categorize or combine these technology programs.

4.1 CONTROL SYSTEM

4.1.1 Evaluation of Alternate Power Transfer and Drive Devices

Slip rings and flex harnesses are power transfer devices most commonly used in spacecraft. However, these systems, principally the slip ring approach, require many mechanical interfaces. Potential reliability advantages can be envisioned with the use of rotary transformers for power transfer and direct drive linear induction motors for drive power. Potential payoffs in reduced maintenance or logistic requirements and lower friction justify further study of these devices for the MPTS.

4.1.1.1 Background

Slip rings and flex harnesses are the only flight-demonstrated methods of power transfer across rotating joints. Because of the project scale of the MPTS, in size current carrying capacity, and mission duration, it is deemed critical to further evaluate rotary transformers and linear induction drive devices.

These devices are relatively new applications for a space environment. A rotary transformer and linear induction motor drive combination has many advantages including no wear or wear products, no arcing, negligible friction, no viscous drag from liquid contact, and energy transfer relatively unaffected by the presence of oil, water, or other contaminants. Further design and experimental work is required to determine the practibility of such a device to the MPTS.

4.1.1.2 Desired Output

- Conceptual design to determine feasibility, weight and cost of rotary transformer/linear induction motor

- Outline of scaled down prototype test program which will lead to development of full scale model.

4-1

4.1.2 Detailed Control System Analysis

The preliminary analytical study performed in support of this contract included an assessment of probable pointing accuracy, control torque requirements, horsepower requirements and control system bandpass frequency. These results were obtained using simplified system models so that the most significant factors could be studied. These simplifications may result in not identifying key dynamics problems associated with spacecraft to antenna structural dynamics and non-linearities in the mechanical elements of the control system.

4.1.2.1 Background

A more in-depth study which considers non-linearities and structural dynamics would modify and complicate the control system design. The first step in a refined study would be the development of an accurate set of structural modes of vibration for all frequencies up through that of the control system bandpass frequency. This is required to understand system stability and performance in a realistic manner.

These bending modes couple into antenna motions through friction effects in the bearings and gear trains, and by physically perturbing the antenna through motion cross-coupling into its two-axis gimbal system. The preliminary study documented here addressed these effects; however, a much more detailed investigation is required.

The torque drive-gear chain system has within it the factors of flexibility, friction, backlash, and hysteresis. These were briefly considered in the preliminary study. They were neglected in the preliminary analysis, but they must be considered in more detail.

Disturbance forces which must be considered in further analysis efforts are due to angular momentum cross-coupling, gravity gradient, magnetic field interaction, and solar pressure. Preliminary study indicated that these might be initially neglected because of the dominating influence of friction forces and structural mode oscillations, which were considered.

It is possible that detailed study efforts will show that many of these aforementioned factors are critical effects on control design and performance. It may also be found that it is not possible to calculate or estimate some of these factors with sufficient accuracy to provide the necessary control performance accuracy. In that case a type of "adaptive" control design may be required where a special estimator logic (Kalman Filter) can update the knowledge of these factors and adjust the control system gains appropriately.

4.1.2.2 Desired Output

* Detailed control system design
* In-depth stability analysis
* Pointing accuracy sensitivity to configuration uncertainties
* Full 3-dimensional math-model simulation demonstration.

4.2 STRUCTURAL SYSTEM

4.2.1 Composite Structures and Assembly Techniques

The attractive combination of strength and mass properties peculiar to advanced composites makes these materials strong candidates for the antenna structure. High strength, stiffness, and low thermal expansion are desirable properties. The initial studies of the MTPS shows these materials to be cost competitive.

4.2.1.1 Background

Up to this time much of the mechanical properties data for advanced composites have been established for short-duration aircraft and spacecraft missions. The antenna structural designs would employ composites in much thinner gauges than has been normally used. Development of mechanical properties in thin sections (5 mil range) must be verified. Durability of organic matrix materials in orbit must be reliably predicted based on sound test data. These verification tests for long-duration life times (30 years) must be initiated as soon as possible.

Methods of assembly and manufacture in space must be evaluated to determine overall feasibility of composites to MTPS application. Creep fatigue from thermal cycling in a space environment should be a long-term advanced study for these materials. Bonding methods used to join members in a space environment needs definition.

4.2.1.2 Desired Output

* Sufficient data to support design of MTPS structure using thin members in a geosynchronous altitude environment for a 30-year period. This data should determine materials strength degradation due to fatigue, radiation, temperature and outgassing
* Methods for manufacture in space. Low cost methods of transporting raw materials to a space-based factory and subsequent automatic manufacture of basic structural elements
* Methods of joining and bonding basic structural elements into large structure.

4-3

4.2.2 Tension Brace Antenna Feasibility Assessment

4.2.2.1 Background

The Tension Brace concept may offer weight and cost advantages over a built-up section approach. The flat array is relatively insensitive to out-of-plane thermal distortions since the braces maintain a positive force on the flat array tension wires. The brace and flat array wires can serve as both structural members and conducting elements.

In order to assess the concept feasibility structural arrangement drawings must be drawn, structural members need to be sized, the combined effects of thermal cycling, long term creep on wires, joints and braces need to be evaluated, and the feasibility of using structure for power transmission needs definition. In addition, methods of assembly to produce a flat pre-tensioned array in space needs to be evaluated along with alternate materials and relative costs.

4.2.2.2 Desired Output

- Preliminary drawings of configuration options and selection of one of the following:
  - Square array
  - Triangular array
  - Round array
- Selection of rectangular, triangular or radial grid for the flat array
- Recommendation of the number of braces per assembly, brace size and wire size
- Material options
- Method of assembly in space
- Long term strength/thermal and creep effects on wires and braces
- Structural weight/cost analysis comparing three tension brace options with built-up section approach.

4.2.3 Local Crippling Stress Evaluation

A study is required for the prediction of local compression crippling failure modes of very thin (0.1 - 0.15 mm) structural sections for various materials. The study should include tubular as well as other structural shapes such as hat sections, channels angles, sections of circles, etc. Of prime interest in the evaluation are the effects of initial imperfections induced in the fabrication process.

4.2.3.1 Background

Some test data has been generated in the low thickness ranges and are summarized in the NASA Handbook of Structural Stability. However, the thickness does not extend in the ranges expected for the antenna structure; in addition, various materials should be evaluated such as the graphite/epoxy, Kevlar 49/epoxy, etc.

4.2.3.2 Desired Output

Local instability design curves as function of parameters such as section geometry, initial imperfections, materials properties, applied axial compression load and temperature-load time histories.

4.2.4 Design Environments

A study of all the structural design environments induced on the antenna during launch into low and synchronous orbit is necessary. This study should establish the design conditions induced during fabrication and assembly in space, with consideration being given to the 30-year life requirement.

4.2.4.1 Background

No data is available on the design environments for large structures of the type to be used on the antenna. Of particular interest (and related to the fabrication process) are the environments induced in assembly, operation and refurbishment during the 30-year life.

4.2.4.2 Desired Output

Structural design environments including acoustic, shock, acceleration, vibration, temperature, meteoroid, etc.; in addition the above are affected and influenced by the 30-year life operation.

4.2.5 Optimum Antenna Structures

The cost of the MPTS is strongly dominated by the mass of the antenna support structure. Significant cost savings will be offered by an optimum structural arrangement for the environmental conditions and stiffness requirements. A study that takes into consideration the following factors should be performed:

- Geometry
- Design environments including effects of meteoroids
- Life requirement (fracture, creep, fatigue creep buckling, etc.)

- Materials applications

- Stiffness requirements —

- Feasibility of fabrication and assembly

Consideration to be given to various configurations of structural elements and shapes.

4.2.5.1 Background

None available on large space structures of this type.

4.2.5.2 Desired Output

Design data and typical structural design arrangements which will satisfy the expected requirements.

4.2.6 Finite Element Model Development

Finite element models of selected structural arrangements are needed to evaluate the antenna structural responses to thermal and dynamic loads These models would ensure that a particular design configuration would satisfy the deflection limitations and pointing accuracy requirements. As part of this study to develop finite element models, consideration could be given to developing a member loading system by increasing or relaxing cable loads based on a deflection sensing system in conjunction with an on-board computer and cable loading/unloading drive system. The objective of this system is to correct any large induced deflections which may occur in the 30-year life due to load and thermal distortions as well as creep.

4.2.6.1 Background

None available.

4.2.6.2 Desired Output

Feasibility of typical design concepts to meet requirements.

4.2.7 Composite Waveguide

The MPTS waveguide will experience extremes in thermal environment and may require tight dimensional and electrical stability throughout these extremes. Composites offer the potential to meet these requirements at low weight and high strength.

4.2.7.1 Background

The Air Force Materials Laboratory at Wright-Patterson Air Force Base (Ref 17 and 19) has completed studies on manufacturing methods for dimensionally stable composite

microwave components. Components were made of graphite/epoxy and in all cases were found to meet criteria of temperature stability, reproducibility and reasonable cost. These components were tested for mechanical and electrical properties in a temperature range between 117 to 394°K (-250 to 250°F).

Application to the MPTS would require cost-effective manufacture of composite components in significantly larger lengths, and tested in a much harsher environment: 50 to 600°K (-370 to 620°F). Manufacturing techniques for interfacing microwave conversion devices such as amplitrons and klystrons are required. Materials other than graphite could lead to a more cost-effective total system. One such material is Kevlar. This material has a tendency to degrade in the presence of UV radiation and coating methods to preclude this degradation would be required.

4.2.7.2 Desired Output

- Manufacturing methods for long length composite material
- Material tests at the temperature extremes
- Radiation characteristic testing
- Manufacture costs
- Extent of UV degradation
- Suitable protective coatings.

4.3 THERMAL SYSTEM

4.3.1 Maximum Temperature

For a given microwave converter efficiency and antenna diameter, the power transmission capability of the MPTS is limited by the maximum permissible structural temperature. Potential payoffs for greater power transmission and wider selection of structural materials to choose from warrant studies for reducing the maximum temperature experienced by the structure.

4.3.1.1 Background

The Gaussian waste heat distribution of the MPTS causes peak temperatures in the center of the antenna support structure that are 200°K hotter than the temperatures at the edges. If one material is to be used efficiently throughout the structure, all of the structure should be near the maximum working temperature of the material. This will maximize the transmission capability of the MPTS. Studies are required to evaluate

various techniques for smoothing out the Gaussian waste heat distribution. (An important byproduct of this smoothing will be smaller temperature differences between structural members.) Techniques for smoothing the distribution that should be investigated are: (1) the use of geometrically and spectrally selective radiators, (2) heat pipes to transport heat away from the center and (3) through the selection of the constant ρ in the microwave converter spacing equation $1 = 1$ min. $\exp (r/\rho)^2$. It is recognized that this constant will affect the microwave transmission efficiency and the total power that can be handled by the MPTS. A study that includes the effect on structural temperatures is required to establish the ρ value that results in the maximum power received on Earth.

As part of this study to increase the power transmission capability of the MPTS and increase the choice of structural materials, it is recommended that the effect of coatings on reducing the maximum structural temperature be investigated. Selective use of coatings will also offer minimization of temperature differences between structural members.

4.3.1.2 Desired Outputs

- Conceptual design of geometrically and spectrally selective radiators along with their attendant MPTS power level increments

- Performance requirements, installation considerations, and redundancy aspects of heat pipe designs along with their predicted power level increments. Due to the high temperatures (300 – 500°K) the heat pipe designs will involve new developments

- Selection criteria for the spacing constant ρ that provides maximum power received on the ground for a given antenna size and maximum structural temperature

- Candidate coatings for the structural members with their attendant power level increments. Consideration for minimizing temperature differences between elements by selectively coating the members should be part of this study. The degradation performance of the coatings must be examined so as to ensure the 30-year design life of the MPTS. A test program for obtaining the necessary degradation data should be outlined as part of this study.

4.3.2 Transient Analysis

The greatest uncertainty in the stress levels that the structural members will experience is due to the stress induced by the different transient thermal responses of the various structural members. To ensure that the lightest possible structure is used

this uncertainty must be eliminated, i.e., a detailed study of the transient thermal performance of the structure must be performed.

4.3.2.1 Background

Twice each year the MPTS will be shadowed from the Sun by the Earth. While in the Earth's shadow there will be no waste heat. The only source of heat to the MPTS will be $5-6$ w/m^2 from the Earth's infrared emission and albedo. The structure will drop to approximately 75°K (-335°F) during the 72 minute occult period. Stresses will be induced as a result of components with low thermal inertia cooling and shrinking more rapidly than the "heavier" ones. The counterpart of this problem with the MPTS coming out of the shade and into the sunlight will also have to be investigated since the members will be stressed differently in the two situations. Identification and modelling of the critical support structure elements will be required. A thermal model of the antenna waveguide/radiator surface will be necessary to provide the thermal inputs to the structure as the entire MPTS moves in and out of the Earth's shadow.

4.3.2.2 Desired Output

- Transient temperature responses of critical structural members during cool-down and heat-up as the MPTS goes in and out of Earth's shadow

- The stresses induced in the structural members as a result of differential contractions/expansions caused by the different temperature responses.

4.4 ASSEMBLY

4.4.1 Assembly Cost

The greatest uncertainty in establishing accurate cost estimates for the MPTS is the estimate of assembly cost. In the development of assembly cost estimates, the amount of resources (manpower, facilities and materials) required to produce the end product must be known. Manpower costs are of two types: recurring and non-recurring. Recurring is the effort associated with the fabrication, assembly, integration and test of flight hardware. Non-recurring cost is the effort associated with manufacturing and testing prototype or test hardware. This effort also includes the cost of tooling and peculiar support equipment.

4.4.1.1 Background

Three basic methods of developing manufacturing cost estimates are used: grass roots, analogous and parametric. Grass roots estimates are based on building up from detailed estimates and require good definition of the parts to be fabricated, the methods

to be used and the equipment required. Analogous estimates use comparisons with past programs. This method requires historical cost data and the exercise of judgment to determine a representative program for comparison and adjustment for varying complexity factors. Parametric estimates use mathematical formulas based on significant variables related to physical or performance characteristics of the system.

Since there is no historical data based for space antennas, a combination of grass roots and analogous techniques is required to develop cost estimates. A baseline design is required which is sufficiently detailed to determine the cost drivers and major cost elements. These can then be related to cost data on fabrication, assembly, and erection for large aluminum structures or ground based antennas.

4.4.1.2 Desired Outputs

- Baseline design to determine:
  - Element fabrication method
  - Joint design
  - Materials
  - Assembly and erection procedures
  - Packaging and delivery techniques
  - Alignment procedures
  - Tooling and equipment requirements
  - Facility requirements

- Analysis of cost data for erection of representative aluminum structures

- Preliminary plan for manufacture on earth

- Analysis of space assembly techniques

- Analysis of astronaut capabilities to perform assembly tasks

- Analysis of special equipment requirements.

4.4.2 Man's Role in Assembly and Maintenance

The Apollo and Skylab programs demonstrated man's capability to work successfully in zero gravity. Future work in space will require teams of men to assemble enormous structures across vast areas over weeks or months. The jobs that man can and must do in the transport, assembly, positioning and maintenance of the MPTS need to be identified. The equipment needed for these jobs and the design of the MPTS to aid job conduct strongly influences the operational concepts selected.

4.4.2.1 Background

The assembly of the MPTS involves these human factor and safety concerns:

- Life support equipment
- Mobility and restraint methods/devices
- Special tools and aids
- Stability and structural integrity of space structure when "man handled"
- Work site volume, power, attitude control, etc., requirements
- Manipulator interfaces: electrical, mechanical and procedural
- Environmental protection requirements for solar flames, micrometeorites and microwave radiation
- Safety in mating large structures and installing/checking out high voltage/ high amperage equipment.

Maintenance of the MPTS requires answers to these questions before design concepts are firmed:

- Should the system ever have a planned shutdown? For what reason and for how long?
- Will maintenance by men be done from the microwave radiating side of the antenna? From the heat rejection side of the assembly?
- What materials or devices can be tailored to protect men and/or equipment from microwave radiating hazards, but still provide visual information on activity progress?
- Are equipment requirements for MPTS assembly operations compatible with equipment requirements for maintenance? Should they be compatible?

4.4.2.2 Desired Outputs

- Remote control activity descriptions
- Crew roles and job descriptions
- Crew equipment requirements
- Crew safety constraints
- Work site requirements
- Maintenance philosophy
- Simulation requirements.

Section 5

CONCLUSIONS AND RECOMMENDATIONS

5.1 CONCLUSIONS

The following summarizes significant conclusions for the mechanical systems and flight operations.

a.   Rectangular grid structural arrangement with triangular has section is recommended for basic members of the transmitting antenna structure.

b.   Aluminum, graphite epoxy, and graphite polymide are recommended candidate materials.

c.   Aluminum materials result in the probable lowest cost and development risk program with thermal limits being their most critical area.

d.   Composites are attractive for low thermal distortion and high temperature operation (polymide), but ultra-violet compatibility, and outgassing leading to rf generator contamination need investigation.

e.   Assuming the Shuttle as the transportation system, low altitude assembly is recommended. The associated transportation and assembly cost for $10.5M/launch is estimated to be near 600 $/kg.

f.   Advanced transportation system needed for low cost of large payloads to earth orbit at relatively low launch packaging densities for the payload. Low cost advanced transportation system required to transport assembled or partially assembled systems from low earth orbit to geosynchronous equatorial orbit.

g.   Orbital assembly requires remote controlled manipulators.

h.   Maximum on orbit manufacturing and assembly will be necessary when using the Shuttle transportation or other options with small volume capacity requiring high launch packaging densities to achieve payload performance.

5.2 RECOMMENDATIONS

Technology issues for mechanical systems are listed and discussed in Section 4 of Section 8 (Mechanical Systems and Flight Operations). This listing identifies areas in technology where more work needs to be done and suggests approaches for accomplishing these tasks. The following simplified list is incorporated here as recommendations for further detailed investigation.

a.   Evaluate alternate power transfer and drive devices for the rotary joint.

b.   Conduct detailed control system analysis.

c.   Conduct detailed investigations of composite structures and assembly techniques.

d.   Investigate tension-brace concepts and compare them with the built-up section approach.

e.   Evaluate the local crippling stress characteristics of the basic thin material elements of the structure.

f.   Establish the design environments for launch into low earth orbit, transfer to synchronous orbit as well as those associated with fabrication and assembly.

Section 6

REFERENCES —

1. GAC Memo ASP-611-M-1018; SSPS Baseline Mass Properties; 16 Nov 1972

2. GAC Memo ASP-611-M-1004; Sensitivity of Attitude Control Propellant Requirements to SSPS Deviation Angle Limits; 21 Aug 1972

3. GAC Memo ASP-611-M-1011; Forces Resulting From the Electromagnetic Radiation of Energy From the SSPS Antenna; 1972

4. Lewis Research Center – NASA CR-2357; Feasibility Study of a Satellite Solar Power Station; Feb 1974

5. GAC Memo ASP-611-M-1005; SSPS Rotary Joint Friction Torque Characteristics; 1972

6. GAC Memo ASP-611-M-1011; Forces Resulting From the Electromagnetic Radiation of Energy From the SSPS Antenna; 1972

7. GAC Memo ASP-611-M-31; SSPS Rotating Joint – Preliminary Study Progress Report; 20 April 1972

8. LMSC – A981486; Space Station Solar Array Technology Evaluation; Dec 1970

9. GAC Memo ASP-611-M-1008; Review and Update Baseline Configuration; 25 Aug 1972

10. E. I. DuPont, A-87903; Properties and Characteristics of "Kevlar" 49, Yarn and Composites

11. GAC Memo MPTSS-74-003; Orientation Meeting With Raytheon on Microwave Power Transmission System Study; 6 Aug 1974

12. GAC Memo MPTSS-74-004; August Progress Report – Microwave Power Transmission Systems Study; 8 Aug 1974

13. GAC Memo MPTSS-74-011; October Progress Report – Microwave Power Transmission Studies; 3 October 1974

14. GAC Memo ASP-611-M-1003; SSPS Microwave Antenna Deflections Due to Temperature; 31 July 1972

15. GAC Memo ASP-611-M-1000; SSPS Microwave Antenna Temperatures; 27 July 1972

16. GAC Memo MPTSS-74-007; Subtask 3.1.2-1, Preliminary Structural Design Options; 26 Aug 1974

17. AFML-TR-74-70, LTN Project No. 461-2; Manufacturing Methods for Dimensionally Stable Composite Microwave Components; May 1974

18. IBM No. 74W-00033; Space Tug Autonomy Analysis Study; 18 Jan 1974

19. AFML-TR-71-105, Vol II, Advanced Composite Material Study for Millimeter Wavelength Antennas; Oct 1971

20. G. Hosh, R. and Husom, G., "Achievement of Synchronous Orbit Using Electronic Propulsion," AIAA Paper 69-275; March, 1969

21. Mickelsen, W. R., "Future Trends in Electric Propulsion," AIAA Paper 66-595; June, 1966

22. GAC Memo MPTSS-74-013; Summary Data - Structural Analysis Microwave Power Transmission System; 4 October 1974

23. SAE Aerospace Handbook - Part 4C "Spacecraft Thermal Balance", p. 615

24. ASP-946-5-61, "Study of Requirements for Assembly and Docking of Spacecraft in Earth Orbit," NAS8-27860; March 1972

25. MSC-02464; SD70-546-1 "Shuttle-Launched Modular Space Station, Volume 1, Concept Definition," NAS9-9953; January 1971

26. GDCA-DDA72-006, "Research and Applications Module (RAM) Phase B Study," NAS8-27539; May 1972

27. XM-TN-160, "Experiment Module Concepts Study," NAS8-25051; May 1970

28. MSFC Doc., "Preliminary NASA Payload Descriptions," July 1974

29. ASP 583-R-3, "Satellite Solar Power Station," November 1971